



The University of
Nottingham

SCHOOL OF CHEMISTRY

Single-Carbon Atom Insertion into Aromatic Heterocycles

Author:

Benjamin W. Joynson

20202412

Supervisor:

Dr Liam T. Ball

*Thesis submitted to the University of Nottingham
for the degree of Doctor of Philosophy, May 2023*

'It is not down on any map; true places never are'

HERMAN MELVILLE – *Moby-Dick; or, the Whale*

Table of Contents

Abstract	i
Acknowledgements	ii
List of Abbreviations	iv
1. Introduction	1
1.1 Aromatic Heterocycles	2
1.1.1 Aromaticity	2
1.1.2 Five-membered aromatic heterocycles	3
1.1.3 Chemical properties of five-membered heterocycles	4
1.1.4 Prevalence of five-membered aromatic heterocycles	5
1.1.5 Synthesis of five-membered aromatic heterocycles	6
1.1.6 Six-membered aromatic heterocycles.....	9
1.1.7 Chemical properties of six-membered heterocycles	10
1.1.8 Prevalence of six-membered aromatic heterocycles	12
1.1.9 Synthesis of six-membered aromatic heterocycles.....	12
1.1.10 Comparison of five- and six-membered aromatic heterocycles.....	16
1.2 Skeletal Editing.....	18
1.2.1 Carbon Atom Insertion.....	19
1.2.2 Nitrogen Atom Insertion.....	24
1.2.3 Carbon atom deletion.....	27
1.2.4 Atom Transmutation.....	29
1.3 Carbenes	31
1.3.1 Carbene Reactivity	32
1.3.2 Carbene precursors	32
1.3.3 Metal Carbenoids	33
1.3.4 Carbenes and carbenoids in cyclopropanations	35
1.3.5 Diazirines	37
1.4 Project Outline and Aims	39

2. Single Carbon Atom Insertion with Zinc Carbenoids	41
2.1 Introduction.....	42
2.1.1 Halocyclopropanation.....	42
2.2 Hypothesis and Chapter Aims	44
2.3 Development of reaction conditions	45
2.3.1 Initial Studies	45
2.4 Modification of protecting group.....	47
2.5 Addition of zinc halides	48
2.6 Subsequent optimisation.....	50
3. Single Carbon Atom Insertion with Arylchlorodiazirines.....	53
3.1 Introduction.....	54
3.1.1 Arylchlorodiazirines.....	54
3.1.2 Chlorodiazirines in organic synthesis.....	54
3.2 Project Hypothesis and Aims.....	56
3.3 Development of reaction conditions	56
3.3.1 Initial Studies	56
3.3.2 Protecting group modification.....	57
3.3.3 Carbene capture with rhodium	59
3.3.4 Diazirine stoichiometry.....	61
3.3.5 Reaction optimisation	61
3.4 Comparison to Levin et al.	67
3.4.1 Limitations of Levin's work	68
3.4.2 Direct comparison of reaction conditions	70
3.5 Substrate scope of indoles	72
3.5.1 Electron-deficient indoles.....	72
3.5.2 Precipitation optimisation	74
3.5.3 Expanded substrate scope.....	77
3.5.4 Incompatible substrates	79
3.6 Substrate scope of diazirines	80
3.6.1 Synthesis of amidine hydrochlorides	80
3.6.2 Synthesis of chlorodiazirines.....	82
3.6.3 Application of diazirines to atom insertion	85
3.7 Substrate scope of pyrroles.....	87

3.7.1	Optimisation of pyrrole atom insertion.....	88
3.7.2	Modified pyrrole substrate scope	89
3.8	Robustness screen.....	92
3.8.1	Methodology robustness.....	92
3.8.2	Poorly tolerated functionalities	95
3.9	Application to complex substrates	97
3.9.1	Tryptophan modification.....	97
3.9.2	Modification of dipeptides	98
3.10	Functionalisation of azinium salts	99
3.10.1	De-alkylation.....	100
3.10.2	Oxygenation.....	102
3.10.3	Reduction	104
3.11	Thermal stability of chlorodiazirines.....	108
3.11.1	Differential scanning calorimetry (DSC)	109
3.11.2	Avoiding isolation of diazirines	115
3.11.3	Applications to flow chemistry	115
4.	Conclusions and Future Work.....	119
4.1	Conclusions.....	120
4.2	Future Work.....	121
5	125
5.	Experimental	125
5.1	General Information.....	126
5.2	Synthesis of compounds relevant to Chapter 2.....	127
5.2.1	Optimisation and General Procedures	127
5.2.2	Synthesis of protected indoles	129
5.2.3	Synthesis of 3- <i>H</i> quinolines.....	132
5.3	Experimental details relevant to Chapter 3	133

5.3.1	Optimisation and General Procedures	133
5.3.2	Synthesis of protected azoles	135
5.3.3	General Procedure 2 (GP-2): Ring expansion of <i>N</i> -benzylindoles.....	169
5.3.4	General Procedure 3 (GP-3): Ring expansion of <i>N</i> -benzylpyrroles	188
5.3.5	Synthesis of Amidine Hydrochlorides	196
5.3.6	Synthesis of 3-chloro-3-aryl-3 <i>H</i> -diazirines (GP-4).....	202
5.3.7	Functionalisation of Azinium Salts	208
5.3.8	Robustness Screen	213
5.4	DSC Analysis	219

6. References	223
----------------------------	------------

Abstract

The desire for highly selective and general methods for the functionalisation of complex molecules is particularly prevalent in the field of drug discovery, as the facile modification of pre-existing entities can lead to the rapid diversification of existing drug libraries. In turn, this could lead to the more efficient identification of potential drug candidates. Building upon the general theme of skeletal editing, this thesis details the development of methodologies to transform heteroaromatic scaffolds – namely indoles and pyrroles - by the insertion of a single carbon atom.

The work described in Chapter 2 outlines the development of a methodology to achieve the ring expansion of indoles *via* a cyclopropanation/fragmentation strategy to the corresponding quinoline with the use of zinc carbenoids. While the desired transformation was achieved in modest yields, the highly reactive nature of the carbenoid intermediate led to poor compatibility with unprotected indoles, while protected indoles proved inert in most cases.

Chapter 3 details the development and application of a robust protocol to achieve carbon atom insertion by a similar strategy, employing arylchlorodiazirines as photo-activated carbene precursors. Protection of the indole nitrogen proved key to high conversion and – along with the tuning of the reaction solvent – allowed for precipitation of the azinium salt product and facile isolation by filtration. An extensive substrate scope revealed tolerance of a range of functional groups, both on the azole and diazirinyl partners. The exploration of substrate scope was assisted by a robustness screen of a number of medically-relevant functional groups, revealing the potential application to complex molecules. Consequently, the methodology was applied to the modification of tryptophan and tryptophan-containing peptides. Functionalisation of the azinium salt products was also explored, focusing in particular on reduction chemistry to give access to a range of three-dimensional architectures.

A hazard assessment of arylchlorodiazirines was also carried out as literature reports have often noted their thermal instability though extensive analysis has not yet been undertaken. The explosive nature of arylchlorodiazirines was analysed by the use of differential scanning calorimetry (DSC). From this data, along with predictors derived from it, the thermal stability of these diazirines was assessed and measures to avoid potential hazards were proposed and discussed.

Acknowledgements

Foremost, I must of course thank Liam. Your mentorship and guidance throughout my PhD have been invaluable and has allowed me to become the chemist I am now. It has been an immense pleasure to carry out this PhD under your supervision, particularly for the support - both scientific and moral – you have provided these past years that has made me appreciate chemistry all the more. I look forward to staying in touch and hearing about what the group has been up to.

Though they have all (mostly) moved onto greener pastures, I must thank the past Ball Group members. Lorenzo, for his mentorship in the lab and assistance with dodgy chemistry as well as for his world-renowned tiramisu and his keen interest in finding me a girlfriend. Tom, your breadth of chemical knowledge is inspiring and you are a fantastic teacher. Aaron, your advice and positivity was always deeply appreciated, and your support truly made me a better chemist. I'll always welcome your input whether it's chemistry advice or another great book or TV recommendation. Katie, the true queen of C41, you are an exceptional chemist and it was a pleasure to work alongside you. Your dedication to chemistry (and Sue's coffee) is truly inspirational. Desiree, your ability to laugh at pretty much anything is honestly infectious and hopefully one day I will properly understand dielectric spectroscopy.

I could not have done this PhD without my two closest friends here in Nottingham: Charlie and Gemma. Charlie, it is honestly impressive how many things we have in common. Whether it's music, climbing, or routinely going insane every day past 3pm, we're always on the same page. I have enjoyed every second of working side by side both in the lab and the office, even if it does involve you showing me the worst idea for a reaction I have ever seen. You've always been there for me and it has been a joy doing this PhD with you. Gemma, your support and advice both in the lab and out has meant the world to me and I simply could not have done it without you. From our early days sharing a fume-hood to sharing a house you have always had the time for me and I know I could always turn to you for support. You have always been there to brighten my day and I'm truly thankful.

Of course, a huge thank you to the remaining Ball Group members. Alessio, your positivity and constant ideas inspire me to be a better scientist. You are a fantastic chemist and it has been a pleasure working with you and your commanding use of British catchphrases. Martyna, it's impressive that someone can make me laugh and go mad so frequently. You are a joy to

be around in the lab and you're a presence I will sorely miss. Dr Ben, you've referred to me as the dark reflection of yourself which I must agree with, we do have a strange amount in common. It's been excellent working with you, and I very much enjoyed our lunch break viewings of University Challenge. Sudheesh, you are a joy to work with and your positivity is uplifting. Your ideas and advice are always welcome and appreciated. My lab children, Tash, Ben, and Sam, you have truly made me go insane. While I do occasionally look at you in the way a tired father looks at a hyperactive toddler, you three collectively have made me laugh more times than I can count. Andy, Joseph, and Louis, it has been great to watch you grow as chemists and I wish you all the best for your time in the Ball Group.

I must of course thank Eli Lilly and Co. for the funding and the opportunity to be here in the first place. A particular thank you to my industrial supervisor Graham Cumming for all his ideas and advice over the years. Thank you as well to the analytical for all their behind-the-scenes work in fixing the NMR and MS after I break them. A particular thank you to Shaz for all his assistance. I appreciate all the (totally unnecessary) 30k scan carbons.

Finally, I have to thank all the people outside the chemistry building who have supported me all this time. To the Tuesday night D&D crew: Charlie, Em, Gemma, Luke, and Tom, for taking my mind off chemistry and instead focusing on figuring out how to fix the encounter that you've just broken. Thank you for being a part of this journey and for listening to me do silly voices.

I of course have to thank my good friend James. You've always been there for me every step of the way, well before my PhD and certainly well beyond it. I am truly grateful for your support and selflessness over the decade or so we've known each other and more than anyone you've helped me become the person I am today. I would not be here without you. Finally, to my parents, thank you for all your unending support and for helping me on this journey. Perhaps one day I'll properly explain to you what it is I actually do.

List of Abbreviations

Common abbreviations used are listed in the Journal of Organic Chemistry abbreviations guideline for authors.ⁱ The main abbreviations used in this thesis are listed below, SI units are omitted:

aq.	aqueous
atm.	atmosphere(s)
calcd.	calculated
cat.	catalyst, catalytic
δ	chemical shift
equiv.	equivalents
PMB	<i>para</i> -methoxybenzyl
R	generic side group
TFA	trifluoroacetic acid (or acetate)
TIPS	triisopropylsilyl
TMS	trimethylsilyl
Ts	<i>para</i> -toluenesulfonyl (tosyl)
X	(pseudo)halide

ⁱ http://pubs.acs.org/userimages/ContentEditor/1218717864819/jocea_h_abbreviations.pdf
(Accessed 19/03/23)

1

Introduction

Abstract

This chapter highlights the underlying chemistry of aromatic heterocycles, their prevalence in nature and medicine, as well as their chemical reactivity and methods for their synthesis. The key synthetic concept of ‘molecular editing’ and its sub-category ‘skeletal editing’, as well as the classes of reagent central to this thesis, are introduced. A specific focus is drawn to the class of skeletal edit known as ‘atom insertion’ though other skeletal editing strategies such as atom deletion and atom exchange are mentioned. This introduction focuses on the modification of aromatic ring systems and thus the molecular editing of non-aromatic scaffolds is omitted. Finally, Section 1.3 focuses on the chemical properties of carbenes and their applications in organic synthesis.

The content of the second section of this Chapter on skeletal editing has been communicated in the following review: B. W. Joynton* and L. T. Ball*, *Helv. Chim. Acta*, **2023**, e202200182.

1.1 Aromatic Heterocycles

Aromatic heterocycles are ubiquitous motifs in both pharmaceuticals and natural products.^{1,2} The presence of a heteroatom in the skeletal core results in vastly different chemistry than their carbocyclic counterparts, and the presence of a stable, aromatic system differentiates them further from saturated heterocycles. This section aims to highlight and explain the key phenomena exhibited by aromatic heterocycles and compare these properties between different heterocyclic congeners.

1.1.1 Aromaticity

The concept of aromaticity and its consequences are highly important in organic chemistry.³ The term generally refers to cyclic π -conjugated compounds that are more stable than their linear analogues.⁴ Aromaticity manifests in abnormal chemical properties including: bond lengths that are intermediate between typical single and double bonds and the ability to induce a current when exposed to an external magnetic field, leading to distinctive ^1H NMR spectroscopic shifts.⁵ The most commonly known aromatic compound is benzene, first isolated in 1825 by Michael Faraday though its structure was not determined until 1865 by Kekulé.⁶ Heteroaromatic compounds, replacing one or more carbon atoms for a different element, commonly feature isoelectronic first-row elements such as nitrogen and oxygen, as the similarly-sized p-orbitals provide optimal overlap with carbon to produce a sufficient π -conjugated system.⁷ Despite the weaker overlap, aromatic compounds of 3rd row elements such as sulfur and phosphorus are known.⁸

There are several requirements for a compound to be aromatic. Firstly, the compound must be cyclic and contain a continuous ring of p-orbitals. These orbitals (and therefore the molecule) must be planar to ensure optimum overlap and conjugation. The final requirement is commonly known as Hückel's rule. This is the requirement that the number of electrons in the π -conjugated system must be equal to $4n+2$, where n takes an integer value (e.g. $n=1$ for benzene).⁹

In heteroatomic aromatic systems, the electrons the heteroatom provides to satisfy Hückel's rule can be derived from two scenarios (Figure 1.1). In the case of five-membered rings such as pyrrole or furan, the heteroatom donates a lone pair to participate in the π -system (1 electron from each of 4 carbon p-orbitals + 2 electrons from heteroatom lone pair = 6 electrons). For furan and thiophene, only one lone pair from oxygen and sulfur respectively is incorporated

into the aromatic sextet. In six-membered systems such as pyridine or the pyrylium cation, the heteroatom only needs to provide 1 electron to achieve aromaticity and thus a single electron in the relevant p-orbital is donated. This leaves a heteroatom lone pair orthogonal to the π -system and therefore cannot overlap with the conjugated system and is free to participate in further reactivity.⁴ Heterocycles containing more than one heteroatom such as 1,2- or 1,3-azoles possess both types of heteroatom where the lone pair of one heteroatom is incorporated into the aromatic sextet (enamine type) while only one electron is provided from the other (imine type).⁷

In addition to monocyclic aromatic heterocycles such as pyrrole and pyridine, benzo-fused bicyclic heterocycles, such as indole and quinoline, are also aromatic. The additional four carbon atoms of the benzo-fused ring provide another four π -electrons to give a total of 10, satisfying Hückel's rule ($n=2$). The reactivity of these heterocycles is somewhat analogous to their monocyclic counterparts, although substitution chemistry can vary as discussed in section 1.1.3.

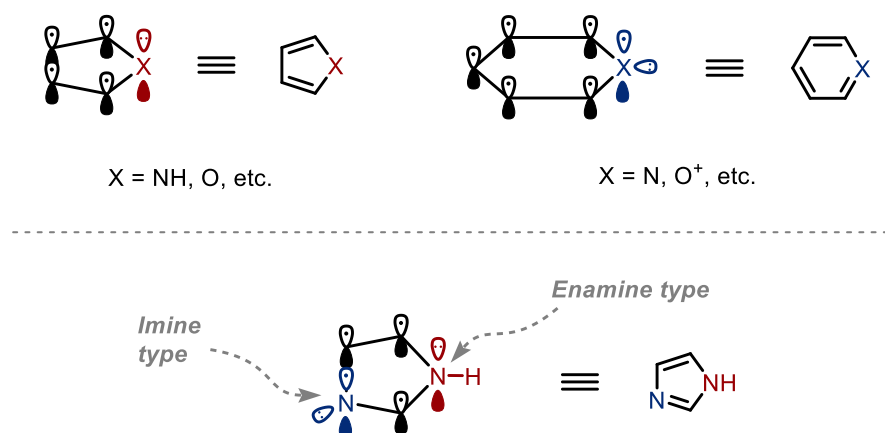


Figure 1.1. Orbital descriptions of aromatic heterocycles highlighting the differing roles of the heteroatom

1.1.2 Five-membered aromatic heterocycles

The first class of compounds relevant to this thesis are five-membered aromatic heterocycles, mainly those containing nitrogen. Two of the most common compounds of this class in nature and pharmaceuticals are pyrrole and indole (Figure 1.2).



Figure 1.2. Two five-membered aromatic heterocycles: pyrrole and indole

Pyrrole, from the Greek *pyrrhos* (πυρρός, “reddish, fiery”), is a monocyclic aromatic heterocycle and was first detected in 1834 as a constituent of coal tar.^{10,11} Pyrrole is isoelectronic with the cyclopentadienyl anion, although the greater electronegativity of the nitrogen atom compared to carbon leads to the formation of a dipole. While the inductive effects of nitrogen draw electron density towards it and away from the carbon atoms, mesomeric effects lead to the formation of partial negative charges on carbon and partial positive charges on nitrogen. Between these opposing effects, the mesomeric contribution is more dominant, resulting in the formation of a dipole *away* from nitrogen. The formation of this dipole towards carbon has led to pyrroles being described as ‘electron-rich’ or ‘ π -excessive’.⁷

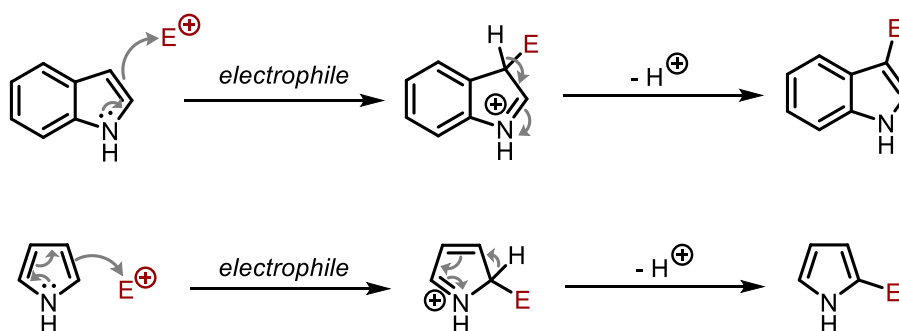
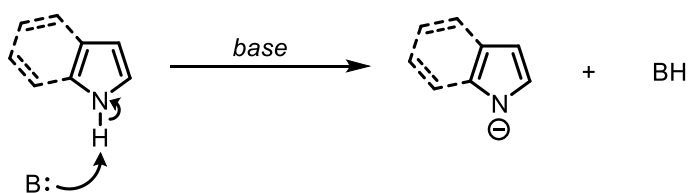
Indole, derived from *indigo*, from which it was first synthesised, is a bicyclic aromatic heterocycle, consisting of a pyrrole unit with a benzo-fused ring. It was first isolated in 1866 as the basic structure of indigo and has been identified in coal tar.¹² The properties of indole can be extrapolated from those of pyrrole; despite the inductive effects of nitrogen, indoles are considered electron-rich due to dominating mesomeric effects.

1.1.3 Chemical properties of five-membered heterocycles

Due to the requirement for six π -electrons in the aromatic sextet, the nitrogen of pyrrole must provide its lone pair to achieve aromaticity. The main consequence of this is the lower affinity for nitrogen to react with electrophiles (under neutral conditions). This ultimately means indoles and pyrroles are very weak bases.¹³ Further highlighting the lack of nucleophilic reactivity at nitrogen, protonation occurs at C3 and C2 respectively. However, azoles of this class are weak acids and can be deprotonated upon exposure to a sufficient base (Scheme 1.1A). Diazoles such as imidazole possess both enamine and imine type nitrogen atoms and therefore possess amphoteric character (imidazole $pK_a = 14.5$, $pK_{aH} = 7.1$).¹⁴

Like protonation, the addition of electrophiles to five-membered heterocycles also typically occurs at carbon (Scheme 1.1B). Due to the addition of a benzo-fused ring, the regioselectivity of the addition of electrophiles to pyrrole and indole differs, with addition to C2 and C3 respectively. Addition at C2 of pyrrole occurs due to favourable resonance forms in the

resulting cationic intermediate. Attack at C3 is feasible, although partial rates of addition favour C2 (3.9×10^{10} vs. 2.0×10^{10} for hydrogen/deuterium exchange of *N*-methylpyrrole).¹⁵ This regioselectivity can be inverted by introducing steric bulk at nitrogen with groups such as triisopropylsilyl (TIPS); kinetically favouring attack at C3. Indoles, on the other hand, exhibit high regioselectivity to electrophilic attack at C3 (C3/C2 2600:1 in Vilsmeier acylation).¹⁶ The high selectivity is derived from the high energy barrier resulting from disruption of the entire aromatic system; attack at C2 disrupts the entire 10π aromatic system, whereas attack at C3 retains a 6π component in the benzo-fused ring.



Scheme 1.1. A: Reaction of five-membered heterocycles with base. B: Reaction of five-membered heterocycles with electrophiles.

1.1.4 Prevalence of five-membered aromatic heterocycles

A number of five-membered aromatic heterocycles occur naturally and are common structural motifs in pharmaceuticals. The most obvious example of these heterocycles in nature is the presence of indole in the essential amino acid tryptophan, and the presence of imidazole in the amino acid histidine (Figure 1.3). For indole specifically, its presence in tryptophan means it is a highly common motif in a number of alkaloids, most famously tryptamine and ergot alkaloids such as psilocybin and LSD (lysergic acid diethylamide) as well as neurotransmitters such as serotonin and melatonin.¹⁷ In pharmaceuticals, a 2014 study found that indoles were the 9th most common heterocycle found in FDA-approved pharmaceuticals and the 4th most common aromatic heterocycle.¹ Pyrroles are far less common in pharmaceuticals, although drugs containing pyrroles show anti-inflammatory, antifungal, antitumor properties.¹⁸ Most

famously, a key pyrrole core can be found in the blockbuster drug atorvastatin which was used by more than 45 million people worldwide and made \$12 billion in 2005.¹⁹ Pyrrole does not occur naturally, though the pyrrole structural motif is present in a number of enzyme cofactors and natural products and is notably found in porphyrin rings in key compounds such as heme, vitamin B12, and chlorophyll.²⁰

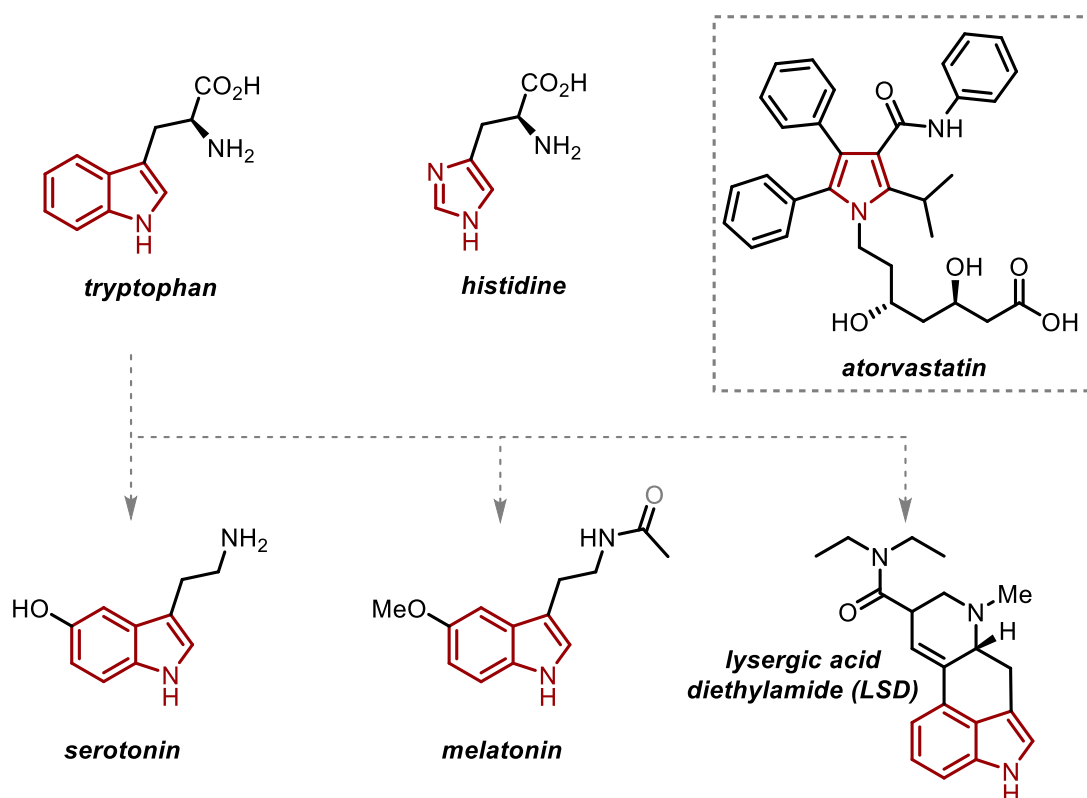


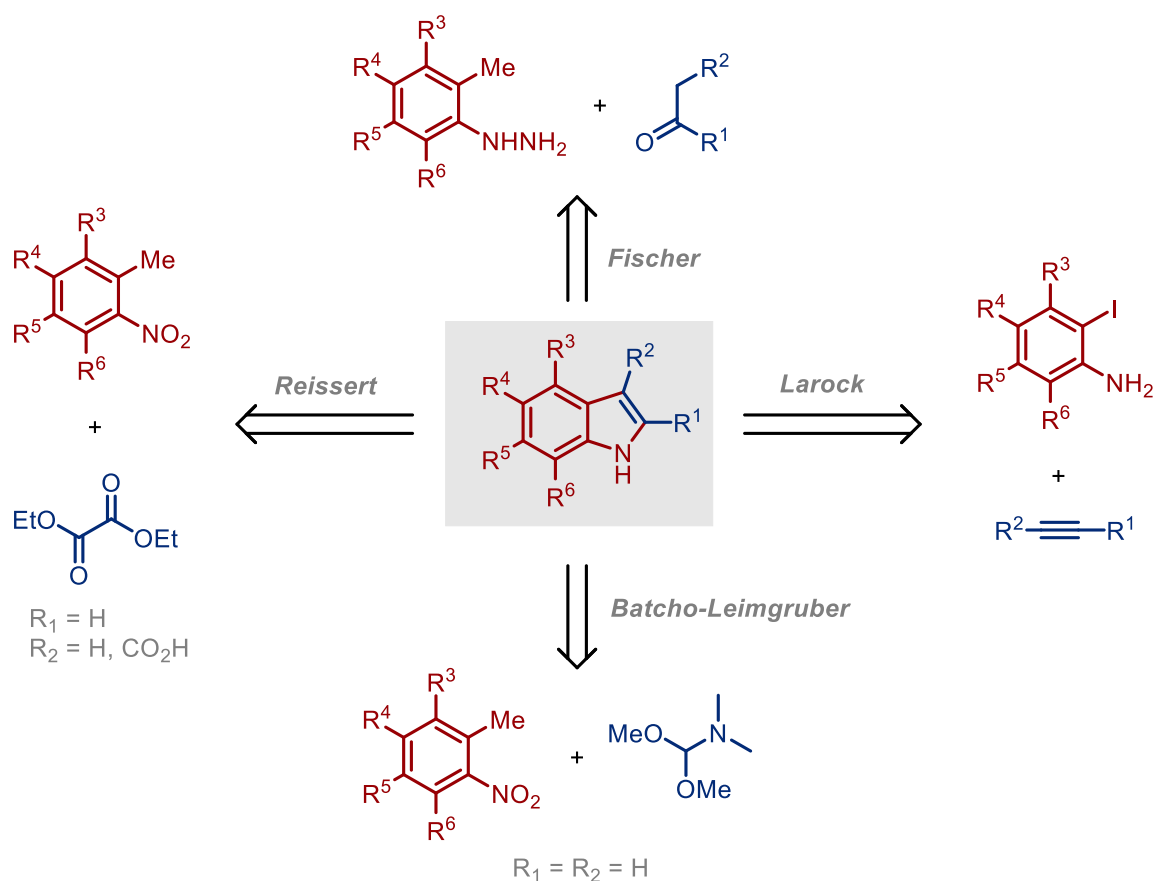
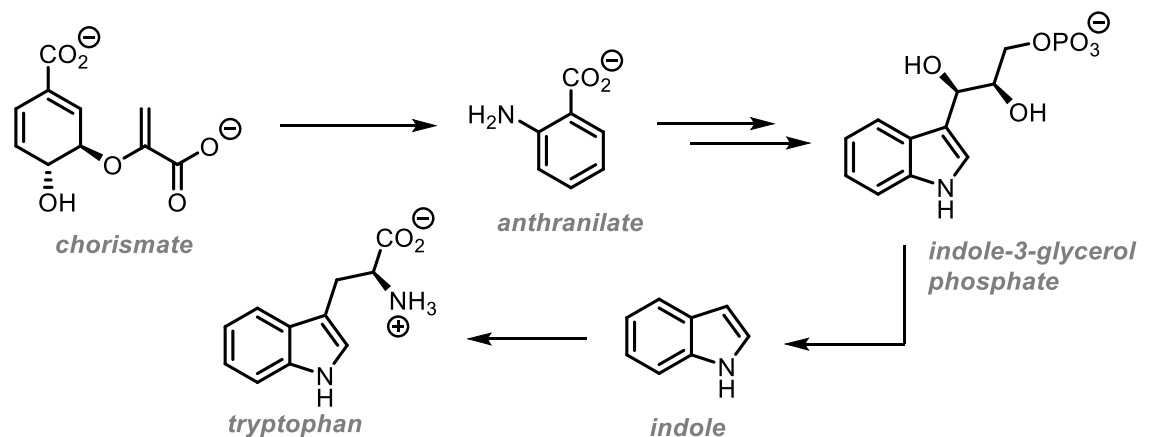
Figure 1.3. Natural sources of indole, highlighting those derived from tryptophan, and the pharmaceutical atorvastatin bearing a central pyrrole core.

1.1.5 Synthesis of five-membered aromatic heterocycles

There are myriad synthetic disconnections available to synthesise indoles (Scheme 1.2).²¹ In nature, indole - and by extension tryptophan - is biosynthesised from chorismate through its conversion to anthranilate.²² Ring cyclisation, followed by decarboxylation affords indole-3-glycerol phosphate, which is converted to indole. Finally, enzymatic reaction with serine then affords tryptophan.

One of the most well-known indole syntheses is the Fischer indole synthesis.²³ This method involves the acid-catalysed coupling of an aryl hydrazine with a ketone. After hydrazone formation, a key [3,3]-sigmatropic rearrangement takes place which forms the desired indole after condensation with loss of ammonia. The reaction tolerates a wide range of substitution patterns though regioselectivity issues arise when employing unsymmetric ketones. A common method for indole synthesis is the functionalisation and subsequent reduction of nitroarenes.²⁴

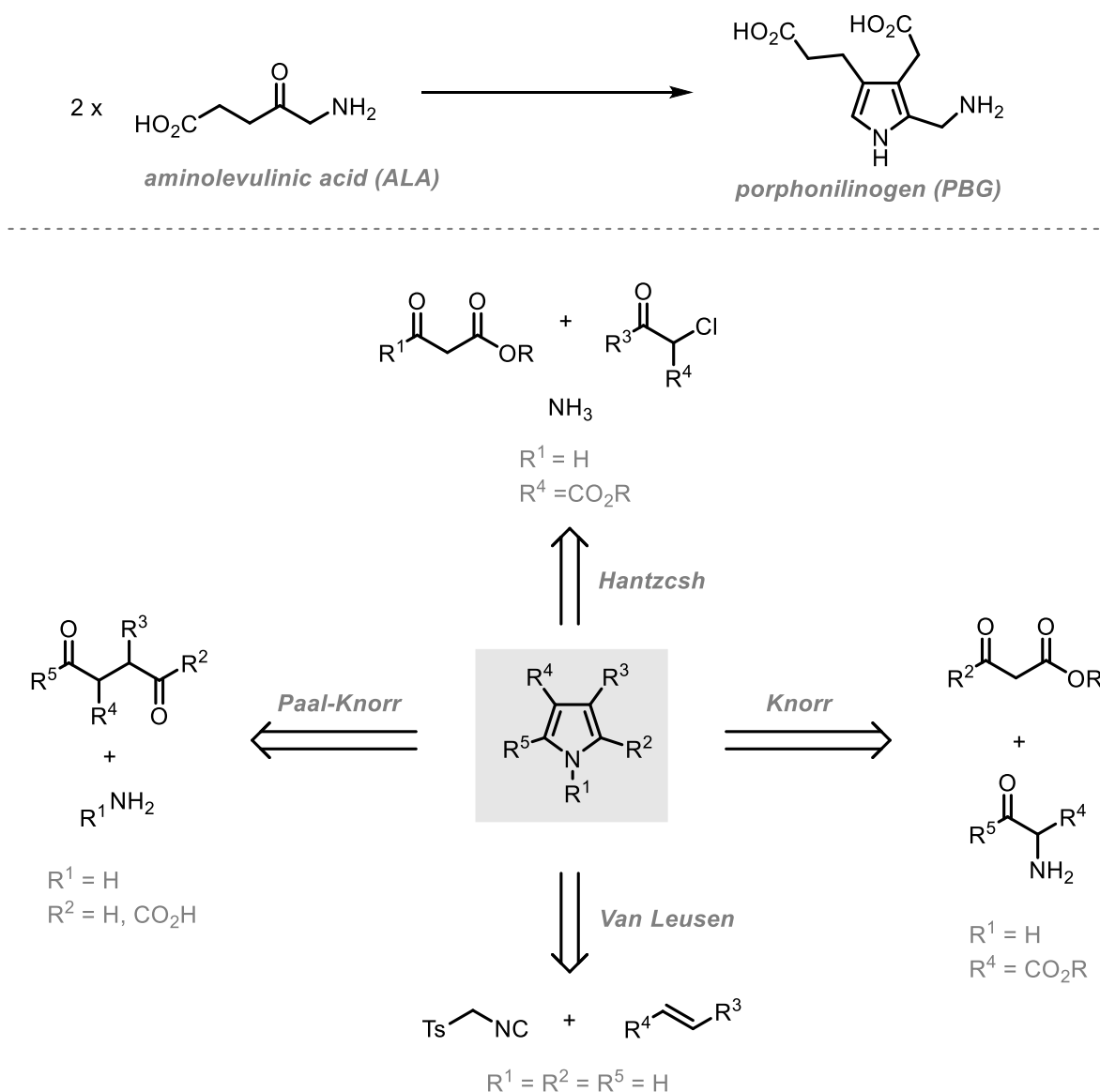
These methods often exploit the relative acidity of *ortho*-methyl nitroarenes to alkylate *ortho* to the nitro group. Cyclisation and aromatisation are then triggered by reduction to the aniline, with the cyclisation often assisted by acid. Methods utilising nitroarenes include the Batcho-Leimgruber²⁵ and Reissert syntheses.²⁶



Scheme 1.2. A: Biosynthesis of indole. B: Retrosynthetic disconnections for the synthesis of indoles.

Another commonly-used indole synthesis is the Larock synthesis.²⁷ This palladium-catalysed method couples an *ortho*-iodoaniline and an alkyne in the presence of a base. A number of bases can be used, and the reaction shows high functional group tolerance. Like

the Fischer synthesis, issues with regioselectivity can arise although the sterically bulkier alkyne group is placed at C2. To reach 2-unsubstituted indoles (that would be unattainable with the terminal alkyne) bulky silyl groups are incorporated into the alkyne component to force the synthesis of the 2-silyl indole.²⁸ The unprotected indole can then be obtained by deprotection with a fluoride source such as TBAF (tetrabutylammonium fluoride).



Scheme 1.3. A: Biosynthesis of PBG. B: Retrosynthetic disconnections in the synthesis of pyrroles.

Like indoles, there are a variety of methods to synthesise pyrroles with various substitution patterns (Scheme 1.3). As pyrrole does not occur naturally, no biosynthesis exists. However, there exists a biosynthesis for pyrrole-containing porphobilinogen (PBG), the building block of porphyrins.²⁹ The key building block is aminolevulinic acid (ALA), synthesised from glycine and succinate. Enzymatic condensation of two ALA units *via* a Knorr-type mechanism (*vide infra*) forms PBG.

Poly-substituted pyrroles can be accessed by methods such as the Hantzsch and Knorr syntheses. The Hantzsch reaction is a three-component reaction of a β -ketoester, an α -haloketone, and ammonia. Condensation of ammonia and the ketoester leads to the formation of an enamine. Nucleophilic attack of the enamine into the carbonyl of the haloketone forms, after proton transfer, an α,β -unsaturated imine which displaces the chloride, leading to ring formation. Base-promoted aromatisation leads to the pyrrole product. The Knorr synthesis is mechanistically similar, though the reaction employs an α -aminoketone rather than the haloketone and ammonia. Other pyrrole syntheses include the Van Leusen reaction of TosMIC (*para*-toluenesulfonylmethyl isocyanide) and a Michael acceptor, and the Paal-Knorr synthesis from 1,4-diketones and a primary amine.^{30–32}

1.1.6 Six-membered aromatic heterocycles

The second class of molecules central to this thesis are six-membered aromatic heterocycles, particularly those containing nitrogen. Two common heterocycles of this class are pyridine and quinoline (Figure 1.4).



Figure 1.4. Two six-membered aromatic heterocycles: pyridine and quinoline.

Pyridine, from the Greek *pyr* ($\pi\upsilon\rho$, fire) and the suffix *-idine*, denoting a nitrogen-containing cyclic compound, was first isolated by Anderson in 1851 by the heating of animal bones.³³ Its structure was first postulated by Korner and Dewar and later confirmed by its reduction to piperidine.^{34,35} The first synthesis of pyridine by Ramsay in 1876 involved the pyrolysis of acetylene and hydrogen cyanide.³⁶ Pyridine is isoelectronic with benzene, with replacement of one carbon atom with nitrogen. As five carbon atoms each provide one π -electron, the nitrogen atom needs to supply only one electron to achieve aromaticity, as opposed to two in pyrrole and indole. This results in the nitrogen lone pair being available for reactivity.

Like five-membered heterocycles, the nitrogen atom induces a dipole in the σ -framework of the molecule due to the higher electronegativity of nitrogen compared to carbon. However, unlike five-membered heterocycles, the inductive polarisation stabilises mesomeric resonance in which the nitrogen atom is negatively charged. This ultimately results in the inductive and

mesomeric polarisation acting in the same direction, inducing partial positive charges on carbon. Due to this, pyridine is described as electron-poor or π -deficient.

Quinoline was first isolated by Runge in 1834 from coal tar and originally named *leukol* (white oil in Greek).¹⁰ It was subsequently isolated by Gerhardt from reaction of cinchona alkaloids such as quinine with potassium hydroxide, which he named *chinoisin* from which the name quinoline is derived.³⁷ As the bicyclic counterpart of pyridine, quinoline is isoelectronic with naphthalene. The chemistry of quinoline is generally analogous to that of pyridine, with the most obvious exception being substitution.

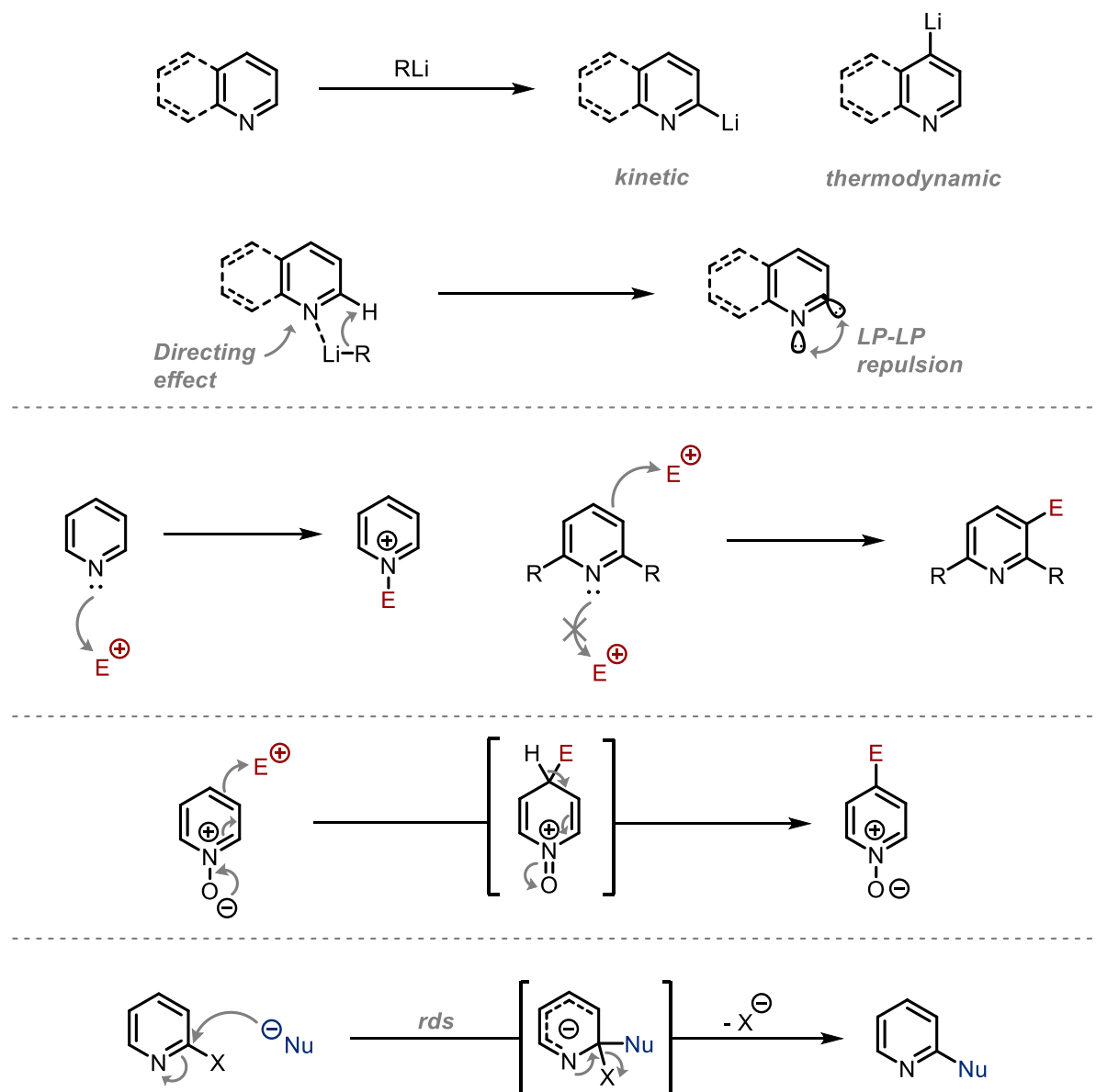
1.1.7 Chemical properties of six-membered heterocycles

As the nitrogen lone pair is not incorporated into the aromatic sextet, it is available for reaction with electrophiles. As a consequence, pyridine and quinoline are weak bases ($pK_{\text{aH}} = 5.2$ and 4.9 respectively).³⁸ Pyridines and quinolines are also very weakly acidic and can be deprotonated only upon exposure to a strong non-nucleophilic base (Scheme 1.4A). The regioselectivity of deprotonation is dependent on reaction conditions.³⁹ Deprotonation at C2 is kinetically favoured due to the directing effect of the nitrogen lone pair on the metal cation (or partial positive charge in a polarised M-C bond). However, deprotonation at C4 is thermodynamically favoured as the resulting anion is more stable. When deprotonation at C2 occurs, the resulting interaction between the filled orbital and the nitrogen lone pair is destabilising, whereas the opposed dipoles are distant enough to avoid this destabilisation.

While the electrophilic aromatic substitution of five-membered heterocycles is facile, the opposite is true for their six-membered congeners. The presence of a Lewis-basic nitrogen atom complicates reaction with electrophiles at carbon, as reaction at nitrogen will occur much faster than at carbon (Scheme 1.4B). Electrophilic substitution can be facilitated by the introduction of electron-donating activating groups to the ring system, especially ones that sterically hinder the nitrogen atom. Additionally, substitution at carbon can be achieved by deactivating the nitrogen atom to attack by reducing its nucleophilicity, such as in the case of 2,6-dibromopyridine where the bromine atoms both electronically deactivate and sterically hinder the nitrogen centre. In cases where electrophilic substitution at carbon is possible, substitution takes place at C3. If C3 is already substituted, attack takes place at either C2 or C6 if these positions are unsubstituted.⁴

Electrophilic substitution can be further facilitated by oxidation to the *N*-oxide (Scheme 1.4C). The activating effect of the oxygen atom results in both higher nucleophilicity and

electrophilicity. This increase in reactivity is accompanied by changes in regioselectivity, as pyridine *N*-oxides undergo substitution at C2 and C4. Strongly acidic conditions should be avoided due to potential protonation of oxygen, quenching the activating effects. Although these properties are also present for quinolines, electrophilic substitution readily takes place, albeit on the benzo-fused ring. In an acidic environment, electrophilic substitution passes through the *N*-protonated intermediate, resulting in much lower rates of substitution (10^{10} times slower than isoelectronic naphthalene).⁴⁰



Scheme 1.4. A: Lithiation of six-membered heterocycles. B: Reaction with electrophiles. C: Enhancement of nucleophilicity with *N*-oxides (attack at 4-position shown). D: $\text{S}_{\text{N}}\text{Ar}$ chemistry.

The electron-deficient, imine-like properties of pyridines also facilitate nucleophilic aromatic substitution (Scheme 1.4D). In this case a sufficient nucleofuge, typically a halide, is required. The halide atom also facilitates addition by inductive withdrawal of electrons making the carbon centre more electrophilic. Addition of a nucleophile results in a Meisenheimer intermediate analogous to the tetrahedral intermediate in carbonyl additions. Collapse of this intermediate with expulsion of the halide reforms aromaticity. Notably, the reactivity of 2- and 4-halopyridines shows an inverse trend to substitution mechanisms such as S_N2 reactivity with respect to nucleofugality. In S_N2 reactions bromides and iodides are more reactive than earlier halogens, whereas generally the inverse is true for S_NAr . The rationale for this difference falls in the rate-determining step for S_NAr .⁴¹ Generally, the initial attack of the nucleophile and formation of the Meisenheimer intermediate is rate-determining and therefore more inductively withdrawing halides such as fluoride and chloride both enhance the electrophilicity of carbon, as well as stabilise the intermediate.⁴² In some cases however, the rate-determining step is collapse of the intermediate or the reaction follows a concerted mechanism.⁴³

1.1.8 Prevalence of six-membered aromatic heterocycles

Pyridines are common structural motifs in both natural products and pharmaceuticals. In nature, a pyridine core is present in a number of important alkaloids and biological co-factors such as: nicotine, NAD (nicotinamide adenine dinucleotide), a key co-enzyme in metabolism, and vitamin B3 (niacin). In pharmaceuticals, a 2014 study found that pyridines are the second most common heterocycle and the most common aromatic heterocycle in FDA-approved drugs including the pheniramine class of anti-histamines, cerivastatin, and the anti-inflammatory roflumilast.¹ Quinolines are less prevalent in pharmaceuticals though many antimalarial drugs such as chloroquine, which appears on the WHO's list of essential medicines, are commonly used worldwide.¹ The quinolone structural motif is more common and is found in drugs such as ofloxacin and ciprofloxacin.⁴⁴ The most well-known examples of naturally-derived quinolines is the cinchona family of alkaloids, from which quinoline gets its name.⁴⁵ These include quinine, the historical treatment for malaria, and cinchonidine, which sees use as a ligand in asymmetric synthesis.⁴⁶

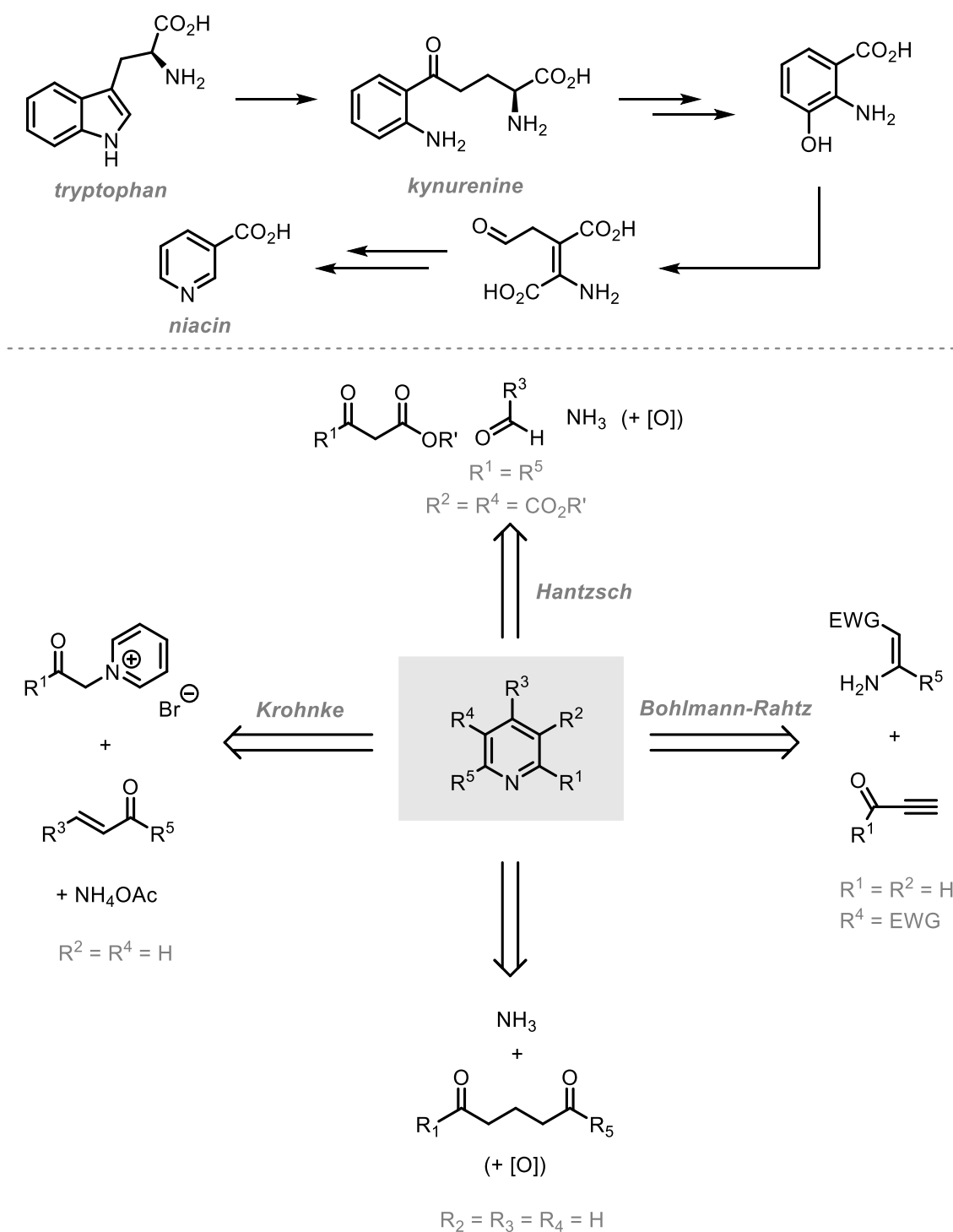
1.1.9 Synthesis of six-membered aromatic heterocycles

Pyridine itself does not occur naturally, but both mammals and bacteria synthesise vitamin B3 (niacin) though the biosynthetic routes differ. Mammals synthesise niacin from tryptophan,

firstly by oxidative cleavage of the indole olefin and hydrolysis of the resulting formamide to afford kynurenine (Scheme 1.5A). Similar cleavage of the aniline arene and condensation affords the pyridine ring which is decarboxylated to give niacin.⁴⁷ By contrast, bacteria and some plants synthesise niacin *via* condensation of glyceraldehyde 3-phosphate and aspartic acid.⁴⁸

The syntheses of pyridines are dominated by condensation and annulation chemistry (Scheme 1.5B). The Hantzsch synthesis of pyridines involves the four-component coupling of two 1,3-ketoester units, an aldehyde, and a source of ammonia to afford a dihydropyridine.⁴⁹ This stable intermediate must then be oxidised to afford the aromatic pyridine, although these compounds are useful reductants in organic synthesis.^{50,51} Condensation of ammonia and the ketoester affords an enamine. A second key intermediate is formed by the Knoevenagel condensation of another ketoester unit and the aldehyde to form an α,β -unsaturated ketoester. Attack of the enamine into this Michael acceptor provides the acyclic core and after tautomerism, condensation of the amine and the ketone followed by loss of deprotonation affords the stable dihydropyridine.

The Bohlmann-Rahtz pyridine synthesis is related mechanistically to the Hantzsch synthesis as an enamine derived from a ketoester is employed, although the use of an ynone removes the need for aromatising oxidation.⁵² Michael addition of the enamine into the ynone affords an isolable dienone. A key drawback of the protocol is the geometry of the alkenes that results from Michael addition (*2Z-4E*) restricts the required attack of the amine into the carbonyl. Therefore, heating is required to isomerise both alkenes to the *2E-4Z*-dienone that is now geometrically predisposed to the desired nucleophilic attack. Condensation with loss of water produces the pyridine product. In response to this limitation, one-pot variations have been developed.⁵³⁻⁵⁶



Scheme 1.5. A: Biosynthesis of niacin. B: Retrosynthetic disconnections in the synthesis of pyridines.

Michael addition also facilitates pyridine synthesis in the Krohnke annulation.^{57,58} Deprotonation of an α -pyridinium methyl ketone and subsequent attack into an α,β -unsaturated ketone leads to the formation of a 1,5-dicarbonyl. Condensation of ammonia and enamine formation leads to the attack of the amine into the second carbonyl, forming the six-membered ring. Base-mediated elimination of the pyridine nucleofuge forms the dihydropyridine, and loss of water leads to formation of the aromatic system. Similarly,

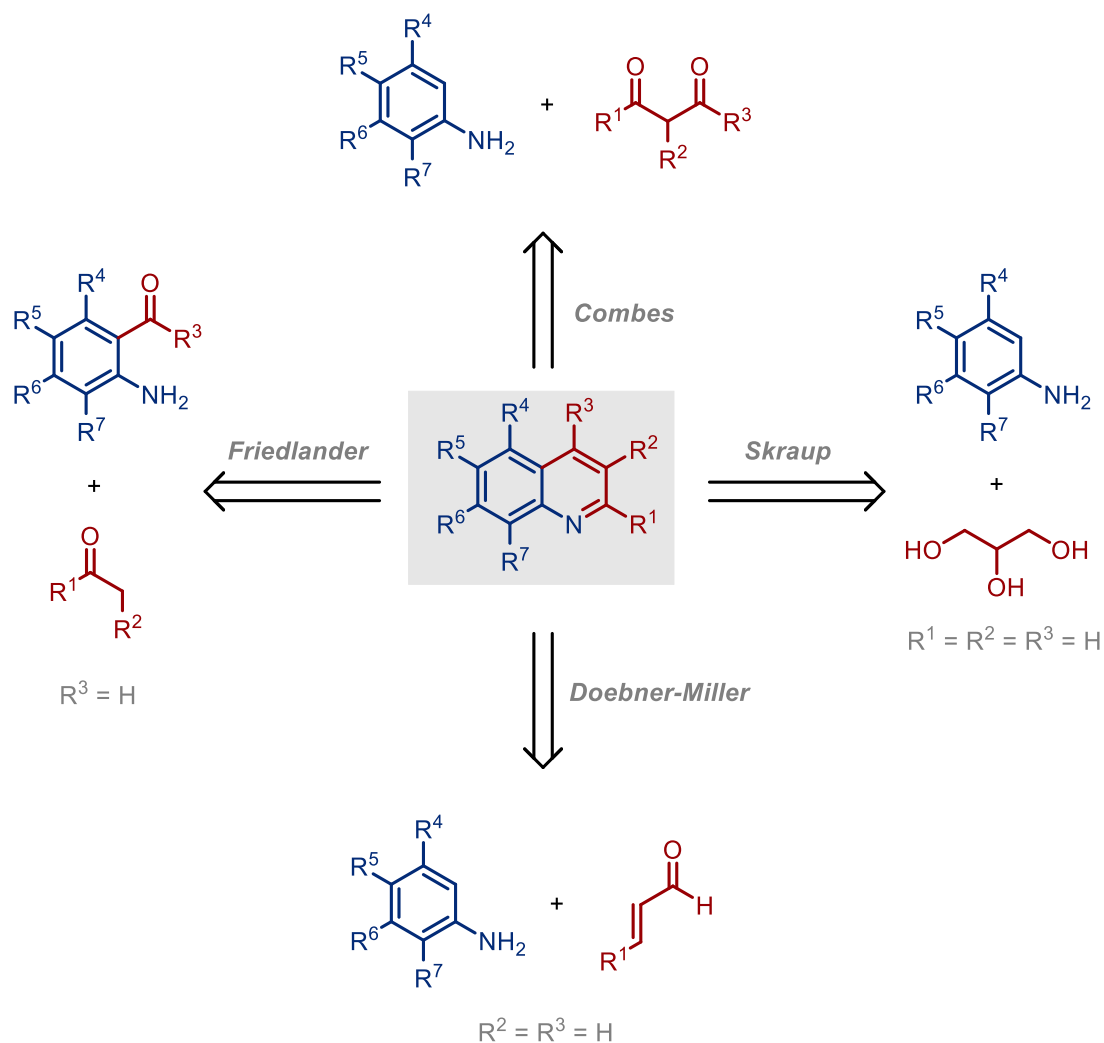
pyridine synthesis can be achieved from the corresponding 1,5-dicarbonyl and an ammonia source, although due to the lack of a sufficient nucleofuge, an exogenous oxidant is required to achieve aromaticity.⁵⁹

Classical syntheses of quinolines are often limited to the additions of anilines into carbonyl compounds with various methods utilising different three-carbon units in the annulation (Scheme 1.6). The Combes synthesis employs a 1,3-diketone as the coupling reagent with an aniline.⁶⁰ Condensation of the aniline with the diketone under acid catalysis affords an imine which tautomerises to the enamine. The electron-rich arene then undergoes S_EAr with the second carbonyl unit, forming the six-membered ring. Rearomatisation of the benzo-fused ring and acid-mediated loss of water affords the quinoline. One major requirement for the aniline partner is an unsubstituted *ortho* position due to the required S_EAr step and subsequent deprotonation.

The Skraup synthesis proceeds *via* a similar mechanism though glycerol is utilised as the three-carbon unit.^{61,62} Under the strongly acidic conditions, glycerol undergoes elimination of two hydroxy groups to afford acrolein *in situ*. Michael addition of the aniline into the acrolein leads to an intermediate analogous to the Combes synthesis. Friedel-Crafts and dehydration then affords the dihydroquinoline. The quinoline is then achieved by oxidation, typically by reaction with the nitrobenzene solvent.⁶³

The Doebner-Miller modification is related to the Skraup synthesis, utilising an enal as the Michael acceptor.⁶⁴ Mechanistic investigations by Denmark and co-workers determined that the reaction proceeds *via* condensation of one aniline unit with the enal and subsequent fragmentation. Addition of another aniline unit to the Michael acceptor results in cyclisation after S_EAr. Elimination of the pendant aniline unit and rearomatisation leads to the final quinoline.⁶⁵

The Friedlander synthesis also allows for either the acid- or base-promoted formation of quinolines from 2-aminobenzaldehydes and an enolisable ketone.⁶⁶ There are two different proposals for the reaction mechanism.⁶⁷ In one case, condensation of the aniline nitrogen and the second carbonyl results in imine formation. An *intramolecular* aldol reaction between the resulting enamine into the *ortho*-aldehyde leads to ring formation, and loss of water forms the aromatic system and affords the quinoline product. The second postulated mechanism involves an *intermolecular* aldol prior to imine formation.



Scheme 1.6. Retrosynthetic disconnections in the synthesis of quinolines.

1.1.10 Comparison of five- and six-membered aromatic heterocycles

Taking into account the previous sections, it is clear to see the difference in chemical properties inherent to five- and six-membered aromatic heterocycles. The electron-rich nature of indole and pyrrole facilitates electrophilic aromatic substitution whereas the electron-deficient nature of pyridine and quinoline hinders S_EAr chemistry. Additionally, the inverse is true for S_NAr chemistry. Acid-base chemistry is also markedly different for both classes of compound.

The differences in properties are not limited to chemistry. The physicochemical properties of the aromatic heterocycles also vary depending on ring size. One obvious difference in properties is derived from acid-base chemistry and involves the interactions between the rings and amino acid residues in enzyme active sites. Six-membered rings are capable of hydrogen-bonding with polar protic residues and forming salt bridges. Five-membered rings - absent of

imine-type nitrogens - are less prone to hydrogen bonding although the electron-rich nature presents the opportunity for considerable π -stacking interactions with aromatic residues.

Two commonly utilised parameters in determining the properties of drug candidates are the dimensionless partition coefficient, $\log P$ (or computed partition coefficient $\text{clog}P$) and polar surface area, PSA (measured in \AA^2).⁶⁸ Partition coefficient describes the lipophilicity of the molecule in question and is the logarithm of the ratio of concentrations of the substrate in a biphasic organic (typically) 1-octanol/water mixture (equation 1.1).⁶⁹ Higher $\log P$ values describe a more lipophilic substrate, capable of penetrating lipid bilayers and the blood-brain barrier whereas a lower value represents a more water soluble substrate capable of dissolving in aqueous media such as blood. Balancing solubility in this manner is key to drug efficacy. Computed partition coefficients ($\text{clog}P$) are typically employed rather than experimentally-derived values. Polar surface area (PSA) is defined as the sum of the surface area of all polar atoms in a molecule. Similar to $\log P$, polar surface area is used to determine the permeability of drug candidates through cell membranes. Molecules with polar surface areas greater than 140 \AA^2 are typically poor at permeating membranes.⁷⁰

$$\log P = \log_{10} \frac{[S]_{1\text{-octanol}}}{[S]_{\text{water}}} \quad (1.1)$$

Table 1.1 highlights the variation on chemical and physicochemical properties between five-membered (indole) and six-membered heterocycles (quinoline). A clear difference can be observed for both partition coefficient (exacerbated by its logarithmic nature) and polar surface area. Therefore, drug molecules containing either of these congeners would likely have significantly different *in vivo* characteristics. Chemical methodologies that can produce either heteroaromatic core, or even interconvert between them, are therefore of great synthetic interest.

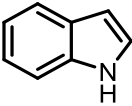
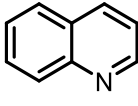
Property		
$\text{p}K_a$	16.2 ⁴	<i>ca.</i> 35
$\text{p}K_{aH}$	-3.5 ¹³	4.93 ³⁸
$\text{clog}P$	2.132	2.029
PSA / \AA^2	12.03	12.36

Table 1.1. Comparison of chemical and physicochemical properties of indole and quinoline. $\text{clog}P$ and PSA values calculated in ChemOffice ChemDraw Professional 20.0.

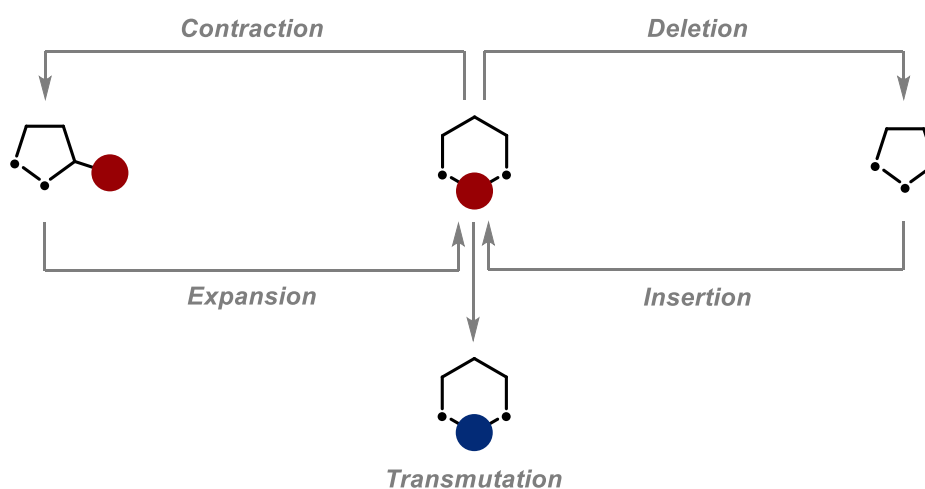
1.2 Skeletal Editing

Due to the different chemical and physical properties possessed by five- and six-membered heterocycles, interconversion between them would be a greatly appealing synthetic transformation for medicinal chemists. One of the foremost aims of synthetic organic chemistry is the ability to achieve the site-selective modification of complex and highly functionalised molecules. This imposing objective has piqued the interest of synthetic chemists due to the potential to develop methodologies that are both general to a wide range of substrates and are synthetically and operationally simple. This drive toward the development of these protocols is particularly resonant in the field of medicinal chemistry, in which the ability to selectively functionalise complex molecules directly affects the speed and efficiency at which chemical libraries can be expanded and therefore affects the rate at which new drug candidates can be discovered.

It is only in recent years that the term ‘molecular editing’ has entered the nomenclature of organic synthesis. This term, also referred to initially as ‘site-directed mutagenesis’⁷¹ or (hetero)arene interconversion^{72,73}, has been defined as ‘the insertion, deletion, or exchange of atoms in highly functionalised compounds at will and in a highly specific fashion’.⁷⁴ Due to this broad definition, its application in the literature is understandably vague and predominantly involves the modification of accessible functionalities on the periphery of molecules, such as C-H activation chemistry. While there are clear advantages to these methods, the exploitation of accessible functionalities leaves core molecular scaffolds such as ring systems untouched.

In answer to this, the term ‘skeletal editing’ was outlined by Sarpong, Levin, and co-workers as the precise modification of molecular skeletons, mainly ring systems.⁷⁴ Three classes of molecular edit were outlined: (1) Insertion, (2) deletion, and (3) transmutation (Scheme 1.7). Insertion refers to the introduction of a new atom (carbon or heteroatom) into an existing ring system, increasing ring size. Deletion is by contrast the removal of an atom from a ring system, leading to a net decrease in ring size. Levin’s review further sub-divided reactions increasing ring size to insertions and expansions.⁷⁴ The nuance derives from the origin of the inserted atom. In insertions the atom introduced into the ring system is provided by an exogenous reagent whereas expansion implies the atom is already tethered to the ring in question. The same is true for contraction and deletion. In this case, the deleted atom is removed completely, whereas in contractions the atom remains part of the molecule, but not as part of the ring

system. For the sake of simplicity, insertion and expansion, as well as deletion and contraction, will be used interchangeably. The final class, atom transmutation, alters the atomic composition of the ring, while maintaining the same ring size.



Scheme 1.7. Definitions of transformations within the field of skeletal editing.

1.2.1 Carbon Atom Insertion

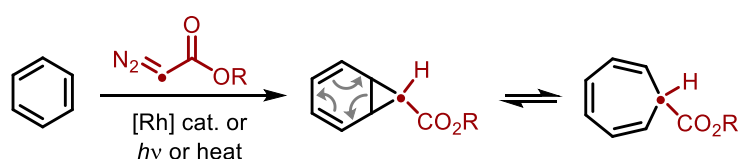
Despite the intrinsic synthetic challenge present in the insertion of single atoms into rings, atom insertion methodologies have been known for over a century although methodologies are typically limited to carbonyl chemistry in aliphatic systems. Examples of such reactions include the Baeyer-Villiger and Beckmann rearrangements.^{75,76} However, the inherent stability of aromatic systems means the insertion of atoms into aromatic frameworks is far less common. Despite this, there are methodologies that have achieved either carbon or heteroatom insertion.

Arguably the most well-known carbon atom insertion method into aromatic systems is the Buchner ring expansion (Scheme 1.8A).⁷⁷ First reported in 1885, this method proceeds by the reaction of an arene with a carbene or carbenoid generated from a diazoester to form a bicyclo[4.1.0]heptadiene. 6π -Electrocyclic ring opening leads to a one-carbon ring expansion to the corresponding non-aromatic cycloheptatriene. Generation of the required carbene can be achieved utilising heat, light, or a transition metal catalyst. Despite the simplicity and appeal of this reaction, it suffers from poor regioselectivity when employing substituted arenes. More recent work has remedied this with improvements to regioselectivity^{78,79} as well as reaction scope.^{80–82} An enantioselective variant has also been demonstrated in flow.⁸³

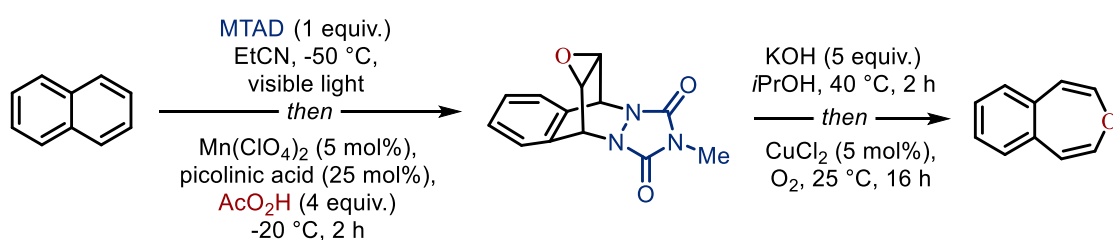
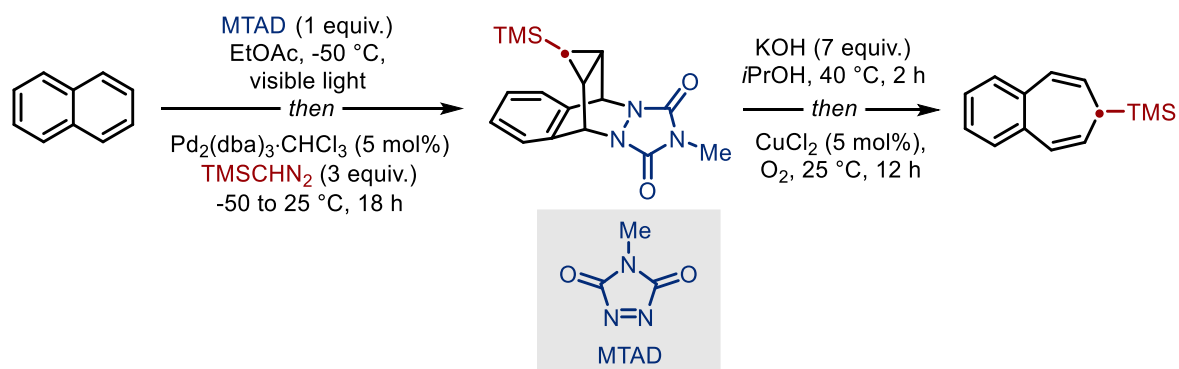
Carbon insertions into arenes can also be achieved *via* other means. Sarlah and co-workers demonstrated the insertion of a carbon atom into polyarenes achieved by a

dearomative-cycloaddition/cyclopropanation strategy (Scheme 1.8B).⁸⁴ Light-mediated [4+2] cycloaddition of arenes with MTAD (4-methyl-1,2,4-triazoline-3,5-dione) produces a non-aromatic adduct bearing a cyclic olefin. This olefin could then be cyclopropanated by a Pd-catalysed method utilising trimethylsilyl diazomethane. Retro-[4+2] cycloaddition is achieved by the partial hydrolysis of the urazole, followed by copper-catalysed aerobic oxidation and subsequent extrusion of dinitrogen. Similar to the Buchner ring expansion, a 6π -electrocyclic ring opening then afforded the product. This protocol has also been similarly applied to the synthesis of benzoxepines by Mn-catalysed epoxidation of the MTAD adduct.⁸⁵

A. Buchner, 1885



B. Sarlah, 2022

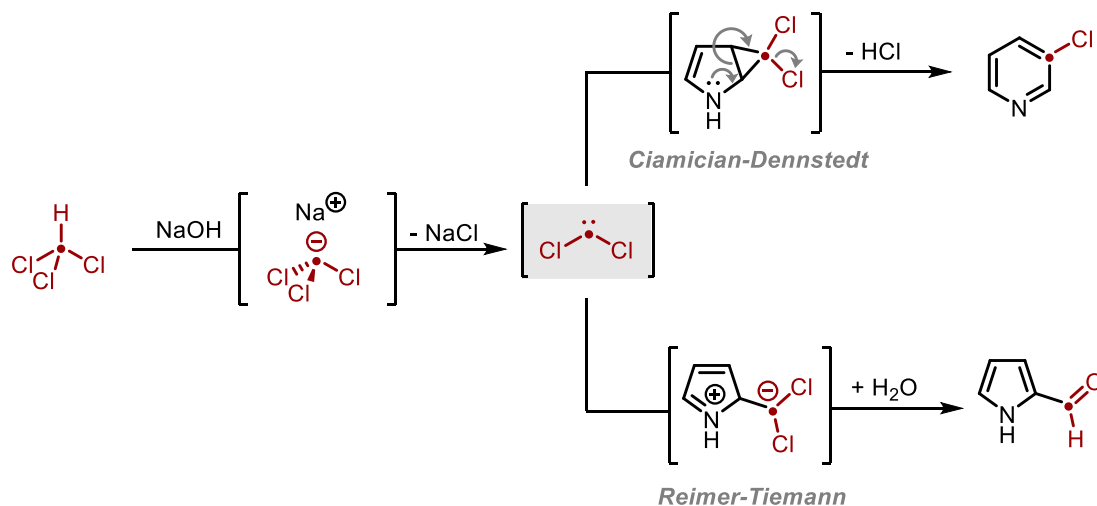


Scheme 1.8. A: Buchner ring expansion of arenes with diazoesters. B: Carbon (and oxygen) atom insertion *via* sequential dearomatisation and cyclopropanation.

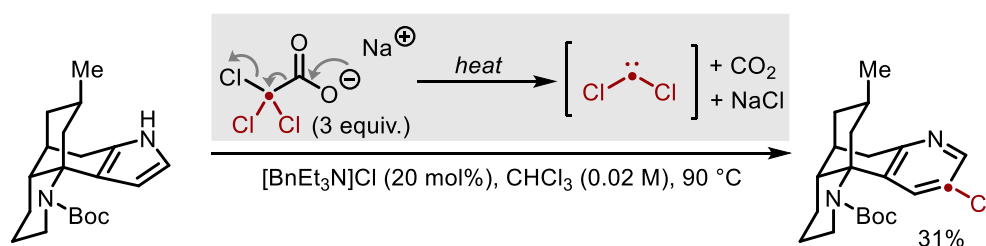
While carbon atom insertion into benzenoids has obvious synthetic appeal, the impact of carbon atom insertion protocols becomes most clear when applied to heteroaromatic molecules. Inserting a carbon atom into a heterocycle can have drastic effects on the chemistry of that ring. For example, insertion of a carbon atom into indole, a weakly acidic compound predisposed to electrophilic aromatic substitution (S_EAr), could transform it into a quinoline,

a basic compound capable of undergoing nucleophilic aromatic substitution (S_NAr). This polarity shift opens new avenues in the development of new drug molecules and how they interact with residues in active sites (see section 1.1 for further discussion).

A. Ciamician-Dennstedt, 1881



B. Dai, 2021

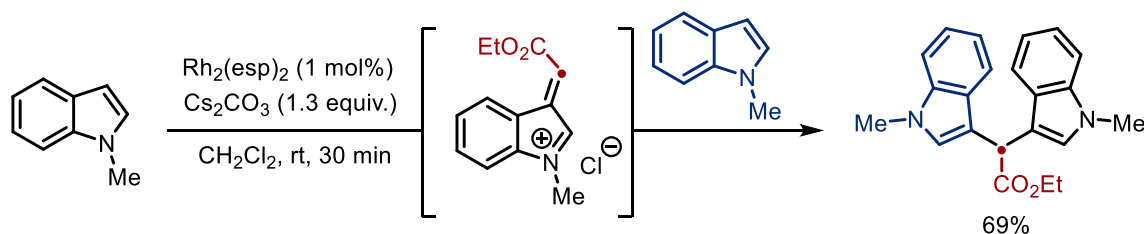
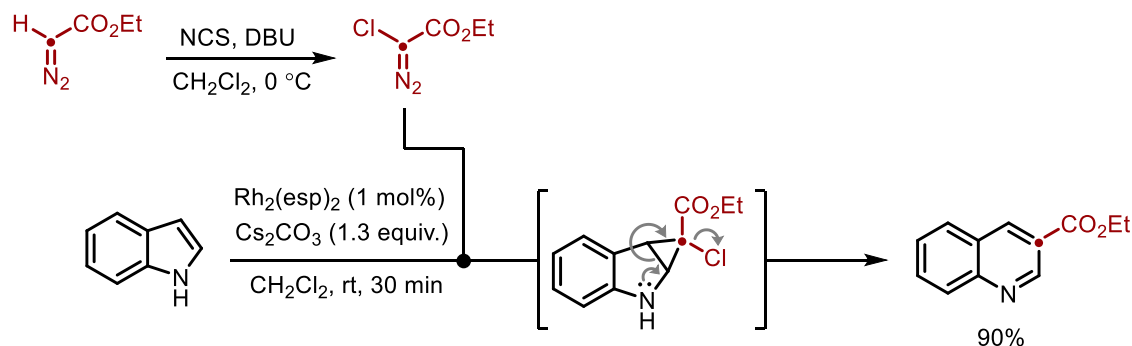


Scheme 1.9. Ring expansion of pyrroles with dichlorocarbene and the competing Reimer-Tiemann formylation. B: Application of Ciamician-Dennstedt reaction in total synthesis.

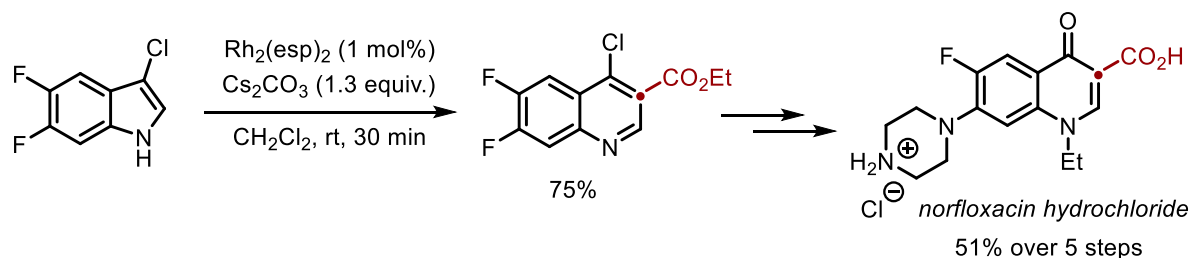
The classical method to achieve carbon atom insertion into aromatic heterocycles such as pyrrole and indole is the Ciamician-Dennstedt reaction (Scheme 1.9A).⁸⁶ The reaction proceeds by generation of a dihalocarbene from the corresponding haloform in basic media. This carbene is capable of cyclopropanating the enamine-like double bond present in both indole and pyrrole. Subsequent fragmentation with extrusion of chloride as a nucleofuge results in rearomatisation and product formation. Despite its synthetic appeal, the reaction is plagued by poor yields due to the competing Reimer-Tiemann formylation, affording yields up to *ca.* 40%.⁸⁷ Other carbene precursors have been employed in modifications of the transformation to counteract the poor functional group compatibility of the highly basic conditions required for carbene formation of haloforms. The thermally-activated carbene precursor sodium trichloroacetate was utilised by Dai and co-workers in the total synthesis of lycopodium alkaloids in a key step transforming the pyrrole core to the corresponding chloropyridine,

which was achieved in a 31% yield Scheme 1.9B).⁸⁸ This chloride substituent could then be further modified by reduction or by Pd-catalysed cross-coupling.

A. Bonge-Hansen, 2015



B. Bonge-Hansen, 2019



Scheme 1.10. A: Rh-catalysed carbon atom insertion with halodiazoacetates with undesired dimerisation upon N-alkylation. B: Ring expansion of chloroindoles to quinolones in the synthesis of norfloxacin hydrochloride.

While dihalocarbenes are competent carbenes for the ring expansion of pyrroles and indoles, only one halide is required as a nucleofuge for the fragmentation step. This would allow for the introduction of other functional groups utilising the same reaction mechanism. In 2015, Bonge-Hansen and co-workers reported the ring expansion of indoles utilising α -halodiazoacetates as carbene precursors (Scheme 1.10A).⁸⁹ In the presence of a Rh(II) catalyst, the corresponding Rh-carbenoid is generated which can facilitate the Ciamician-Dennstedt type reaction in the presence of a base. The halodiazoacetates are readily available from the corresponding diazoester and an electrophilic halide source such as *N*-halosuccinimides. However, these substrates are unstable at ambient temperatures and are stored in solution. Additionally, an electron-withdrawing ester group is required to achieve this modest level of

stability, which severely limits the scope of substituent that can be introduced to the 3-position of the quinoline product. Despite these limitations, the reaction proved robust and produced high yields across a broad scope of indole starting materials.

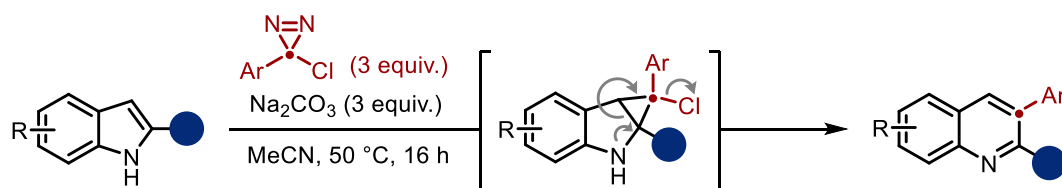
Attempts to protect the indole nitrogen led to either no reaction, in the case of Boc protection, or adverse reactivity when a methyl group was employed. In this latter case, competitive C3-alkenylation was observed which generated a competent Michael acceptor. This intermediate could then undergo nucleophilic attack from the methyl indole starting material to form a dimeric C3-alkylated product. This methodology was later utilised by the same group in the ring expansion of 3-chloroindoles (Scheme 1.10B).⁹⁰ The resulting 4-chloroquinoline-3-carboxylates could then be hydrolysed to the corresponding 4-quinolone. This strategy was utilised in the synthesis of norfloxacin from a 3-chloroindole.

A powerful, recent addition to the arsenal ofazole ring expansions was reported by Levin and co-workers in 2021. This methodology utilises chlorodiazirines as thermally-activated carbene precursors. These diazirines are more stable than their diazo isomers and therefore aryl rings could be incorporated as substituents. While mentioned briefly here, this work will be discussed in detail within Chapter 3 to best highlight the complementarity between the methodology described in that chapter and that of Levin's.

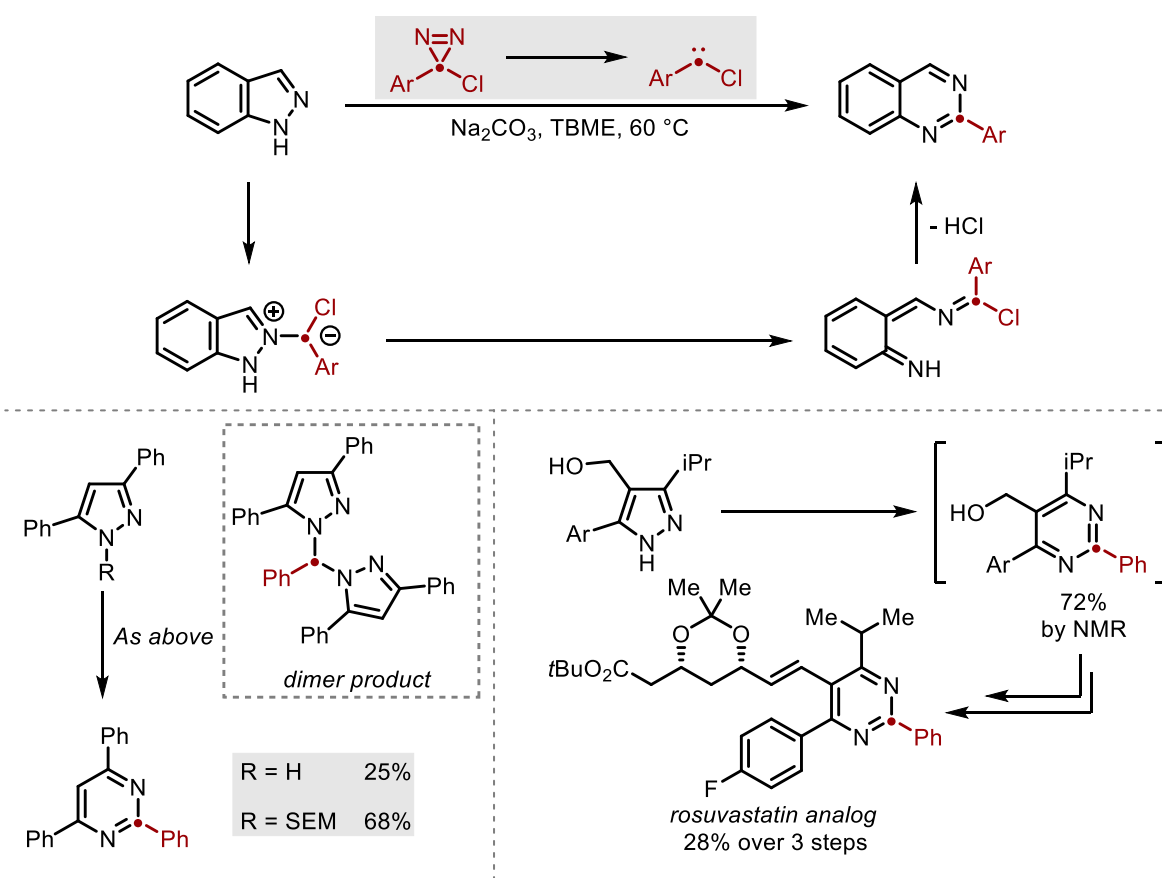
In addition to Ciamician-Dennstedt type reactions, carbenes have been utilised in the ring expansions of other aromatic heterocycles. In 2022, Levin and co-workers reported the ring expansion of pyrazoles and indazoles to pyrimidines and quinazolines respectively by cleavage of the N-N bond found in both (Scheme 1.11).⁹¹ In this reaction, rather than a cyclopropanation event, the carbene undergoes nucleophilic attack from the Lewis basic nitrogen atom present in diazoles to form a nitrogen ylide. N-N cleavage then proceeds *via* a 6π -electrocyclic ring opening. The ring-opened intermediate then undergoes a condensation reaction to achieve the desired pyrimidine or quinazoline. The reaction was found to tolerate a broad range of substrates on both the diazole and diazirine starting material. In some cases, competitive dimerization was observed which was minimised by SEM (trimethylsilylethoxy methyl) protection. There were two main limitations to the scope highlighted by the authors: electron-deficient diazoles and those that were insoluble in the TBME solvent. The protocol

has been applied to complex substrates and used in the synthesis of an analog of rosuvastatin, in which the key atom insertion step was achieved in a 72% yield.

A. Levin, 2021



B. Levin, 2022



Scheme 1.11. A: Ring expansion of indoles with arylchlorodiazirines. B: Ring expansion of pyrazoles highlighting enhanced reactivity upon SEM-protection and applications to late-stage modification.

1.2.2 Nitrogen Atom Insertion

The insertion of a nitrogen atom into the aromatic framework of molecules facilitates a significant change to the chemical and physicochemical properties of molecules. Factors such as (Lewis) basicity, H-bonding capabilities and partition coefficient can be greatly altered by the inclusion of a new nitrogen atom. This skeletal edit is arguably of greater interest to

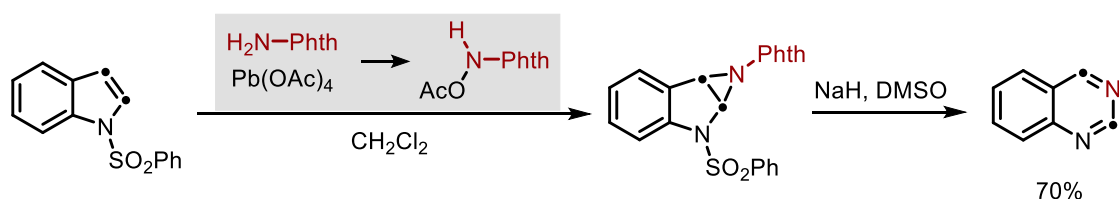
medicinal chemists than carbon atom insertion due to the significant changes that nitrogen insertion invokes.

Methodologies to achieve nitrogen atom insertion have been known for many decades but reports are often foundational in nature and lacking significant substrate scope and functional group tolerance. Analogous to the carbon atom insertion into indoles mentioned above, nitrogen insertion can be achieved using the same mechanism by utilising nitrene or electrophilic nitrogen chemistry. In 1987, Kumar reported the insertion of a nitrogen atom into indoles, affording the corresponding quinazoline (Scheme 1.12A).⁹² This reaction proceeds by initial aziridination with *N*-aminophthalimide and Pb(OAc)₄ of the olefin present in a benzenesulfonyl protected indole. Analogous to the Ciamician-Dennstedt reaction, fragmentation with expulsion of the phthalimide nucleofuge facilitated by removal of the protecting group leads to ring expansion and rearomatisation. Later studies by Atkinson suggests the reaction proceeds *via* an *N*-acetoxyaminophthalimide as opposed to a nitrene, formed by oxidation with Pb(OAc)₄.⁹³

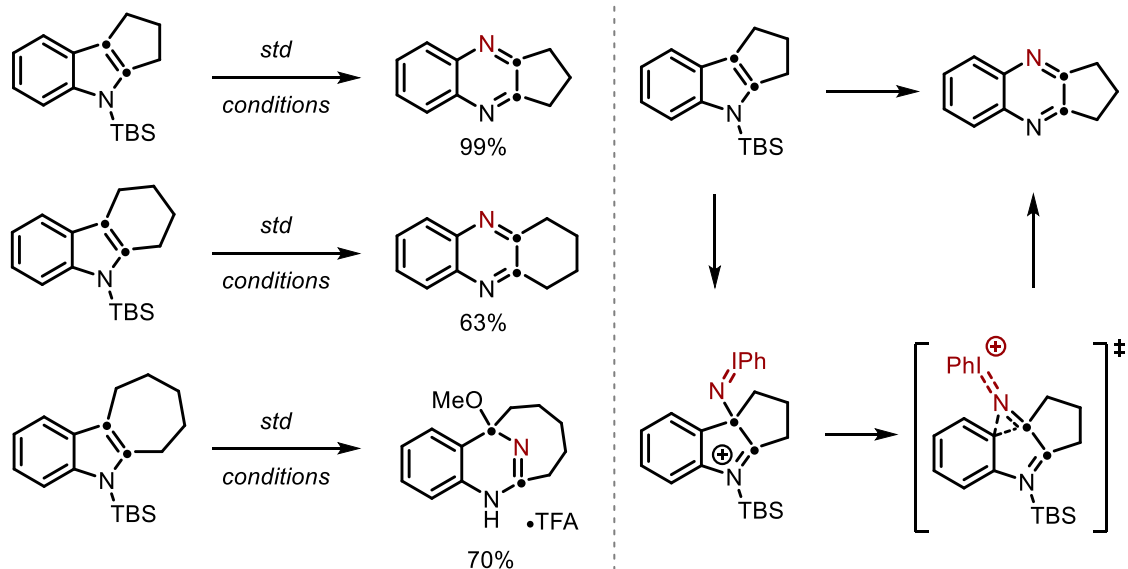
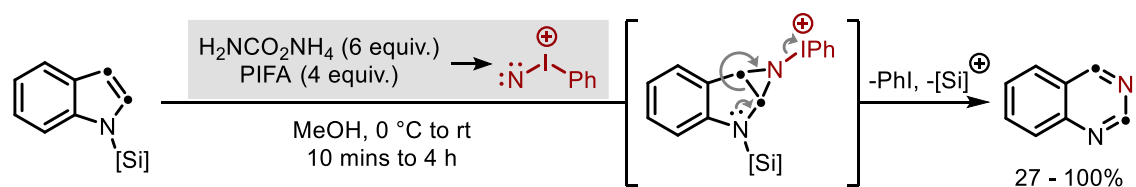
A far more general variant of the reaction was reported in 2022 by Morandi and co-workers (Scheme 1.12B).⁹⁴ In this case, initial aziridination is achieved by the formation of a nitrene from the ammonia source ammonium carbamate and the hypervalent iodine(III) reagent PIFA (bis(trifluoroacetoxy)iodobenzene). The reaction is proposed to proceed *via* step-wise aziridination and the formation of a cationic intermediate. Fragmentation and expulsion of the iodobenzene nucleofuge leads to formation of the quiazoline. A silyl protecting group was found to be crucial to reactivity due to: (1) the deleterious interaction of the nitrene and indole N-H, (2) the stabilisation of the cationic intermediate, and (3) the ease at which the protecting group is cleaved upon formation of the quiazoline. The reaction showed a broad scope including medicinally-relevant functional groups and was successfully applied to a range of complex substrates containing indoles. Intriguingly, when the protocol was applied to indoles bearing 2,3-fused rings, the isomeric quinoxaline was obtained in high yields. The authors propose that the high strain imposed by the fused ring prevents the desired fragmentation reaction. Instead, computational analysis suggested a transition state in which the aziridinyl nitrogen inserts into the C3-C4 σ -bond. This specific reactivity was observed for five- and six-membered fused rings. The desired fragmentation was observed for seven-membered fused rings, although the product was obtained as a dihydroquinoline with addition of the methanol solvent.

The insertion of nitrogen atoms into azoles is not limited to aziridination chemistry. In 1971, Maeda and co-workers reported the *N*-insertion into imidazoles utilising an oxidative cleavage/condensation strategy.⁹⁵ Irradiation with blue light in the presence of a methylene blue photocatalyst resulted in oxidative cleavage of the imidazole C=C bond to afford an amidoaldehyde intermediate. *In situ* condensation of both carbonyls with ammonia led to the formation of *s*-triazines. The same approach was later employed in the conversion of indoles to quiazolines.⁹⁶

A. Kumar, 1987



B. Morandi, 2022



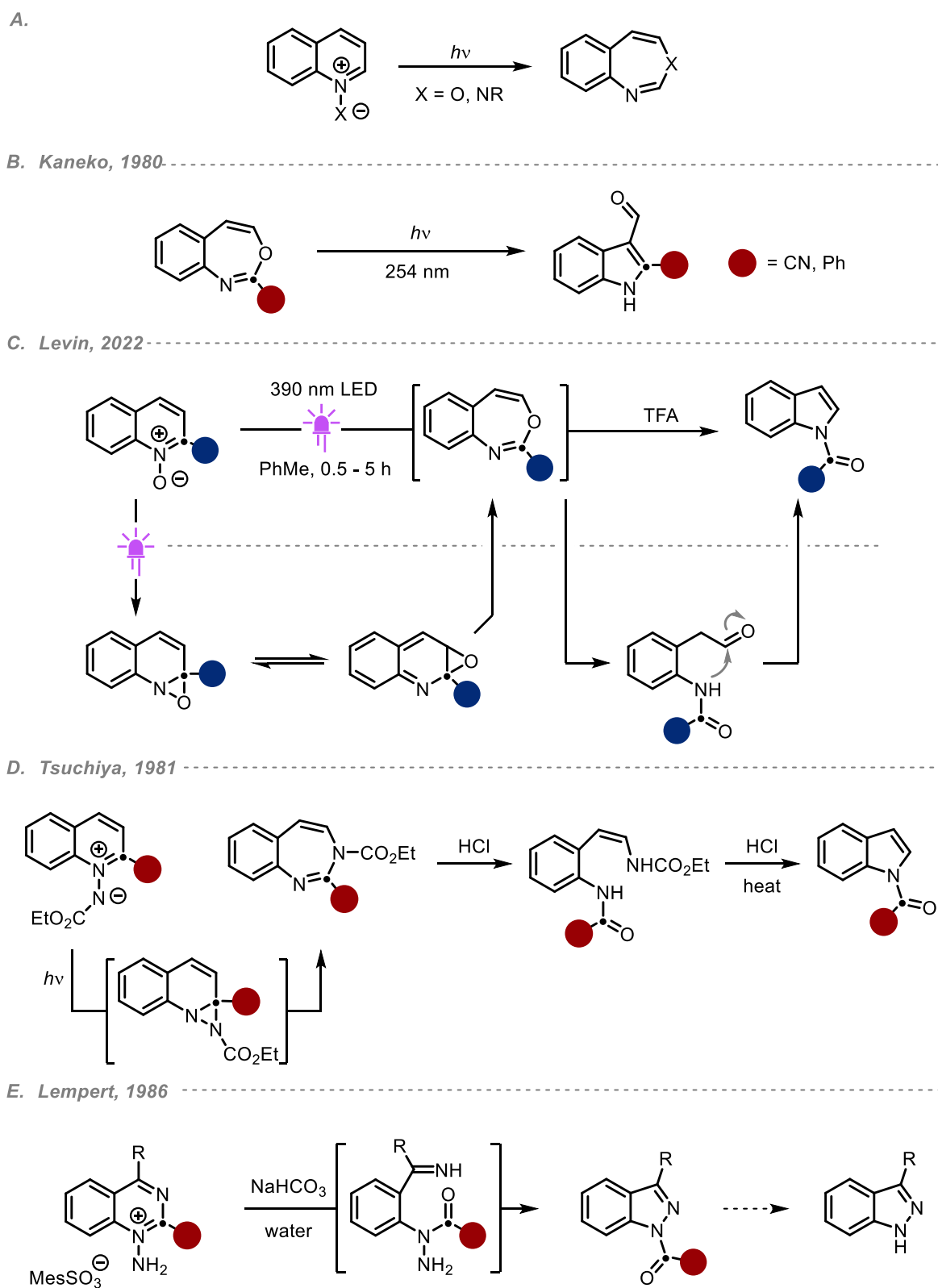
Scheme 1.12. Nitrogen atom insertion. A: Insertion with *N*-acetyloxyphthalimide. B: Insertion with iodonitrenes highlighting unexpected regioselectivity with fused indoles.

1.2.3 Carbon atom deletion

The direct opposite to atom insertion, atom deletion implies the removal of one or more atoms from an aromatic skeleton. The deleted atom can either be extruded from the molecule completely or remain tethered on the newly contracted ring. One of the more prominent and well-explored classes of atom deletion are the ring contraction of quinoline *N*-oxides and *N*-amides to indoles and other five-membered azoles. These reactions all proceed *via* an initial light-mediated ring expansion to a benzoxazepine or benzodiazepine (Scheme 1.13A); the subsequent ring contraction can then be achieved using a number of methods.

In 1980, Kaneko and co-workers reported the light-mediated ring contraction of benzoxazepines to 3-formyl indoles (Scheme 1.13B).^{97,98} A thermal ring contraction was also reported for 3-carboxymethyl indoles. Despite the obvious appeal of these transformations, these early reports were limited by substrate scope and modest yields. However, in 2022, Levin and co-workers reported the one-pot ring contraction of quinoline *N*-oxides (Scheme 1.13C).⁹⁹ This methodology generalised the method to a broad range of substrates and functional groups. The use of narrow-band 390 nm light avoided deleterious two-photon processes observed when Hg lamps were employed. After initial ring expansion to the benzoxazepine, *in situ* acidolysis promoted both the ring opening and subsequent ring contraction to afford 1-acylindoles. The acyl group could then be removed by treatment with hydrazine.

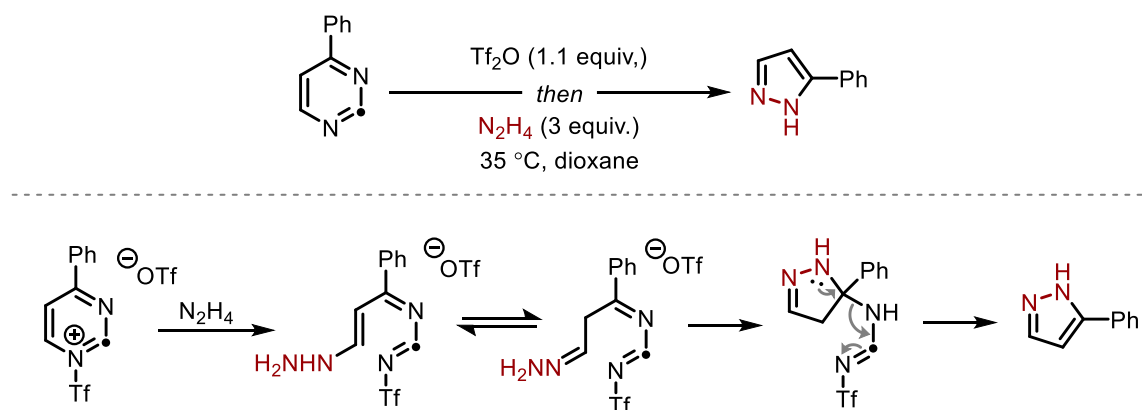
Like *N*-oxides, quinoline *N*-amides undergo a light-promoted ring expansion to benzodiazepines. Tsuchiya and co-workers reported the photochemical ring expansion and subsequent ring contraction *via* analogous condensation triggered by acidolysis (Scheme 1.13D).^{100,101} The method relies on electron-rich quinolines for good yields, as electron-deficient examples suffered from competitive N-N bond cleavage. The ring expansion is proposed to proceed by formation of a 3-membered diazirane formed by nucleophilic attack of the exocyclic nitrogen at C2. C-C bond cleavage then affords the seven-membered ring. The amido-enamine could be accessed by treatment with HCl, and heating at 80 °C with HCl led to ring closure with loss of ethyl carbamate. A similar strategy was employed in the synthesis of indazoles from quinazolines (Scheme 1.13E).¹⁰² Oxidation to the *N*-amide followed by base-mediated ring opening and condensation affords the 1-acylindazole.



Scheme 1.13. Atom deletion strategies. A: Ring expansion of quinoline oxides/amides. B: Initial studies of benzoxazepine ring contraction. C: General protocol developed by Levin. D: Ring contraction of quinoline N-amides. E: Ring contraction of quinazolines.

In addition to benzo-fused heterocycles, the ring contraction of pyrimidines to pyrazoles has been reported by Sarpong and co-workers (Scheme 1.14).¹⁰³ Computational calculations led to a proposed mechanism involving initial triflation of a pyrimidine nitrogen with Tf₂O followed by nucleophilic attack with hydrazine which leads to a Zincke intermediate. The subsequent tautomerisation followed by ring closure affords the five-membered ring. Expulsion of an amidinyl nucleofuge then leads to rearomatisation and the pyrazole product. While a carbon atom is deleted from the ring, both pyrimidinyl nitrogen atoms are also replaced by the hydrazine nitrogen atoms.

Sarpong, 2022



Scheme 1.14. Ring contraction of pyrimidines to pyrazoles *via* ring-opening.

1.2.4 Atom Transmutation

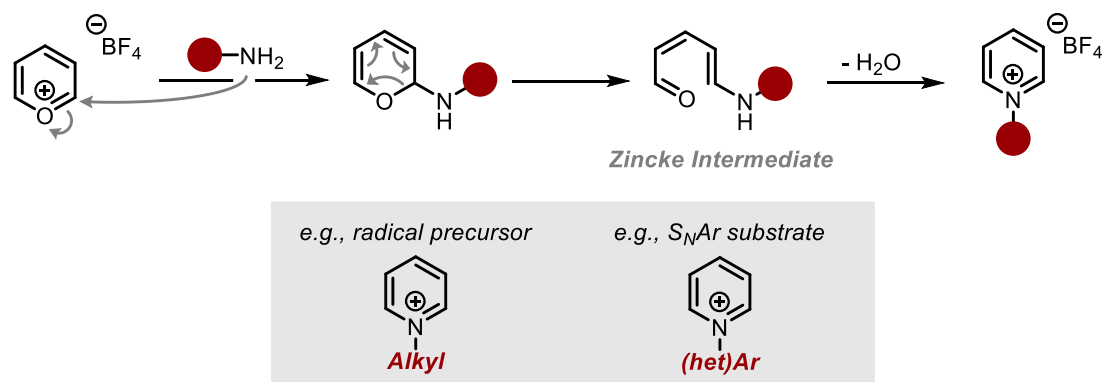
The final class of skeletal edit is the transmutation of atoms within molecular skeletons. Some atom transmutations, notably [4+2] cycloadditions/retro-cycloadditions of five-membered rings, occur concomitantly with atom insertions. However, there are a number of atom transmutations that occur without modulating ring size. One of the most well-known examples of atom transmutation in organic synthesis is the formation of Katritzky salts from pyrylium salts (Scheme 1.15A).¹⁰⁴ The resulting pyridinium salt products are competent substrates for radical chemistry and can also be employed as nucleofuges in S_NAr chemistry.^{105–}

107

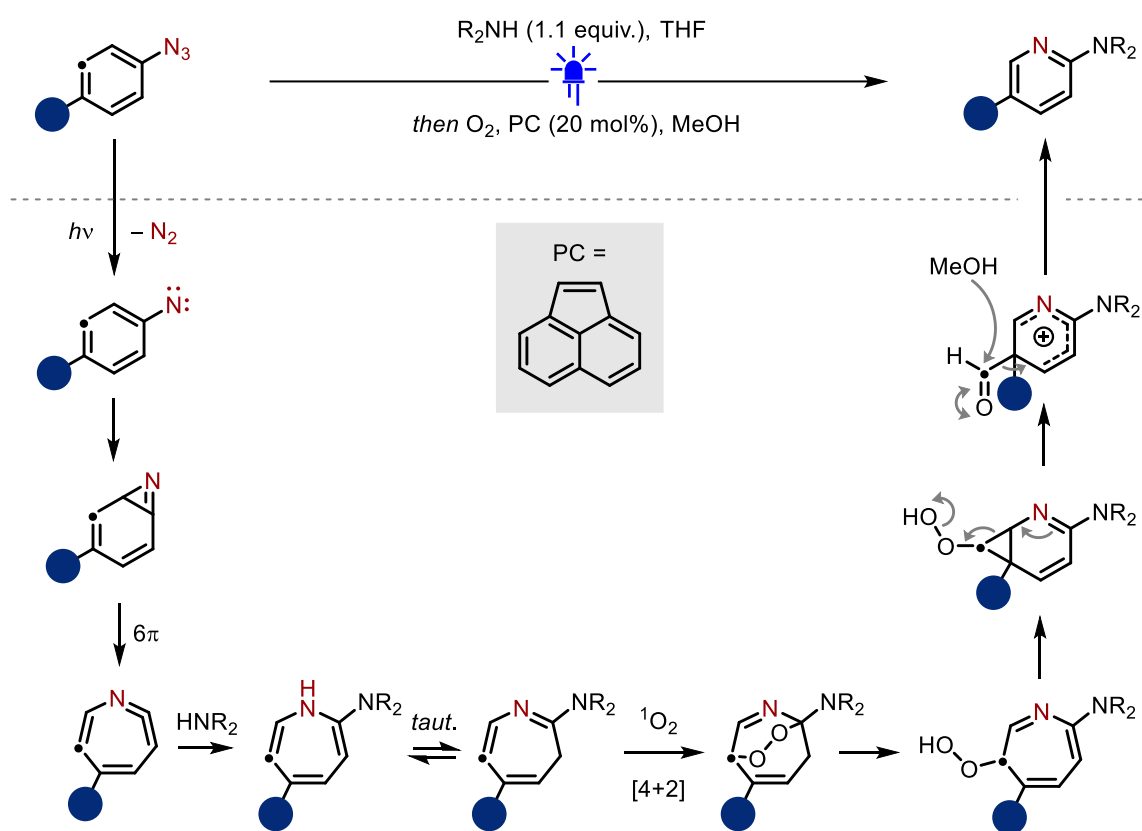
In addition to heteroatom-heteroatom transmutation, carbon-heteroatom exchange has also been reported in recent years. In 2022, Burns and co-workers reported the light-mediated transmutation of azidoarenes to aminopyridines (Scheme 1.15B).¹⁰⁸ In the mechanism proposed by the authors, photolysis of the azido group forms a nitrene with extrusion of dinitrogen. This nitrene is capable of inserting across the arene π-bond, forming a non-

aromatic 2*H*-azirine. A thermal 6π electrocyclic ring opening affords a cyclic ketimine which is captured by a secondary amine, subsequent tautomerism provides a stable 2-aminoazepine. Exposure to photochemically-generated singlet oxygen then affords a peroxy-bridged species. Ring opening, followed by a second 6π electrocyclic ring opening affords a Wheland intermediate that is quenched by solvolytic deformylation to afford the 2-aminopyridine product.

Katritzky



Burns, 2022



Scheme 1.15. A: O-to-N atom transmutation. B: C-to-N transmutation *via* N-insertion and ring contraction.

1.3 Carbenes

Given their relevance in the insertion of carbon atoms into molecular skeletons – the topic of this thesis – the following section will discuss the structure, reactivity, and generation of carbenes.

Carbenes are neutral compounds that feature a divalent carbon atom with only six valence electrons.¹⁰⁹ Due to this low valency, carbenes are highly reactive, even with typically inert functional groups (e.g. C-H bonds).¹¹⁰ The central carbenic carbon can adopt either a linear or bent geometry, implying sp and sp^2 hybridisation respectively.¹¹¹ The linear geometry features two non-bonding degenerate orbitals (p_x and p_y). The bent geometry breaks this degeneracy to form non-degenerate σ - and p_π -orbitals (Figure 1.5). Due to the degeneracy of the frontier orbitals in the linear geometry, linear carbenes tend to adopt the *triplet* electronic configuration (Figure 5). Bent carbenes can adopt several electron configurations with two different spin-states: *singlet* or *triplet*.¹¹¹ The spin-state adopted by the bent carbene is dependent on the substituents bonded to the carbon atom. Electron donating substituents induce a small σ - p_π gap and therefore promote the triplet state. Electron withdrawing substituents stabilize the σ non-bonding orbital, increasing its s -character while leaving the p_π orbital unchanged. This increases the σ - p_π gap, favouring the singlet state. Steric factors can also influence spin-state. Due to the steric bulk of the phenyl rings (in addition to electronic effects), diphenylcarbene possesses a triplet ground-state.¹¹²

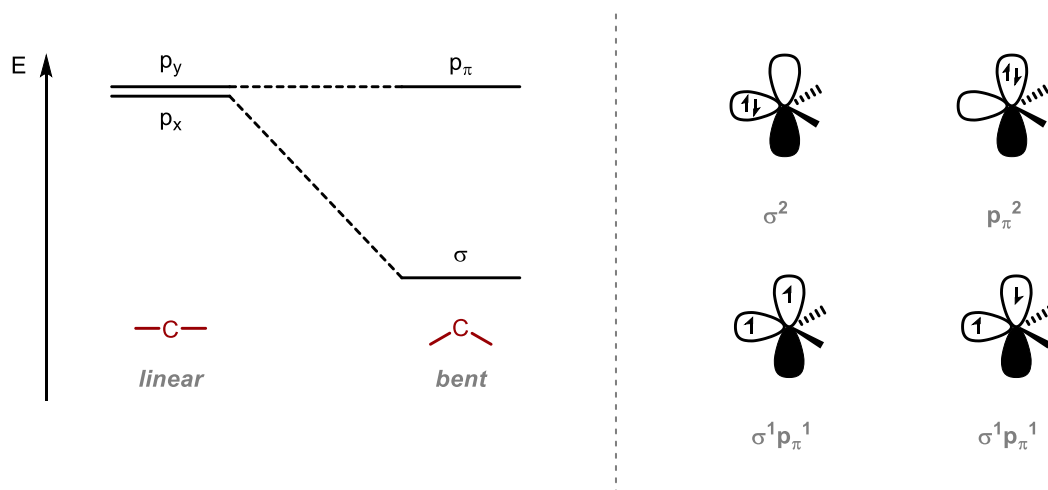


Figure 1.5. Left: Frontier orbital energy diagrams of linear and bent carbenes. Right: Electron configurations in carbenes. Bent geometry is shown for clarity.

1.3.1 Carbene Reactivity

The structural nature of carbenes means they are highly reactive. The reactivity of a carbene is dictated by its ground-state spin state – singlet or triplet. Triplet carbenes are especially reactive as they can be considered as diradicals. Decomposition routes for carbenes of this nature involve dimerization, although very bulky substituents can prevent reaction, increasing their lifetimes, and bond insertion reactions.¹¹³ Carbenes possess a unique type of reactivity in which the carbene unit can insert between X-H bonds such as O-H, N-H and, despite their inertness, C-H bonds.¹¹⁴ These insertions readily occur due to frontier orbital matching between the carbene σ and p_{π} orbitals and the X-H σ and σ^* orbital. For a singlet carbene the orbital overlap means insertion follows a concerted mechanism that generally allows retention of stereochemistry. Due to the diradical nature of triplet carbenes, insertion reactions are step-wise and form a radical intermediate that typically does not retain stereochemistry.¹¹³ Carbenes are also capable of reacting with double bonds *via* cheletropic addition, affording three-membered rings.¹¹⁵

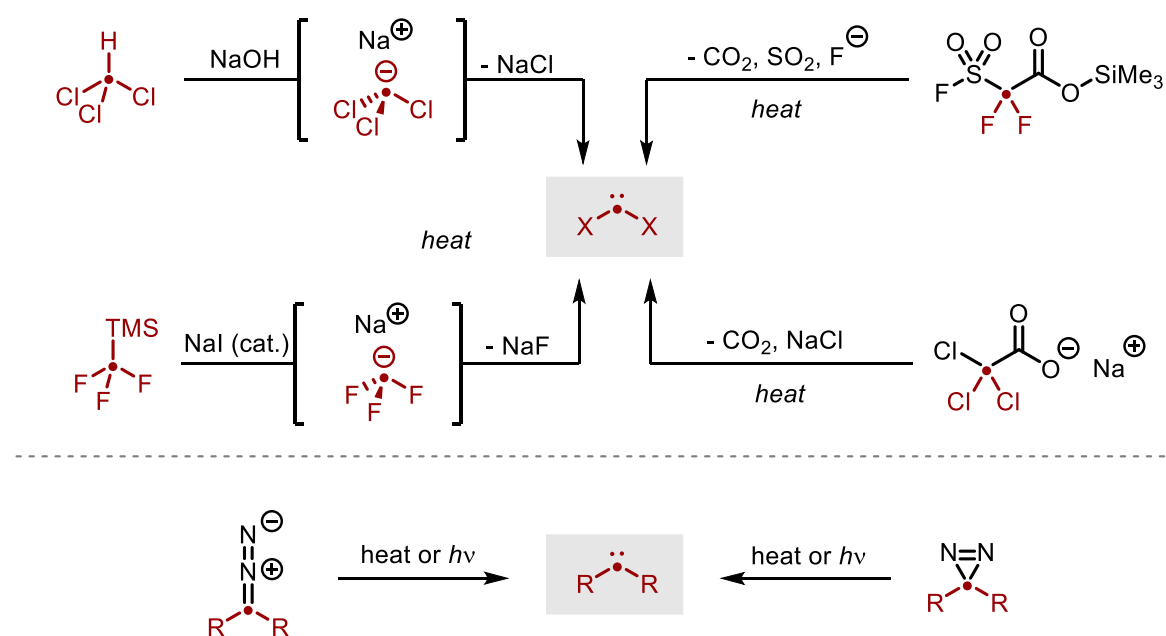
Depending on the substituents, singlet carbenes can be described as either nucleophilic or electrophilic due to both the presence of a filled and vacant orbital. Carbene philicity can be described using various scales including the experimentally-determined philicity scale proposed by Moss, based on the competitive cyclopropanation of different alkenes, referenced to dichlorocarbene.¹¹⁶ Other three-dimensional philicity scales have also been devised.¹¹⁷ Typical nucleophilic singlet carbenes include: dialkylcarbenes, dialkoxycarbenes, and aminoalkylcarbenes. Electrophilic carbenes include: dihalocarbenes, dialkylidenecarbenes, and acylcarbenes.

1.3.2 Carbene precursors

Due to their high reactivity, carbenes must be generated *in situ* from an appropriate precursor. These precursors typically require heat, light, and/or the generation of a highly stable by-product such as a gas or metal salt to promote carbene formation (Scheme 1.16). Dihalocarbenes are among the most easily available carbenes due to the array of precursors available. The first synthesis of dichlorocarbene was reported in 1855 by Geuther, who suggested that the hydrolysis of chloroform in alkaline conditions proceeded through a carbene intermediate.¹¹⁸ Deprotonation of chloroform leads to the corresponding trichloromethyl salt and extrusion of the metal chloride affords the carbene. In addition to dichlorocarbene, dibromocarbene¹¹⁹ and diiodocarbene¹²⁰ are readily produced using the same method from the

corresponding haloform. Another common method for the generation of dihalocarbenes is the thermal decomposition of halogenated esters/carboxylates such as sodium trichloroacetate or the difluorocarbene precursor TFDA (trimethylsilyl fluorosulfonyldifluoroacetate).^{121,122} The formation of these carbenes is entropically driven by extrusion of gaseous by-products. Difluorocarbene can also be generated by the thermolysis of TMSCF₃ in the presence of sodium iodide.¹²³

Carbenes bearing non-halogen substituents such as dialkylcarbenes or carbene itself can be readily generated by the thermolysis or photolysis of the appropriate precursor. Diazo compounds such as diazomethane as well as diazirines are typically-employed functional groups as carbene formation is driven by the extrusion of dinitrogen upon heating or irradiation.¹²⁴



Scheme 1.16. Methods of generating free carbenes. A: generation of dihalocarbenes. B: generation of dialkylcarbenes.

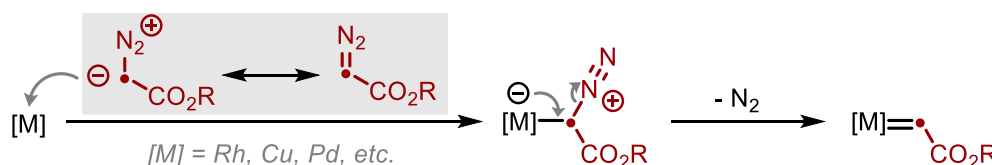
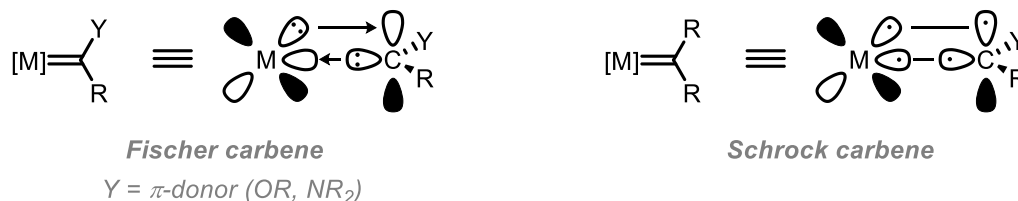
1.3.3 Metal Carbenoids

The term carbenoid was first introduced in 1964 by Moss and Closs to describe compounds that exhibit similar reactivity to carbenes without being free divalent carbon species.¹²⁵ These carbenoids are typically much more stable - and their reactions are more selective.¹²⁶ One method of achieving typical carbene reactivity while increasing stability is by bonding the carbenic carbon to an appropriate transition metal. Metal carbenoids can therefore be described as a compound containing a carbon atom with a double bond to a metal centre. There exist two types of metal carbene complex: Fischer and Schrock carbenes.¹²⁷ While not free carbenes, these transition metal complexes are commonly referred to as carbenes.¹⁰⁹

Fischer carbenes typically include a low oxidation state middle-to-late transition metal with π -acceptor ligands and π -donor substituents bonded to the carbenic carbon atom.¹²⁸ The carbene exists in the singlet state and the 'M=C double bond' is formed by donation of lone pairs by both the carbon atom and the metal (Scheme 1.17A). Because of this Fischer carbenes do not contain a 'true' metal-carbon double bond. As a result, Fischer carbenes are nucleophilic at the metal atom and electrophilic at carbon.¹²⁹ Schrock carbenes however include a high oxidation state early transition metal and no π -acceptor ligands or π -donor substituents. The carbene carbon atom is found in the triplet state and thus bonding between the carbon atom and metal is analogous to the C=C bond in an alkene.¹²⁸ Therefore, Schrock carbenes can be considered to have a true M=C double bond. They exhibit opposite reactivity to Fischer carbenes as they are electrophilic at the metal atom and nucleophilic at carbon.¹³⁰

Some of the most widely used transition metal carbenoids in organic synthesis are those of rhodium and copper. These carbenoids can be readily formed from copper and rhodium salts and diazo compounds. Due to their nucleophilicity at carbon, diazo compounds can react with transition metals and extrusion of dinitrogen facilitates the formation of the metal-carbon double bond (Scheme 1.17B).¹³¹ Due to their instability, diazo compounds typically require electron-withdrawing groups such as esters to stabilise the partial negative charge build up at carbon.^{132,133} Like free carbenes, the reactivity of rhodium and copper carbenoids involves insertion and cyclopropanation reactions.^{131,134} Metal carbenoids with chiral ligands are commonly used in enantioselective variations of these reactions.¹³⁵

While zinc is classified as a transition metal, its electronic configuration contains a closed d-shell configuration ($[\text{Ar}]3d^{10}4s^2$) and thus its reactivity is much more analogous to that of alkaline earth metals such as magnesium ($[\text{Ne}]3s^2$). Alkali metals, alkali earth metals, and zinc form carbenoids whose structure differs to that of transition metals. While metal carbenes possess a metal-carbon 'double bond', these alkali metal carbenoids are instead organometallic compounds that possess a tetravalent carbon bonded to both a sufficient nucleofuge, typically a halide, and the metal atom. It is the elimination of the metal and nucleofuge as a highly stable salt that provides the driving force for the carbene-like reactivity (Scheme 1.17C). These carbenoids can be readily prepared by metal-halogen exchange of gem-dihalogenated compounds.

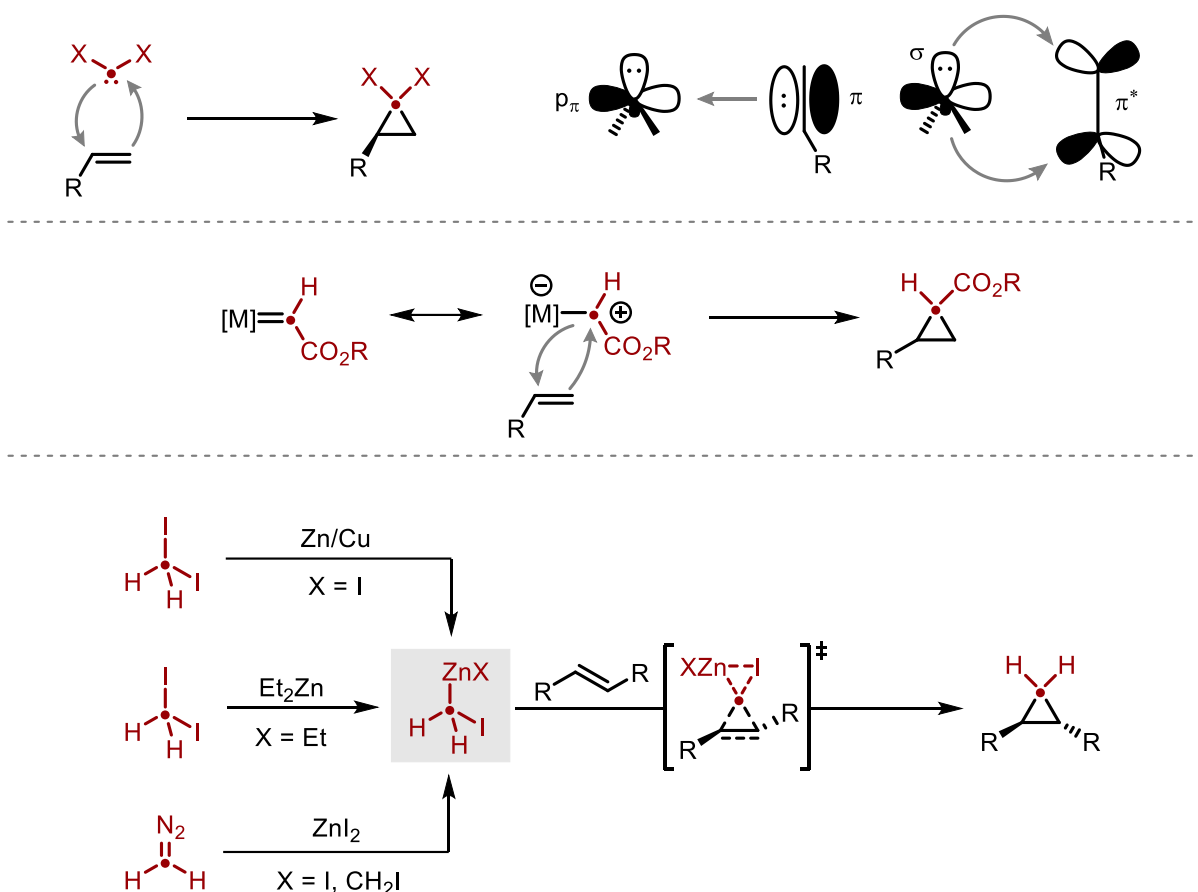


Scheme 1.17. A: Orbital interactions of Fischer and Schrock carbenes. B: Generation of metal carbenoids from diazoesters. C: Generation of carbenoids derived from alkali metals.

1.3.4 Carbenes and carbenoids in cyclopropanations

One of the more well-explored applications of carbenes and carbenoids is the cyclopropanation of alkenes and cyclopropanation of alkynes (Scheme 1.18A). Free carbenes readily react with alkenes in a concerted, chelotropic [2+1] cycloaddition. The orbital interactions of this reaction are analogous to that of bond insertion reactions mentioned earlier. The vacant p_{π} -orbital of the carbene interacts with the filled π -bond of the alkene, whereas the filled carbene σ -bond interacts with the alkene π^* -bond. As with bond insertion reactions, there is little orbital overlap when the carbene takes a linear approach to the alkene and sufficient overlap can only be achieved when the carbene approaches from side-on.

Carbenoids of metals such as rhodium, copper, and palladium can also undergo cyclopropanation with alkenes. After generation of the carbenoid by reaction with a diazoester, a concerted attack of the rhodium-carbon bond into the olefin and attack of the olefin into the carbenic carbon occurs, resulting in the cyclopropane (Scheme 1.18B). Metal carbenoids are often employed in cyclopropanation reactions due to the relative stability of carbenoids compared to free carbenes as well as the ease at which they form compared to thermally- and photolytically-activated carbenes, resulting in milder reaction conditions. Additionally, chiral ligands can be employed at the metal centre to impart enantioselectivity.



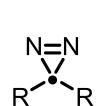
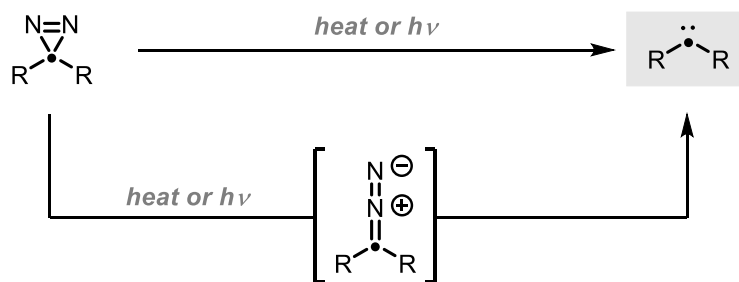
Scheme 1.18. Synthesis of cyclopropanes from carbenes. A: Orbital interactions. B: Cyclopropanation with metal carbenoids. C: Mechanism for Simmons-Smith cyclopropanation.

The most well-established reaction involving zinc carbenoids is the Simmons-Smith cyclopropanation, first reported in 1958 (Scheme 1.18C). This reaction generates a carbenoid from a zinc/copper couple and diiodomethane of the structure IZnCH_2I . Since then, several other methods have been developed to generate the desired carbenoid. Wittig and Wingler prepared IZnCH_2I and the bis(iodomethyl)zinc reagent from ZnI_2 and diazomethane and Furukawa and co-workers reported that the Zn/Cu couple previously employed could be replaced with diethylzinc to generate EtZnCH_2I .^{136,137} The simple reaction mechanism of cyclopropanation by this zinc carbenoid involves a ‘butterfly’ transition state in which a concerted chelotropic addition of the CH_2 unit is concomitant with extrusion of ZnI_2 though more complex, multi-metallic mechanisms have been postulated computationally.^{138,139} The protocol is highly general and can be applied to various substituted olefins and is commonly utilised in total synthesis.¹⁴⁰ It is an especially powerful method for substrates with Lewis basic directing groups as these moieties facilitate diastereoselective cyclopropanation by coordination with the zinc centre.

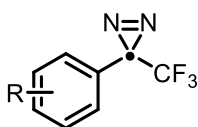
Methods have also been developed that include an additive to enhance the reactivity of the carbenoid.¹⁴¹ Several methods have been developed utilising zinc carbenoids with strongly electron-withdrawing anionic ligands, allowing for the cyclopropanation of unfunctionalised olefins. One of the most common is the introduction of an equimolar amount of trifluoroacetic acid to produce iodomethyl zinc trifluoroacetate ($\text{F}_3\text{CCO}_2\text{ZnCH}_2\text{I}$, so-called Shi's reagent).¹⁴² Charette and co-workers have developed carbenoids with other ligand variants including phenoxides and phosphates.^{143,144} The phosphate variant is particularly valuable as solutions of the carbenoid can be stored for several days, removing the need to form the carbenoid in each reaction. Lewis basic directing groups as well as chiral auxiliaries can also be used to enable stereoselective cyclopropanation.^{145–147}

1.3.5 Diazirines

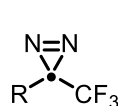
The structure of the diazirinyl functional group facilitates the generation of free carbenes with a wide range of substituents. Notably, the three-membered ring possessing a $\text{N}=\text{N}$ double bond allows for the facile extrusion of dinitrogen along with the release of ring strain to generate the singlet carbene.¹⁴⁸ Carbene generation can be achieved both thermally and photolytically although decomposition of aryldiazirines can initially proceed *via* the isomeric diazo group (Scheme 1.19A).^{149,150} The triplet state of carbenes derived from diazirines can also be achieved by energy transfer from an excited triplet-state photocatalyst.¹⁵¹ Due to the ease with which the free singlet carbene can insert into X-H bonds paired with the long-wavelength UV and short irradiation times required, damage to biological tissues and residues is diminished and alkyl diazirines are commonly employed as probes in photoaffinity labelling.¹⁵² There exist four classes of *internal* diazirine (Scheme 1.19B). The most common are type A, dialkyl diazirines, and type B, aryl trifluoromethyl diazirines. Type C, alkyl trifluoromethyl diazirines, and type D, alkyl difluoromethyl diazirines, are rare or unknown until recently.¹⁵³ Each class of diazirine is readily synthesised from the corresponding carbonyl (Scheme 1.19C). Formation of oxime followed by activation with TsCl allows for the formation of the diazirane intermediate upon addition of ammonia. Oxidation with iodine in the presence of base affords the diazirine. This mild synthesis and the relative stability of the resulting diazirine allows for the creation of complex labelling agents.^{154–156}



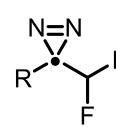
Type A
R = alkyl



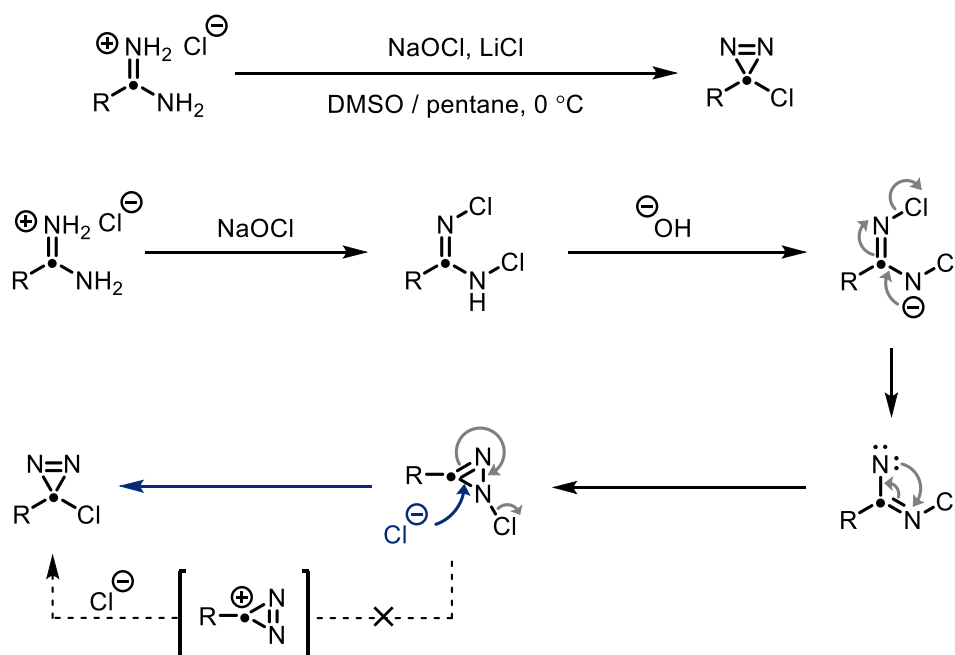
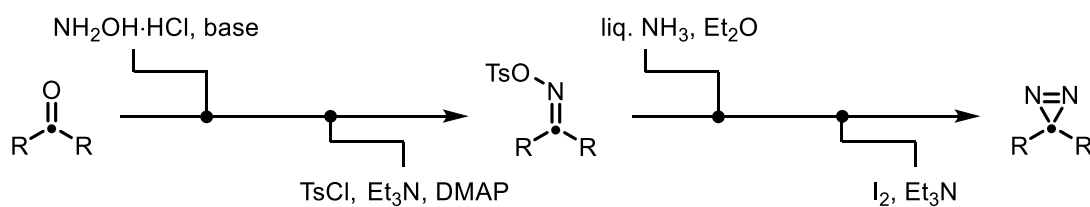
Type B



Type C
R = alkyl



Type D
R = alkyl



Scheme 1.19. A: Generation of carbenes from diazirines. B: Classes of diazirine. C: Synthesis of dialkyldiazirines. D: Synthesis of arylchlorodiazirines via Graham oxidation highlighting mechanistic insights.

Diazirines are not limited to these four types, however. A common class of *terminal* diazirines are 3-halodiazirines. These are readily prepared from the corresponding amidinium salt *via* the Graham oxidation with the corresponding hypohalite (Scheme 1.19D).¹⁵⁷ The mechanism of this transformation has been investigated extensively and is believed to proceed *via* a nitrene intermediate.¹⁵⁸ The initial step involves conversion of the amidine to the N,N'-dichloroamidine which then forms a nitrene in the presence of the hydroxide base. Nitrene insertion then occurs to form the three-membered 2*H*-diazirine ring.

The mechanism for the formation of the 3*H*-diazirine postulated by Graham has been disputed. Graham initially proposed that the conversion to the diazirine proceeded *via* a diazirenium cation isoelectronic to the corresponding cyclopropenium ion with formation of the nitrogen-nitrogen double bond.¹⁵⁷ This carbocation would then be attacked by a halide anion to afford the 3*H*-diazirine. However, another mechanism was proposed in which a S_N2' reaction could occur without the formation of a formal cation.¹⁵⁹ This mechanism is generally accepted as substitution reactions (with a mechanism analogous to the final step of halodiazirine formation) on diazirines bearing an electron-withdrawing group (R = CF₃) occur readily.^{160,161} The cation in this case would be highly unstable due to the inductive effects of the trifluoromethyl group. While this synthesis limits one of the substituents to chloride or bromide depending on the hypohalite employed, displacement of this halide for another functional group such as a methoxy group or fluoride is possible by employing the corresponding nucleophile. As before, this displacement is believed to proceed *via* a S_N2' mechanism.^{162,163} Additionally, by converting the second substituent to a competent leaving group, both substituents can be altered. Nitration of 3-phenoxy-3-chloro-3*H*-diazirine followed by treatment with TBAF (tetrabutylammonium fluoride) afforded 3-fluoro-3-chloro-3*H*-diazirine, a photolytically-generated source of a mixed dihalocarbene.¹⁶⁴

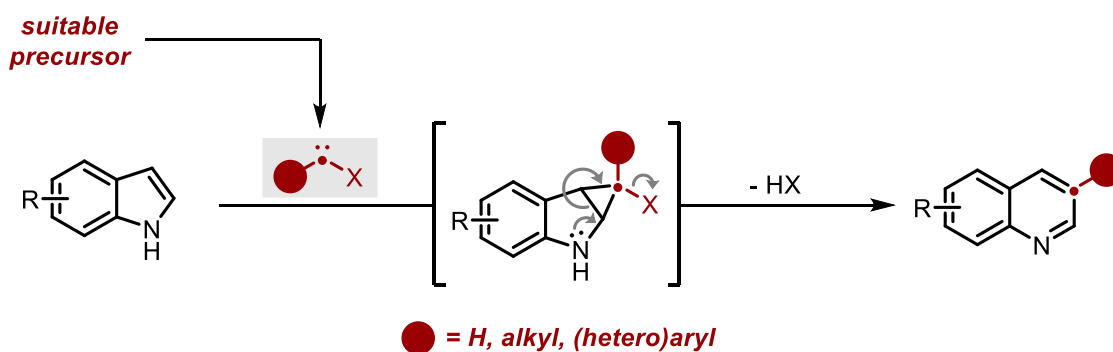
1.4 Project Outline and Aims

The stark contrast in chemical and physicochemical properties possessed by five- and six-membered aromatic heterocycles presents an interesting synthetic challenge: is a robust method for the late-stage conversion of indoles and pyrroles to their six-membered congeners with a wide range of substituents achievable? If this can be achieved in a general fashion, it would potentially allow for chemical libraries of indole- and pyrrole-containing drug candidates

to be rapidly transformed to a new six-membered skeleton, drastically altering the properties of the drug.

As outlined in section 1.2.1, methodologies for this specific transformation are known, though the range of substituents that can be installed as part of the carbynyl fragment are limited to halogens in the case of dihalocarbenes, or electron-withdrawing groups in the case of diazoesters. Therefore, at the time this research began, there existed a gap in the literature for the corresponding transformation achieved with more electronically-neutral groups, such as alkyl and aryl groups. Additionally, the scope of the reactions is limited with respect to the starting azole and the methodologies have not yet been applied to more complex compounds such as drug APIs. Taking this into account, we outlined a series of project aims that would resolve the drawbacks with previous reports.

The primary aim of this project is therefore to develop a novel methodology for the insertion of a single carbon unit into indoles, and later pyrroles. Based on previous work, this would be achieved by reaction with a carbene possessing a leaving group as a substituent. To begin, an appropriate carbene precursor must first be identified. This precursor must contain a sufficient nucleofuge to achieve the desired transformation but must also ideally possess a broad range of substituents that have not yet been reported. Once this has been realised, the methodology would then have to be optimised in line with typical measures of reaction efficacy, notably: reaction yield, substrate scope, atom economy, and ease of purification/isolation. The resulting protocol would then need to tolerate a range of substituents on both the indole scaffold and the carbene precursor for optimum applicability. For applications to late-stage functionalisation, the method must be tolerant not only of simple indoles and pyrroles, but also highly-functionalised molecules possessing a wide range of functional groups.



Scheme 1.20. General scheme for the carbon insertion into the aromatic framework of indoles.

2 Single Carbon Atom Insertion with Zinc Carbenoids

Abstract

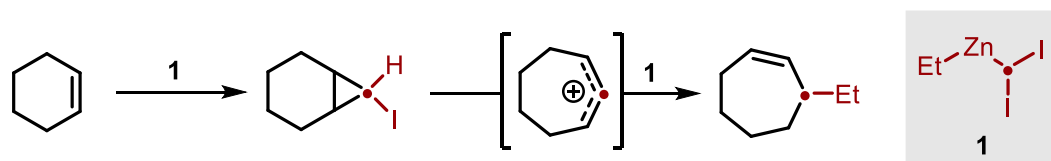
The development of a methodology to achieve the single carbon ring expansion of indoles to quinolines employing zinc carbenoids as carbonyl synthons is presented. Optimisation of a system developed from modifications to the well-established Simmons-Smith cyclopropane synthesis resulted in the novel transformation of 5-fluoroindole to 6-fluoroquinoline. This transformation marks the only known example of the insertion of a simple C-H unit into the indole skeleton in a single step, albeit in low yields.

2.1 Introduction

As seen in section 1.3.4, the Simmons-Smith reaction is a powerful tool for the cyclopropanation of olefins. However, the reaction is most known for the installation of a simple CH₂ unit. The single carbon atom insertion rationale invoked in section 1.2.1 requires a cyclopropanation reaction that installs a (pseudo)halocyclopropane such that the desired fragmentation can take place.

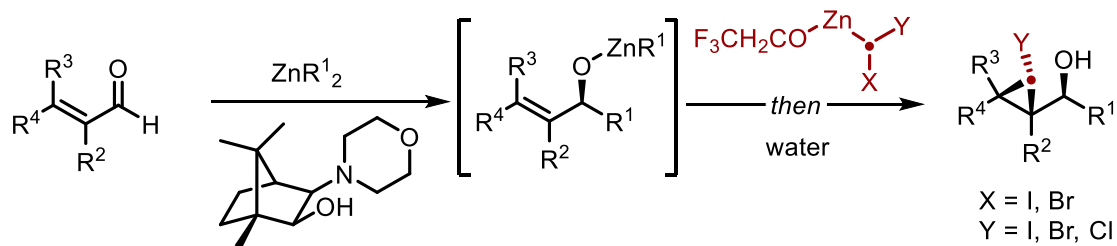
2.1.1 Halocyclopropanation

Methods for the halocyclopropanation of olefins have been known for decades. In 1971, Nishimura and Furukawa reported the iodocyclopropanation of cyclohexene with diethylzinc and iodoform.¹⁶⁵ Pioneering work in the field was reported by Hashimoto and Miyano who developed the carbenoid **1** (so-called Hashimoto's reagent) similarly from diethylzinc and iodoform and applied it in the cyclopropanation and subsequent ring expansion of cyclic olefins (Scheme 2.1).¹⁶⁶



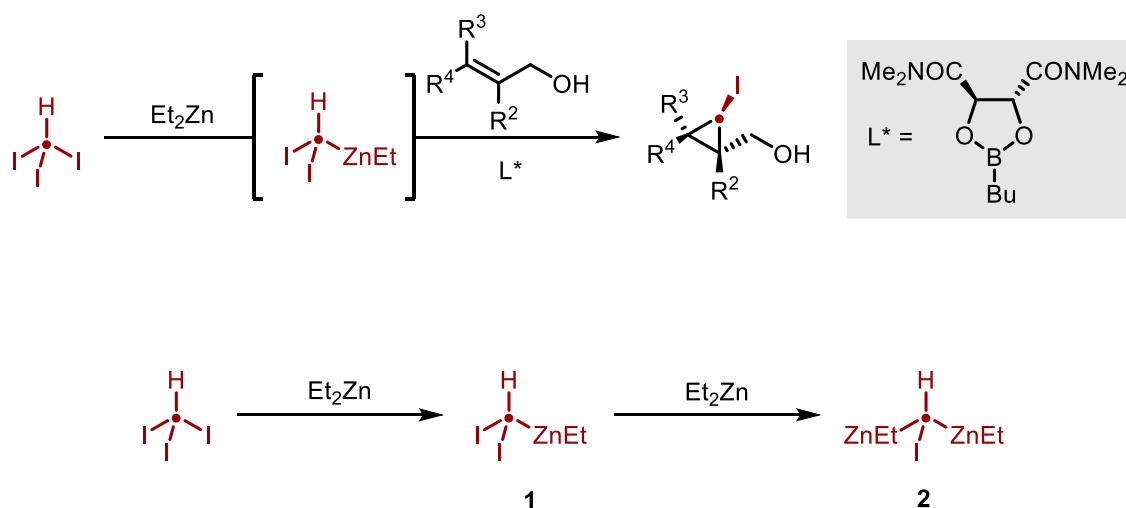
Scheme 2.1. Iodocyclopropanation of cyclohexene with carbenoid **1**.

The enantioselective iodocyclopropanation of allylic alcohols has more recently been developed by Walsh and co-workers who achieved tandem nucleophilic addition of zinc nucleophiles to aldehydes followed by stereoselective cyclopropanation with a similar carbenoid and a chiral ligand.¹⁶⁷ While initially only a small number of iodocyclopropanes were synthesised, a more comprehensive study was later undertaken.¹⁶⁸ Also explored in this report was the enantioselective cyclopropanation with other halide substituents derived from bromoform or mixed haloforms.



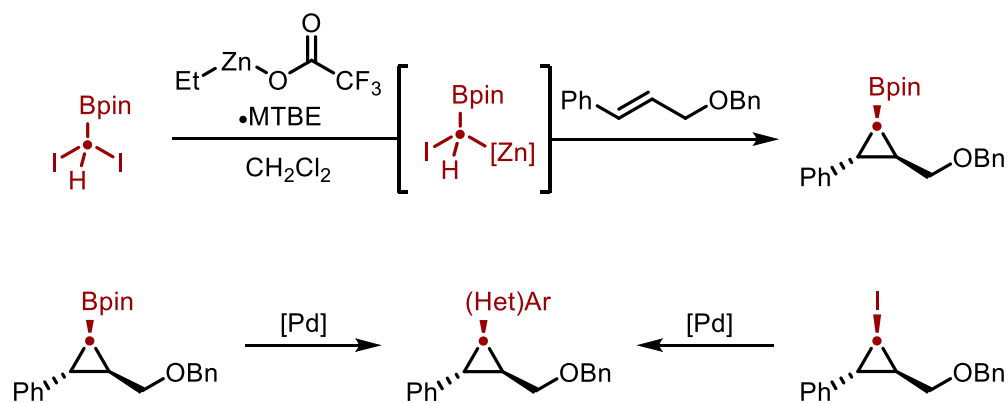
Scheme 2.2. Enantioselective alkylation/halocyclopropanation developed by Walsh and co-workers.

Extensive exploration of (enantioselective) halocyclopropanation methodologies has been performed by Charette and co-workers.¹⁶⁹ The protocols developed for Simmons-Smith reactions of this class are necessarily restricted to allylic alcohols due to the required coordination of both the zinc species and a chiral Lewis acid to achieve high diastereoselectivity. In addition to the development of reaction methodologies, mechanistic insights have also been reported.¹⁷⁰ The stoichiometric ratio of diethylzinc and iodoform was found to be important in achieving high conversion due to deleterious formation of a *gem*-dizinc carbenoid **2**.



Scheme 2.3. Top: Enantioselective iodocyclopropanation of allylic alcohols developed by Charette and co-workers. Bottom: Formation of the *gem*-dizinc carbenoid **2**.

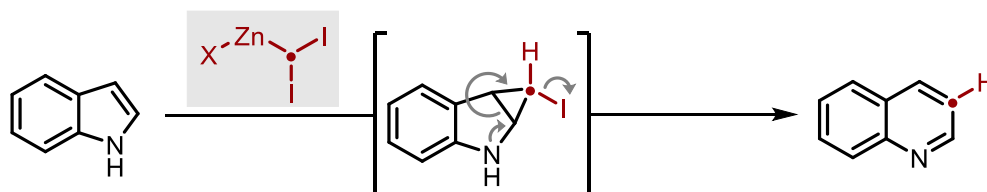
Charette and co-workers have similarly employed mixed haloforms in the synthesis of other halocyclopropanes.^{171–173} Additionally, the second non-halide substituent can also be altered from a simple H atom to access more complex and useful functionalities. Charette reported the borocyclopropanation of allyl ethers by a similar Simmons-Smith type reaction.¹⁷⁴ The resulting cyclopropyl boronic esters were then employed in cross-coupling chemistry to further highlight the structural complexity that can be achieved with these conditions. Both coupling chemistry¹⁷⁰ and lithium-halogen exchange¹⁶⁹ have been used to further functionalise the analogous halocyclopropane products.



Scheme 2.4. Borocyclopropanation of allylic ethers. Arylation of both borocyclopropanes and iodocyclopropanes.

2.2 Hypothesis and Chapter Aims

By utilising zinc carbenoids based on Hashimoto's reagent and the pioneering work of Charette and co-workers on asymmetric halocyclopropanation, these carbenoids could potentially be applied to the ring expansion of indoles. Considering the typical limitation of the carbenoids to allylic alcohols and their derivatives, it was anticipated that significant optimisation would be required to achieve high conversions to the cyclopropane intermediate. A second major limitation of these reagents is their high basicity, potentially leading to undesired side reactivity with unprotected indoles. Taking these limitations into account, the aims of this project were to identify and optimise reaction conditions for the halocyclopropanation of indole, assuming the subsequent fragmentation would be favourable due to rearomatisation. Once optimal conditions had been identified, exploration of the reaction scope, functional group tolerance and limitations could then be undertaken.

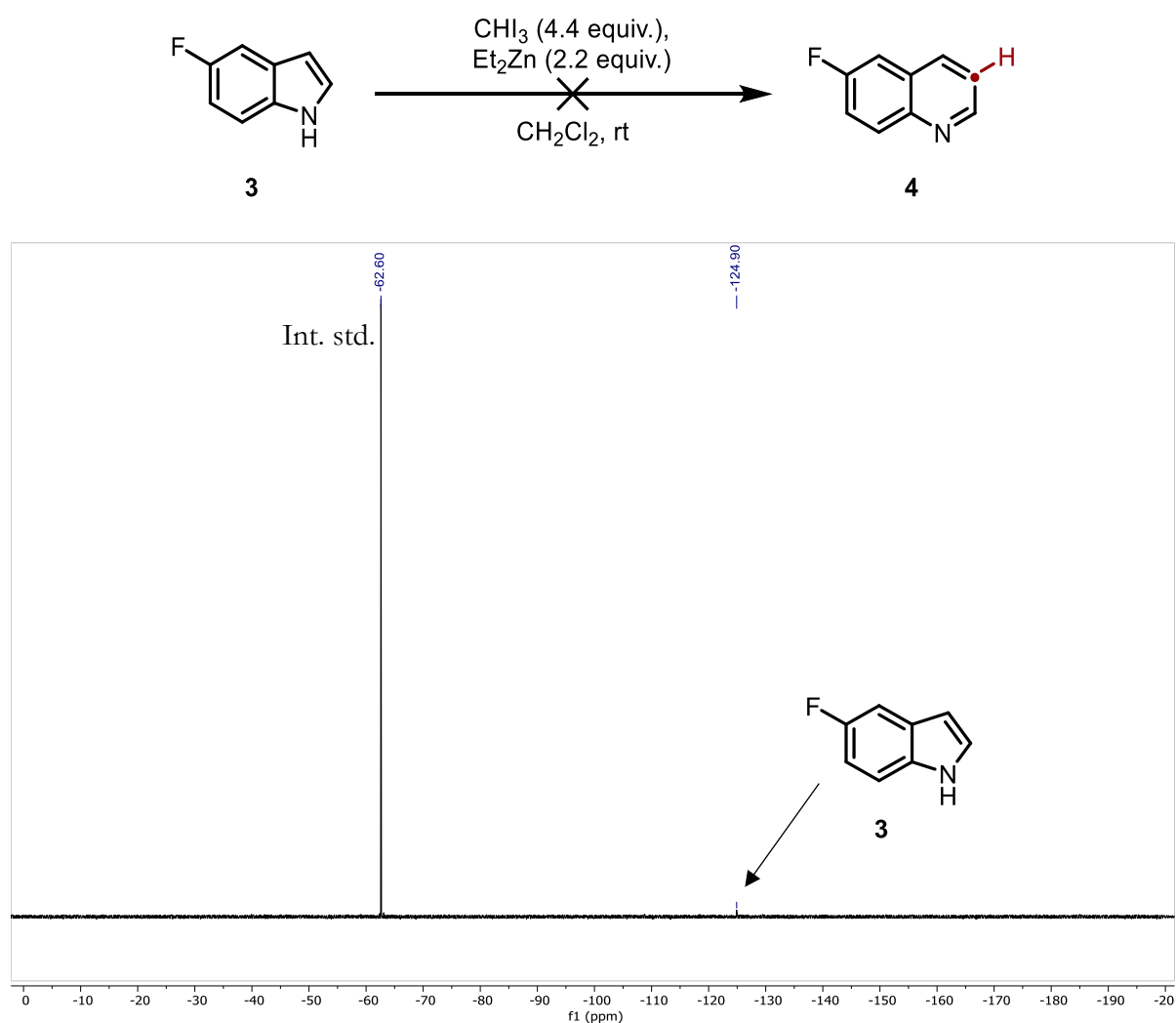


Scheme 2.5. General scheme for zinc-mediated carbon atom insertion.

2.3 Development of reaction conditions

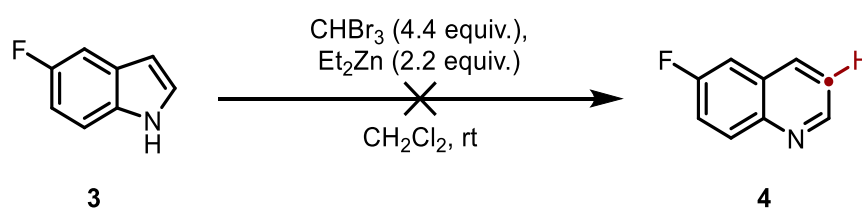
2.3.1 Initial Studies

5-Fluoroindole **3** was chosen as the model substrate to test the above hypothesis due to the ease of reaction monitoring by ^{19}F NMR spectroscopy. Initial conditions for the cyclopropanation were identical to those reported by Charette for the cyclopropanation of allyl ethers/alcohols.¹⁷³ A notable requirement for this system is the need for >2 equivalents of the zinc carbenoid due to the relative acidity of the free indole N-H. Taking this into account, the indole was subjected to the conditions shown in Scheme 2.6. After stirring for 4 h, NMR analysis showed only trace amounts of the product. Additionally, very little starting material was present in the filtered reaction aliquot, suggesting almost total decomposition under the reaction conditions.



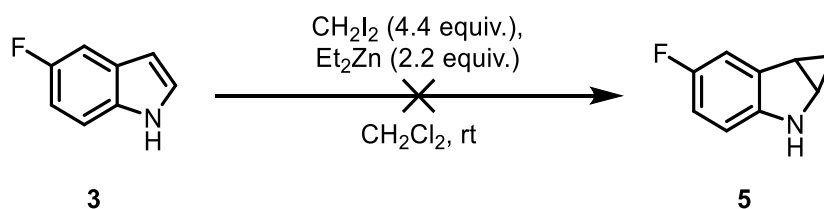
Scheme 2.6. Initial conditions for the ring expansion of **3** with a zinc carbenoid. Representative ^{19}F NMR spectrum of a reaction aliquot after 4 hours. 0.2 mmol scale.

Due to the almost quantitative consumption of the starting material, further investigations were undertaken to account for the missing mass balance. The Lewis basicity of the quinoline nitrogen makes them competent ligands for transition metals, including zinc.^{175,176} It was hypothesised that the quinoline product could ligate to the zinc salts produced during cyclopropanation, and that the resulting Lewis adduct may not be soluble in the reaction solvent. Consistent with this proposal, a precipitate was observed in the reaction mixture, although its identity was not determined. The resulting reaction mixture was therefore washed with both aqueous ammonia and Rochelle's salt in an attempt to liberate any product from complexation to zinc salts. Under these conditions, only trace amounts of the product could be detected by ¹⁹F NMR spectroscopy, suggesting significant decomposition as we first proposed. As the reaction aliquots were filtered prior to analysis to remove any insoluble material, it could be assumed that the starting material had decomposed to form this precipitate. Considering the insolubility of iodoform in dichloromethane, the reaction was also attempted with bromoform (Scheme 2.7). Under these conditions, similar total consumption of the starting material was observed, with only trace amounts of the product formed.



Scheme 2.7. Ring expansion of **3** with a bromoform-derived carbenoid. 1.0 mmol scale. Yields determined by ¹⁹F NMR spectroscopy.

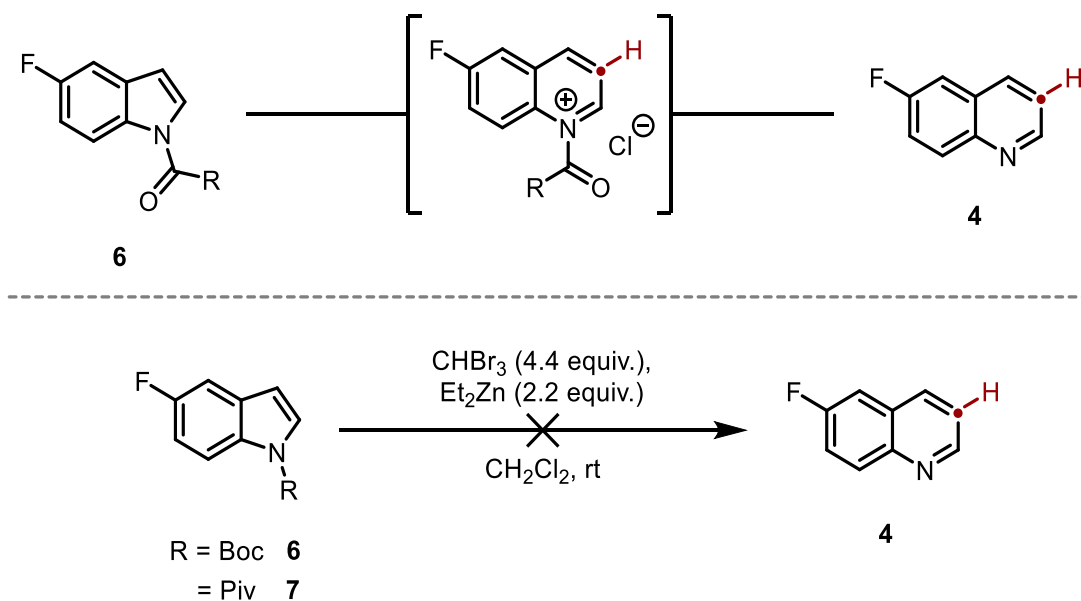
Since the total consumption of the indole was observed, the compatibility of the substrate with the classical Simmons-Smith conditions - rather than just halocyclopropanation methodologies - was investigated. To achieve this, **3** was subjected to standard Simmons-Smith conditions with diiodomethane as opposed to iodoform. Under these standard conditions, the resulting cyclopropanation **5** was not observed, suggesting incompatibility of the free indole with these conditions.



Scheme 2.8. Attempted Simmons-Smith cyclopropanation of **3**. 1.0 mmol scale. Yields determined by ¹⁹F NMR spectroscopy.

2.4 Modification of protecting group

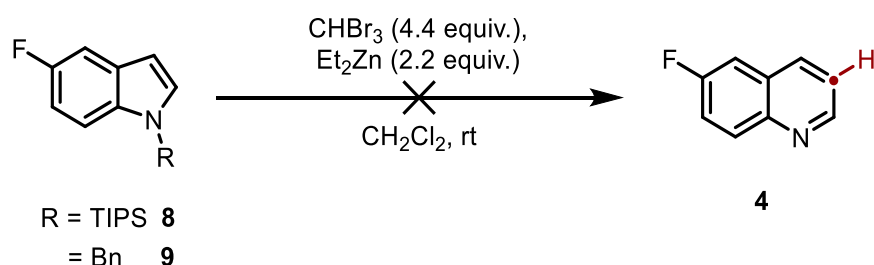
Since the unprotected 5-fluoroindole **3** proved incompatible, it was proposed that a protected indole would be better tolerated as deprotonation of the indole nitrogen is prevented. The cyclopropanation of protected indoles has been reported, employing Boc (*tert*-butoxycarbonyl) and Piv (2,2-dimethylpropanoyl) protecting groups, though not with zinc carbenoids.^{115,177–179} It can also be theorised that protection with an amide-like functional group would allow for *in situ* cleavage of the protecting group due to the instability of the resulting acyl quinolinium salt. The iodocyclopropanation shown in Scheme 2.9 on indoles protected with both groups was therefore carried out. However, under these conditions only starting material was observed after 16 hours for the Boc-protected indole. Although the decomposition of the indole had been prevented by indole protection, the substrate was totally unreactive. The same result was also observed for the Piv-protected substrate. Notably, in these cases a precipitate was observed prior to the addition of the indole suggesting possible precipitation of the carbenoid or decomposition.



Scheme 2.9. Top: Ring expansion of amide-protected indoles with *in situ* protecting group cleavage. Bottom: Attempted ring expansion of Boc- and Piv-protected indoles **6** and **7**. 1.0 mmol scale. Yields determined by ¹⁹F NMR spectroscopy.

Considering the poor reactivity of amide/carbamate-protected indoles under these conditions, the reactivity of more electron-rich indoles was investigated. In particular, a focus was placed on benzyl and silyl-protected indoles. In these cases, it was anticipated that silyl protection would lead to a similarly unstable *N*-silyl quinolinium salt which could be

deprotected *in situ*. On the other hand, a benzyl protected indole may allow for the formation of the stable quinolinium salt. Application of the ring expansion methodology to indoles **8** and **9** (Scheme 2.10) similarly provided no conversion to the desired quinoline **4**. However, in contrast to the reaction of unprotected indole **3**, the mass balance was primarily unreacted starting material.



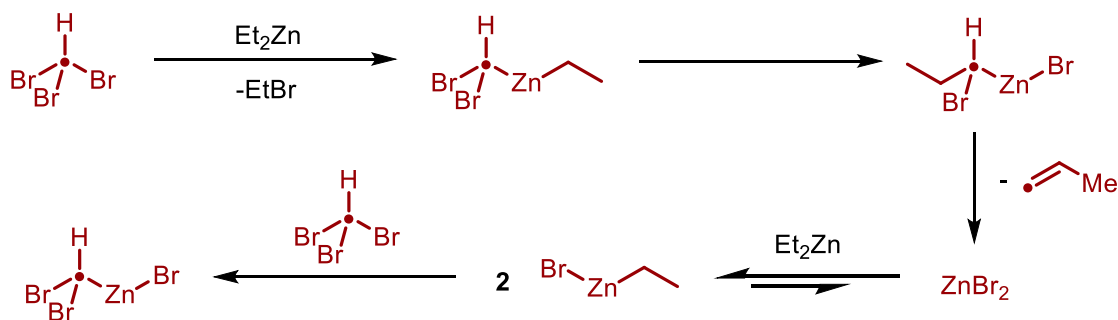
Scheme 2.10. Attempted ring expansion of **8** and **9**. 1.0 mmol scale. Yields determined by ^{19}F NMR spectroscopy.

Based on these observations, the carbenoid system was simply not reactive enough with the starting material to achieve the desired transformation. Modifications to conditions to aid reactivity were therefore required.

2.5 Addition of zinc halides

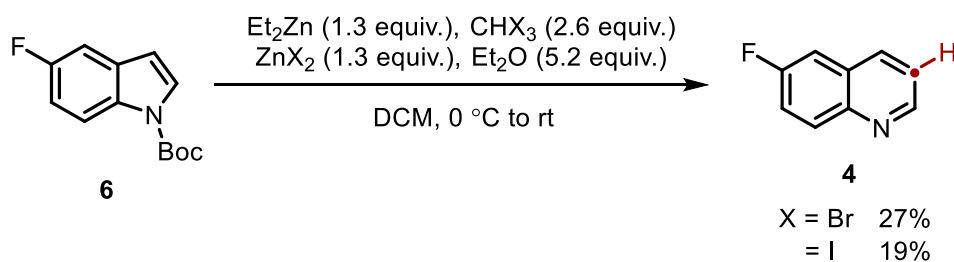
The bromocyclopropanation of allylic alcohols was reported by Charette and co-workers in 2015.¹⁷² In this report, the authors note similar observations to those observed in the present system when employing bromoform. In particular, when diethylzinc and bromoform were mixed, a precipitate quickly formed. The authors determined that this was in fact zinc(II) bromide, suggesting rapid decomposition of the carbenoid. Stabilisation was achieved by the addition of ligating ethers, with 2 equivalents of diethyl ether proving optimal.

The authors also suggested the active carbenoid in this transformation was in fact a carbenoid possessing a bromide ligand derived from a Schlenk equilibrium (Scheme 2.11) of diethylzinc and any zinc dibromide present. To bypass the deleterious side reactivity of the carbenoid, the active carbenoid could be accessed directly by reaction of diethylzinc with bromine or zinc(II) bromide in the presence of diethyl ether.



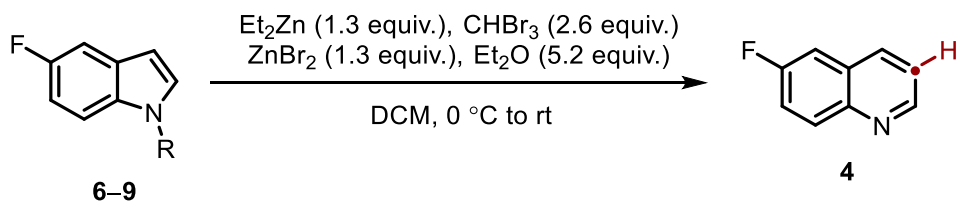
Scheme 2.11. Decomposition of the zinc carbenoid and the resulting Schlenk equilibrium.

With this knowledge, this new method was applied to the ring expansion of indoles. Knowing that unprotected indoles were not tolerated, this method was explored with Boc-protected indole **6**. Gratifyingly, after 16 hrs a 27% yield of the free quinoline product was observed, suggesting *in situ* deprotection. The same method was also applied to the generation of the iodomethylzinc carbenoid by reaction with zinc(II) iodide. In this case, a slightly lower 19% yield was determined by NMR spectroscopic analysis.



Scheme 2.12. Ring expansion of **6** with a carbenoid derived from Et_2Zn and ZnX_2 . 1.0 mmol scale. Yields determined by ^{19}F NMR spectroscopy.

With these promising results, and considering other protecting groups were simply unreactive, these new conditions were reapplied to other protected indoles. However, each indole proved unreactive, and no product was observed.

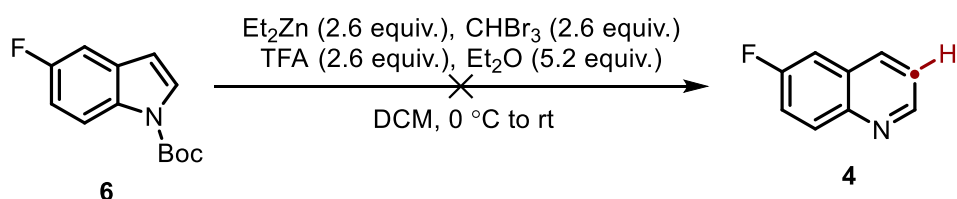


Entry	Protecting group, R	Yield of 4 / %
1	Boc (6)	27
2	Piv (7)	0
3	TIPS (8)	0
4	Bn (9)	0

Table 2.2. Re-evaluation of protecting groups with successful conditions. 1.0 mmol scale. Yields determined by ^{19}F NMR spectroscopy.

2.6 Subsequent optimisation

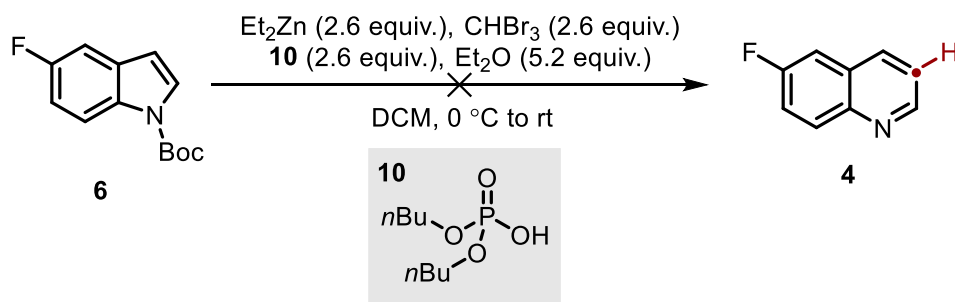
With this information, optimisation of the transformation of Boc-protected indole **6** was pursued. Initially, the identity of the second non-carbon ligand at the zinc centre was investigated. The electrophilicity of the carbenoid can be enhanced by introducing a trifluoroacetate ligand (so-called Shi's reagent) and can be used to cyclopropanate non-activated olefins.¹⁸⁰ When applied to the present transformation however, no further increase in yield was observed.



Scheme 13. Attempted ring expansion with a TFA-based carbenoid. 1.0 mmol scale. Yields determined by ^{19}F NMR spectroscopy.

To reduce the operational complexity of the transformation, exploration of other carbenoid systems was considered. Charette also developed a carbenoid system with a phosphonate ligand that is stable in solution for several days.¹⁴⁴ The successful use of this carbenoid would allow for optimisation to be carried out much faster. Before a stock solution was prepared, a

reaction was carried out with direct formation of the carbenoid to determine if the reaction with this carbenoid was feasible. Under these conditions, however, no conversion was observed after 16 hrs.



Scheme 14. Attempted ring expansion with a stable carbenoid. 1.0 mmol scale. Yields determined by ^{19}F NMR spectroscopy.

Ultimately, the Simmons-Smith reaction may have applications in carbon atom insertion, but the nature of the active species may lead to additional issues with substrate compatibility due to the high reactivity of zinc carbenoids. Although carbon insertion had been achieved in low yields, at this point the exploration of milder, more robust methods of carbon atom insertion was desired.

3

Single Carbon Atom Insertion with Arylchlorodiazirines

Abstract:

By utilising arylchlorodiazirines as photo-activatable sources of halocarbenes, the ring expansion of a range of protected indoles and pyrroles to the corresponding *N*-alkyl azinium salts was achieved. Protection of the indole nitrogen was found to be key to reactivity and precipitation of the azinium salt allowed for facile isolation by filtration. Both the scope of the azole and diazine partners were investigated, aided by a comprehensive robustness screen, which allowed for application to complex substrates. Functionalisation of the resulting products was investigated, focusing in particular on reduction chemistry. The thermal stability of diazirines as synthetic reagents is also discussed.

The results presented in this Chapter have been communicated in the following manuscript:
B. W. Joynson, G. R. Cumming, and L. T. Ball*, *Angew. Chem. Int. Ed.*, **2023**, e202305081.

3.1 Introduction

In the previous chapter, a synthetic route towards the one-carbon ring expansion of 5-fluoroindole with zinc carbenoids was outlined. While low yields were achieved, further experimentation led to no further increase in reaction yield. Additionally, the generation of the carbenoid and the subsequent reaction proved operationally complex and tedious. We therefore set out to identify a new class of carbene or carbenoid that could be readily isolated for ease of use, and most importantly, afford high yields of the desired atom-inserted product.

3.1.1 Arylchlorodiazirines

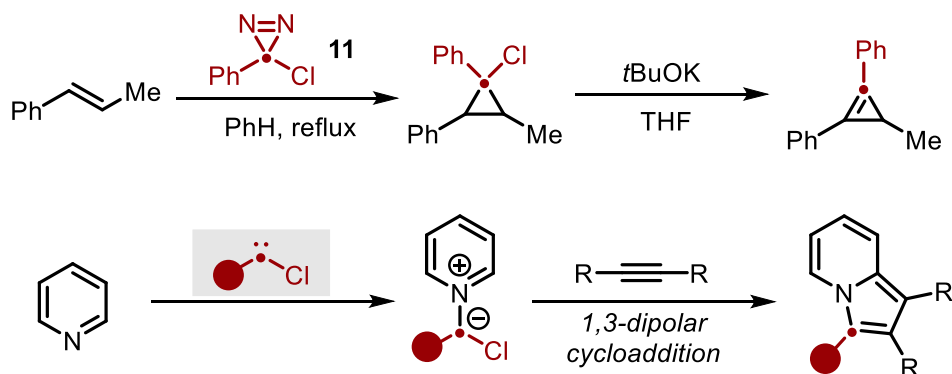
There are many notable carbene precursors that are bench-stable such as tri- and dichloroacetates (dichlorocarbene)⁸⁸ and TMSCF_3 (difluorocarbene),¹²³ but these precursors ultimately fail to fulfil the project aims due to both carbene substituents being limited to halides which only allow for the synthesis of 3-haloquinolines. One class of carbene precursors that proved promising were 3-chloro-3-aryl-3*H*-diazirines (henceforth referred to as ‘chlorodiazirines’ or simply ‘diazirines’). The diazirinyl functional group is structurally similar to that of the diazo functional group with the added benefit of enhanced stability.¹⁴⁹ This increased stability allows for the incorporation of functional groups, such as aryl groups, in place of the electron withdrawing groups required for diazo compounds, such as esters and phosphonates.¹⁵⁹

The corresponding free carbene can be generated readily *via* photolysis (UV-A) or by heating, potentially providing mild and functional group-tolerant reaction conditions.¹⁴⁹ Additionally, the diazirines are isolable and are stable for months when stored in a freezer. It should be noted that diazirines of this class have been reported to be explosive, and indeed thermodynamic data for 3-phenyl-3-chloro-3*H*-diazirine suggest this.¹⁸¹ Still, these diazirines present a synthetically useful carbynyl cation for the installation carbon atoms bearing non-EWG functional groups into the indole skeleton.

3.1.2 Chlorodiazirines in organic synthesis

Halodiazirines have seen use as synthetic reagents in the transformations and synthesis of organic compounds, though investigation into the synthesis of functionalised diazirines is still lacking. As carbene precursors, their reactions are typical of singlet carbene reactions, with the

added benefit of being able to install aryl rings as substituents due to the greater stability of the aryl diazirinyl functional group compared to other carbene precursors. These reactions include notably cyclopropanations¹⁸² as well as cycloadditions facilitated by the formation of nitrogen ylides by reaction of the free carbene with a tertiary amine/azine.^{183–186} The presence of the chloride atom as a potential nucleofuge presents additional complexity and synthetic utility to the typical reactions of carbenes and allows for the synthesis of cyclopropenes as well as aromatic heterocycles such as pyrroles *via* elimination.

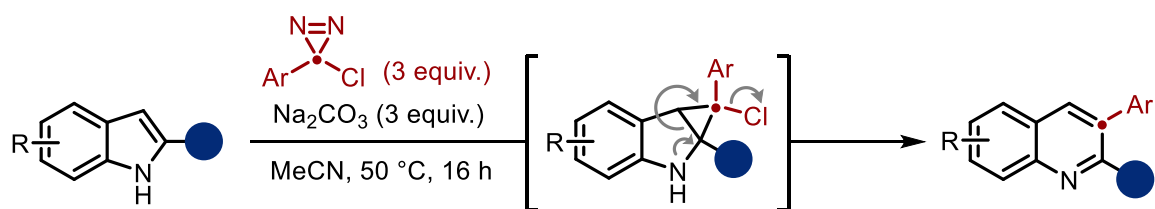


Scheme 3.1. Top: Cyclopropane synthesis reported by Padwa. Bottom: General scheme for [3+2] mediated by chlorodiazirines.

Despite these methods, it is worth noting that the application of chlorodiazirines as carbonyl synthons is underexplored in the literature, presenting an opportunity to apply these reagents in the single atom insertion into ring systems.

It should be noted that during the course of the research carried out in this section, an almost identical transformation was reported by Levin and co-workers.¹⁸⁷ The reaction outline will be mentioned here, but more detailed insights into the reaction such as the scope and mechanistic investigations will be mentioned when appropriate to the reaction developed in this chapter as a means of comparison. The aims for this project were set out prior to the release of this publication and are thus similar in concept to Levin's work.

The protocol reported employs chlorodiazirines as carbene precursors to cyclopropanate indoles and pyrroles, which spontaneously undergo a fragmentation reaction analogous to previous carbon atom insertions into pyrroles and indoles. The use of diazirines in this context allows for installation of aryl rings into heteroaromatic frameworks, which has previously been limited to halides or electron-withdrawing groups. Carbene generation was achieved by heating at 50 °C, without the need for harsh conditions or a transition metal catalyst. Additionally, a superstoichiometric base was employed to remove the HCl produced by the desired reaction as well as some decomposition pathways of chlorodiazirines.



Scheme 3.2. Carbon atom insertion into indoles and pyrroles developed by Levin and co-workers.

3.2 Project Hypothesis and Aims

Having identified chlorodiazirines as potential carbene precursors for the atom insertion into aromatic heterocycles, a number of key aims for this project were developed. These were mostly identical to the aims set out in the previous chapter but build upon the observations made during that research. Initially, the development and optimisation of the carbon atom insertion into indoles would be explored with the hope that it could be later applied to pyrroles and potentially other nitrogen heterocycles such as indazoles and benzimidazoles. This protocol would have to utilise mild conditions for the activation of the carbene and we envisioned that UV-A irradiation (365 nm) would achieve this. As diazirines can simply be added to the reaction mixture and the reaction initiated by irradiation, this remedies the issues with multiple additions seen with the use of zinc carbenoids, making the system far more user-friendly. The reaction would also have to tolerate a wide range of azole substrates as well as various substituents on the diazirine itself, as previously only small libraries of chlorodiazirines have been synthesised. Finally, for application in the modifications of late-stage drug targets, the reaction would have to tolerate medicinally-relevant functional groups.

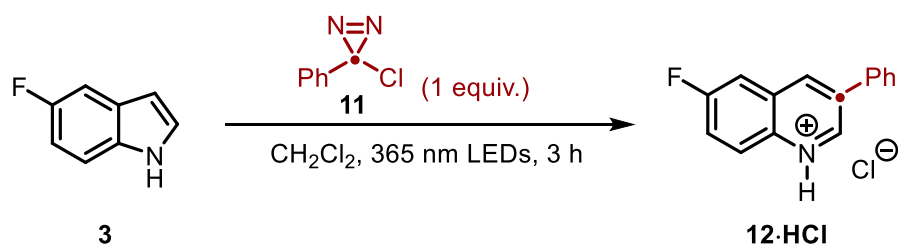
3.3 Development of reaction conditions

3.3.1 Initial Studies

The initial strategy involved irradiating an equimolar amount of 3-phenyl-3-chloro-3H-diazirine **11**, prepared by the Graham oxidation of benzamidine hydrochloride,¹⁵⁷ at 365 nm in the presence of 5-fluoroindole **3** (Table 3.1, entry 1). After 3 hours of irradiation in CDCl₃ on an NMR sample scale, only ca. 15% conversion was observed to a product spectroscopically consistent with the 3-arylquinolinium hydrochloride. The majority of the remaining mass balance was indole **3** with some unknown side products present. Although poor conversion

was observed, this suggested reaction feasibility and that significant optimisation would have to be undertaken to achieve high yields of the desired product. Replicating the reaction using toluene as the solvent led to no conversion to the desired product. When the reaction scale was increased to 1 mmol, similar conversions were observed in anhydrous dichloromethane compared to CDCl_3 .

Based on these results, it was clear that only a small portion of the photolysed diazirine **11** was reacting with the indole, with other side reactions such as dimerisations dominating. When the reaction was attempted with 1.5 equivalents of diazirine, no further conversion was observed (entry 2). The formation of a quinolinium hydrochloride is consistent with the production of HCl as a by-product. Assuming this had a deleterious effect on reaction yield, we envisioned the inclusion of a stoichiometric base would improve yields. However, the inclusion of NaHCO_3 also led to no further increase in yield (entry 3), though the free quinoline was observed by ^{19}F NMR spectroscopy rather than the salt.



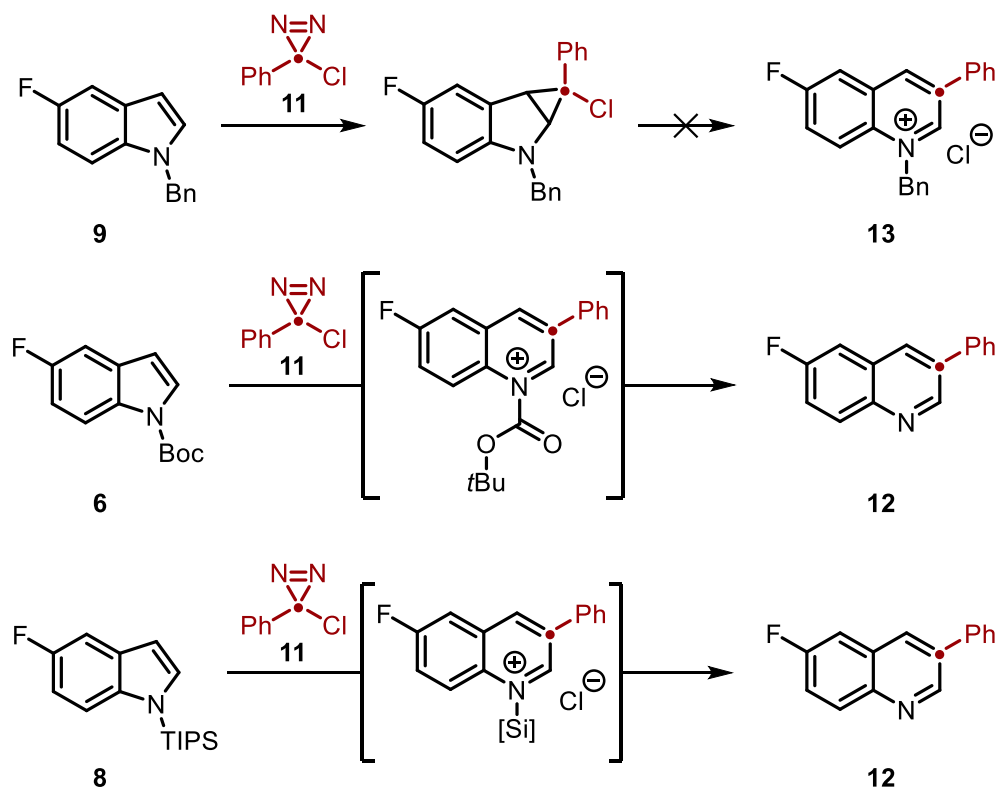
Entry	Deviation from above	Conversion to 12 / %
1	None	15
2	1.5 equiv. of 11	15
3	1 equiv. NaHCO_3 added	9 ^a

Table 3.1. Initial studies into the ring expansion of **3**. ^aAs free quinoline product. Conversions determined by ^{19}F NMR spectroscopy.

3.3.2 Protecting group modification

With the poor conversions of the unprotected indole, we next sought to modify the indole substrate by incorporating a nitrogen protecting group. This would avoid any reactions with the indole nitrogen, consistent with the strategy outlined in the previous chapter. It should be noted that the nature of the protecting group can drastically alter the electronic properties of the indole core (Scheme 3.3). Therefore, an initial range of three protecting groups were screened. The first, benzyl, would increase electron density at the indole core though the lack

of lability may result in the formation of the ‘halted’ cyclopropane if fragmentation to the quinolinium salt is not thermodynamically favoured. The Boc (*tert*-butoxycarbonyl) group would serve as the antithetical protecting group. It would transform the *N*-atom into amide-like functional group, decreasing electron density, though may act as a more capable electrofuge and be cleaved *in situ* upon ring expansion. Finally, silyl protecting groups would offer a middle ground, increasing electron density but also leading to an unstable *N*-silyl quinolinium salt, which would be deprotected *in situ*.



Scheme 3.3. Protecting group strategy highlighting potential shortcomings of alkyl protecting groups and possible benefits of labile groups

The Boc protected indole **6** proved unreactive, most likely attributed to the reduction in electron density preventing attack of the highly electrophilic carbene. Despite the opposite electronic character, TIPS (triisopropylsilyl) also proved unreactive though a small amount of the quinolinium salt **13** was observed for the benzylated indole, in each case returning the starting indoles **8** and **9** after irradiation for 3 hrs. Due to the presence of starting materials **8** and **9**, we inferred that the limitation was not the indole itself, but rather the irradiation time. For ease of reaction monitoring by ^{19}F NMR spectroscopy, a fluorinated diazirine analogue **14** was synthesised to monitor both the product formation and the diazirine decomposition.

Monitoring the reaction for 3 hrs showed a significant portion of the diazirine **14** remained unreacted (Figure 3.6), suggesting slow formation of the carbene or other reactive

intermediates. With this knowledge, the reaction time was increased from 3 hrs to overnight (16 hrs) to allow for increased carbene formation. Despite this increase in reaction time, no further product was observed in either the unprotected or protected indoles with other diazirine side-products present.

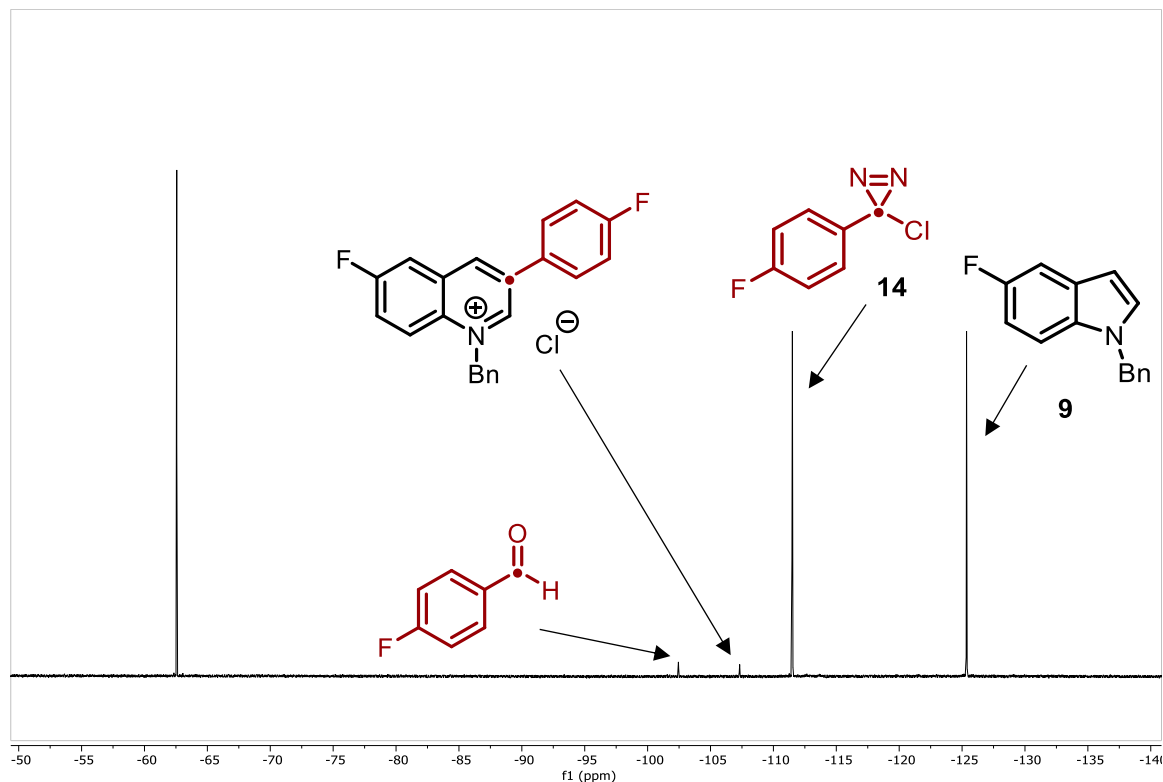
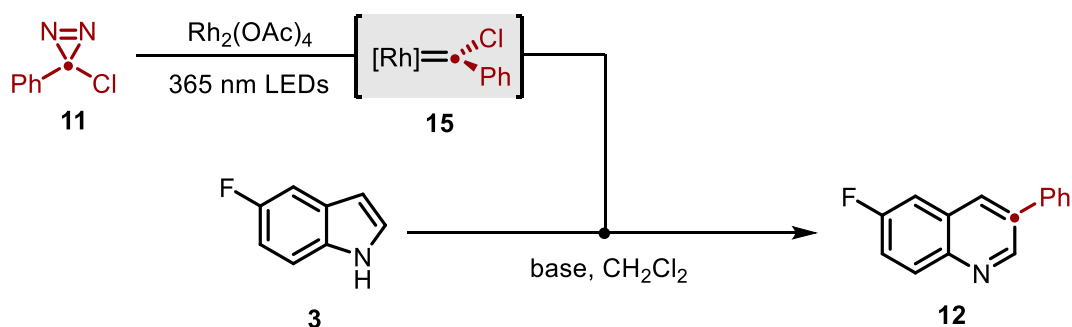


Figure 3.6. ^{19}F NMR spectrum of crude reaction mixture after 3 hrs. Int. std. = 4,4'-(trifluoromethyl)-1,1'-biphenyl. D1 = 30 s. Quinolinium 4-fluoroarene peak is obscured by diazirine **14**.

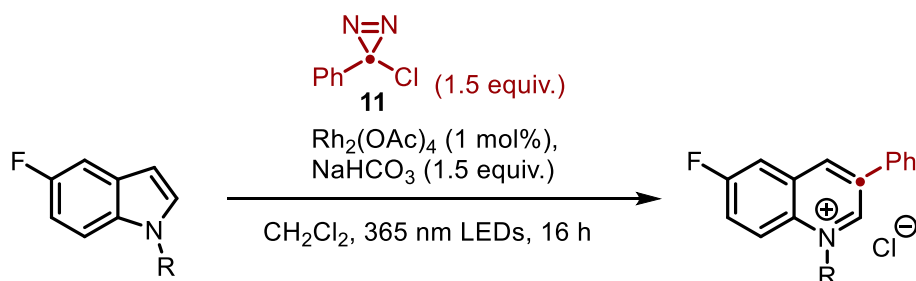
3.3.3 Carbene capture with rhodium

Having observed a large degree of deleterious decompositions of the fluorinated diazirine following extended irradiation, the development of a more selective system was investigated such that the carbene is more easily able to react with the desired indole. A potential promising modification to the method might be the inclusion of a Rh(II) salt to form a metal carbenoid (Scheme 3.4). As shown by Bonge-Hansen and co-workers, Rh-carbenoids are competent reagents for the cyclopropanation of indoles in the carbon atom insertion reaction.^{89,90} In this case however, photolysis of the diazirine would produce the carbene *in situ*, allowing for the formation of carbenoid **15** resulting from what would be a highly unstable diazo compound using typical methods.



Scheme 3.4. Rationale for the inclusion of Rh(II) salts in the ring expansion methodology.

Once again using the work of Bonge-Hansen as a template, the reaction was performed in the presence of 1 mol% $\text{Rh}_2(\text{OAc})_4$ and a superstoichiometric amount of an inorganic base. Unlike the previous examples using Rh-carbenoids, the use of the free indole did not afford a significant amount of product, although small amounts of the benzyl quinolinium salt were observed when employing the benzylated indole. Additionally, the TIPS-protected indole afforded small amounts of the quinoline product, although lower than the initial tests. Attempts to optimise the transformation proved unproductive. Both NaHCO_3 and Cs_2CO_3 gave similar results, although slightly higher NMR yields were observed using NaHCO_3 . As the rhodium appeared to have little effect on the selectivity of the carbene reactions, the next course of action was to greatly increase the amount of diazirine employed.

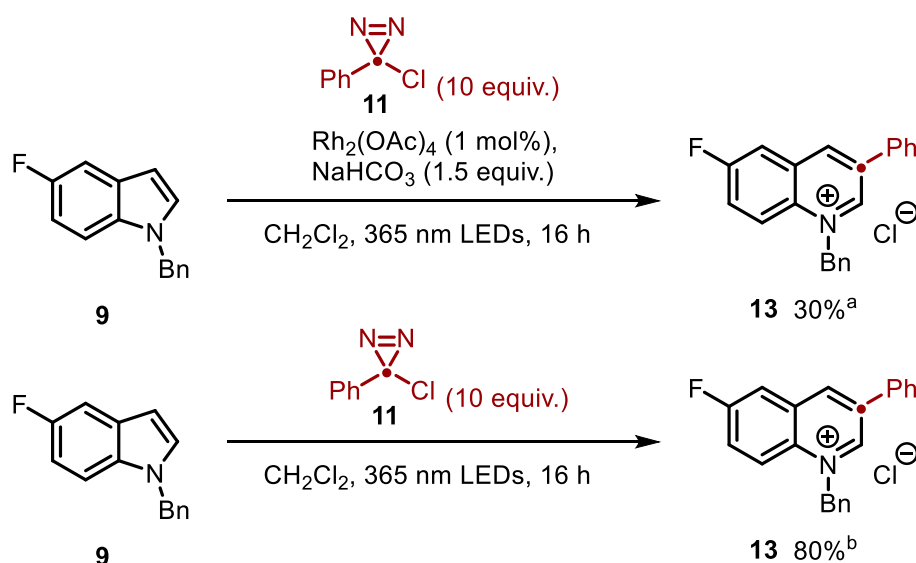


Entry	Protecting Group, R	Base	Yield of 12 or 13 / %
1	Bn (9)	NaHCO_3	9
2	Bn (9)	Cs_2CO_3	<5
3	TIPS (8)	NaHCO_3	<5
4	TIPS (8)	Cs_2CO_3	0

Table 2.2. Rh-mediated ring expansions of protected indoles **12** and **13**. 0.2 mmol scale. Yields determined by ^{19}F NMR spectroscopy.

3.3.4 Diazirine stoichiometry

If the selectivity of the carbene cyclopropanation could not be controlled *via* a transition metal, it was hypothesised that increasing the amount of carbene available over the course of the reaction may increase yields. Therefore, the reaction of benzylated indole **9** was carried out with 10 equivalents of **11**. While 10 equivalents is a significant excess of the reagent, it was anticipated that this stoichiometry would give insight into whether the reaction is feasible and optimisation would involve decreasing diazirine stoichiometry. When employing 10 equivalents of **11** in the rhodium-catalysed variation, a 30% yield of the quinolinium salt was obtained (Scheme 3.5). Considering the stoichiometry of **11** was having a clear effect on yield, the reaction was repeated in the absence of both the rhodium catalyst and the inorganic base. Under these conditions, a precipitate was observed after irradiation for 16 hrs. NMR analysis showed the precipitate to be the pure quinolinium salt, which was isolated in an 80% yield (Scheme 3.5). The lack of any additives in this transformation increased potential appeal by increasing atom economy. With the identification of these conditions, we set out to optimise the reaction conditions further.

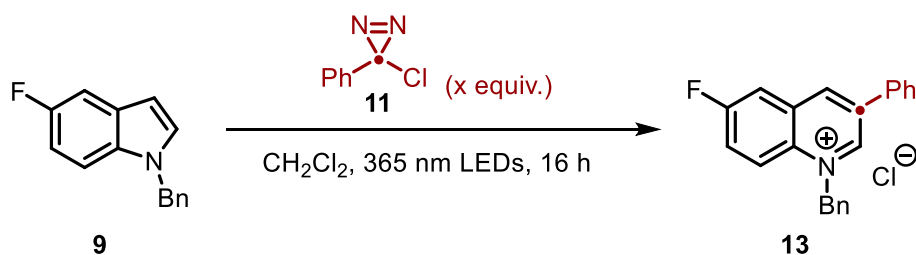


Scheme 3.5. Top: Reaction employing 10 equivalents of **11**. Bottom: 10 equivalents of **11** in the absence of any additives with isolation of precipitates. ^aNMR yield. ^bIsolated yield.

3.3.5 Reaction optimisation

The first obvious optimisation is to decrease the amount of diazirine used to a synthetically-viable amount. Although a superstoichiometric amount is clearly required, the use of 10 equivalents decreases the viability of this procedure for practical applications. Decreasing the amount of **11** to 5 equivalents resulted in no significant alteration in yield (Table 3.3,

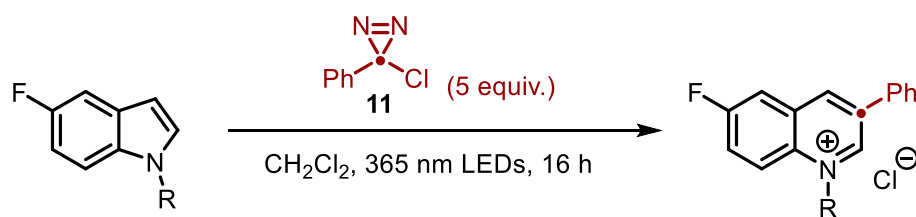
entry 2) and decreasing further to only 3 equivalents of **11** reduced the yield only slightly to 77% (entry 3), though this may be a result of the intrinsic error in calculating NMR yields and yields are in fact very similar. For further optimisations, 5 equivalents were employed although later reactions would prove 3 equivalents gave equal yields and was ultimately selected as the optimal choice. This appears to be the limit for the transformation, as performing the reaction with 2 equivalents of **11** resulted in a 65% yield which, while modest, is a significant reduction in yield compared to using 3 equivalents (entry 4). In each case, full precipitation of the salt was observed in the DCM solvent which allowed for facile isolation of the pure product by simple filtration of the reaction mixture.



Entry	Equivalents of 11 , x	Yield of 13 / %
1	10	80
2	5	82
3	3	77
4	2	65

Table 3.3. Optimisation of stoichiometry of **11** in the ring expansion protocol. 0.2 mmol scale. Yields determined by ^{19}F NMR spectroscopy.

Having identified suitable reaction conditions regarding the diazirine, investigations into the indole substrate were undertaken. While excellent yields were observed for the benzyl indole **13**, the ideal synthesis of the free quinoline **12** from the indole is hampered both by the initial benzylation of the indole, but also by a subsequent deprotection step, decreasing the ideal atom economy of the process. Therefore, an exploration into the compatibility of a number of protecting groups was undertaken. Based on earlier observations, an alkyl protecting group similar to benzyl is likely required to improve electron density although at this point only Boc had been employed as an outlier to this group. A range of protecting groups were therefore screened, as shown in Table 3.4.

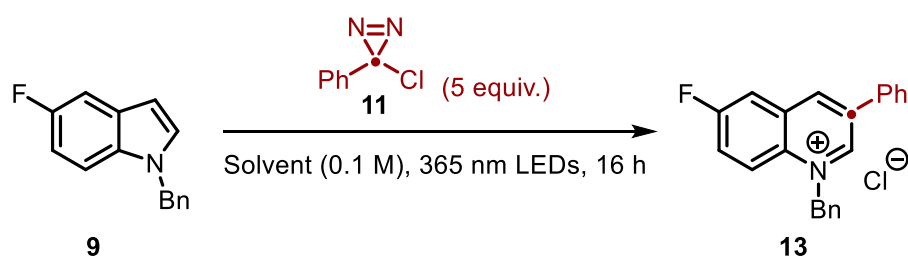


Entry	Protecting group, R	Yield / %
1	Bn	82
2	PMB	51
3	Me	28
4	Allyl	6
5	MOM	5
6	TIPS	0
7	SEM	0
8	Boc	3 ^a
9	Piv	0
10	Ts	0

Table 3.4. Optimisation of protecting group. 0.2 mmol reaction scale. Yields determined by ¹⁹F NMR. ^aAs unprotected quinoline. PMB = *para*-methoxybenzyl; MOM = methoxymethyl; TIPS = triisopropylsilyl; SEM = trimethylsilylethoxy methyl; Boc = *tert*-butoxycarbonyl; Piv = 2,2-dimethylpropanoyl (pivaloyl); Ts = *p*-toluenesulfonyl.

As expected, alkyl protecting groups proved most effective, with benzyl (entry 1) remaining the optimal protecting group. PMB (*para*-methoxybenzyl, entry 2) also proved effective, providing a 51% yield, though the salt exhibited higher solubility in the DCM solvent. Methyl provided a modest yield of 28% (entry 3), with the resulting quinolinium salt proving far more soluble once again. The other alkyl groups tested, allyl (entry 4), MOM (methoxymethyl ether, entry 5), and SEM (trimethylsilyl ethoxymethyl, entry 6), gave poor NMR yields in both cases. Despite possessing similar electronic properties to alkyl groups, the silyl group TIPS afforded no product. As before, Boc gave poor yields, although the free quinoline was observed in a 3% yield by ¹⁹F NMR. Protecting groups of similar electronic character - pivaloyl (entry 9) and tosyl (entry 10) - proved unreactive, providing further evidence that an electron-rich indole is paramount for efficient transformation.

While dichloromethane is a highly efficient solvent for this transformation, a screen of a number of solvents and their effects on the reaction protocol was carried out (Table 3.5). It was anticipated that less polar solvents would decrease the solubility of the salt product further, potentially increasing isolated yields. Both toluene and TBME (*tert*-butylmethyl ether) provided lower yields in each case (entries 2 and 3). As a comparison, more polar solvents were screened to judge the solubility of the resulting salt and the effect of the solvent on yield. Acetonitrile afforded a modest yield of 20% (entry 4) with no observed precipitation while no product nor precipitated were observed when methanol was employed (entry 5). The lack of reactivity when employing methanol is likely due to the protic, nucleophilic nature of the solvent interacting with the carbene generated by competitive O-H insertion, preventing desired reactivity. The poor yield when employing acetonitrile may arise from similar origins with the solvent undergoing Ritter-type additions into the carbene, though the far less nucleophilic nitrile has a weaker affinity to degrade the carbene.

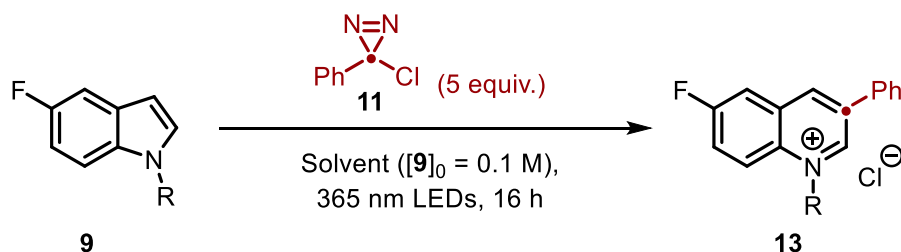


Entry	Solvent	Yield of 13 / %
1	CH₂Cl₂	82
2	PhMe	37
3	TBME	49
4	MeCN	20
5	MeOH	0

Table 3.5. Optimisation of reaction solvent. 0.2 mmol reaction scale. Yields determined by ¹⁹F NMR. TBME = *tert*-butylmethyl ether.

Having investigated the impact of protecting groups and solvents, optimisation of the general reaction conditions was then performed. The standard conditions of the reaction are highlighted in Table 3.6. To avoid potential side reactions of the highly reactive carbene with water, anhydrous solvents had been employed in all reactions thus far. Using commercial-grade

dichloromethane without drying beforehand resulted in a drastic decrease in yield to 42% (entry 2), suggesting competitive reaction with water (or other impurities) present in the solvent. When oxygen and atmospheric water were excluded from the solvent by degassing (sparging with dinitrogen), a slightly higher yield of 55% was observed (entry 3), though reaction with the water still remained significant.



Entry	Deviation from above	Yield of 13 / %
1	None	82
2	Aerobic, undried CH ₂ Cl ₂	42
3	Degassed, undried CH ₂ Cl ₂	55
4	0.2 M	37
5	0.05 M	80
6	Scratched MW tube	81
7	6 h reaction time	65
8	No UV light + darkness	4

Table 3.6. Optimisation of various reaction conditions. 0.2 mmol scale. Yields determined by ¹⁹F NMR spectroscopy. Degassed refers to sparging with dinitrogen for 30 mins. Scratched refers to a reaction vessel bearing considerable surface damage.

It was anticipated that the reaction concentration could have significant effects on the formation of the desired product. A higher concentration could potentially lead to more competitive inter-carbene reactions such as dimerisations as the concentration of the free carbene would be intrinsically greater. Additionally, as the product precipitates over the course of the reaction, at higher concentrations, the resulting solid would more greatly obfuscate the UV light compared to lower concentrations and light would penetrate to a lesser degree. Indeed, increasing the concentration two-fold resulted in a significant decrease in yield to 37% (entry 4). By contrast, it was hypothesised that decreasing the concentration would aid light penetration and hinder carbene dimerisations but also alter the reaction rate of the desired

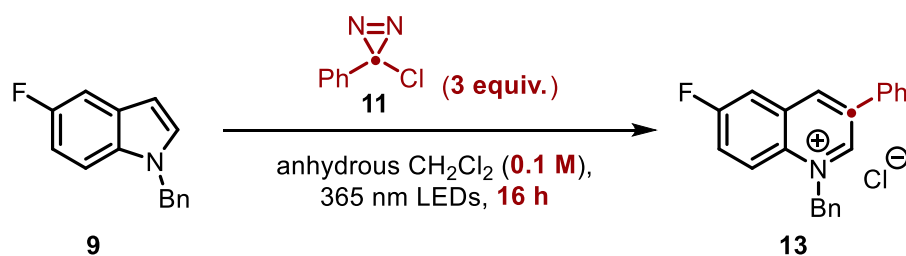
process and aid dissolution of the product in the greater volume of solvent. When the reaction was performed at a concentration of 0.05 M with respect to **9** an almost identical yield of 80% was observed (entry 5) suggesting that despite the potential drawbacks, the reaction tolerates a lower concentration than 0.1 M. For practicality reasons, the reaction concentration was maintained at 0.1 M as it is more economical in solvent.

As the reaction is driven by photolytic activation of the carbene, the penetration of the light into the reaction vessel might affect conversion. Over time, reaction vessels, especially microwave tubes - in which these reactions were carried out - are damaged by mechanical stirrers. This has the effect of creating a translucent haze in the flask due to the scattering of light on the scratches. While the effect is obvious for visible light, we aimed to test whether the effect on UV light was drastic enough to decrease yields to ensure compatibility between experiments and to account for variability in glassware quality. When employing a heavily-damaged translucent reaction vessel, no significant change in yield was observed (entry 6), allowing for any flask to be employed in the transformation.

A further avenue of exploration for optimisation was reaction time. Early on in the project, it was determined that a 16 hour reaction time was required for full conversion of the diazirine. However, under these new optimised conditions, we sought to return to this parameter to determine if the reaction is complete in a shorter timescale, ideally allowing for the reaction to be carried out in under one working day. Halting the reaction after 6 hrs resulted in an observed yield of 65% (entry 7) which, while high, remains a significant enough deviation from the optimum that it was decided to maintain the overnight reaction time in the optimised conditions.

Finally, the necessity of UV irradiation was investigated to determine whether it is required for high yields. Diazirines are known to decompose to the carbene *via* thermolysis and are unstable at room temperature for extended periods of time (*ca.* 24 hrs) when neat. To determine whether the reaction proceeded *via* a significant thermal pathway, the reaction was carried out without UV irradiation and wrapped in foil to avoid ambient photolysis at 30 °C. The higher temperature was used due to the heat radiated by the UV lamp which, despite cooling with a fan, can cause temperatures within the photoreactor to reach 30 °C over the 16 hour period. After 16 hours, only 4% of the product was observed (entry 7), providing evidence that photolytic generation of the carbene dominates under standard conditions.

The conditions shown in Scheme 3.6 were identified as suitable for further investigation and were therefore carried forward to study the reaction scope and limitations.

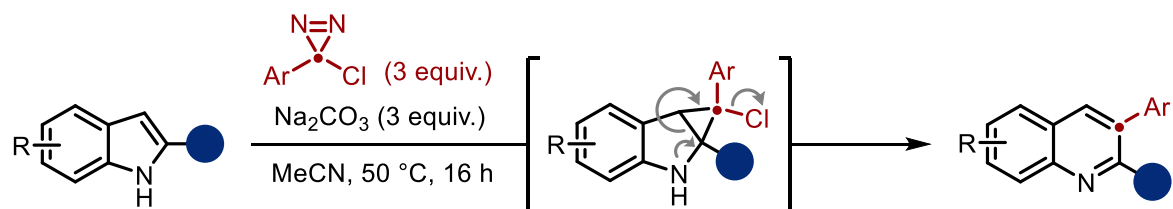


Scheme 3.6. Working reaction conditions.

3.4 Comparison to Levin et al.

Shortly after optimisation was completed, and prior to any meaningful explorations into substrate scope, a very similar transformation was reported by Levin and co-workers.¹⁸⁷ While it was mentioned at the beginning of this chapter, it is worth reiterating the conditions developed by Levin and co-workers and how they compare to the protocol designed herein.

Levin and co-workers reported the insertion of a carbon atom into the aromatic skeleton of *unprotected* indoles and pyrroles utilising chlorodiazirines as we have (Scheme 3.7). Notably, three equivalents of diazirine were found to be optimal, consistent with our own findings, in addition to the inclusion of three equivalents of Na_2CO_3 as a base. The most notable differences are the method of activation of the diazirine, which was achieved thermally rather than photolytically, and the solvent employed, which was acetonitrile rather than dichloromethane. The reaction protocol allowed for the transformation of a number of substituted indoles bearing various functional groups. This allowed for the editing of functionalised molecules such as tryptophan and the pyrrolic core of atorvastatin. Additionally, the chemistry was applied to the synthesis of quinoline cyclophanes.



Scheme 3.7. Single carbon atom insertion with chlorodiazirines developed by Levin and co-workers.

3.4.1 Limitations of Levin's work

While the chemistry could be applied to a range of functionalised substrates, there exists a clear limitation of the substitution pattern of the starting material. Specifically, a substituent at the 2-position of the starting azole is required for high yields. This is exemplified by the reported yields of two quinolines formed from a substituted and unsubstituted indole **16** and **17** (Figure 3.1).

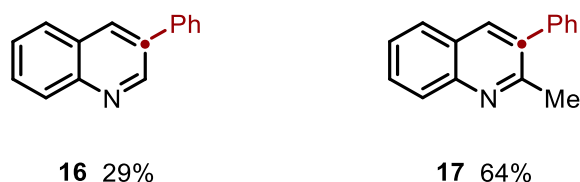
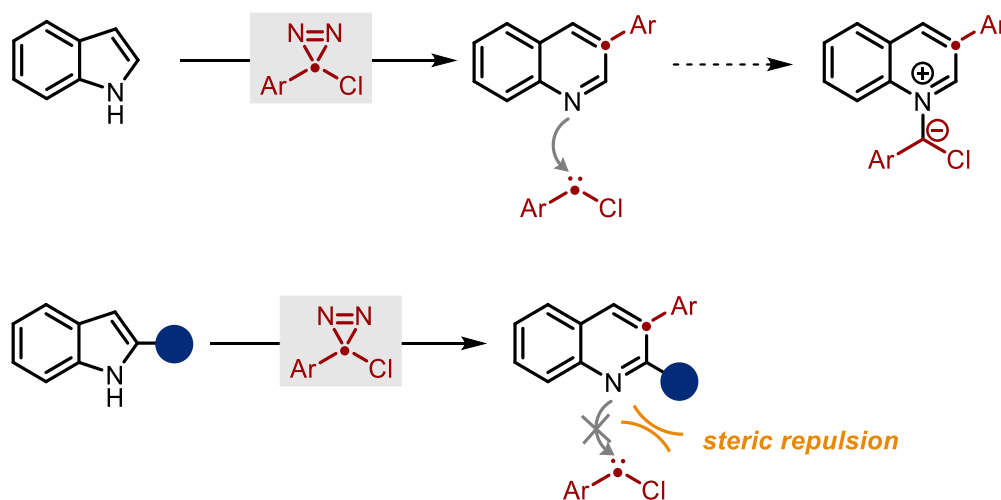


Figure 3.1. Comparison of yields for substrates with and without substitution at the 2-position. Reported as isolated yields.

The authors report the rationale for this difference as a deleterious interaction of the *product* with the carbene, rather than the starting material. The nucleophilic nitrogen of the product is capable of undergoing addition into the free carbene, resulting in a nitrogen ylide, both decomposing the starting material and quenching the reactivity of the free carbene. The introduction of a substituent, typically alkyl or aryl, at the 2-position introduces a steric blocker, kinetically disfavoring attack of the carbene. This interaction was further demonstrated by the inclusion of quinoline as an additive in the ring expansion of 2-phenylindole (Table 3.7, entry 2), which afforded the quinoline product in a 15% yield, compared to 68% in its absence (entry 1).



Scheme 3.8. Mechanistic rationale for the importance of 2-substitution postulated by Levin.

Further quenching studies were also undertaken. The inclusion of the inorganic base is paramount in achieving high yields. By quenching the HCl formed during ring expansion, the

Na_2CO_3 acts as a chloride abstractor, sequestering the chloride anion from solution. This is essential because - like the quinoline product - chloride is nucleophilic enough to undergo addition into the carbene. Carrying out the reaction of 2-methylindole in the presence of TBAC (tetrabutylammonium chloride) led to a 21% yield of **17** with 69% of the starting material **18** remaining (entry 3). Benzal chloride **22** formed from reaction of chloride with the carbene was also isolated in an 11% with respect to diazine stoichiometry. When the quenching study was applied to a 2-unsubstituted indole, the dimerised product **21** was detected in a 67% yield, with the formation of only trace amounts of the desired product. In this case, benzal chloride **22** was isolated in a 34% yield.

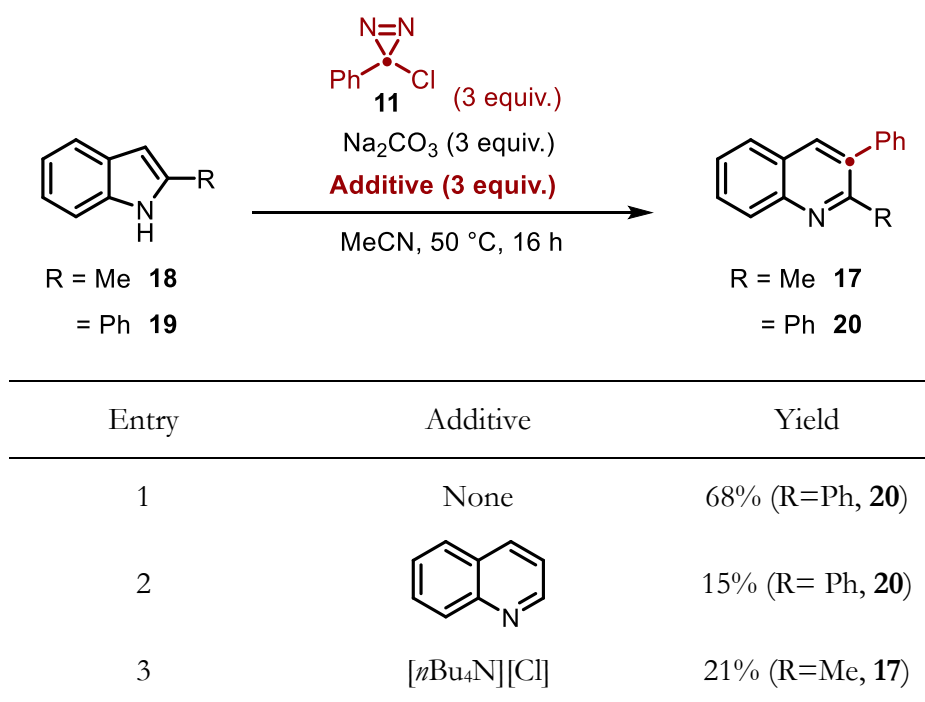


Table 3.7. Quenching studies performed by Levin and co-workers. Isolated yields.

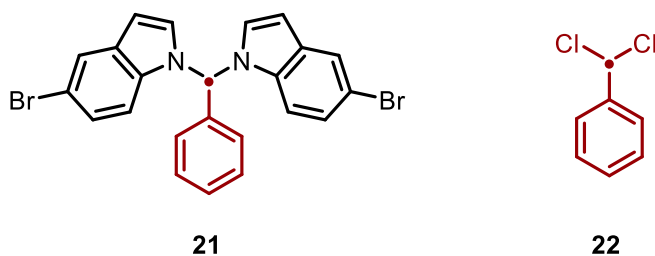


Figure 3.2. By-products formed in the presence of additives reported by Levin.

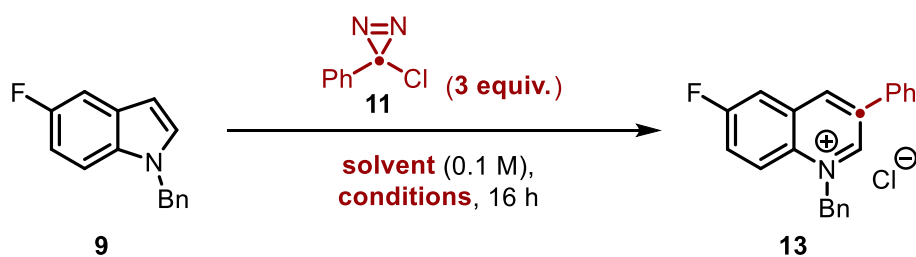
These studies reveal a significant limitation in Levin's work: namely, the requirement for substitution at the 2-position restricts the scope ofazole substrate that can be employed. In contrast, this consideration does not apply to the transformation developed herein.

The lack of need for a substituted indole can be explained due to the indole nitrogen, and by extension the quinolinium salt product, already being protected and is therefore inert to attack from the electrophilic carbene. The rationale for the lack of base is more subtle. As the quinolinium salt precipitates from solution as the chloride salt, it sequesters chloride from the reaction mixture, decreasing available chloride without an exogenous reagent. With this, it was decided that substrate scope would focus on the synthesis of 2*H*-quinolinium salts as these quinolines would otherwise be unachievable in good yield when utilising Levin's methodology.

3.4.2 Direct comparison of reaction conditions

With a greater understanding of the rationale for the choice of azole and base, comparison of other differences, particularly the choice of solvent and method of carbene generation, was investigated. A series of reactions were undertaken utilising Levin's conditions with the substrates employed in our own reaction.

The ring expansion of **9** was carried out in both dichloromethane and acetonitrile, with each reaction also being carried out under photolytic conditions (365 nm LEDs) or at 50 °C for four reactions in total. The results of this investigation are shown in Table 3.8.



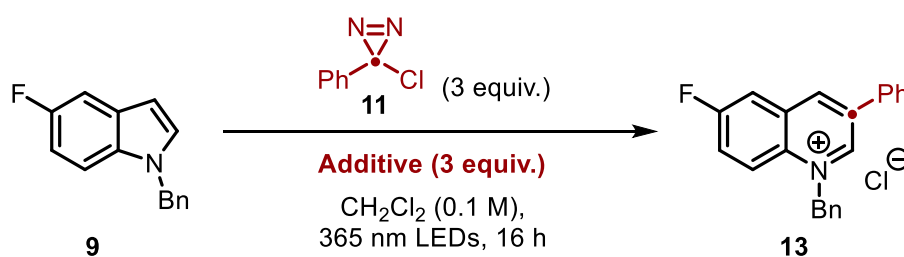
Entry	Solvent	Conditions	Yield of 13 / %	9 / %
1	CH ₂ Cl ₂	<i>hν</i> (365 nm)	82	2
2	CH ₂ Cl ₂	50 °C	64	19
3	MeCN	<i>hν</i> (365 nm)	20	35
4	MeCN	50 °C	16	34

Table 3.8. Comparison of conditions based on the work of Levin et al. 0.2 mmol scale. Yields determined by ¹⁹F NMR spectroscopy.

Compared to standard photolytic conditions, thermolysis in dichloromethane affords good yields after 16 hrs (entry 2), though significantly decreased. As seen previously, acetonitrile is a poor solvent for this transformation (entry 3), despite the report from Levin utilising this

solvent. Yields are likely diminished by the greater solubility of the product in this solvent increasing the concentration of chloride in solution; this is consistent with the observation that a significant portion of starting material remained. As expected, combining both the poorer thermolysis and acetonitrile solvent resulted in further diminished yields (entry 4).

As part of our own mechanistic understanding of the reaction, the quenching studies performed by Levin to confirm the effect of Lewis basic functionality on the reaction were repeated. Identical to their studies, the ring expansion procedure was carried out in the presence of 3 equivalents of the Lewis base additive. Both quinoline and TBAC were employed as additives, though the reaction was also carried out in the presence of 2-methylquinoline, not reported by Levin, to confirm the blocking effects of the 2-substituent (Table 3.9).



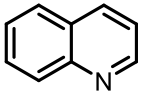
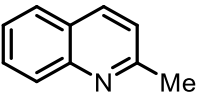
Entry	Additive	Yield of 13 / %
1	None	82
2		7
3		21
4	[<i>n</i> Bu ₄ N]Cl	0

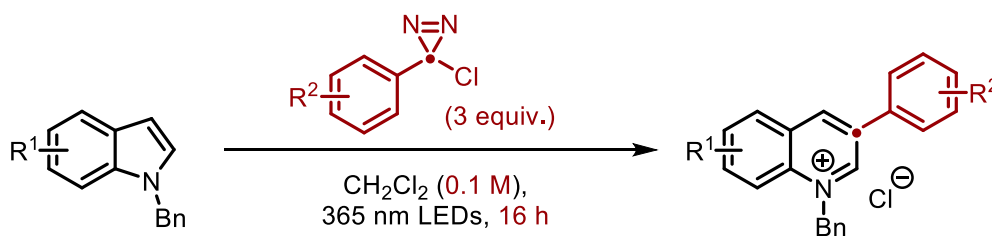
Table 3.9. Quenching studies of the ring expansion of **9**. 0.2 mmol scale. Yields determined by ¹⁹F NMR spectroscopic analysis.

As expected, the inclusion of 3 equivalents of quinoline (entry 2) led to almost total quenching of reactivity due to addition into the carbene consistent with Levin's findings. When 2-methylquinoline was employed, a significant but smaller decrease in yield was observed with 21% of the product **13** formed by NMR spectroscopic analysis (entry 3). Although this decrease in yield is substantial, 3 equivalents were employed with equal stoichiometry to the diazirine and therefore should result in near total quenching of the carbene. In this case, the 21% yield suggests the methyl group is successfully preventing carbene addition. Consistent

with Levin's findings, the inclusion of 3 equivalents of TBAC led to no product formation (entry 4).

3.5 Substrate scope of indoles

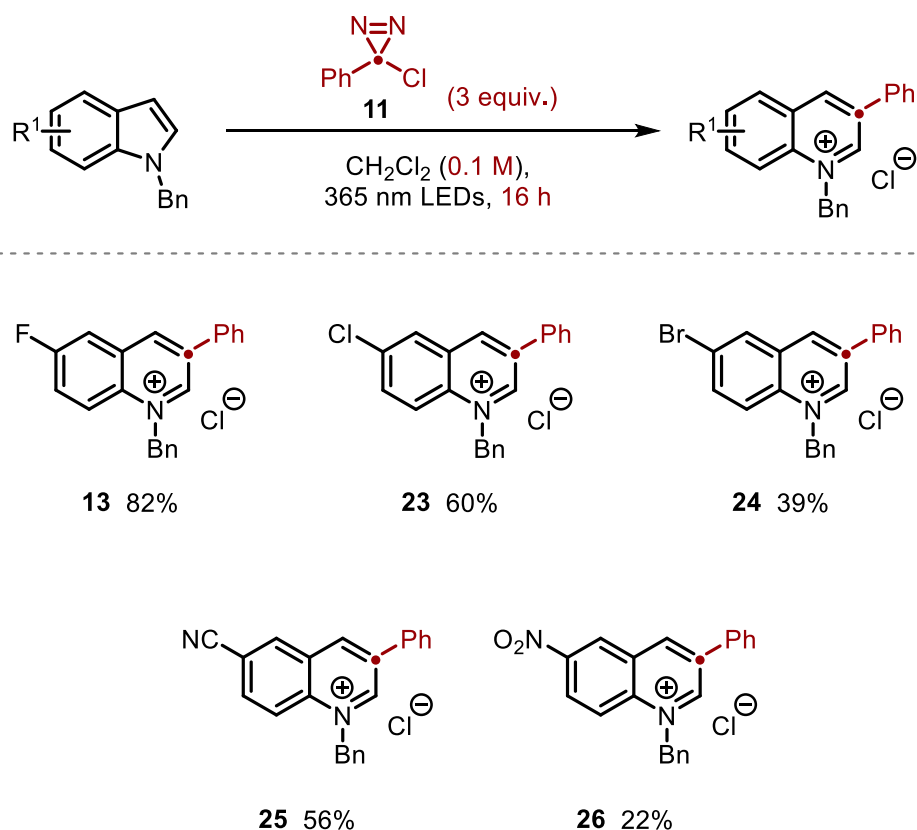
With the optimised conditions in hand and a greater understanding of the mechanistic nuances of the reaction, the protocol could now be applied to a range of substituted indoles. The investigation was designed to explore the tolerance of electronically- and sterically-diverse substrates bearing common functional groups in the transformation. Since the reaction involves the coupling of an indole with a diazirine, the substitution of both partners could be modified (Scheme 3.9), allowing for a comprehensive understanding of steric and electronic effects.



Scheme 3.9. General scheme for the exploration of substrate scope.

3.5.1 Electron-deficient indoles

The first class of substituted indoles investigated were indoles bearing electron-withdrawing substituents. Ideally, this would test the limitations of the reaction as, based on protecting group optimisation, we postulated that a nucleophilic indole is key to high reactivity. The incorporation of electron-withdrawing substituents was expected to reduce nucleophilicity and potentially decrease yields. For an even comparison, all substituted indoles were reacted with diazirine **11**.



Scheme 3.10. Initial substrate scope of electron-deficient indoles. 0.2 mmol scale. Isolate yields

Initial exploration of scope returned moderate yields of electron-deficient indoles (Scheme 3.10). The reaction tolerated halides at the 5-position, with 5-chloroindole and 5-bromoindole affording the quinolinium salts **23** and **24** in 60% and 39% yields respectively. Although modest, these yields are considerably higher than those reported by Levin and have the additional benefit of providing additional functional handles for cross-coupling chemistry. A 5-cyanoindole was also well tolerated by the reaction and the product **25** was achieved in a 56% yield. Unfortunately, a 5-nitroindole afforded poor yields, achieving **26** in a 22% after 16 hours. This can likely be attributed to the strong electron-withdrawing effect of the nitro group ($\sigma_{\text{para}} = +0.72$) as well as potential excitation of the nitro group to a reactive diradical, which can be achieved with purple LEDs (390 nm).^{188,189}

Considering the decreased nucleophilicity of electron-deficient indoles, increasing the stoichiometry of **11** would potentially improve yields for these substrates. Indeed, subjecting the previous indoles to the reaction conditions employing 5 equivalents of **11** afforded improved yields in each case as shown in Figure 3.3 with the exception of **13** and **25**, the yields of which remained near identical.

3 equiv. **11** → 5 equiv. **11**

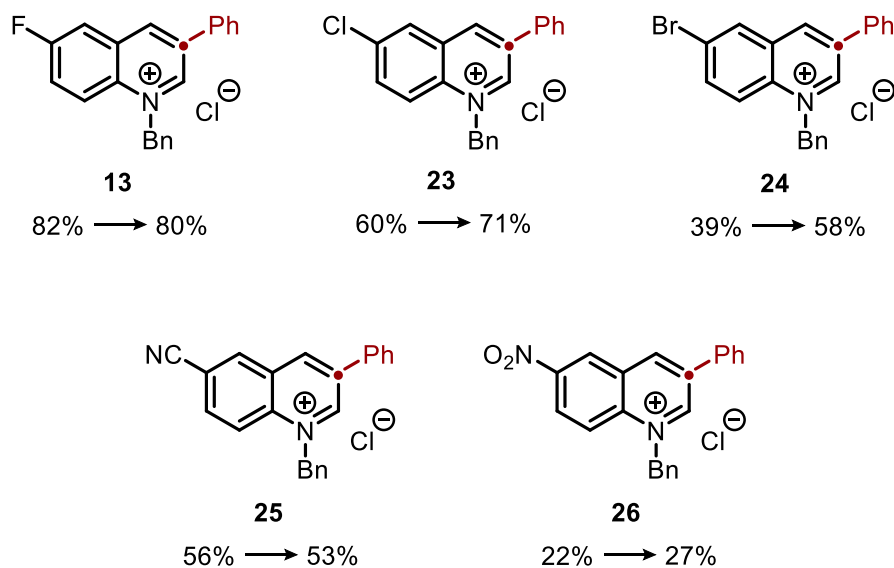
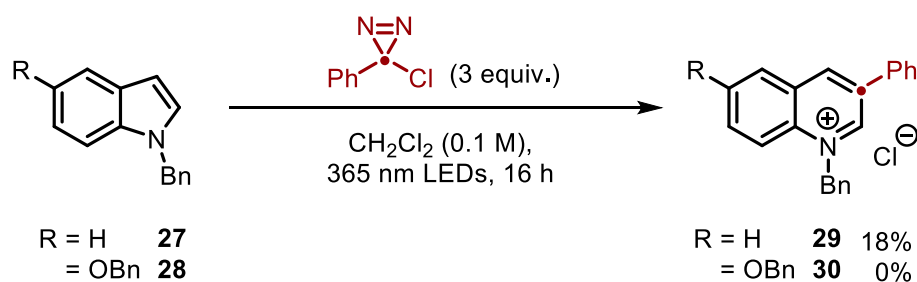


Figure 3.3. Effect of diazirine stoichiometry on yields for electron-deficient indoles. 0.2 mmol scale. Isolated yields.

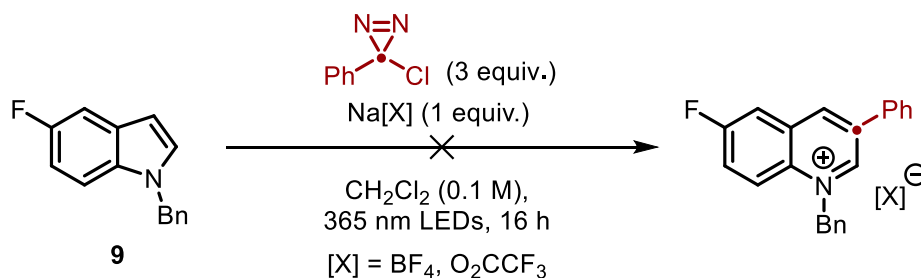
3.5.2 Precipitation optimisation

With electron-deficient indoles well tolerated by the reaction, the scope of electron-neutral and -rich indoles was considered (Scheme 3.11) including indole itself as a centre-point for electronic factors. However, when the methodology was applied to indole **27**, only an 18% isolated yield of the salt **29** was observed. This was quickly attributed to poor precipitation of the quinolinium salt from the dichloromethane solvent, lowering yields. The reaction was thus attempted again, but with a modified work-up in which the solvent was removed *in vacuo* and the resulting solid triturated with toluene. Unfortunately, similar yields were observed compared to simple isolation, suggesting the precipitation is paramount for high yields. Moreover, when the more lipophilic 5-(benzyloxy)indole **28** was employed, no precipitation of salt **30** was observed. Re-optimization of the procedure to enhance precipitation of the salt product and increase reaction yields was therefore required.



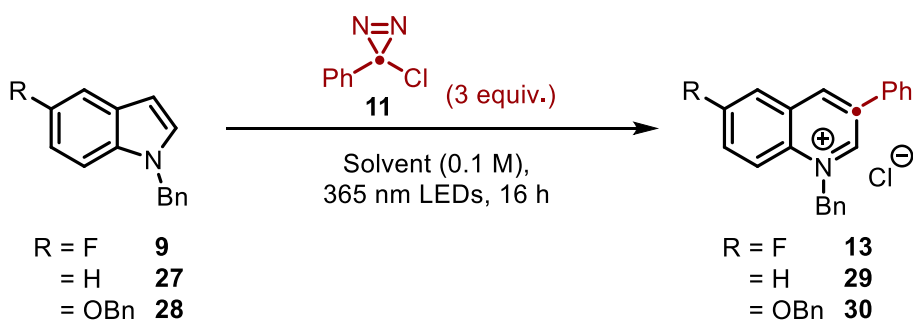
Scheme 3.11. Poor yields observed for electron-neutral/lipophilic indoles. 0.2 mmol scale. Isolated yields.

To improve precipitation, a salt additive could be added to perform an *in situ* salt metathesis and produce a less organic-soluble quinolinium salt. Initial tests used sodium tetrafluoroborate (NaBF_4) and sodium trifluoroacetate (NaTFA) as anion sources (Scheme 3.12). In each case, no reactivity was observed, and significant degradation of the anions was observed by ^{19}F NMR spectroscopy, suggesting the additive was in fact reacting with the carbene.



Scheme 3.12. Effect of sodium salt additives on precipitation.

With the knowledge that additives could potentially quench reactivity, any stoichiometric additives were avoided and instead modification of the bulk solvent system to be less polar - and therefore assist precipitation of the salt - was investigated. From the previous solvent screen, we identified both toluene and TBME as potential candidates. As dichloromethane was by far the optimal solvent, a mixture of CH_2Cl_2 and a less polar solvent such as toluene or TBME could prove optimal, likely with CH_2Cl_2 as the major component. A second solvent optimisation screen was therefore devised. This screen tested various ratios of CH_2Cl_2 with either toluene or TBME on three different indole substrates: *N*-benzyl-5-fluoroindole **9**, which precipitated fully in neat CH_2Cl_2 , *N*-benzylindole **27**, which partially precipitated, and *N*-benzyl-5-(benzyloxy)indole **28**, which showed no precipitation. The results of this screen can be seen in Table 3.10.



Entry	Solvent	Yield 13 / %	Yield 29 / %	Yield 30 / %
1	CH ₂ Cl ₂	82	18	0
2	3:1 CH ₂ Cl ₂ / PhMe	84	57	20
3	1:1 CH₂Cl₂ / PhMe	54	70	76
4	3:1 CH ₂ Cl ₂ / TBME	49	66	44
5	1:1 CH₂Cl₂ / TBME	69	70	74

Table 3.10. Optimisation of mixed solvent systems for three products of varying solubility. 0.2 mmol scale. Isolated yields.

By incorporating 25% PhMe into the bulk solvent system (while maintaining a 0.2 M concentration with respect to the indole), yields increase drastically for both **29** and **30** to 57% and 20% respectively while the yield of **13** remained almost identical to the reaction in solely CH₂Cl₂ (entry 2). By utilising a 1:1 v/v mixture of toluene and CH₂Cl₂, the isolated yield decreased for **13** to 54% while yields for both **29** and **30** increase even further to 70% and 76% respectively (entry 3). Higher yields derived from the more lipophilic indoles **27** and **28** in a high volume fraction of toluene is consistent with the less polar solvent system assisting precipitation and increasing yields. By replacing toluene with TBME, an identical trend was observed though greater yields of **29** and **30** were observed in the 3:1 mixture with TBME compared to toluene (entry 4). Additionally, the decrease in yield observed for **13** in the 1:1 mixture was higher with TBME compared to PhMe (entry 5).

Based on these results, the 1:1 solvent mixtures proved optimal, though at the expense of lower yields for quinolinium salts that previously had no issues with precipitation. Therefore, for further exploration of reaction scope, the 1:1 CH₂Cl₂/PhMe solvent mixture would be employed. While the TBME systems showed equal reactivity, issues would later arise regarding the solubility of the indole *starting materials* in these solvent mixtures that were avoided when using toluene.

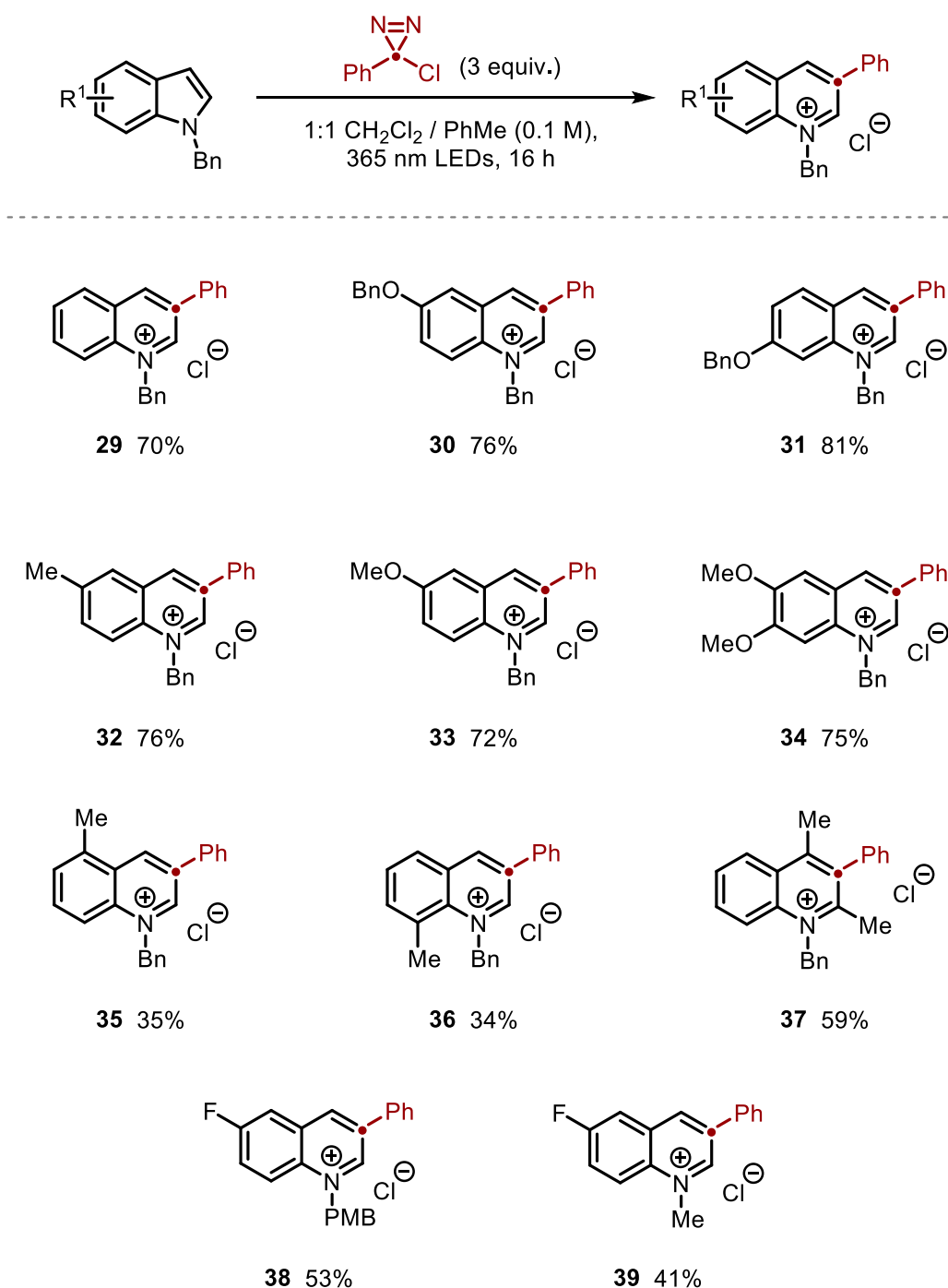
3.5.3 Expanded substrate scope

With the reaction optimised once more, a full exploration of the scope of the reaction could be undertaken. Employing the new solvent system, a number of substituted indoles were well tolerated by the reaction protocol (Scheme 3.13). Continuing the previous trend, indoles substituted at the 5-position were particularly efficient substrates in addition to 6-substituted indoles as 6-benzyloxyindole achieved similar yields of the salt **31** to that of the 5-substituted isomer and was isolated in a 72% yield. An 81% yield was achieved for the quinolinium salt **32** derived from 5-methylindole although a significant decrease was observed for the 6-methoxyquinolinium salt **33**, though still in a decent 58% yield. This can be likely attributed to the increased electron density leading to the formation of unwanted side-products. In the case of the ring expansion of **13**, ^{19}F NMR analysis of the reaction mixture would reveal other resonances of similar chemical shift to the indole starting material. Considering their similarity to the starting indole, these were attributed to C-H insertion products - consistent with Bonge-Hansen's findings with *N*-alkylated indoles - rather than cyclopropanation events.⁸⁹ Although these by-products were not isolated or further characterised, it is consistent with previous observations that more electron-rich indoles have a higher propensity to undergo C-H insertion and therefore the lower yield of **33** could be attributed to this,⁸⁹ though other electron-rich indoles such as **30** and **34** do not share this phenomenon and were isolated in good yields.

By far the most significant limitation of substitution in previous methodologies has been substitution at the 4- and 7-positions. While this substitution pattern remains problematic in the present protocol (see section 3.5.5), methyl groups were tolerated in both the 4- and 7-position and quinolinium salts **35** and **36** were isolated in 35% and 34% yields respectively. Additionally, while Levin and co-workers highlighted that a protecting group is not required for 2-substituted indoles, our methodology provided 2,3-disubstituted quinolinium salt **37** in a 59% yield. The transformation of substrates of this substitution pattern presents novel methods to achieve 2-substituted quinolinium salts which can be troublesome when attempted *via* simple alkylation with a benzyl halide due to steric hindrance resulting in sluggish reactivity and poor yields.¹⁹⁰

With the new solvent system in place, substrates that previously observed greater solubility in dichloromethane could now be reassessed. Namely, the reaction of the other protected indoles that gave moderate yields in dichloromethane: a PMB-protected indole and a methyl-protected indole. In the new solvent system **38** was obtained in near identical yields compared to solely dichloromethane, though greater precipitation was observed for **39** in addition to

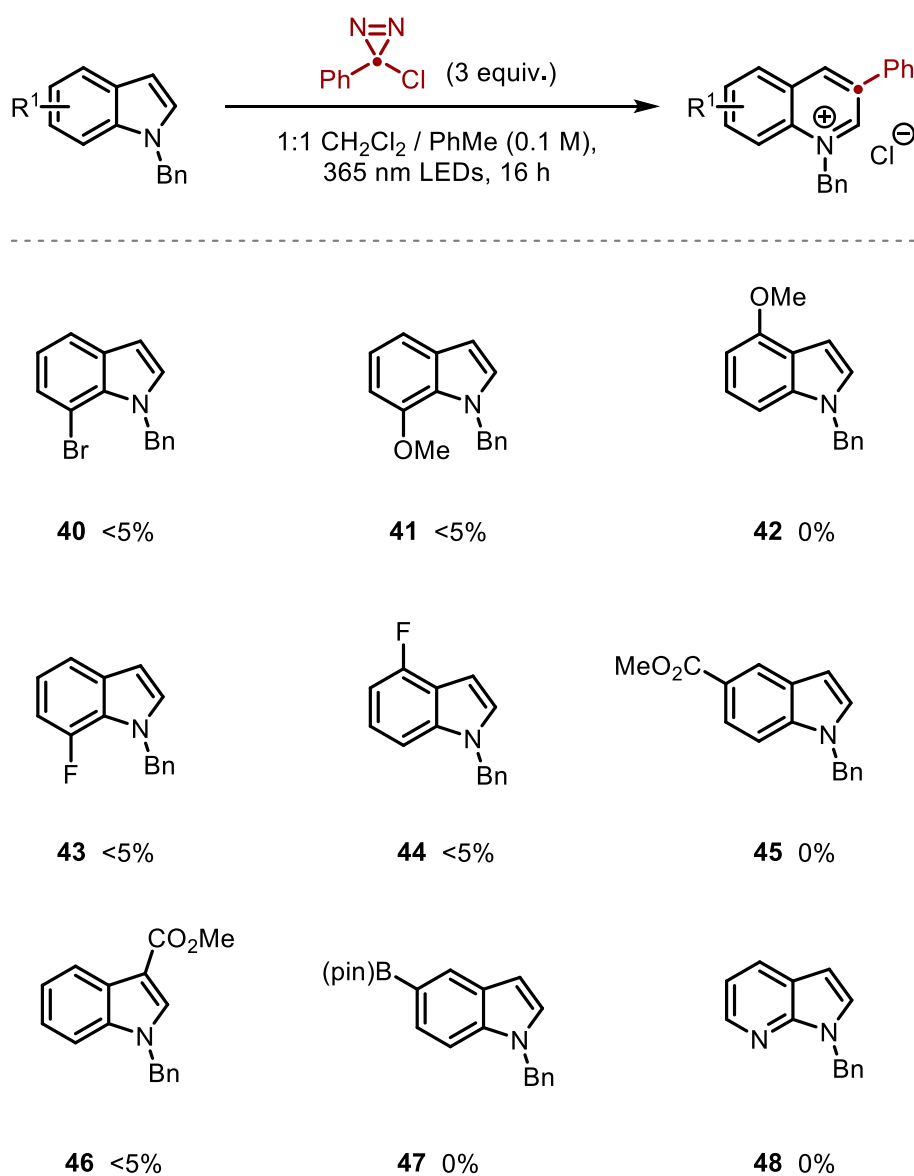
higher yield and was isolated in a 41% yield. Although it is clear that benzyl remained the optimal protecting group, the success of other groups allows for orthogonality in deprotection strategies.



Scheme 3.13. Expanded substrate scope to include lipophilic indoles. 0.2 mmol scale. Isolated yields. PMB = *para*-methoxybenzyl.

3.5.4 Incompatible substrates

As with any methodology, there were a number of substrates and substitution patterns that proved incompatible (Scheme 3.14). As mentioned previously, several 4- and 7-unsubstituted indoles proved unreactive or returned only trace amounts of the product (detectable by HRMS). Indoles bearing substituents of opposing electronic character such as 7-bromo- and 7-methoxyindoles **40** and **41** also proved unreactive. Interestingly, 4- and 7-fluoroindoles **43** and **44** also proved unreactive. While fluoro substituents are typically considered as sterically similar to protons, considering Hammett parameters relative to the indole nitrogen shows similar electronic character to their 4-bromo counterparts ($\sigma_{\text{meta}}(\text{F}) = +0.34$, $\sigma_{\text{meta}}(\text{Br}) = +0.39$), which are known to be problematic.



Scheme 3.14. Incompatible substrates in the ring expansion protocol. 0.2 mmol scale.

Another class of substrates not tolerated by the reaction conditions were some electron-poor indoles. Indole **45** bearing a 5-methyl ester proved unreactive and no product was detected by HRMS. Introducing an ester group to the heterocyclic core of the indole (**46**) led to trace amounts of product. A boronic ester-bearing indole **47** also did not provide the desired ring-expanded product. While the functional group is only weakly electron-withdrawing ($\sigma_{\text{para}} = +0.12$), there may also be deleterious interactions with the boronic ester as C-B bond insertions are known.^{191,192} While the ring expansion of substituted azaindoles would allow for further expansion of molecular complexity, the ring expansion of azaindole **48** led to no formation of product. The incompatibility of azaindoles is likely a combination of the diminished electron-density compared to isoelectronic carbocyclic indoles in addition to the presence of a Lewis basic site of reactivity resulting in deleterious carbene interactions.

3.6 Substrate scope of diazirines

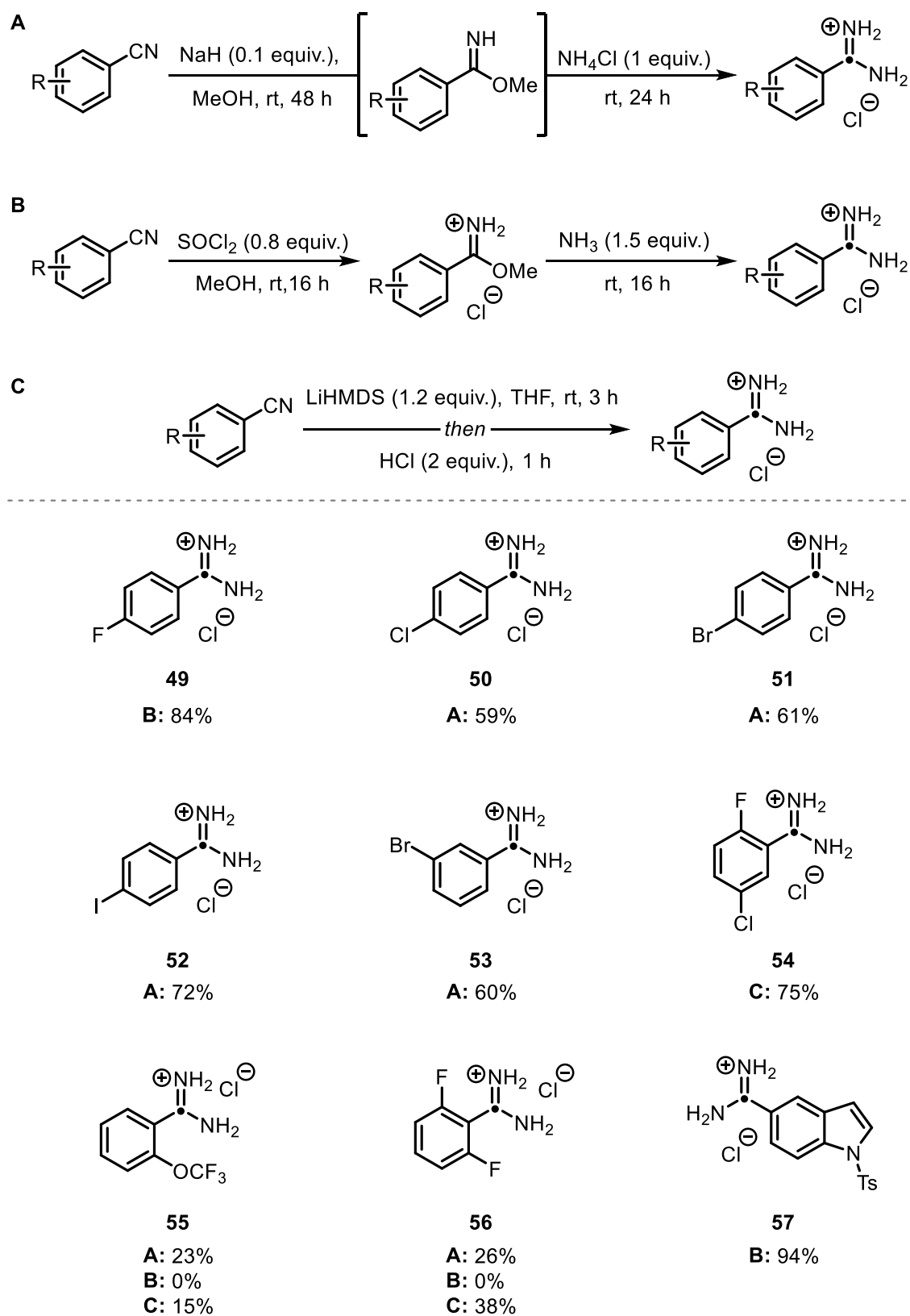
With an understanding of the functional group limitations and substitution patterns of the indole starting material, the scope of the chlorodiazirine coupling partner was investigated. Due to the lack of exploration in the synthesis of substituted diazirines in the literature, their synthesis in addition to synthesis of their amidine precursors is a topic of discussion in itself.

3.6.1 Synthesis of amidine hydrochlorides

While a large number of amidine hydrochlorides are commercially available, several functionalised amidines were unavailable or were too costly for the desired reaction scale. Therefore, we sought to identify methods to synthesise the amidinium salts from more simple and cost-effective starting materials. In addition to facilitating the present study, methods for the synthesis of bespoke amidines also further improves the applicability of this chemistry.

The most common method of synthesising amidine hydrochlorides is from the parent benzonitrile. Synthesis can be achieved *via* a number of routes: either acid- or base-mediated formation of an imidate intermediate followed by reaction with an ammonia source, or by direct addition of a nitrogen nucleophile. In total, three methods were used to synthesise amidines with the reaction protocol dependent on the electronic nature of the starting material, with more electron-rich nitriles favouring acidic conditions and electron-poor favouring basic

conditions. The yields of amidines synthesised from these methods are illustrated in Scheme 3.15.



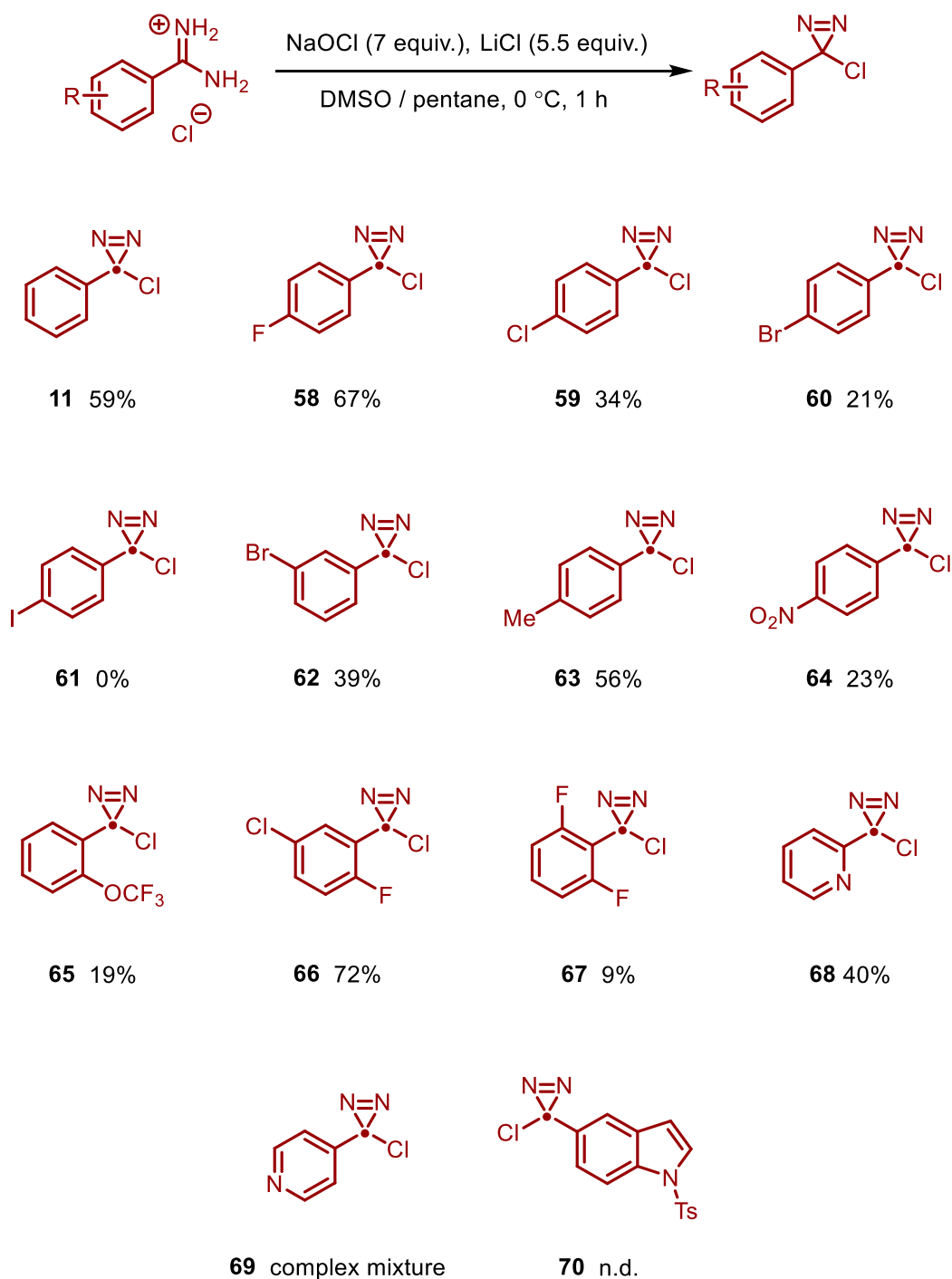
Scheme 3.15. Synthesis of amidine hydrochlorides via base mediated (A), acid mediated (B) or nucleophilic addition (C). 5-20 mmol scale. Isolated yields.

para-Substituted amidines, in addition to 3-bromo amidine **53** afforded good yields in most cases and could be synthesised readily on >10 mmol scales without purification. When the synthesis of *ortho*-substituted amidines **55** and **56** was attempted under basic conditions, poor yields were obtained after 72 hrs. Reaction under acidic conditions **B** also returned only starting material. In these cases, the synthesis with LiHMDS (**C**) proved most appropriate though with similarly poor yields. In each case, poor reactivity was attributed to *ortho*-substitution preventing nucleophilic attack. Using method **C**, amidinium salt **54** was also achieved in a 75% yield despite *ortho*-substitution. Despite poor observed yields, the diazirine derived from amidinium salt **56** presented an interesting variation to Suzuki-Miyaura cross-coupling as the corresponding boronic acid is prone to protodeboronation.¹⁹³ Additionally, as the protecting group screen revealed that tosyl indoles were inert to reaction, tosyl indole amidine **57** was synthesised as ring expansion with the corresponding diazirine would highlight substrate orthogonality.

3.6.2 Synthesis of chlorodiazirines

With the desired amidinium salts synthesised in addition to those purchased from commercial suppliers, exploration into the synthesis of chlorodiazirines could be undertaken. The Graham oxidation was employed using the conditions listed below in each case. Yields for the isolated diazirines are highlighted in Scheme 3.16.

The oxidation tolerated a range of functional groups such as F, Cl, and Br, giving rise to diazirines **58**, **59**, and **60**. In most cases, the major product is the diazirine with only a small portion of the mass balance being degradation products such as the corresponding aldehyde. The remaining mass corresponded to the starting amidine in each reaction with varying degrees of reactivity. Lower yields can therefore be attributed to poor conversion unless specified. In the case of **60**, increased reaction times led to no further increase in yield. While **60** was afforded in low yields, more respectable conversion was observed for its *meta*-isomer **62** which was isolated in a 39% yield. The inclusion of halides into the diazirines would potentially allow for the further functionalisation of the products *via* cross-coupling chemistry. Therefore, in addition to **60**, we attempted the synthesis of iododiazirine **61**. In this case, no diazirine was obtained and ¹H NMR and HRMS spectra were consistent with λ^3 -iodanes suggesting preferential oxidation of the iodine over the amidine nitrogen.



Scheme 3.16. Synthesis of arylchlorodiazirines *via* Graham oxidation. Isolated yields. 5 or 10 mmol scale.

Noticeably absent from this scope are strongly electron-donating substituents such as alkyl ethers. Due to the energetic nature of diazirines, the synthesis of these compounds was purposely avoided as the destabilising nature of the electron-rich arene could increase the propensity of violent decomposition (see section 3.11). Therefore, the most electron-rich diazirine synthesised was 4-methylphenyl diazirine **63**, which was synthesised in a 56% yield.

While *para*- and *meta*-substituted amidines afforded the corresponding diazirine in decent yields in most cases, *ortho*-substitution patterns are more nuanced. Due to the highly reactive nature of the free carbene, there is the potential for deleterious bond insertion reactions with X-H bonds.¹¹¹ With this knowledge, the choice of *ortho*-substituted diazirines were specifically tailored to functional groups lacking X-H bonds which would then ideally translate into high yields of the corresponding quinolinium salts. The synthesis of *ortho*-fluoro-substituted diazirines was investigated, not only because of the strong C-F bond disfavoring insertion, but also due to the potential to solve longstanding issues in the cross-coupling of *ortho*-fluoroarenes. The Suzuki-Miyaura cross-coupling of the corresponding boronic acid is challenging due to the propensity to undergo protodeboronation (the half-life of the corresponding boronic acid of diazirine **67** is only 5 seconds at 70 °C in water/dioxane at pH 9).¹⁹³ Therefore, the ring expansion of indoles with the insertion of arenes of this nature would circumvent these challenges. However, both the synthesis of the amidine **56** and the diazirine **67** resulted in poor yields. Due to the difficulty in accessing the desired amount of material, ring expansion with this diazirine was not attempted. While this lack of reactivity may result from the di-*ortho* substitution pattern, mono-*ortho* substituted diazirines proved more accessible. 2-Fluoro-5-chlorophenyldiazirine **66** was isolated in an excellent 72% yield considering the typical yields of diazirines. While 2-trifluoromethoxydiazirine **65** was obtained in poor yield, sufficient material was isolated to be employed in the ring expansion reaction.

A similar rationale for the inclusion of 2-heterocyclic diazirines within the scope was also employed. The infamous ‘2-pyridyl problem’ in cross-coupling chemistry also stems from the affinity for 2-pyridylboronic acid to readily undergo protodeboronation,¹⁹⁴ with a half-life of *ca.* 30 seconds depending on conditions.¹⁹⁵ In this case, the 2-pyridyldiazirine **68** was accessed cleanly in a 40% yield. By contrast, the synthesis of the 4-pyridyl diazirine **69** proved more challenging. Although its synthesis has been reported before,¹⁸⁷ when attempted, the reaction produced a complex mixture of products including the diazirine which ultimately made its isolation difficult.

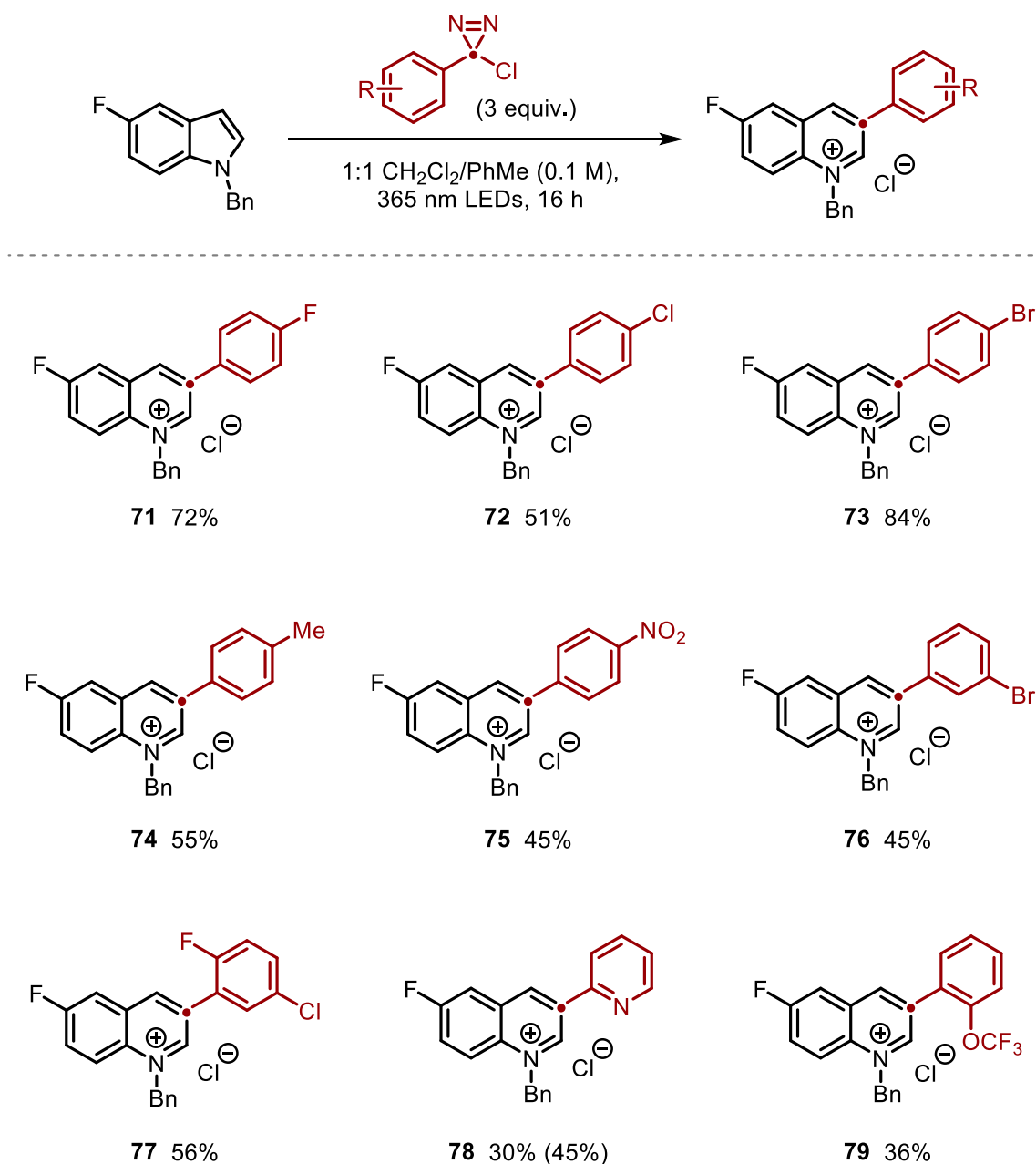
As mentioned previously, as tosyl indoles are inert to the ring expansion reaction conditions, the synthesis of a Ts-protected indolyl diazirine would potentially allow for the coupling of two indole units and demonstrate reaction orthogonality. However, under the standard conditions of the Graham oxidation, no diazirine **70** was observed. This was attributed to the poor solubility of the diazirine (and likely any intermediates) in the pentane phase of the biphasic mixture. While there are literature examples of modified procedures in other solvents such as dichloromethane, these methods involve the synthesis and isolation of

unstable and energetic *N*-chloroamidines.¹⁹⁶ Due to the unexpected difficulty of this synthesis and the increased hazards present, the idea was ultimately abandoned.

3.6.3 Application of diazirines to atom insertion

With a range of diazirines synthesised, they could be applied to the ring expansion protocol. In each case, unless specified, 3 equivalents of the diazirine were employed under the standard conditions mentioned previously. *N*-Bn-5-fluoroindole **9** was utilised as the standard substrate due to its high yields when employing simple phenylchlorodiazirine **11**. This would also allow for the straightforward detection of any side-products by ¹⁹F NMR spectroscopy and to probe conversion in the event that no precipitation occurs. When 4-fluorophenyldiazirine **58** was initially screened, only DCM was employed as the solvent rather than the DCM/toluene mixture. Since the quinolinium salt derived from fluoroindole **9** showed no issues with precipitation, we inferred that substitution of the diazirine would also enhance precipitation, particularly when substituted with groups such as halides. However, the initial reaction led to no precipitation of the product, despite confirmation of its formation by both NMR spectroscopy and HRMS. In lieu of this, the less polar 1:1 DCM/toluene mixture was employed throughout the scope. This has the added benefit of normalising the reaction conditions further to a single solvent system, except for the products derived from the initial scope of electron-poor indoles. The full scope of diazirines can be seen in Scheme 3.17.

para-Substituted diazirines bearing halides were well tolerated by the reaction conditions with the fluoro-, chloro-, and bromophenyl quinolinium salts **71**, **72**, and **73** obtained in 72%, 51%, and 84% yields respectively. The high yield obtained from bromodiazirine **60** is especially valuable, as this methodology allows for arylation without the need for cross-coupling chemistry, leaving the bromide free for further functionalisation. A 55% yield was of the product **74** was observed when employing 4-methylphenyldiazirine **63**, despite the greater electron density compared to other substituted diazirines. A *para*-nitro group was also well tolerated, affording the quinolinium product **75** in a 45% yield. The higher yield of the salt derived from the nitro-substituted diazirine **64** compared to the nitro-substituted indole implies the importance of an electron-rich indole in the reaction as shown by the 27% isolated yield of **26** obtained from the 5-nitroindole. In addition to *para*-substituted examples, the *meta*-substituted 3-bromodiazirine **62** afforded the corresponding quinolinium salt **76** in a 45% yield.



Scheme 3.17. Scope of chlorodiazirines in the ring expansion methodology. 0.2 mmol scale. Isolated yields. Yields reported in brackets were obtained employing 5 equivalents of diazirine.

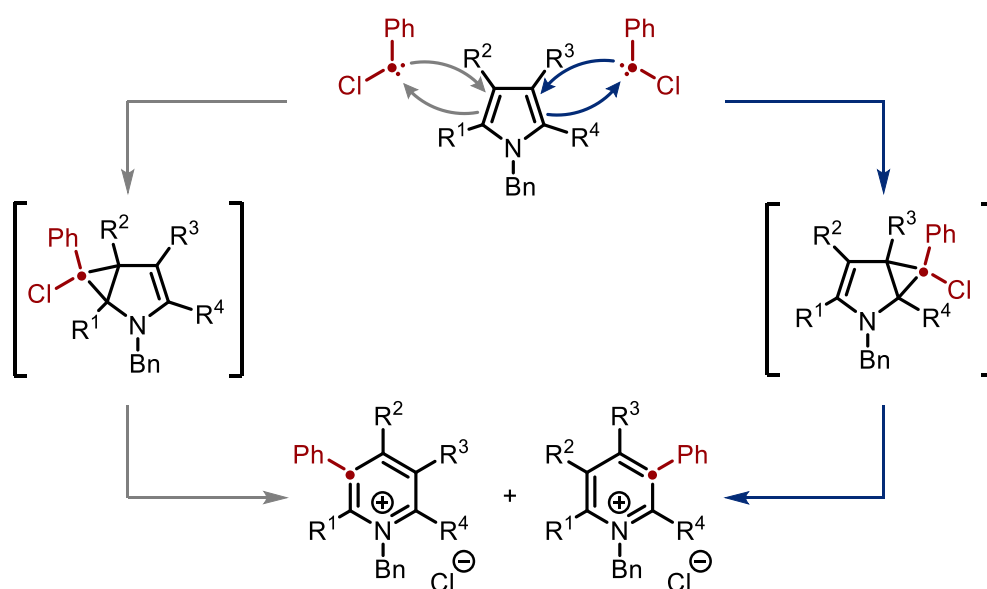
Despite issues in the synthesis of the diazirines themselves, *ortho*-substituted diazirines performed well under the reaction conditions with 2-fluoro-5-chlorodiazirine **70** affording the corresponding quinolinium salt **77** in a 56% yield. The more sterically-encumbering 2-(trifluoromethoxy)diazirine **65** provided the quinolinium salt **79** in a 36% yield.

Earlier investigations into the effects of Lewis basic functionalities had revealed that six-membered heterocycles, including quinolines, led to decomposition of the carbene and decreased yields (Table 3.9). However, 2-pyridyldiazirine **68** afforded the quinolinium salt **78** in a 30% yield, despite the knowledge that the inclusion of 3 equivalents of quinoline quenches

the reaction almost entirely. This can be rationalised in two ways. Firstly, the interaction of the pyridyl nitrogen with the carbene may be dissuaded by the steric hindrance of the diazirinyl group itself, preventing reactivity. Secondly, as the pyridyl functional group is present in the product as well, the precipitation of the salt sequesters the problematic functional group from the reaction, increasing yields. The addition of the carbene into the pyridyl functional group was also noted by Levin and co-workers in their report, and in response employed 5 equivalents of this diazine in the reaction. When we repeated the ring expansion with 5 equivalents of **68**, an increase in yield from 30% to 45% was observed.

3.7 Substrate scope of pyrroles

The application of the ring expansion methodology to pyrroles presents additional synthetic challenges due to the two potential sites of reactivity, which leads to the formation of regioisomeric atom insertion products. Additionally, it can be rationalised that the cyclopropanated intermediate could undergo additional cyclopropanation on the remaining olefin, potentially reducing yields of the desired pyridinium salt.

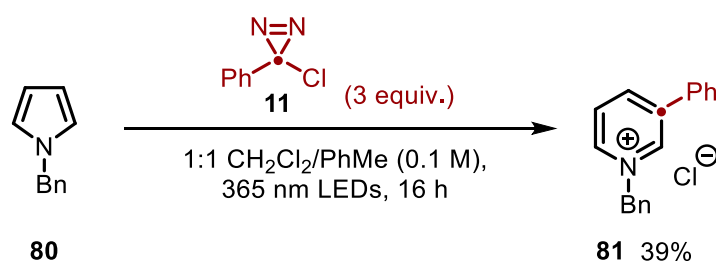


Scheme 3.18. Origin of regioselectivity issues in the ring expansion of pyrroles

3.7.1 Optimisation of pyrrole atom insertion

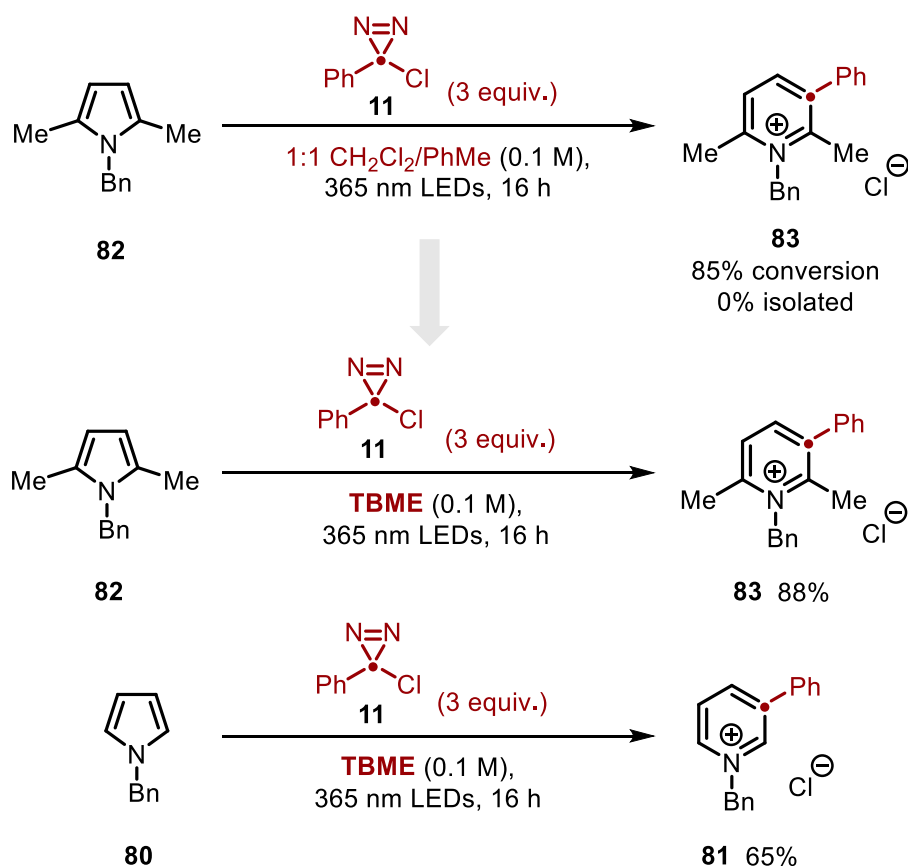
N-Benzylpyrrole was used for initial studies into the ring expansion of pyrroles, as this substrate lacks any substitution and would therefore be expected to return low yields under Levin's conditions. This substrate would therefore highlight to the greatest degree the complementarity of our protocol in the transformation of pyrroles.

Using the conditions outlined in the previous section, the ring expansion of *N*-benzylpyrrole **80** was achieved in a 39% yield (Scheme 3.19). Notably, in this case, precipitation of the salt **85** was not observed, and the pure product was isolated by column chromatography as a viscous gum.



Scheme 3.19. Preliminary ring expansion of benzylpyrrole **80** using standard conditions. 0.2 mmol scale. Isolated yield.

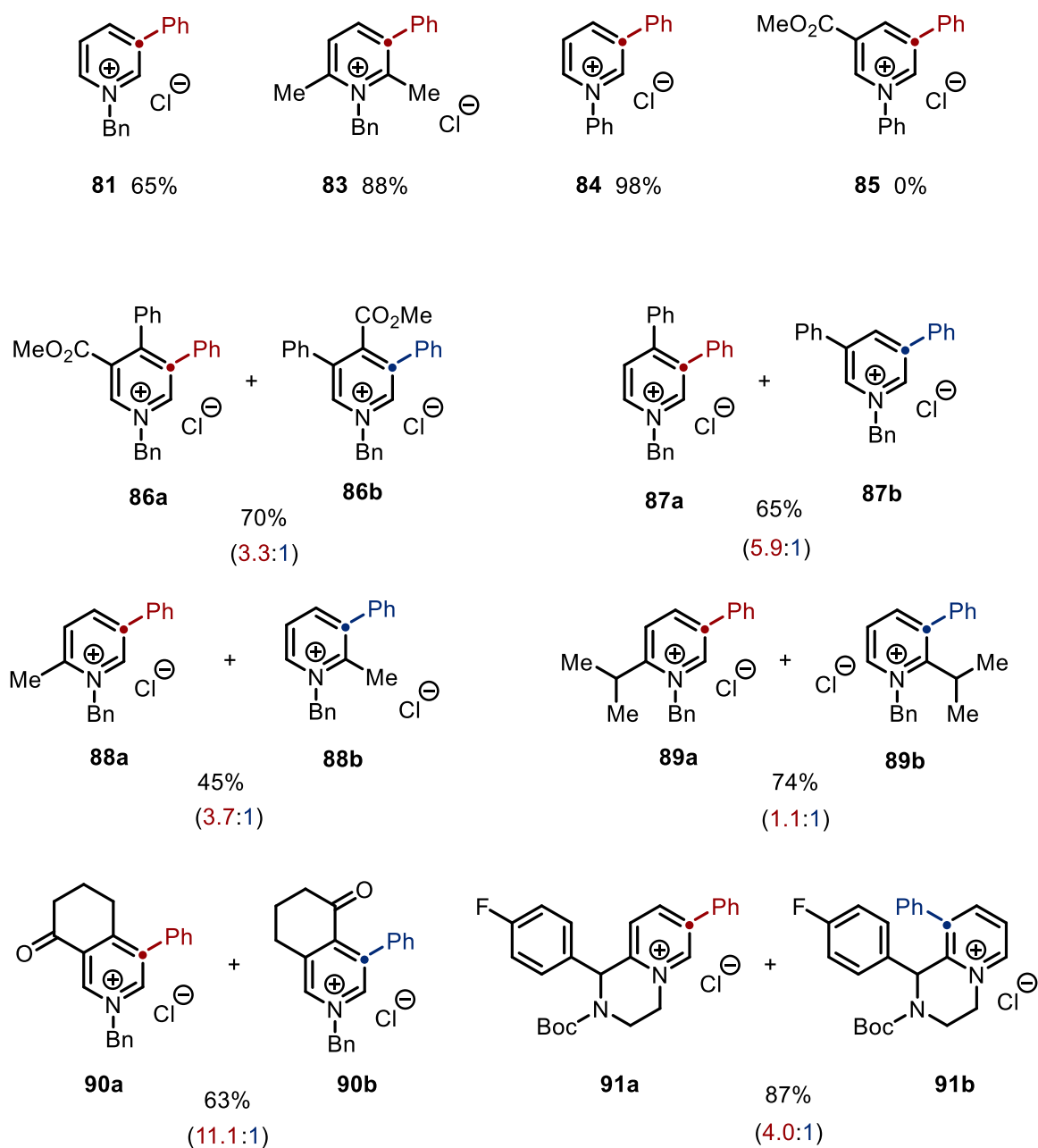
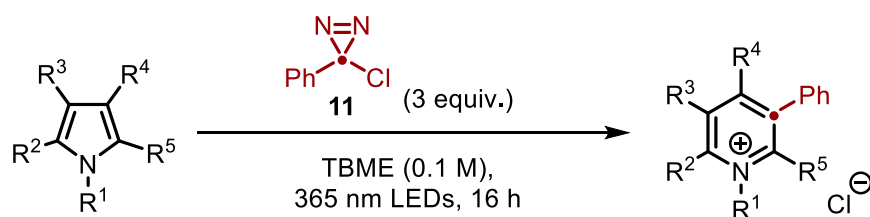
With this initial promising result, we turned our focus to functionalised pyrroles, initially focusing on symmetrical pyrroles. When 2,5-dimethylpyrrole **82** was subjected to the reaction conditions above, no precipitate was observed despite formation of the salt **83** as determined by ¹H NMR in 85% conversion. Attempted trituration from toluene, while successful for some indoles, led to decreased isolated yields in this case. To combat this decreased yield, re-optimisation was once again required to enhance precipitation. Once again, the focus was placed on modifying the solvent system rather than the inclusion of any additives. Due to the poor reactivity in neat toluene, TBME seemed most appropriate. When the ring expansion of **82** was attempted in TBME as the sole solvent, precipitation was observed which, after isolation by filtration, afforded the pure product **83** in an excellent 88% yield (Scheme 3.20). The ring expansion of the unsubstituted pyrrole **80** was then re-attempted, which under the new reaction conditions led to precipitation of the product **81** which was isolated in a 65% yield.



Scheme 3.20. Effect of TBME on the isolated yields of benzyl pyridinium salts **81** and **83**. 0.2 mmol scale. Isolated yields.

3.7.2 Modified pyrrole substrate scope

The use of TBME as the reaction solvent proved paramount in achieving high yields of the far more lipophilic pyridinium salts. Therefore, the exploration of the pyrrole scope was carried out utilising TBME as the sole solvent. As the indole scope determined functional group tolerance, the focus on the pyrrole scope fell on the regioselectivity of the atom insertion into unsymmetric pyrroles. The full scope, including both yields and distribution of isomers, is highlighted in Scheme 3.21.



Scheme 3.21. Substrate scope of pyrroles highlighting regioisomeric products. 0.2 mmol scale. Isolated yields. Regioisomeric ratio (r.r.) determined by ^1H NMR analysis of precipitated product. The r.r. of precipitated products was assumed to be reflective of the r.r. of the bulk system and that the solubilities of the two isomers were identical.

In addition to benzylated pyrroles, *N*-arylated pyrroles were also investigated as competent substrates for the ring expansion as this protecting group had not been screened for indoles. Surprisingly, not only was the phenyl group tolerated by the reaction, but the corresponding *N*-phenylpyridinium salt **84** was isolated in a near quantitative yield.

When *N*-benzylpyrrole 3-methyl ester was subjected to the reaction conditions, no product **85** was observed. This lack of reactivity can be attributed to the electron-withdrawing nature of the ester group lowering nucleophilicity of the pyrrole such that reaction with the carbene is disfavoured and is consistent with previous literature reports.¹⁸⁷ In contrast, when the electron-withdrawing ester is paired with a phenyl ring, the pyridinium salt **86** was isolated in a 70% yield in a 3.3:1 mixture of regioisomers with the major isomer arising from insertion adjacent to the more electron-donating phenyl ring. The ring expansion of 3-phenylpyrrole was also achieved in an 81% yield, with the dominant isomer **87a** resulting from insertion adjacent to the phenyl substituent in a ratio of 5.9:1, incongruous with any steric arguments for atom insertion. An 11:1 ratio of products was observed in the ring expansion of a ketopyrrole to pyridinium salts **90a** and **90b**, which was isolated in a 63% yield. The drastic electronic difference between each position of atom insertion likely dominates the selectivity in this case.

In direct contrast to this result, when 2-methylpyrrole was subjected to the reaction conditions, the opposite regioselectivity was observed in which insertion occurs preferentially to the unsubstituted olefin in to afford pyridinium salts **88a** and **88b** in a 45% yield with a 3.7:1 product ratio. Additionally, carbon atom insertion into 2-isopropylpyrrole occurs does not favour one isomer over the other with a 1.1:1 ratio of regioisomers of pyridinium salts **89a** and **89b**. Finally, to further expand the molecular complexity of the resulting azinium salts, reaction with a non-benzyl alkyl pyrrole was desired, particularly one that would result in the formation of a complex bicyclic system. Gratifyingly, the ring expansion of a pyrrolopyrazine to the corresponding products **91a** and **91b** were achieved in an excellent 87% yield with a regioisomeric ratio of 4.0:1 in favour of insertion distal from the alkyl chain. Based on these results, we rationalised that insertion occurs preferentially at the most electron-rich position, unless the 2-position is sterically hindered.

3.8 Robustness screen

In addition to carrying out a comprehensive substrate scope, it was deemed important to determine the general tolerance of the methodology towards more complex and medically-relevant functional groups. While this could be determined by expanding the substrate scope further, we thought it worthwhile instead to carry out a comprehensive robustness screen. First outlined by Glorius and co-workers,¹⁹⁷ this screen involves carrying out the desired reaction in the presence of an additive bearing the desired functional group. Once the reaction is complete, both the reaction yield and the amount of the (unreacted) additive remaining are quantified. This allows for both the determination of how the functional group alters product yield, but also its tolerance towards the reaction conditions. This has the added benefit of de-convoluting variations in reaction yield when the functional group is directly attached to the substrates, in this case an indole. In these cases, poor yields could be attributed to the functional group itself or the steric/electronic effects that the group imparts on the molecule.

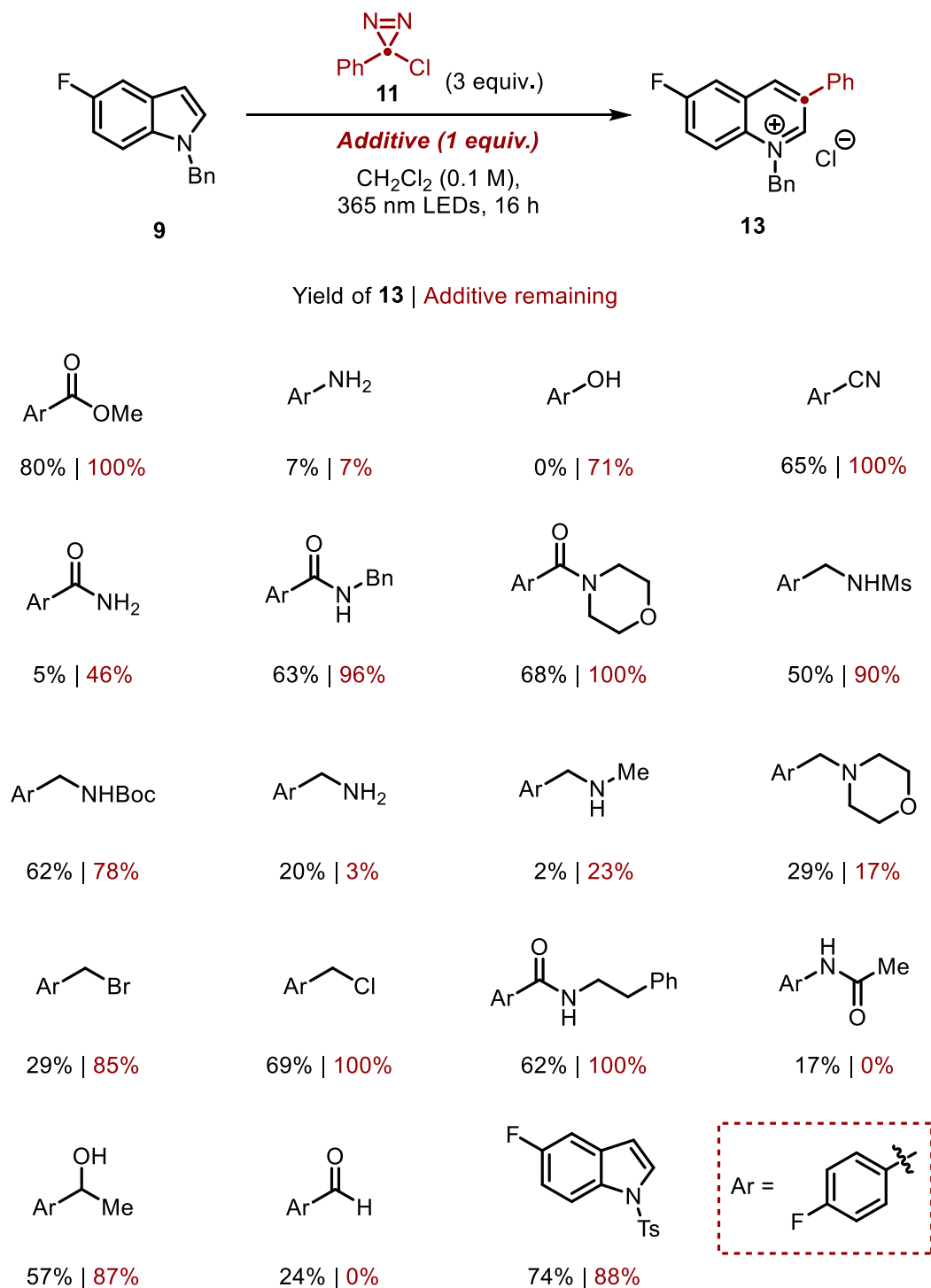
3.8.1 Methodology robustness

Reaction robustness was explored by first identifying a suitable range of functional groups for screening. As mentioned previously, quinolines are known to be problematic and are thus omitted. Ultimately, a tolerance of medically-relevant functional groups, particularly esters and amides, was paramount to the development of this methodology. Substitution of the amide was also an avenue of interest as complex molecules can include a range of primary, secondary, and tertiary amides. The tolerance of nucleophilic groups was also of interest. The focus here was on free amines and alcohols (including anilines and phenols). In the case that these groups were found not to be tolerated, then ideally a protected form would be robust. Further consideration of functional groups was influenced by a study of the most common functional groups in drug discovery by Erti and co-workers.¹⁹⁸

Reaction outcome was determined by ¹⁹F NMR spectroscopy and thus any additives employed were *para*-fluorinated arenes,ⁱ and *N*-benzyl-5-fluoroindole **9** was utilised as the indole for monitoring by ¹⁹F NMR in addition to its known high yields under standard conditions. As the ring expansion of **9** is known to occur readily in CH₂Cl₂, for simplicity (and to aid solubility of the additives in some cases) only the single solvent conditions were used as

ⁱ With the exception of the methyl ester, as the ¹⁹F NMR peak for the *para*-fluoro ester overlapped with that of **13**. A *para*-trifluoromethyl variant was used in this case.

shown in Scheme 3.22. To aid in the discussion of the screen, the data have also been represented graphically in Figure 3.4.



Scheme 3.22. Robustness screen of medically-relevant functional groups. 0.2 mmol scale. Yields and mol-fraction determined by ^{19}F NMR spectroscopy. ^aAr = 4-(trifluoromethyl)phenyl.

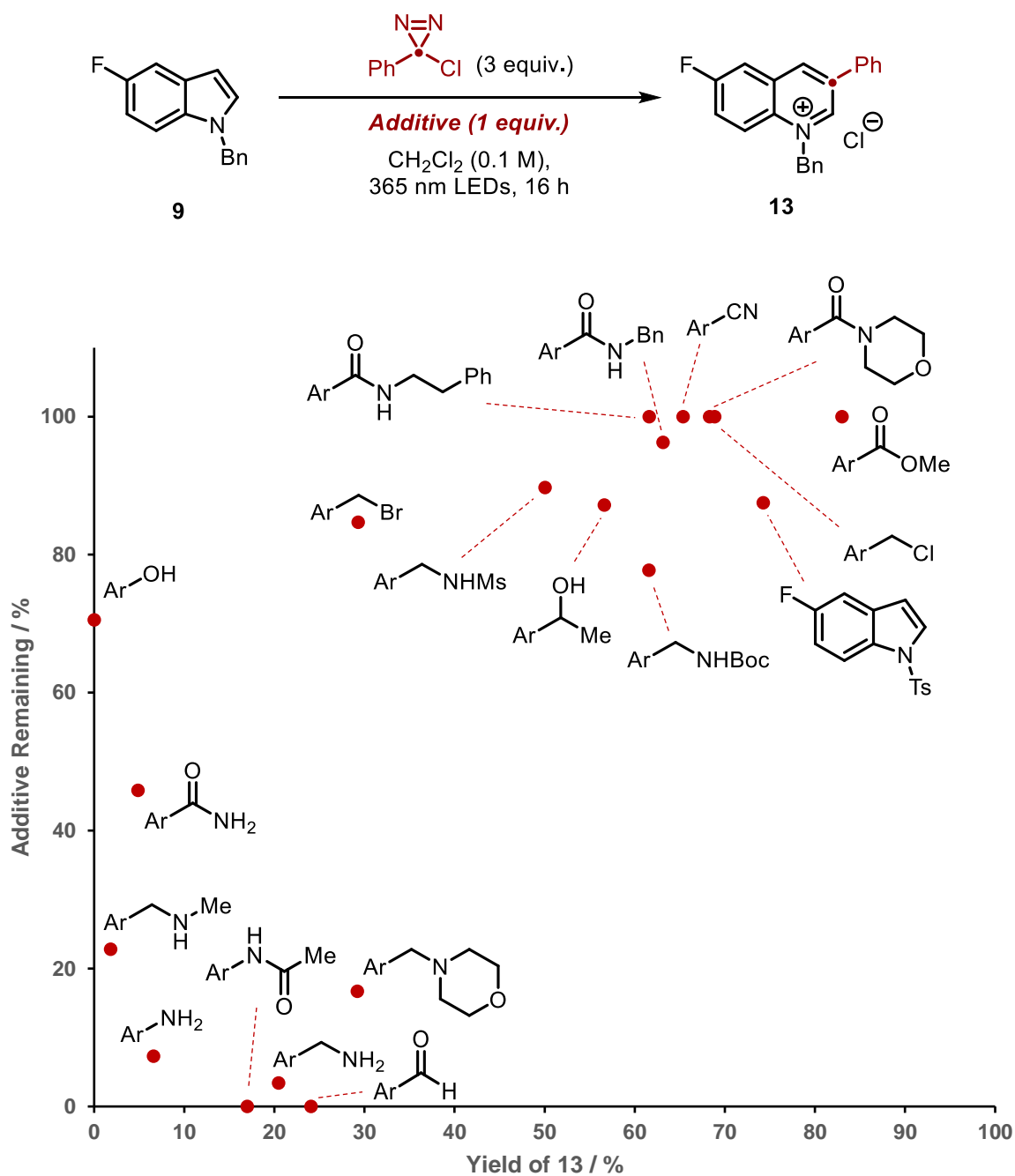


Figure 3.4. Graphical representation of robustness screen relationships.

The screen revealed a number of functional groups that were highly compatible with the reaction conditions. Notably, secondary and tertiary amides were well tolerated as little to no degradation was observed for both a benzyl benzamide and morpholino benzamide (96% and 100% recovered, respectively) after 16 hrs in addition to high yields of **13** (63% and 68% respectively). A phenethylamide was also tested to confirm that amides possessing non-benzylic alkyl chains were resilient to the carbene. Indeed, no additive consumption was observed after 16 hrs and a similarly high yield of **13** (62%) was observed. On the contrary, a

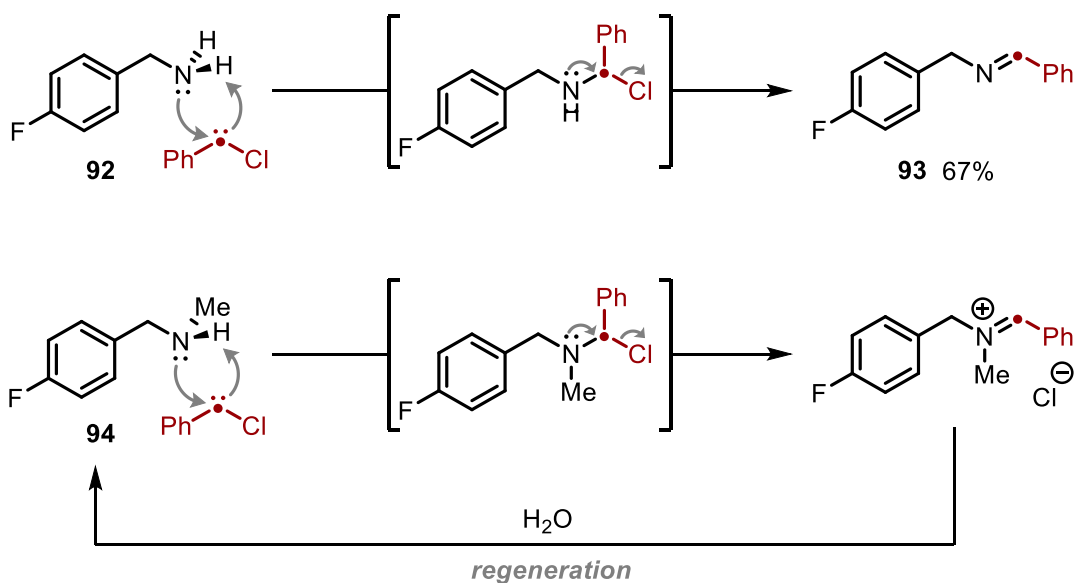
primary benzamide led to poor conversion to **13** (5%) in addition to greater observed consumption, with only 46% remaining intact. Esters also proved to be highly robust functional groups, with no degradation of a methyl benzoate observed in addition to an 80% yield of **13**. With both amides and esters well tolerated, it was clear that the chemistry would tolerate more complex biologically-derived substrates such as tryptophan-containing peptides (*vide infra*).

Consistent with the good yields observed for the nitrile-containing quinolinium salt **25** as part of the indole scope, nitriles were found to be well tolerated by the reaction conditions. Somewhat surprisingly, secondary alcohols also proved to be compatible functional groups with 87% of the alcohol remaining post-reaction though a lower yield of 57% was observed compared to other robust additives. Consistent with findings during optimisation of the protecting group, a tosyl-protected indole proved mostly unreactive and 88% of the additive was observed after 16 hrs with **13** formed in a good yield of 74%.

3.8.2 Poorly tolerated functionalities

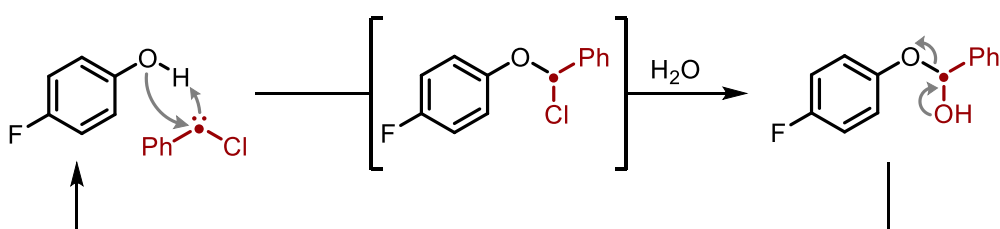
The screen also revealed a number of functional groups that were not tolerated by the reaction and afforded poor yields of the product, high consumption of the additive, or both. As expected, nucleophilic amines proved incompatible with the reaction protocol as primary, secondary, and tertiary amines competitively reacted with the carbene. In the case of primary amine **92**, this was evidenced by the formation of imine **93** in a 67% yield by ¹⁹F NMR by addition of the amine to the carbene, followed by proton transfer and elimination (Scheme 3.23). Despite lower yields of the quinolinium salt **13** (20% vs. 2%) observed in the presence of secondary amine **94** compared to primary amine **92**, a lesser amount of amine **94** was consumed. This can be rationalised by the greater nucleophilicity of the secondary amine but the relative instability of the resulting iminium cation compared to the neutral imine **93** formed from **92**. After quenching the carbene and forming the corresponding iminium salt, hydrolysis may then occur which results in the release of the free amine (Scheme 3.23). This has the effect of quenching the carbene with less apparent net decomposition of the additive.

To combat the incompatible nature of amines, both Boc- and Ms-protected amines were also screened. Gratifyingly, these additives proved far more compatible, with inclusion of the Boc-amine resulting in a 62% yield of **13** with 78% of the additive remaining. A methanesulfonyl-protected amine also led to 50% conversion to **13** with 90% of the additive surviving the reaction.



Scheme 3.23. Top: formation of imine **93** *via* attack of amine into the carbene. Bottom: Rationalisation of carbene consumption with regeneration of the amine *via* iminium salt.

A more drastic example of the regenerative phenomenon can be seen when 4-fluorophenol was incorporated into the reaction. In this case, none of the desired quinolinium salt was observed, yet the phenol was retained in a 71% yield. This is consistent with competitive consumption of the carbene by the phenol with the formation of an unstable intermediate that - upon hydrolysis - results in the extrusion of the additive, seemingly untouched. This can be rationalised by initial addition of the phenol into carbene followed by formation of a hemiacetal upon attack by a nucleophile (possibly water) with loss of chloride (Scheme 3.24). This tetrahedral intermediate could then collapse which would regenerate the phenol. Finally, in addition to amines and phenols, aldehydes proved highly intolerant and yield to total consumption of the additive.



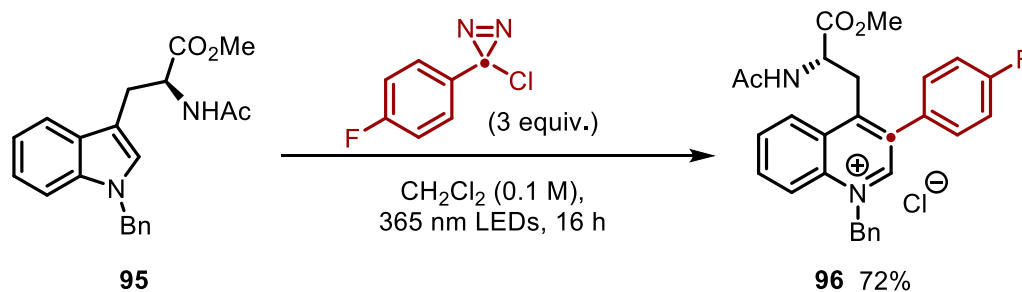
Scheme 3.24. Carbene consumption with regeneration of a phenol.

3.9 Application to complex substrates

With the robustness screen complete, the reaction was found to tolerate important functional groups found in complex molecules, namely esters, amides, and protected amines. With this in mind, the focus of the project turned to the modification of tryptophan-containing molecules.

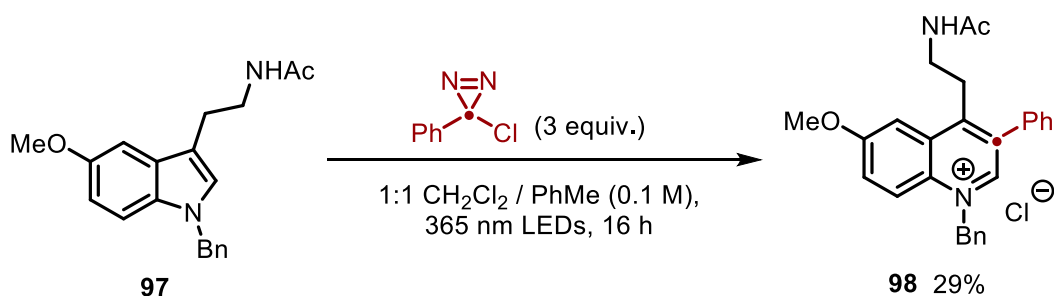
3.9.1 Tryptophan modification

Before more complex targets could be modified, the ring expansion of tryptophan itself had to be investigated. As observed by the robustness screen, this would require an orthogonal protection strategy to protect the α -amine as well as benzylate the indole nitrogen. Ultimately, the chosen substrate included an acetylated amine as well as a methyl ester. The CH_2Cl_2 /toluene mixture was initially chosen as the substrate proved to be soluble in this solvent. Upon subjecting protected tryptophan **95** to the reaction conditions, high conversion to the desired ring expanded product **96** along with high levels of precipitation was observed, which allowed for isolation in a 72% yield (Scheme 3.25).



Scheme 3.25. Ring expansion of protected tryptophan **95**. 0.2 mmol scale. Isolated yield.

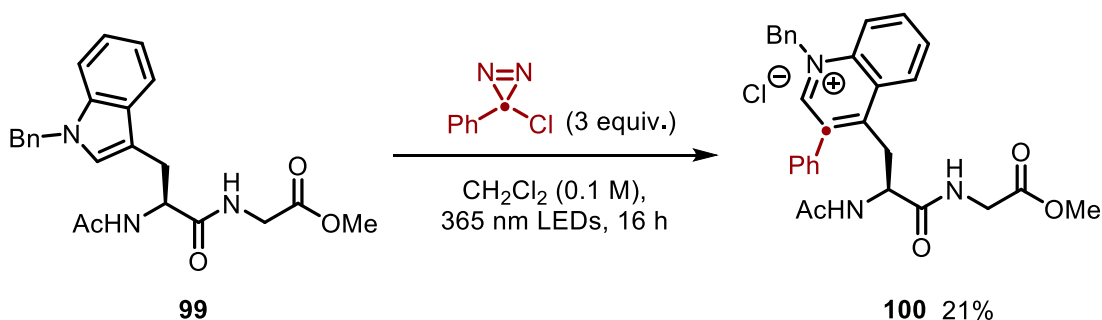
The tryptamine-derived neurotransmitter melatonin was also subjected to the reaction conditions (Scheme 3.26). Melatonin naturally possesses an acetylated amine, making it a perfect choice for this transformation. Despite possessing complementary functionality, subjecting benzylated melatonin **97** to the reaction protocol resulted in a 29% isolated yield of the expanded product **98**. However, NMR analysis revealed only partial precipitation of the product. Attempts to achieve greater yields by trituration with toluene resulted in the co-precipitation of the product and another impurity. Separation of the two products proved difficult, and characterisation of the impurity was not achieved.



Scheme 3.26. Ring expansion of benzylated melatonin **97**. 0.2 mmol scale. Isolated yield.

3.9.2 Modification of dipeptides

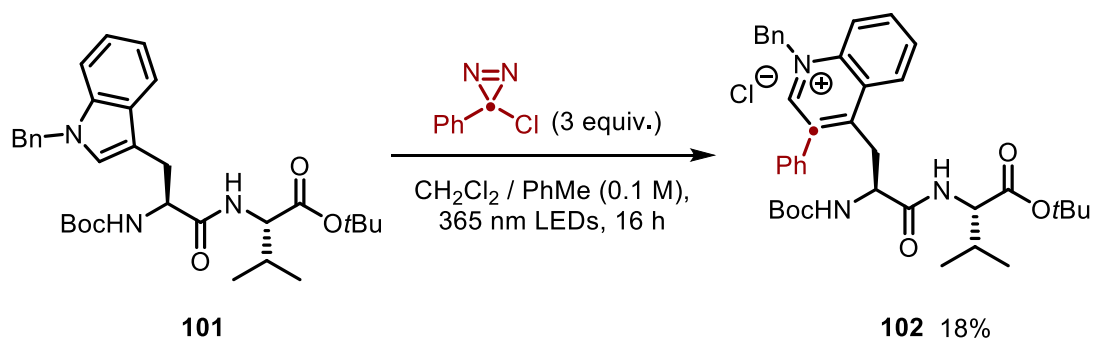
With the promising result obtained from tryptophan **95**, the next route of exploration was the modification of dipeptides. For simplicity, glycine was chosen as the second amino acid and the dipeptide **99** was therefore synthesised. As both protecting groups had proved competent in the tryptophan reaction, the tryptophan *N*-terminus was protected *via* acetylation whereas the glycine *O*-terminus was methylated. Subjecting dipeptide **99** to the ring expansion led to no precipitation of the desired product. Due to solubility issues, the reaction was carried out in solely CH_2Cl_2 instead of the toluene mixture, which likely prevented precipitation of the product. Despite this, removal of the solvent followed by trituration with toluene afforded the product. Unfortunately, similarly insoluble impurities co-precipitated with the product and reverse-phase column chromatography had to be employed to achieve high purity. After purification, the ring expanded dipeptide **100** was isolated in a 21% yield (Scheme 3.27).



Scheme 3.27. Ring expansion of Trp-Gly dipeptide **99**. 0.2 mmol scale. Isolated yield.

The reaction of this dipeptide represents the fine balance of solubility required to achieve optimal yields in this methodology. In this case, the poor solubility of the starting material in the less polar solvent system required the use of a more polar system, which in turn led to no precipitation of the product. To achieve good conversion, this must be reversed such that the starting material is *soluble*, and the product is *insoluble*. A new, more lipophilic peptide **101** was therefore synthesised such that the CH_2Cl_2 /toluene mixture could be employed, and hopefully

lead to full precipitation. Sadly, again no precipitation was observed even in the less polar solvent (Scheme 3.28). Similar isolation methods afforded the product **102** in an 18% yield though impure due to the presence of minor polar impurities. In this case, the peptide **101** was likely too apolar, suggesting a modified peptide capable of precipitation falls somewhere in the middle-ground.



Scheme 3.28. Ring expansion of Trp-Val dipeptide **101**. NMR yield reported.

3.10 Functionalisation of azinium salts

Having successfully synthesised a range of substituted azinium salts, the chemistry of these reagents was explored. The requirement for *N*-alkylation for high conversions necessarily restricts the methodology to the formation of azinium salts instead of the original aim of the project, the free azine. However, these salts themselves are potentially competent precursors for a number of transformations that result in medically-valuable architectures. Therefore, exploration of a range of transformations particular to azinium salts would further the synthetic utility of our ring expansion protocol. For simplicity, the functionalisation of *N*-benzyl-3-phenylquinolinium chloride salt **29** was investigated, though its fluorinated analogue **13** was employed for reaction monitoring (Figure 3.5).

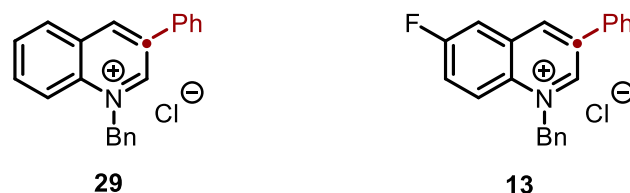
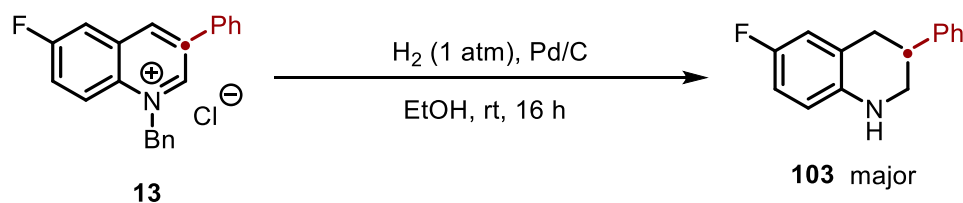


Figure 3.5. Quinolinium salts **29** and **13** chosen for functionalisation studies.

3.10.1 De-alkylation

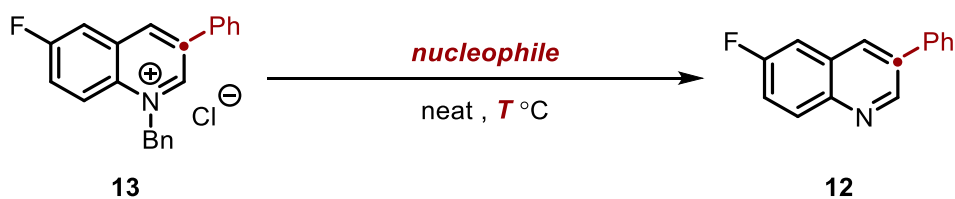
While more divergent transformations were of great interest, the first transformation to be explored was de-alkylation of the N-alkyl protecting group. This would result in completion of the initial aim of this project, albeit in three steps (alkylation/ring expansion/de-alkylation) rather than one.

The classical choice for de-benzylation specifically is Pd-catalysed hydrogenolysis. The hydrogenation of N-benzyl pyridinium salts is well documented and it was therefore anticipated that this method would transfer readily to quinolinium salts.^{199,200} Initial de-benzylation was attempted with the conditions shown in Scheme 3.29. After 16 hrs, NMR spectroscopic analysis revealed cleavage of the benzyl group had occurred in addition to full reduction of the heteroarenium ring to tetrahydroquinoline **103**. Reaction monitoring revealed reduction of the ring occurred selectively prior to benzyl cleavage, ultimately meaning de-benzylation *via* hydrogenolysis was abandoned for this specific transformation but utilised later for other reduction chemistry (see section 3.10.3).



Scheme 3.29. Initial hydrogenation tests on **13**. 0.2 mmol scale.

Instead, de-alkylation *via* S_N2 methods was attempted. Upon reaction with a nucleophile, the azinium group could act as a competent nucleofuge and therefore release the free azine. Similar to hydrogenolysis, S_N2 de-alkylations of pyridinium halides are reported but, are lacking for quinolinium halides.²⁰¹ The first attempt involved de-alkylation with pyridine as the nucleophile (Table 3.11). This was attempted by heating the quinolinium salt in pyridine to reflux as shown in entry 1. However, no conversion was observed after 3 hours. This can be likely attributed to the poor solubility of the salt in pyridine, even at reflux. Similar de-alkylation reactions have also been carried out in N-methylimidazole.^{201,202} While this time dissolution of the salt was achieved at reflux, no conversion to the free azine was observed (entry 2).

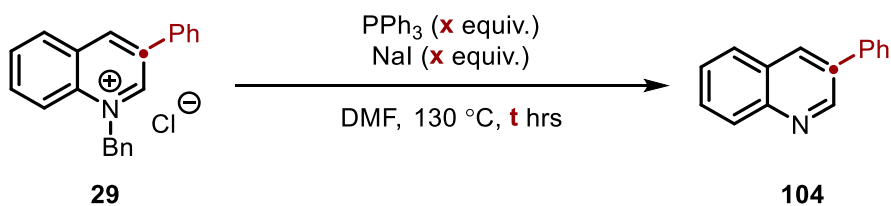


Entry	Nucleophile	T / °C	Yield of 12 / %
1	Pyridine	120	0
2	<i>N</i> -Methylimidazole	140	0

Table 3.11. Attempted de-benzylation with nitrogen-based nucleophiles. 0.2 mmol scale.

Mechanistic studies of nucleophilic pyridinium de-alkylations postulated that rather than direct attack by a *N*- or *P*-nucleophile to the benzylic centre, the counterion of the salt (in their case iodide) undergoes initial attack to release benzyl iodide and the free azine.^{203–205} As the high temperatures required for de-alkylation also promote alkylation, the terminal nucleophile therefore acts as an alkyl halide scavenger, sequestering the reactive benzyl iodide and promoting the equilibrium towards formation of the azine product.

With this in mind, the conditions investigated in those mechanistic studies were recreated. Quinolinium salt **29** was treated with two equivalents of sodium iodide (the authors reported iodide acts as a better nucleophile than chloride) and triphenylphosphine (as the alkyl scavenger) in DMF at 130 °C (Table 3.12, entry 1). Gratifyingly, after only 1 hour, an 82% NMR yield of the product **104** was obtained. Further optimisation was desired as superstoichiometric triphenylphosphine may prove troublesome due to the formation of the phosphine oxide, which is notoriously difficult to remove.²⁰⁶ Repeating the reaction with 2 equivalents of both NaI and PPh₃ for 2 hours resulted in quantitative yields of the free quinoline (entry 2). Decreasing the stoichiometry to 1.2 equivalents resulted in similar quantitative yields of **104** with only a slightly longer 3 hour reaction time required (entry 3). This reaction can be monitored visually as the brightly coloured orange quinolinium iodide formed *in situ* is converted to the colourless quinoline.



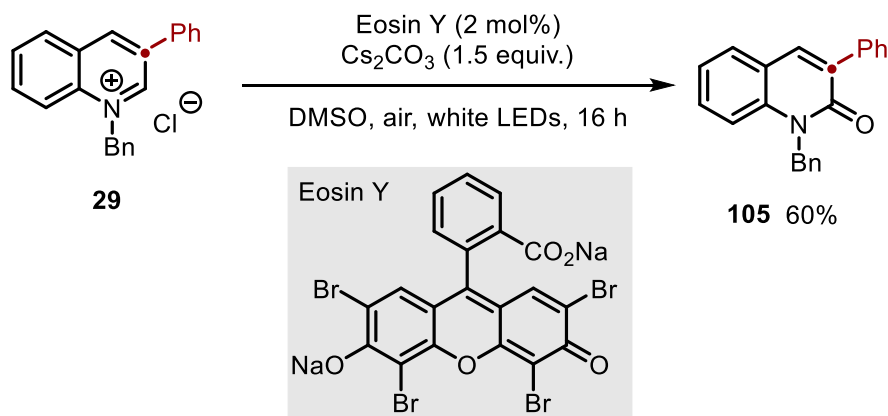
Entry	x	t	Yield of 104 / %
1	2	1	82
2	2	2	100
3	1.2	3	100

Table 3.12. Optimisation of de-benzylation *via* S_N2 with PPh₃ and NaI. 0.2 mmol scale. Yields determined by ¹H NMR spectroscopy against 1,3,5-trimethoxybenzene as an internal standard.

3.10.2 Oxygenation

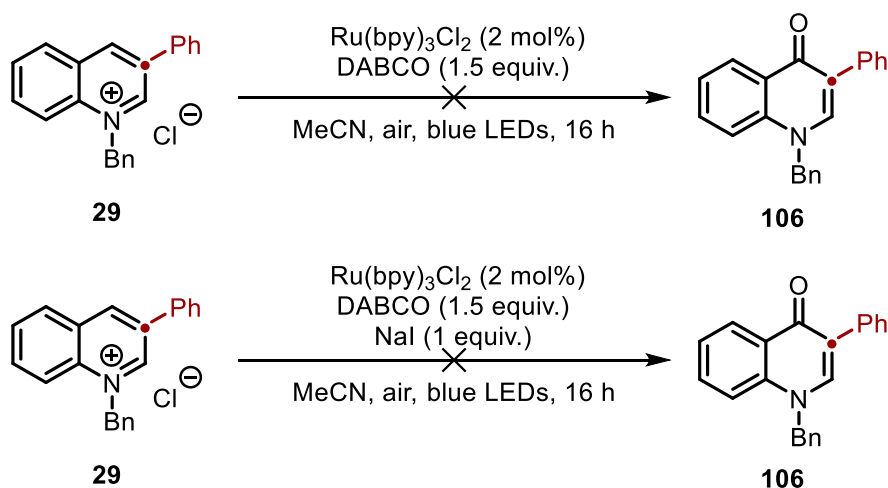
The site-selective oxygenation of azinium salts is also well documented and can be achieved with a number of methods.^{207–209} Due to the presence of quinolone motifs within drug molecules,¹ we began to explore and apply these methods to our quinolinium chloride salts. It should be noted for this transformation, similar to most transformations discussed within this section, the structure of the quinolinium salts formed in our ring expansion methodology typically fall out of the purview of the substrate scope originally reported in the literature. Specifically, these methods have typically not been applied to 3-aryl substituted azinium salts, although other 3-substituted substrates are sometimes employed. Secondly, quinolinium bromides, rather than the chlorides formed from our methodology, are typically the substrate of choice due to their greater solubility in more less polar solvents as well as the ease at which they are accessed. Ultimately, for many transformations, while still highly similar substrates, there is a distinct difference in reactivity between our 3-aryl quinolinium chlorides and the standard quinolinium bromides.

With regards to oxidation, achieving selective oxidation to both 2- and 4-quinolones was the main goal, again to further derivatise the products. Selective 2-oxygenation was achieved by an aerobic oxidation mediated by an Eosin Y photocatalyst and blue light and the corresponding 2-quinolone **105** was isolated in 60% yield (Scheme 3.30).²¹⁰



Scheme 3.30. Selective oxidation of **14** to 2-quinolone **108**. 0.2 mmol scale. Isolated yield.

Selective oxygenation at the 4-position proved more troublesome (Scheme 3.31). The regioselective aerobic oxygenation of quinolinium salts has been reported and can be achieved with a ruthenium photocatalyst and DABCO.²⁰⁹ However, the authors of this paper report that MeCN provided optimal yields for the transformation. When this reaction was attempted with **29**, no conversion to **106** was observed after 16 hours. This was likely due to the poor solubility of the quinolinium chloride salt in acetonitrile. The range of substrates investigated in the paper were restricted to quinolinium bromides, which are more soluble in MeCN and therefore more readily undergo oxidation. The reaction was therefore re-attempted with the addition of one equivalent of sodium iodide to facilitate anion metathesis and form the quinolinium iodide *in situ*, which would hopefully dissolve more readily. Sadly, no conversion was observed in this case. A solid precipitate was observed throughout the reaction consistent with the quinolinium salt suggesting that either anion metathesis was slow, or the salt was simply too insoluble regardless of the counterion. Additionally, the iodide present may also have been non-innocent in this reaction. DMSO was also tested as the reaction solvent due to its success in the previous oxidation, but similarly no reaction was observed, consistent with the authors' findings.

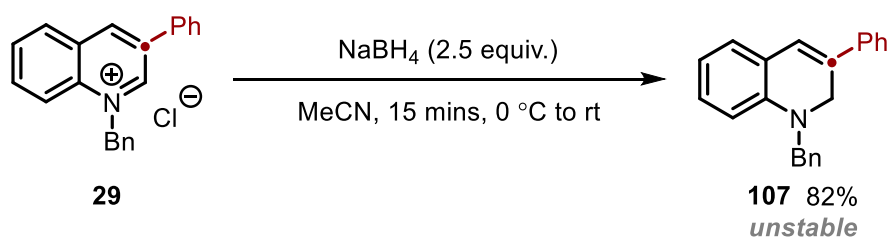


Scheme 3.31. Attempted regioselective aerobic 4-oxidations of **29** with a ruthenium photocatalyst. bpy = 2,2'-bipyridine. 0.2 mmol scale.

3.10.3 Reduction

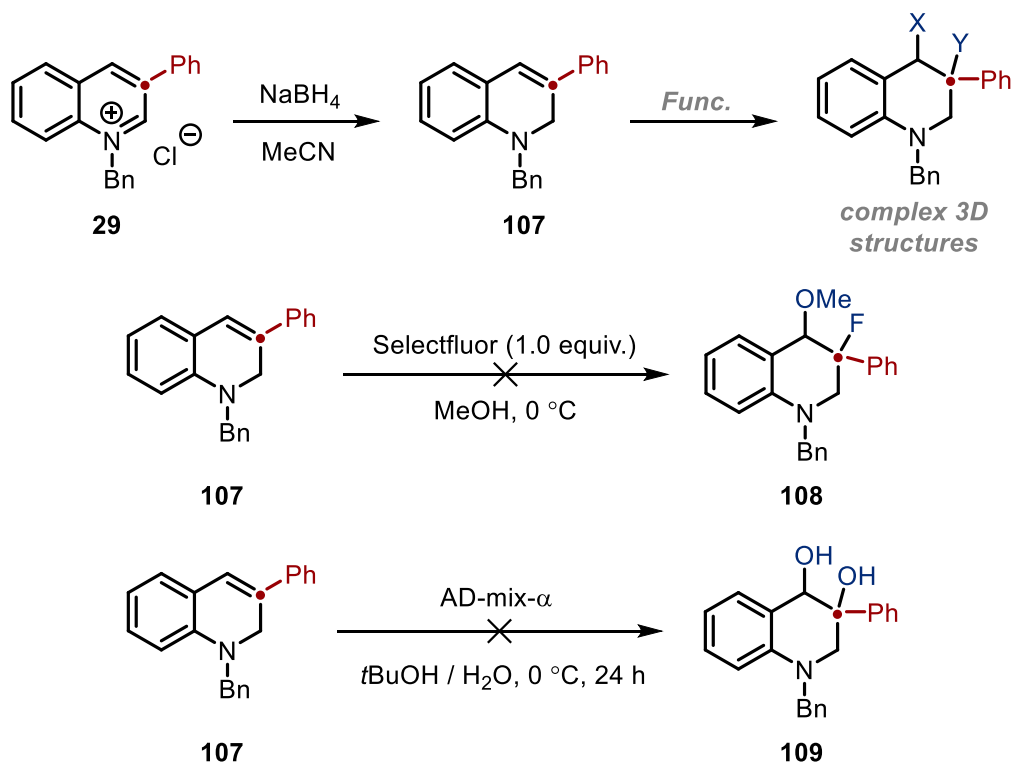
The main avenue of interest for the functionalisation of quinolinium salts was reduction chemistry. The transformation of a planar sp^2 aromatic system to a new 3-D molecular architecture in the form of various reduction products would present interesting new routes to complex structures, particularly due to the increased interest in non-planar systems within the field of medicinal chemistry.²¹¹ Full reduction of the ring would therefore result in the net transformation of an indole into a functionalised piperidine.

Due to the electron-deficient nature of azinium salts, they are competent electrophiles and can be partially reduced by the addition of hydride. Subjecting quinolinium salt **29** to 2.5 equivalents of sodium borohydride in MeCN resulted in full conversion of the salt within 15 minutes selectively to the dihydroquinoline **107** product resulting from addition at the 2-position, which was isolated in 82% yield (Scheme 3.32). Presumably due to the highly conjugated system that results from partial reduction, this compound possesses bright fluorescent yellow colour and emits a strong light blue colour when irradiated with long-wave UV radiation. While the product could be isolated and characterised in the crude mixture, purification by silica gel - as well as both neutral and basic alumina - column chromatography resulted in decomposition of the product. Degradation was also observed after 1 day at room temperature as well as upon storage in a freezer under a nitrogen atmosphere.



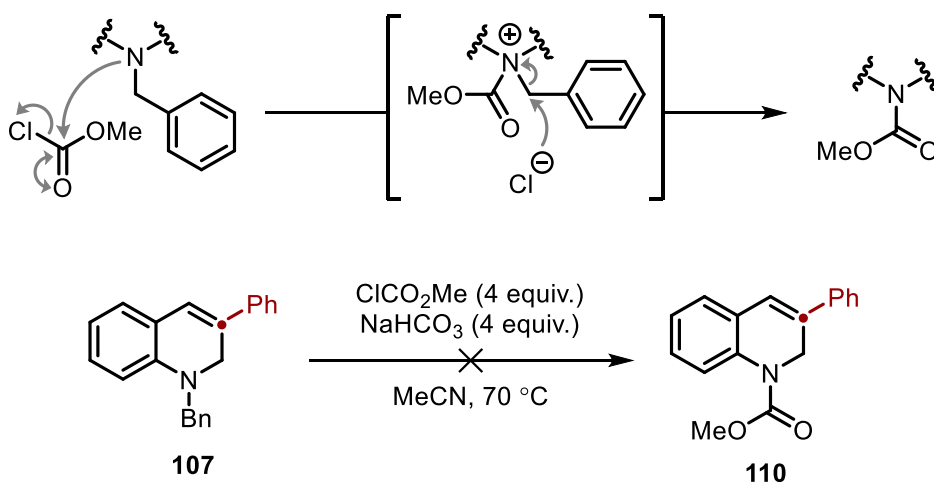
Scheme 3.32. Partial reduction to dihydroquinoline **107** with NaBH₄. 0.2 mmol scale. Isolated yield. Mass of residual solvent deducted.

Due to the instability of the dihydroquinoline **107**, the ‘capture’ of the product by functionalisation of the resulting stilbene-like olefin was attempted (Scheme 3.33). Ideally, this functionalisation would have to be carried out under mild conditions to avoid promoting decomposition. The first attempt at further functionalisation involved methoxyfluorination of the olefin with Selectfluor® in methanol to give **108**. However, under these conditions, quantitative oxidation back to the quinolinium salt **29** was observed. A well-known method of alkene functionalisation to achieve sp³ centres is asymmetric dihydroxylation.²¹² After isolation, the dihydroquinoline was subjected to AD-mix- α . Perhaps due to poor solubility of the salt in *t*BuOH/water solvent mixture, the reaction proved sluggish to the point that decomposition of the dihydroquinoline (at 0 °C) was competitive and poor conversion to **109** was achieved after 24 hrs.



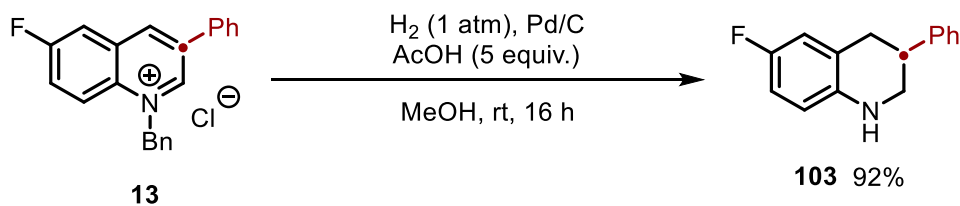
Scheme 3.33. Top: Rationale for molecular complexity *via* reduction. Middle: Attempted methoxyfluorination. Bottom: Attempted asymmetric dihydroxylation. 0.2 mmol scale.

It was proposed that the instability of the dihydroquinoline was due to the electron-rich benzyl protecting group as carbamate-protected dihydroquinolines are known to be stable.^{213,214} The acylation of amines with cleavage of a benzyl protecting group is known and therefore it was envisaged that the dihydroquinoline **107** could be converted to a more stable form by reaction with methyl chloroformate *via* the mechanism shown in Scheme 3.34.^{215,216} Upon subjecting of the benzyl dihydroquinoline **107** to methyl chloroformate in MeCN at 70 °C, only decomposition of the dihydroquinoline was observed with none of the desired product **110** formed. This can likely be attributed to the decreased nucleophilicity of the aniline-like amine in the dihydroquinoline compared to typical aliphatic tertiary amines, for which this method of swapping protecting groups is generally used.



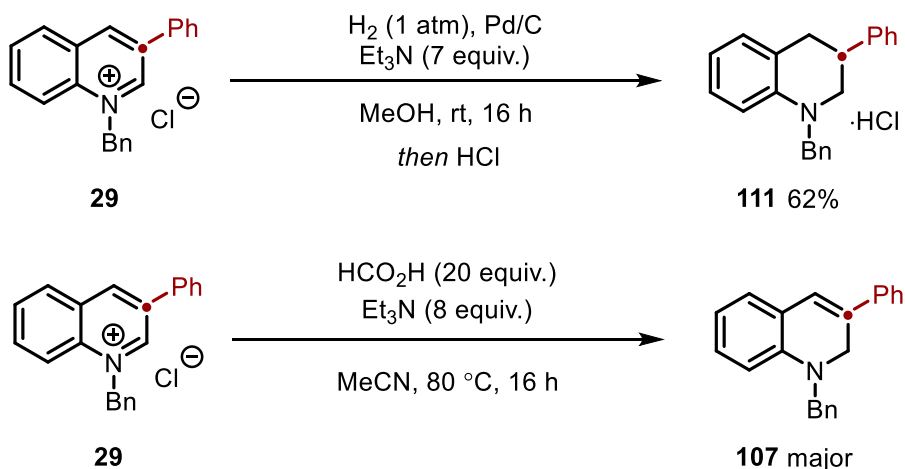
Scheme 3.34. Top: De-benzyl acylation of amines. Bottom: Attempted protecting group swap with methyl chloroformate. 0.2 mmol scale. Determined by ¹H NMR spectroscopy.

As noted in the attempted de-benzylation of the quinolinium salt to the free quinoline, Pd-catalysed hydrogenation selectively reduces the heterocyclic ring prior to benzyl cleavage. With this in mind, access to the tetrahydroquinoline would therefore be facile. Subjecting **13** to hydrogenolysis with 1 atmosphere of hydrogen resulted in full reduction of the ring in addition to benzyl cleavage though conversion was inconsistent over several reactions. Notably, the product was obtained as the hydrochloride salt upon removal of the methanol solvent, suggesting *in situ* formation of HCl. The following reaction mechanism was therefore postulated: reduction of the ring occurs prior to benzyl cleavage, followed by protonolysis of the amine nitrogen. This protonation then enhances cleavage of the benzyl group. Likely enhancing this reactivity further, the addition of acetic acid led to more consistent conversion to the tetrahydroquinoline **103**, which - after basic work-up - was isolated in a 92% yield (Scheme 3.35).



Scheme 3.35. Full reduction of **14** to tetrahydroquinoline **107**. 0.2 mmol scale. Isolated yield.

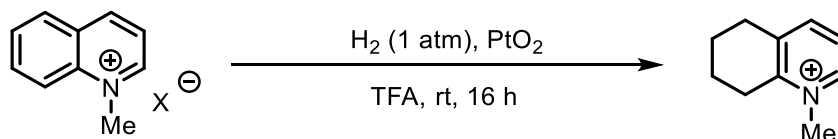
Having proposed the reduction mechanism above, diminishing the amount of acid present would likely halt the reaction after initial ring reduction, without cleavage of the benzyl group. This would give access to the benzyl tetrahydroquinoline and increase the diversity of products accessible from these salts. Indeed, the inclusion of triethylamine resulted in selective formation of the benzyl tetrahydroquinoline product **111** which was isolated in a 62% yield as the hydrochloride salt (Scheme 3.36). A metal-free reduction of the azinium ring was also attempted using chemistry developed by the Donohoe and co-workers which achieves azinium reduction with 5:2 HCO₂H/Et₃N azeotrope.¹⁹⁰ However, under these conditions, the major product observed was dihydroquinoline **107**. This suggests that despite its instability, the stilbene formed is the most stable product under these conditions and reduction of **107** further is disfavoured.



Scheme 3.36. Top: Base-assisted reduction of **33** with retention of the benzyl protecting group. 0.2 mmol scale. Isolated yield. Bottom: Attempted metal-free reduction. 0.2 mmol scale.

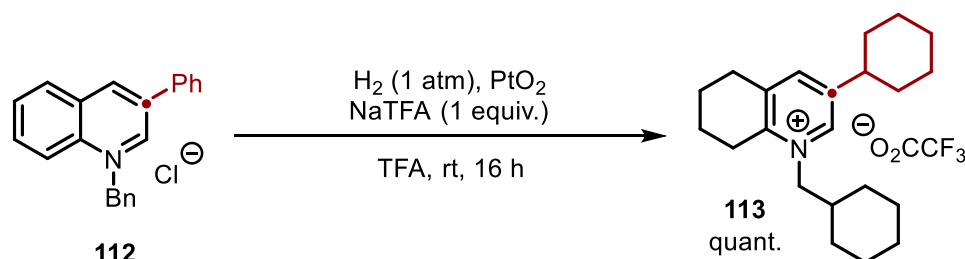
Finally, exploration into more unorthodox reductions that could create unique molecular architectures that would be difficult to access otherwise was undertaken. One method identified was the selective Pt-catalysed reduction of the benzenoid ring within *N*-methyl quinolinium salts, leaving the azinium core intact.²¹⁷ This method required anion exchange to either trifluoroacetate or fluorosulfate prior to reaction to avoid catalyst poisoning. The authors suggest in this case that the chemoselectivity results from solvation of the cationic core

by the trifluoroacetic acid (TFA) solvent, which is significantly enhanced compared to the more lipophilic benzo-fused ring.



Scheme 3.37. Solvent- and catalyst-mediated reduction of arenes with retention of cationic functionality.

The reaction was therefore carried out on salt **112** in the presence of PtO₂ and sodium trifluoroacetate (to sequester the chloride anion) in the TFA solvent. Not only was the benzo-fused ring reduced, but the two additional aryl rings at the 3-position and benzyl group were fully reduced to the corresponding cyclohexane while the central heteroarene core remained untouched (Scheme 3.38). A quantitative yield of pyridinium salt **113** was observed by ¹H NMR analysis.



Scheme 3.38. Reduction of **112** to pyridinium salt **113**. TFA = trifluoroacetate. 0.2 mmol scale. Yield determined by ¹H NMR spectroscopic analysis against 1,3,5-trimethoxybenzene as an internal standard.

3.11 Thermal stability of chlorodiazirines

In addition to the work presented here, chlorodiazirines are emerging as a powerful class of reagents due to their potential to act as carbynyl synthons, and additional publications have reported the use of chlorodiazirines over the course of the work carried out for this thesis.^{91,187} In these reports, in addition to older reports of the synthesis and use of chlorodiazirines, the thermal stability and energetic potential of diazirines is often noted but only anecdotal evidence regarding their stability is reported.^{91,157,187,196} Due to the myriad potential applications of chlorodiazirines in synthetic chemistry, we thought it necessary to carry out a thorough investigation of the thermal stability and the explosive potential of these reagents.

3.11.1 Differential scanning calorimetry (DSC)

To investigate the thermal stability of diazirines, differential scanning calorimetry (DSC) was chosen as the analytical technique of choice over similar techniques such as thermogravimetric analysis (TGA). While TGA may appear to be superior due to the nature of the technique as it is known for monitoring the decomposition of materials, DSC possesses a number of advantages. Firstly, TGA will only identify the temperatures at which decomposition occurs, whereas DSC also allows for the enthalpy of decomposition to be obtained, a highly important parameter for determining if a material is energetic. Additionally, not only has DSC analysis been carried out on a range of diazo compounds,¹³² the compounds with which diazirines are often compared, DSC data for phenylchlorodiazirine **11** is also known, allowing for a direct comparison.¹⁸¹ This study also employed a DSC capsule with a pierced lid (to vent dinitrogen formed) which would likely result in a lower reported exotherm. However, a comprehensive structure-activity relationship for the stability of diazirines has not been carried out, which we sought to remedy.

The work of Bull and co-workers on the stability of diazo compounds and the analysis of peptide coupling reagents by Pfizer served as guidelines for the DSC analysis of diazirines and highlighted key variables of interest.^{132,218} These variables are: enthalpy of decomposition (ΔH_d), onset temperature (T_{onset}) and initiation temperature (T_{init}). ΔH_d is the total energy released (energetic yield) upon decomposition as an exotherm and is typically measured and reported in J g^{-1} or kJ mol^{-1} . T_{onset} is defined as the intersection of the maximum peak gradient and the baseline.ⁱ T_{init} is defined as the temperature at which heat flow, Q , is $>0.01 \text{ W g}^{-1}$ above the baseline (Figure 3.6). From these data, several parameters may be derived to quantify the energetic nature and the ability to which they can be handled safely.

ⁱ In DSC experiments, the baseline is not necessarily 0 W g^{-1} , but rather the lowest value prior to any exothermic or endothermic events and may be positive or negative.

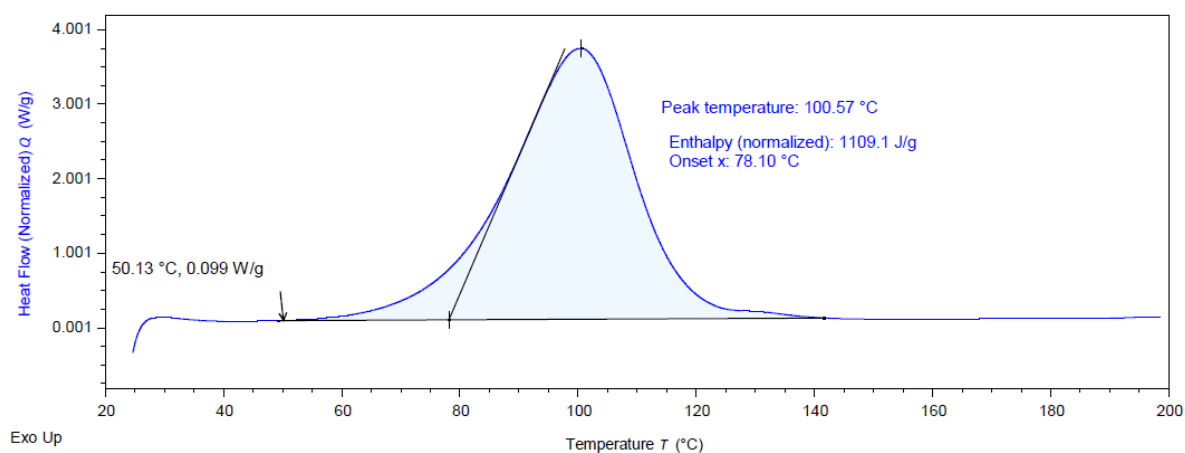


Figure 3.6. A typical DSC plot for diazirine **59**. Exotherms shown upwards. Method: Equilibrate at 25 °C for 1 min, then heat to 180-250 °C (dependent on substrateⁱ) at 5 °C/min. See experimental for raw data. Temperature denoted by arrow refers to T_{init} . Section 5.4 for full DSC methods.

To identify general trends in their stability, a range of diazirines with varying electronics were analysed as T_{onset} shows a strong correlation with the Hammett parameter, σ for phenyl diazoacetates.¹³² Results of the DSC analysis on neat diazirines revealed, in each case, large exothermic decomposition upon heating. The full results can be seen in Table 3.13.

Entry	Diazirine	σ	$T_{\text{init}} / ^\circ\text{C}$	$T_{\text{onset}} / ^\circ\text{C}$	$\Delta H_{\text{d}} / \text{J g}^{-1}$	$\Delta H_{\text{d}} / \text{kJ mol}^{-1}$
1	4-Me-C ₆ H ₄ (63)	-0.17	49	77	-1437	-240
2	Ph (11)	0.00	49	79	-1309	-200
3	4-F-C ₆ H ₄ (58)	0.06	49	77	-1168	-199
4	4-Cl-C ₆ H ₄ (59)	0.23	50	78	-1109	-207
5	4-Br-C ₆ H ₄ (60)	0.23	50	78	-952	-220
6	2-Pyridyl (68)	0.71	62	92	-1884	-289
7	4-NO ₂ -C ₆ H ₄ (64)	0.78	67	87	-1225	-242

Table 3.13. Thermodynamic data for the thermal decomposition of arylchlorodiazirines.

Of the seven diazirines analysed, an exotherm greater than or comparable to known explosive diazo compounds such as ethyl diazoacetate (EDA) and methyl phenyldiazoacetate was observed.¹³² Notably, the initiation temperature for this decomposition is strikingly low at under 50 °C, lower than neat EDA (55 °C neat, 65 °C in solution). Decomposition of more

ⁱ Maximum temperature was initially chosen to be 250 °C, consistent with Bull and co-workers. However, once we were certain the exotherm of interest concluded at <160 °C for a number of samples, the maximal temperature was lowered to 200 °C and then 180 °C.

electron-rich diazirines (entries 1-3) occurs noticeably lower than strongly electron-withdrawing diazirines (entries 6 and 7) with both T_{onset} and T_{init} increasing with σ (Figure 3.7). ΔH_{d} is mostly consistent for each diazirine, with the exception of 4-bromodiazirine **60** (entry 5) and 2-pyridyldiazirine **68** (entry 6). For **60** the lower value for ΔH_{d} can be attributed to the higher mass of the bromine compared to other substituents. In this case, the heavy bromine atom acts as ‘molecular ballast’ as a lower proportion of the molecular mass is incorporated into the energetic functional group. Normalising these data from J g^{-1} to kJ mol^{-1} affords a similar value of ΔH_{d} for **60** though ΔH_{d} for **68** remains far higher at 289 kJ mol^{-1} . This may be attributed to the ‘nitrogen effect’ in which the inclusion of nitrogen atoms into a molecule often leads to greater energetic capabilities.²¹⁹ The generally consistent value of ΔH_{d} in kJ mol^{-1} for each diazirine correlates with the presence of a single energetic moiety per molecule, resulting in an equimolar amount of the energetic group. A comparison of ΔH_{d} and T_{init} with those of other energetic reagents can be seen in Figure 3.8.

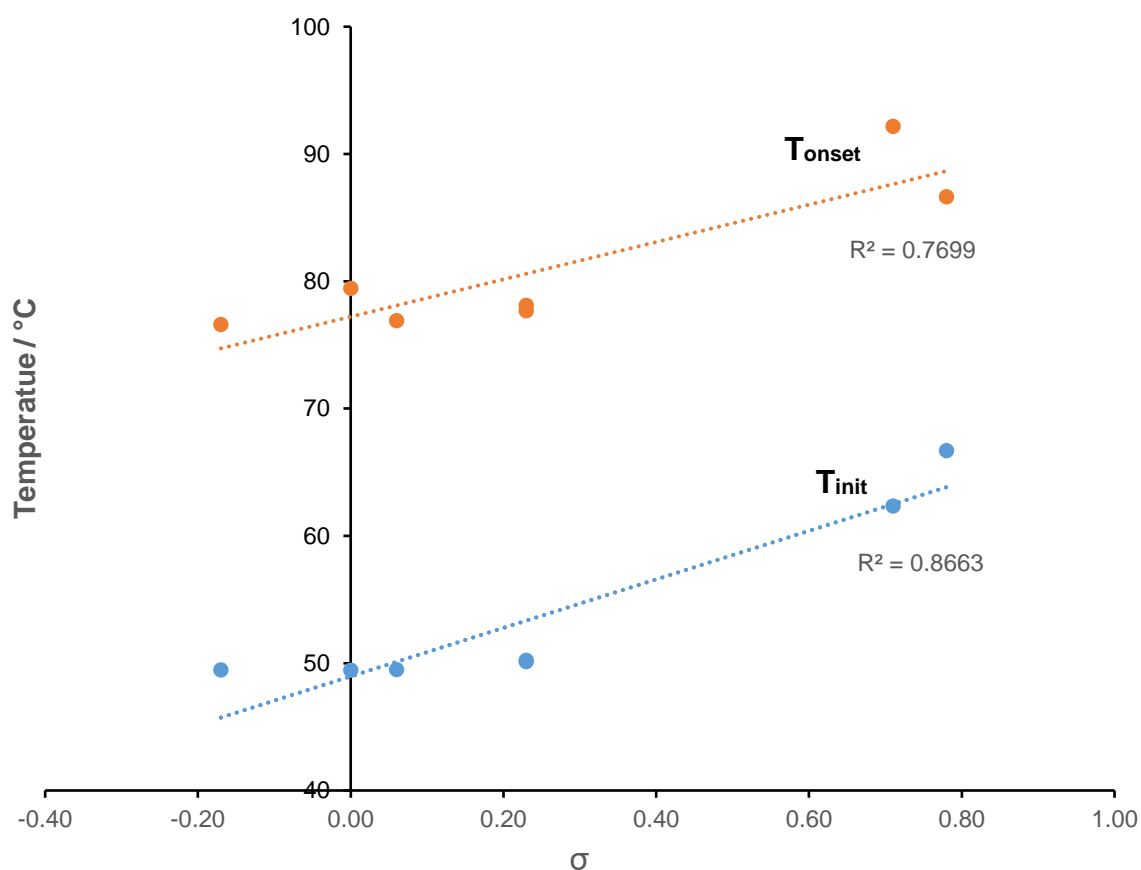


Figure 3.7. Dependence of T_{init} and T_{onset} of diazirine decomposition against Hammett parameter, σ .

In general, arylchlorodiazirines are more energetic than their analogous aryltrifluoromethyldiazirines as well as diazo compounds.^{132,181} It is an important distinction to make that although diazirines are more energetic, diazo compounds necessarily require an electron-withdrawing group to achieve a modicum of stability. For comparison, phenyldiazomethane, arguably the closest diazo isomer to diazirine **11**, is reported to decompose at -80 °C.²²⁰ Diazirines proved less energetic than several common synthetic reagents including tosyl azide (TsN₃)¹³² and the peptide coupling reagent HATU²¹⁸ though were similar in magnitude to DEAD (diethyl azodicarboxylate).¹³² The range of T_{init} for diazirines is comparable to that of EDA (60 °C) but is significantly lower than methyl phenyldiazoacetate (Figure 3.8). Both HATU and TsN₃, which have greater ΔH_d values than the diazirines, have significantly higher T_{init} values. Arylchlorodiazirines therefore undergo decomposition at lower temperatures than diazo compounds and are more energetic, though the latter are significantly stabilised by electron-withdrawing groups.

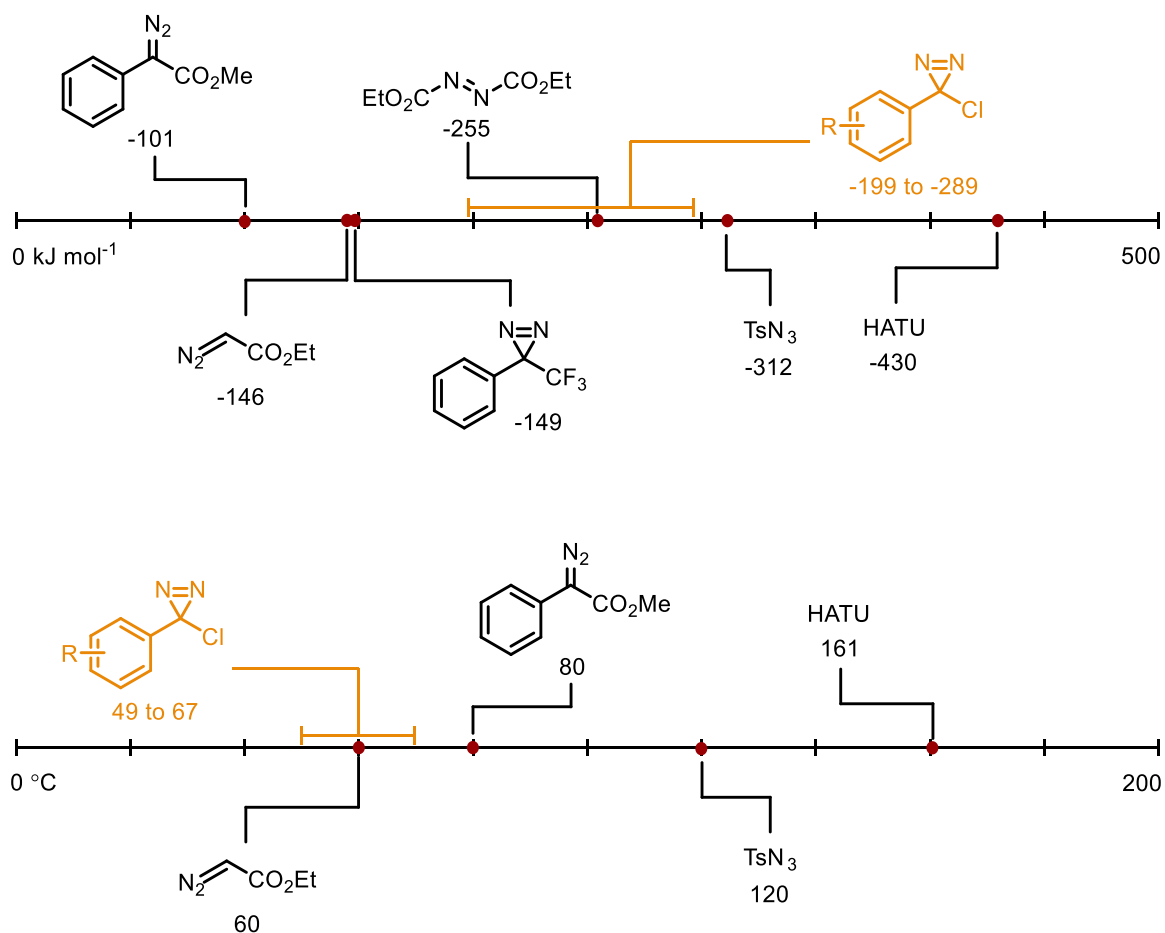


Figure 3.8. Comparison of ΔH_d and T_{init} with common and commercially-available reagents reported to be energetic. Portrayed roughly to scale. T_{init} reported as the lowest reported value.

The parameters discerned above can be used to calculate predictors of the energetic nature of a compound. In a seminal work, Yoshida and co-workers developed a correlation to predict impact (or shock) sensitivity (IS) and explosive propagation (EP) by the experimental determination of these characteristics from known explosives.²²¹ Impact sensitivity as the name suggests describes how to compound reacts to physical stimuli. Other sensitivities are also used, such as friction and electrostatic discharge, though these are less common, and results are more difficult to reproduce.¹³² Impact sensitivity is generally difficult to determine and rudimentary techniques such as the self-explanatory ‘hammer and anvil’ test are employed.^{222,223} Explosive propagation (EP) refers to the ability for the exotherm released by a decomposing molecule to trigger further decompositions through the sample, resulting in an explosive chain reaction. These correlations allow for the prediction of these characteristics in a safe and controlled manner by the use of DSC.

The Yoshida correlations employ ΔH_d and T_{onset} to determine both impact sensitivity and explosive propagation *via* equations 1 and 2 shown below:

$$IS = \log_{10}(Q) - 0.72[\log_{10}(T_{onset} - 25)] - 0.98 \quad (3.1)$$

$$EP = \log_{10}(Q) - 0.38[\log_{10}(T_{onset} - 25)] - 1.67 \quad (3.2)$$

where Q is ΔH_d in cal g⁻¹. A value > 0 in each case predicts that the material will be impact sensitive or undergo explosive propagation. A similar correlation was developed by Pfizer in the assessment of peptide coupling reagents (equations 3.3 and 3.4).²¹⁸ This particular correlation is nearly identical, though the lower T_{init} is employed instead of T_{onset} and smaller coefficients result in a more stringent estimate for both parameters.

$$IS = \log_{10}(Q) - 0.54[\log_{10}(T_{onset} - 25)] - 0.98 \quad (3.3)$$

$$EP = \log_{10}(Q) - 0.285[\log_{10}(T_{onset} - 25)] - 1.67 \quad (3.4)$$

The final characteristic of note is T_{D24} , defined as the temperature at which the time to maximum rate under adiabatic conditions (TMR_{ad}) becomes >24 hrs. Initially employed at GSK, it can be used to approximate a temperature at which the material can be handled with a reasonable margin of safety.²²⁴

$$T_{D24} = 0.7T_{init} - 46 \quad (3.5)$$

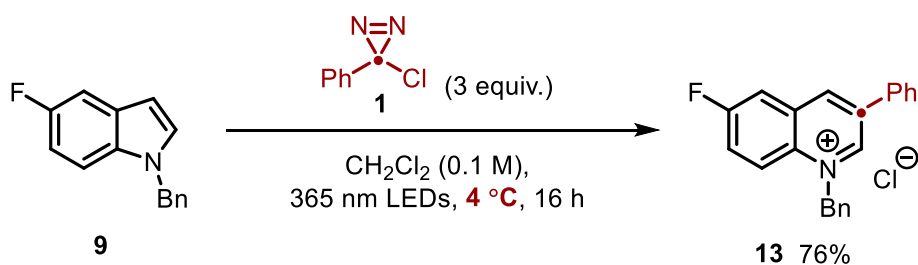
Due to a number of limitations in assumptions made and the sensitivity of DSC, values for T_{D24} are typically given to the nearest 5 °C. Values for IS and EP using both correlations and T_{D24} are shown in Table 3.14.

Entry	Diazirine	Yoshida		Pfizer		T _{D24} / °C
		IS	EP	IS	EP	
1	4-Me-C ₆ H ₄ (63)	0.32	0.22	0.81	0.47	-10
2	Ph (11)	0.27	0.17	0.77	0.43	-10
3	4-F-C ₆ H ₄ (58)	0.23	0.12	0.72	0.38	-10
4	4-Cl-C ₆ H ₄ (59)	0.20	0.10	0.69	0.35	-10
5	4-Br-C ₆ H ₄ (60)	0.14	0.03	0.62	0.29	-10
6	2-Pyridyl (68)	0.39	0.29	0.82	0.54	0
7	4-NO ₂ -C ₆ H ₄ (64)	0.20	0.12	0.61	0.33	0

Table 3.14. Correlations for chlorodiazirines derived from thermodynamic data.

Both correlations indicate that every diazirine tested is both impact sensitive and will undergo explosive propagation, with values > 0 in each case. Only diazirines **59** and **60** (entries 4 and 5) are close to zero for explosive propagation using Yoshida's correlations (0.10 and 0.03 respectively) though the more stringent Pfizer correlation has these values well above zero. Due to the larger proportion of the correlation deriving from ΔH_d (as Q), 2-pyridyl diazirine **68** is identified as particularly sensitive, despite its high initiation and onset temperatures. As T_{D24} is dependent only on T_{init}, both diazirines **64** and **68** can be handled to a reasonably safe degree at 0 °C, compared to -10 °C for all others.

Considering the data reported herein, arylchlorodiazirines are clearly highly sensitive and potentially explosive reagents that can undergo decomposition at temperatures and conditions typical of laboratory chemical reactions. Although the diazirine is in solution as opposed to neat, the conditions reported by Levin and co-workers employ temperatures (50 °C and later 60 °C) close to or above T_{init} for some diazirines and may present a significant safety hazard, particularly when performed in a sealed vessel.^{91,187} On the other hand, the use of photochemical methods of diazirine decomposition allow for controlled decomposition at ambient temperatures, allowing for safer handling of these energetic compounds. To highlight the operational advantages of utilising photochemistry in the ring expansion procedure, we were curious to see whether the reaction could be performed close to T_{D24}. Carrying out photochemical reactions at low temperatures typically requires specialist equipment which limited temperature ranges available to us. However, carrying out the reaction in a cold-room (4 °C) proved operationally simple. Gratifyingly, carrying out the reaction shown in Scheme 3.39 under photolytic conditions at 4 °C resulted in a 76% isolated yield of quinolinium salt **13**.



Scheme 3.39. Ring expansion of **9** performed at 4 °C. 0.2 mmol scale. Isolated yield.

3.11.2 Avoiding isolation of diazirines

As arylchlorodiazirines are clearly energetically sensitive, we sought to continue to develop conditions in which exposure to the *neat* reagents was minimised. One method to achieve this is to avoid isolation of the neat diazirine and simply employ a titrated solution of diazirine generated from the Graham oxidation. Solutions of arylchlorodiazirines carried over from their synthesis have been employed, notably by Padwa and co-workers who utilised a solution of **11** in cyclohexane in a cyclopropanation reaction.¹⁸²

To achieve this, the Graham oxidation of benzamidine hydrochloride was carried out (see section 3.6.2). Rather than separating the pentane layer and extracting the aqueous with diethyl ether, only the pentane was separated which was dried over MgSO₄. This pentane extract was then titrated by ¹H NMR analysis of an aliquot of a known volume of the **11** solution against 1,3,5-trimethoxybenzene as an internal standard. The titre of the solution of **11** was identified to be 0.48 M. Employing this solution in the standard reaction conditions afforded **13** in a 45% yield. Although a sharp decrease compared to the typical yield for this transformation, no methods of purification other than drying with MgSO₄ were employed for the pentane solvent. Additionally, the use of pentane as opposed to CH₂Cl₂ may be the cause of the lower yield. Ultimately, this proved to be a useful preliminary test in carrying out the reaction without exposure to neat diazirines.

3.11.3 Applications to flow chemistry

The next logical step in avoiding neat diazirines is transferring the reaction protocol to flow conditions. Flow chemistry enables the use of highly sensitive reagents by avoiding direct contact and the generation of potentially explosive reagents *in situ*.²²⁵ Flow chemistry would allow for the generation of the diazirine in flow which could then be telescoped to a second

photochemical flow apparatus that would carry out the ring expansion protocol. A general scheme for possible flow conditions is shown in Figure 3.9.

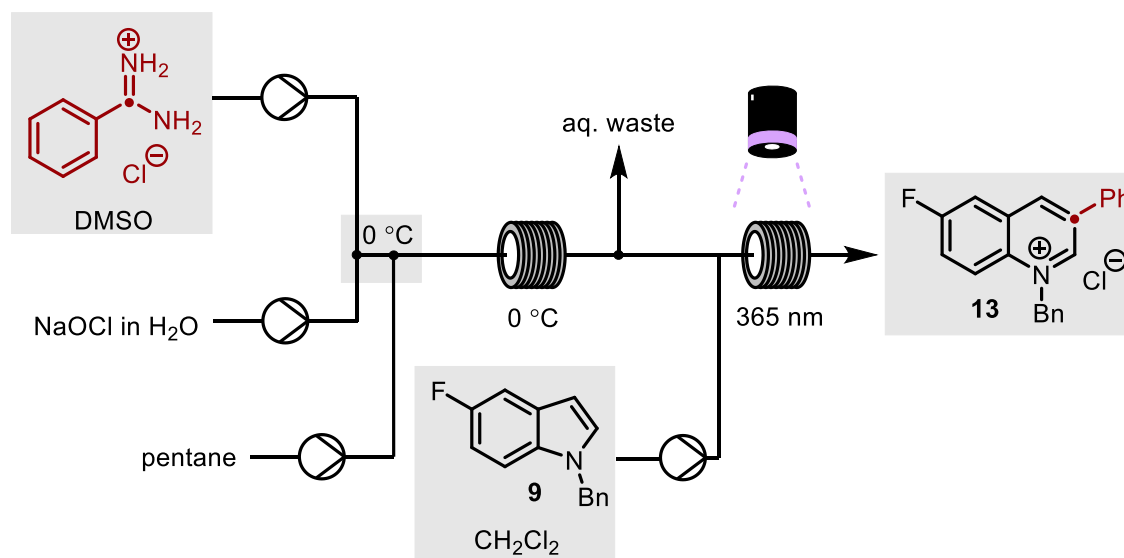


Figure 3.9. Diagram of potential flow apparatus for the tandem Graham oxidation/ring expansion.

There are however major drawbacks with the reaction protocol that inhibit its applicability to flow. Firstly, synthesis of the diazine *via* Graham oxidation occurs in a biphasic mixture. While the use of biphasic conditions in flow is known, specialist flow equipment may be required to enhance both mixing and subsequent separation of the phases. Secondly, the ring expansion protocol produces dinitrogen gas as a by-product. This has two issues: the build-up of pressure would require the use of pressure regulators, and the formation of bubbles within the reaction mixture may disrupt solvent flow. Once again, while problematic, these issues can be resolved with specialist equipment. Finally, the reaction product is a precipitate. This restricts the ability to transfer the product after precipitation and also may result in clogging of the flow equipment (especially the required back-pressure regulators).

Before these issues can be resolved, whether the reaction can be applied to flow chemistry must first be determined. A potential limitation is that a 16 hour reaction time is required for maximum conversion. However, light penetration may be enhanced when employing the narrow flow reactor tubing. As a crude initial test, the reaction was performed in NMR tubes to match the approximate diameter of flow tubing. The reaction was then monitored by ^{19}F NMR spectroscopy. Under these conditions, conversion after 4 hours was poor (Figure 3.10). The reaction was also attempted in typical flow tubing using a plug of the reaction mixture held in place. Similar conversions were observed in this case, suggesting that the reaction was simply too slow to employ a realistic residence time for flow conditions. This is of course using a photoreactor available with an 18 W LED. More powerful LEDs in addition to better light

penetration may afford higher conversions in a shorter time, though access to this equipment was not possible at the time.

While no mechanistic investigations have been undertaken thus far, monitoring this reaction revealed that conversion to **14** occurred linearly, suggesting a zero-order dependence on the indole starting material (Figure 3.10). This therefore implies that the rate-determining step is the – potentially photon-limited - formation of the carbene. There may be a number of possible steps in the decomposition of the diazirine that could be rate-determining, though probing this would require more specialist techniques such as laser-flash photolysis (LFP) and further mechanistic analysis is yet to be undertaken. This does however lend to the idea that the reaction rate may be enhanced by employing a more powerful light source. Considering the evident issues, modification of the reaction protocol under flow conditions was not continued, although it remains an important objective of future work.

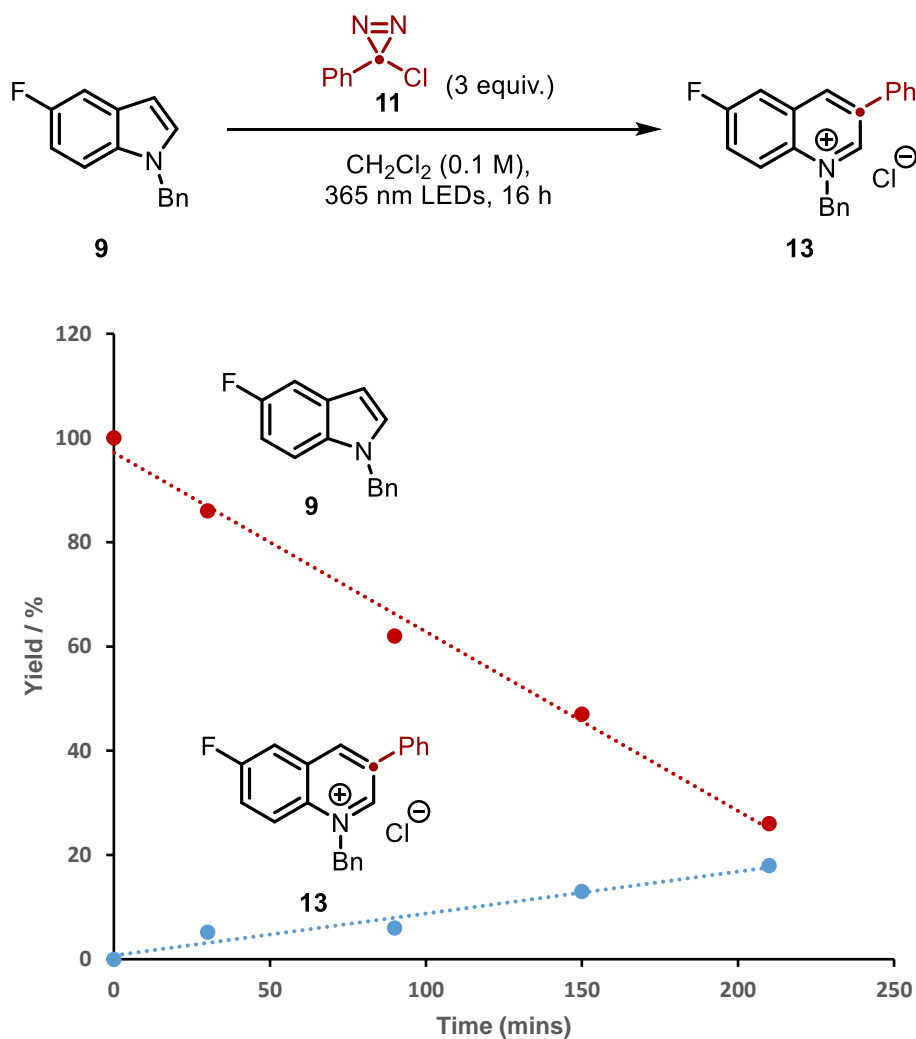


Figure 3.10. Monitoring of ring expansion reaction. Yields determined by ^{19}F NMR spectroscopy.

4

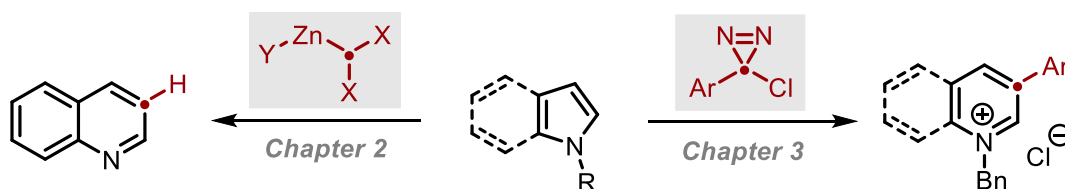
Conclusions and Future Work

Abstract:

This chapter summarises the work reported in this thesis as well as serving as an outlook for further work and transformations that could build upon the work presented here.

4.1 Conclusions

This work has furthered the newly emerging field of skeletal editing by the development and optimisation of two new methodologies that insert a carbon atom into the aromatic skeleton of an azole to achieve the ring expanded product.



Scheme 4.1. Summary of the transformations reported in this thesis.

While full investigations were not fully realised, chapter 2 described the insertion of a single C-H unit into 5-fluoroindole *via* a Simmons-Smith approach. An unprotected indole was found to be incompatible with the reaction conditions and, despite a number of attempts to remedy this, subsequent protection of the indole was ultimately required to achieve low yields of the product. Boc-protection proved most effective, with other amide-like functional groups proving less well tolerated. Alkyl- and silyl-protected indoles also proved unreactive.

In chapter 3, a synthetic protocol to achieve carbon atom insertion was developed and optimised. This method utilised arylchlorodiazirines as photolytically-activated carbynyl synthons that achieve the ring expansion of both indoles and pyrroles by formation of the singlet carbene and cyclopropanation of the indole olefin. Fragmentation of the resulting intermediate led to ring expansion. A benzyl protecting group proved optimal to achieve high yields and, due to the nature of the resulting benzyl quinolinium salt product and the solvent, allowed for isolation of the product by precipitation.

A study of substrate scope revealed tolerance towards a range of substitution patterns and functional groups. Notably, modification of the solvent system had to be undertaken to achieve consistently high yields from indoles bearing more apolar substrates. Precipitation of quinolinium salts derived from electron-deficient indoles proved facile, though increasing the stoichiometry of the diazirine partner was required for higher yields. In addition to the azole, the diazirinyl partner also tolerated a range of functional groups though the synthesis of the diazirines themselves proved difficult for *ortho*-substituted examples.

Application to pyrroles required further re-optimisation of the methodology. Specifically, due to higher solubility of the product in the reaction solvent, employing TBME achieved

optimal yields. Similar to indoles, a range of substitution patterns were well tolerated. In the cases where the resulting pyridinium salt product was unsymmetrical, carbon atom insertion occurred preferentially at the most electron-rich position, unless the 2-position was substituted which appeared to override the electronic preference.

Investigations into functional group tolerance were aided by a Glorius-type robustness screen, which identified that a range of medically-relevant functional groups including esters and amides were well tolerated by the reaction. On the contrary, nucleophilic functional groups such as amines proved incompatible, presumably due to deleterious interactions with the carbene. With the information gained from this screen, the reaction protocol was applied to more complex substrates including the hormone melatonin, a protected tryptophan, and a tryptophan-containing dipeptide.

Functionalisation of the resulting products was also preformed to highlight their synthetic utility. De-alkylation to the free quinoline was carried out *via* an S_N2 reaction as Pd-catalysed hydrogenolysis resulted in reduction of the azinium ring. This was later exploited to achieve both the secondary tetrahydroquinoline and a tertiary tetrahydroquinoline with retention of the benzyl group. Partial reduction to the dihydroquinoline was also achieved though the resulting product proved highly unstable. Attempts to capture this product by further functionalisation failed. A complementary reduction of the arene functionalities in the product was also achieved with retainment of the azinium core. A selective oxygenation of the 2-position was carried out, though due to solubility issues a 4-oxygenation was not achieved.

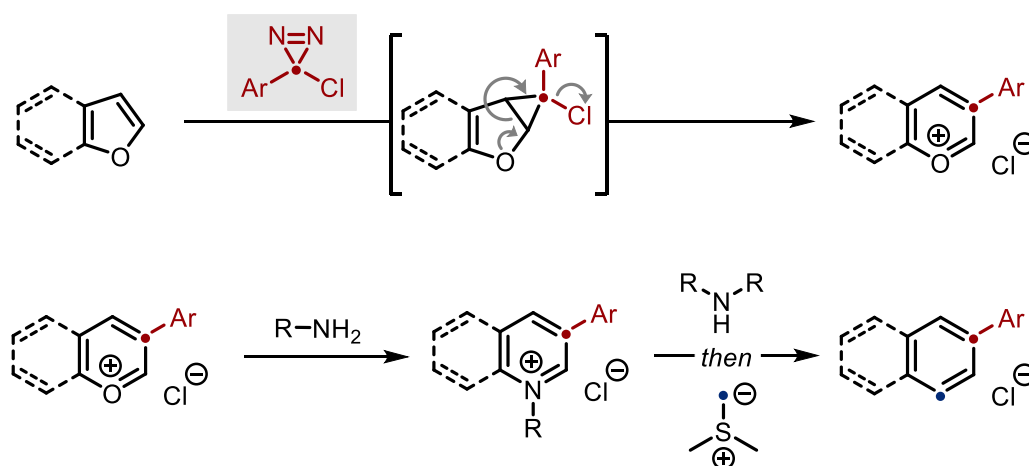
Finally, determination of the thermal stability of the arylchlorodiazirines was carried out by DSC analysis. Several parameters and correlations indicated that every diazirine synthesised is potentially explosive. Methods to avoid handling of the neat diazirine, such as the use of the reagents in solution and transferring the reaction protocol to flow either returned poorer yields or were unsuccessful.

4.2 Future Work

If arylchlorodiazirines are to see any major synthetic use in large-scale industrial applications, methods that avoid their isolation will be required. Further application of the methodology to flow conditions is therefore highly sought after due to its capabilities to form - and react - sensitive substrates in a controlled manner. While not fully realised in this thesis,

application of azole ring expansions to flow remains paramount to the development of this methodology.

While this thesis has focused on the ring expansion of nitrogen heterocycles. A similar rationale can be invoked for the ring expansion of furans. The resulting product of this reaction would be a more unstable pyrilium salt, though this could be feasibly captured by reaction with an amine similar to the reaction of Katritzky salts outlined in section 1.2.4. This would allow for the formal insertion of a carbon atom with additional exchange of an oxygen atom for a nitrogen atom. This particular reactivity could be carried even further. By tailoring the choice of amine incorporated into the aromatic skeleton as described above, nitrogen to carbon exchange could also be achieved, resulting in a formal exchange of oxygen for carbon.²²⁶ The ring expansion of benzofurans in this manner has been reported, though the sole method employs a vast excess of the benzofuran as opposed to the diazirine, which makes application to complex – and labour intensive – substrates less appealing.²²⁷ For this transformation, nitrogen exchange *via* ring opening would be more challenging and may be limited only to monocyclic furans.

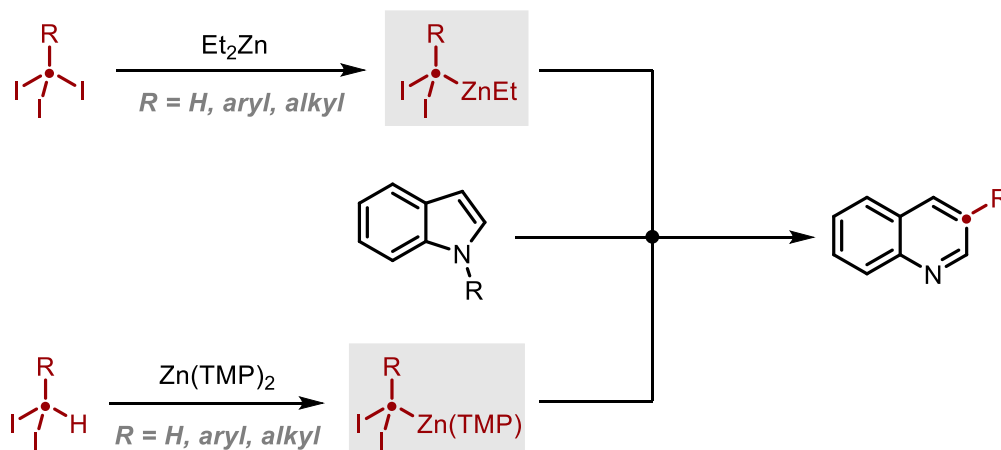


Scheme 4.2. Ring expansion of (benzo)furans. Atom exchange of O-to-N-to-C.

The ring expansion of azoles with zinc carbenoids has been demonstrated here, but significant optimisation would need to be carried out to achieve a robust methodology. Further optimisation would likely require a continuation of a protecting group screen along with modification of the active carbenoid. Application of this chemistry to pyrroles specifically may lead to better conversions due to their reactive nature. However, if an optimised method is realised, a far greater range of substituents could be inserted into the azole than the use of diazirines would allow. As long as the required trihalomethyl compound could be prepared, alkyl, (hetero)aryl, and heteroatomic groups could be inserted. If steric encumbrance does not

allow for their synthesis, it could be envisaged that the relatively acidic dihalomethyl compound could react with a zinc base such as $\text{Zn}(\text{TMP})_2$ to achieve a similar species.

By further development of both the methods described within, the insertion of *any* carbonyl synthon may be achieved, allowing for access to highly diverse heteroaromatic scaffolds.



Scheme 4.3. Zinc-mediated ring expansion achieved by zinc-halogen exchange or deprotonation of *gem*-dihalomethanes.

5

Experimental

Abstract:

Experimental details regarding the synthesis of all compounds mentioned in this thesis are included in addition to any relevant data such as DSC analysis.

5.1 General Information

Reagents were purchased from commercial suppliers and used as supplied. Sodium hypochlorite solution was either purchased from Sigma Aldrich (10-15%) or as commercial bleach (4.5%) and titrated against sodium thiosulfate in the presence of potassium iodide and HCl before use. Procedures requiring inert conditions were conducted in flame-dried glassware under an atmosphere of anhydrous dinitrogen using standard Schlenk techniques. Anhydrous solvents were obtained from in-house solvent purification systems (Inert® ProSolv; dried by passage through activated alumina columns under pressure of Ar) or by drying over activated 3 Å molecular sieves for 48 h followed by distillation. Deuterated chloroform was stored over 4 Å molecular sieves.

Flash column chromatography was accomplished using silica gel 60 Å (40-60 µm particle size) used as purchased from Sigma-Aldrich. Automated column chromatography was performed on disposable columns pre-packed with 50 µm silica gel using a Buchi Pure C-850 FlashPrep equipped with a UV-vis DAD (200-800 nm) and an ELSD detector. Analytical thin-layer chromatography was carried out on aluminium-backed silica gel plates (Merck/EMD Millipore, 60 Å pore size, precoated with a 254 nm-responsive fluorescent dye) and spots were visualised with UV irradiation (254 nm).

Photochemistry was achieved using a HepatoChem EvoluChem™ PhotoRedOx Box and an HCK10120111 (365 nm) LED lamp operating at 18 W with samples kept between 5–7 cm from the light source. Temperatures inside the photo-reactor were monitored and exceeded no more than 5 °C above ambient temperatures after 16 h.

NMR spectra were recorded at 298K on Bruker-Avance 500 or 400 spectrometers (¹H, 500 / 400 MHz; ¹³C, 125 / 101 MHz; ¹⁹F, 471 / 376 MHz). Chemical shifts (δ) are reported in ppm; coupling constants; *J*, are reported in Hz. Signals are reported as singlet (s), doublet (d), triplet (t), quartet (q), multiplet (m), broad (br), apparent (app.) and combinations thereof. Chemical shifts are reported relative to tetramethylsilane (TMS) and referenced to the appropriate residual solvent peaks for ¹H and ¹³C{¹H} NMR respectively:

CDCl₃: 7.26 ppm, 77.16 ppm

CD₃OD: 3.34 ppm, 49.00 ppm

DMSO-d₆: 2.54 ppm, 39.52 ppm

A 30 s relaxation delay time (D1) was used for quantitative ^{19}F NMR spectroscopy. NMR yields were calculated from ^{19}F NMR spectroscopy by comparison of integral ratios with the internal standard 4,4'-bis(trifluoromethyl)-1,1'-biphenyl (δ : -62.6 ppm in CDCl_3), which was prepared according to the literature method.²²⁸ Quantitative ^1H NMR analysis was achieved by comparison to a 1,3,5-trimethoxybenzene internal standard.

High-resolution mass spectrometry (HRMS) was performed using a Bruker MicroTOF spectrometer, with an electrospray ionisation ion source. Infrared spectra of neat compounds were recorded over the range 4000-600 cm^{-1} using a PerkinElmer Spectrum 1000 Series FTIR spectrometer with an ATR diamond cell.

Differential Scanning Calorimetry (DSC) analysis was performed using a TA Discovery DSC with reusable high pressure stainless steel capsules (TA Instruments; #900808.901) and gold-coated copper seals (TA Instruments; 900814.901). Calibration of the empty reference capsule was determined against a capsule containing *ca.* 8 mg of pure indium. Analysis of DSC data was carried out in TRIOS software.

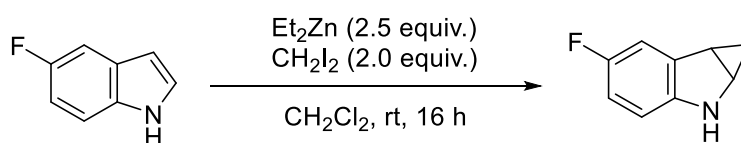
5.2 Synthesis of compounds relevant to Chapter 2

5.2.1 Optimisation and General Procedures

General Optimisation

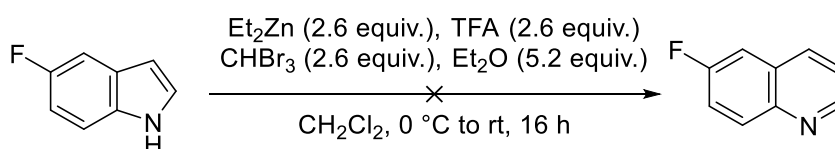
In a flame-dried flask under an atmosphere of dinitrogen, diethylzinc (1.0 M in hexanes, 0.44 mL, 0.44 mmol) was added drop-wise to a mixture of haloform (0.88 mmol) and 4,4'-bis(trifluoromethyl)-1,1'-biphenyl (internal standard) in anhydrous CH_2Cl_2 (1 mL) at rt and stirred for 15 mins. A solution of the indole (0.2 mmol) in anhydrous CH_2Cl_2 (1 mL) was then added dropwise and the reaction flask wrapped in foil to exclude light. The mixture was stirred at room temperature overnight. An aliquot was taken from the reaction mixture which was then filtered *via* syringe filter and analysed by ^{19}F NMR spectroscopy.

Attempted Simmons-Smith reaction with diiodomethane



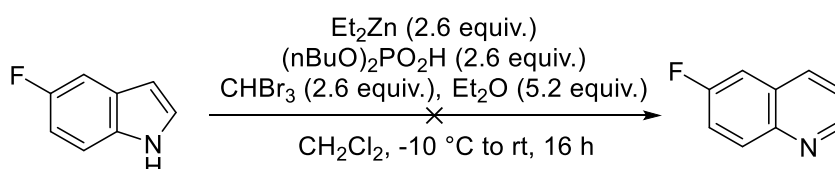
Under inert atmosphere diethylzinc (1.0 M in hexanes, 0.5 mL, 0.5 mmol) was added to a solution of diiodomethane (32 μL , 0.4 mmol) in anhydrous CH_2Cl_2 (1 mL) at 0 °C. The reaction mixture was stirred for 30 mins and then a solution of 5-fluoroindole (27 mg, 0.2 mmol) in anhydrous CH_2Cl_2 (1 mL) was added drop-wise. The mixture was warmed to room temperature and stirred overnight. An aliquot was taken from the reaction mixture which was then filtered *via* syringe filter and analysed by ^{19}F NMR spectroscopy.

Attempted ring expansion with zinc trifluoroacetate carbenoids



In a flame-dried flask under an atmosphere of dinitrogen, TFA (0.10 mL, 1.3 mmol) in anhydrous CH_2Cl_2 (1 mL) was added drop-wise to a second solution of diethylzinc (1.0 M in hexanes, 1.3 mL, 1.3 mmol) and Et_2O (0.27 mL, 2.6 mmol) in anhydrous CH_2Cl_2 (1 mL) cooled to 0 °C. The reaction mixture was stirred for 10 mins after which bromoform (0.11 mL, 1.3 mmol) was added drop-wise. The reaction mixture was stirred for another 30 mins after which a solution of *N*-Boc-5-fluoroindole (118 mg, 0.5 mmol) in anhydrous CH_2Cl_2 (1 mL) was added drop-wise. The mixture was warmed to room temperature and stirred overnight. An aliquot was taken from the reaction mixture and analysed by ^{19}F NMR spectroscopy.

Attempted ring expansion with zinc phosphate carbenoids

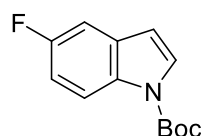


In a flame-dried flask under an atmosphere of dinitrogen, dibutylphosphate (0.26 mL, 1.3 mmol) in anhydrous CH_2Cl_2 (1 mL) was added drop-wise to a second solution of diethylzinc (1.0 M in hexanes, 1.3 mL, 1.3 mmol) and Et_2O (0.27 mL, 2.6 mmol) in anhydrous

CH₂Cl₂ (1 mL) cooled to -10 °C with an ice-salt bath. The reaction mixture was stirred for 10 mins after which bromoform (0.11 mL, 1.3 mmol) was added drop-wise. The reaction mixture was stirred for another 30 mins after which a solution of *N*-Boc-5-fluoroindole (118 mg, 0.5 mmol) in anhydrous CH₂Cl₂ (1 mL) was added drop-wise. The mixture was warmed to room temperature and stirred overnight. An aliquot was taken from the reaction mixture and analysed by ¹⁹F NMR spectroscopy.

5.2.2 Synthesis of protected indoles

N-(*tert*-Butoxycarbonyl)-5-fluoroindole (6)



In a flame-dried flask under an atmosphere of dinitrogen, Boc₂O (2.0 mL, 8.9 mmol) was added to a solution of 5-fluoroindole (1.00 g, 7.40 mmol) and DMAP (90 mg, 0.74 mmol) in anhydrous CH₂Cl₂ (8 mL) at room temperature. The mixture stirred at room temperature overnight. The reaction was quenched by the addition of sat. aqueous NaHCO₃ and the CH₂Cl₂ layer was separated. The aqueous layer was then washed with Et₂O (3 × 10 mL). The combined organics were dried over MgSO₄, filtered, and concentrated *in vacuo*. The crude material was purified by column chromatography (silica gel; 20% EtOAc in CyH) to afford the product as a yellow oil (1.35 g, 78%).

¹H NMR (400 MHz, CDCl₃): δ 8.08 (s, 1H), 7.62 (d, *J* = 3.7 Hz, 1H), 7.21 (dd, *J* = 9.0, 2.6 Hz, 1H), 7.03 (app td, *J* = 9.0, 2.6 Hz, 1H), 6.52 (dd, *J* = 3.7, 0.7 Hz, 1H), 1.67 (s, 9H).

¹³C{¹H} NMR (101 MHz, CDCl₃): δ 159.3 (d, *J* = 238.6 Hz), 149.7, 131.7, 131.5 (d, *J* = 10.1 Hz), 127.6, 116.2 (d, *J* = 9.2 Hz), 112.1 (d, *J* = 25.1 Hz), 107.1 (d, *J* = 4.1 Hz), 106.4 (d, *J* = 23.7 Hz), 84.0, 28.3.

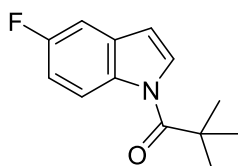
¹⁹F NMR (376 MHz, CDCl₃): δ -121.25 (td, *J* = 9.3, 4.5 Hz).

ν_{max} (neat) / cm⁻¹: 2979, 1731, 1468, 1371, 1353, 1277, 1254, 1155, 1024.

HRMS: calcd. for C₁₃H₁₄FNO₂Na [M+Na]⁺: 258.0901; found 258.0938.

Characterisation data are consistent with literature values.²²⁹

1-(5-Fluoro-1H-indol-1-yl)-2,2-dimethylpropan-1-one (7)



A flame-dried flask under an atmosphere of dinitrogen was charged with 5-fluoroindole (676 mg, 5.0 mmol), DMAP (61 mg, 0.5 mmol), Et₃N (1.05 mL, 7.5 mmol) and anhydrous CH₂Cl₂ (10 mL). The solution was cooled to 0 °C at which point pivaloyl chloride (0.68 mL, 5.5 mmol) was added drop-wise. The resulting mixture was stirred at 0 °C for an additional 10 mins and then warmed to rt and stirred overnight. The reaction mixture was then concentrated *in vacuo*. The crude mixture was re-dissolved in Et₂O (10 mL) and washed with saturated NH₄Cl (10 mL). The two layers were then separated, and the aqueous layer extracted with Et₂O (3 × 10 mL). The combined organic layers were dried over MgSO₄, filtered, and concentrated *in vacuo*. Purification by column chromatography (silica gel; 10% EtOAc in CyH) to give the product as an off-white solid (1.05 g, 4.79 mmol, 96%).

¹H NMR (400 MHz, CDCl₃): δ 8.47 (dd, *J* = 9.0, 4.8 Hz, 1H), 7.78 (d, *J* = 3.8 Hz, 1H), 7.20 (dd, *J* = 8.7, 2.7 Hz, 1H), 7.06 (app td, *J* = 9.1, 2.7 Hz, 1H), 6.58 (dd, *J* = 3.8, 0.7 Hz, 1H), 1.52 (s, 9H).

¹³C{¹H} NMR (101 MHz, CDCl₃): δ 176.9, 159.6 (d, *J* = 239.9 Hz), 133.1, 130.4 (d, *J* = 10.1 Hz), 127.1, 118.4 (d, *J* = 9.0 Hz), 112.7 (d, *J* = 24.3 Hz), 107.9 (d, *J* = 4.0 Hz), 106.0 (d, *J* = 23.8 Hz), 41.2, 28.7.

¹⁹F NMR (376 MHz, CDCl₃): δ -119.80 (app td, *J* = 9.0, 4.8 Hz).

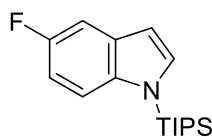
ν_{max} (neat) / cm⁻¹: 3175, 2981, 1693, 1458, 1444, 1309, 1183, 1084, 905.

HRMS: calcd. for C₁₃H₁₄FNONa [M+Na]⁺: 242.0952; found 242.0950.

m.p. / °C: 70–73 (lit. 62-65).²³⁰

Characterisation data are consistent with literature values.²³⁰

N-(Triisopropylsilyl)-5-fluoroindole (8)



To a flame dried flask under an atmosphere of dinitrogen was added 5-fluoroindole (4.00 g, 29.6 mmol) and anhydrous THF (40 mL). A second flame-dried flask was charged with additional THF (40 mL) and NaH (60% in mineral oil, 1.42 g, 35.5 mmol). The second flask was cooled to 0 °C in an ice-water bath and the contents of the first flask added drop-wise. After complete addition, the reaction mixture was warmed to rt and stirred for 30 mins. After cooling once more to 0 °C, TIPSCl (8.2 mL, 38.5 mmol) was added drop-wise after which the mixture was warmed to rt and stirred overnight. The reaction was quenched with NH₄Cl (10 mL) and extracted with EtOAc (3 × 30 mL). The combined organics were dried over MgSO₄, filtered, and concentrated *in vacuo*. Purification by column chromatography (CyH) afforded the product as a brown oil. (6.31 g, 21.7 mmol, 73%).

¹H NMR (400 MHz, CDCl₃): δ 7.40 (dd, *J* = 9.1, 4.3 Hz, 1H), 7.29 (d, *J* = 3.2 Hz, 1H), 7.25 (dd, *J* = 9.3, 2.8 Hz, 1H), 6.88 (app td, *J* = 9.1, 2.8 Hz, 1H), 6.58 (dd, *J* = 3.2, 0.9 Hz, 1H), 1.69 (sept, *J* = 7.5 Hz, 3H), 1.14 (d, *J* = 7.5 Hz, 18H).

¹³C{¹H} NMR (101 MHz, CDCl₃): δ 157.9 (d, *J* = 234.7 Hz), 137.3, 133.0, 131.9 (d, *J* = 10.0 Hz), 114.3 (d, *J* = 9.6 Hz), 109.5 (d, *J* = 25.8 Hz), 105.3 (d, *J* = 22.8 Hz), 104.8 (d, *J* = 4.5 Hz), 18.1, 12.8.

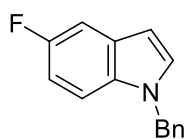
¹⁹F NMR (376 MHz, CDCl₃): δ -125.29 (app td, *J* = 9.3, 4.3 Hz).

ν_{\max} (neat) / cm⁻¹: 2948, 2868, 1465, 1443, 1210, 1143, 882.

HRMS: calcd. for C₁₃H₁₅FNO [M+H]⁺: 292.1891; found 292.1894.

Characterisation data are consistent with literature values.²³¹

1-Benzyl-5-fluoroindole (9)



A flame-dried flask under an atmosphere of dinitrogen was charged with 5-fluoroindole (5.00 g, 37.0 mmol) and anhydrous DMF (40 mL). The solution was added drop-wise to a

second flame-dried Schlenk tube containing a suspension of NaH (60% in mineral oil, 1.78 mg, 2.4 mmol) in anhydrous DMF (2 mL) cooled to 0 °C. The reaction mixture was warmed to rt and stirred for 30 mins. After cooling once more to 0 °C, benzyl bromide (6.6 mL, 55.5 mmol) was added drop-wise and the reaction mixture warmed to rt and stirred overnight. The reaction was quenched with saturated aqueous NH₄Cl (20 mL) and extracted with EtOAc (3 × 20 mL). The combined organics were washed with a 10 wt% aqueous solution of LiCl (20 mL) to remove residual DMF and then dried over MgSO₄, filtered, and concentrated *in vacuo*. Purification by column chromatography (silica gel; 10% EtOAc in CyH) afforded the pure product as a tan solid (6.82 g, 30.3 mmol, 82%).

¹H NMR (400 MHz, CDCl₃): δ 7.34 – 7.26 (m, 4H), 7.19 – 7.14 (m, 2H), 7.12 – 7.07 (m, 2H), 6.92 (app td, *J* = 9.1, 2.5 Hz, 1H), 6.52 (d, *J* = 3.1 Hz, 1H), 5.31 (s, 2H).

¹³C{¹H} NMR (101 MHz, CDCl₃): δ 158.0 (d, *J* = 234.2 Hz), 137.4, 133.0, 130.0, 129.1 (d, *J* = 10.3 Hz), 129.0, 127.9, 126.8, 110.5 (d, *J* = 9.8 Hz), 110.2 (d, *J* = 26.4 Hz), 105.8 (d, *J* = 23.3 Hz), 101.7 (d, *J* = 4.7 Hz), 50.5.

¹⁹F NMR (376 MHz, CDCl₃): δ -125.37 (app td, *J* = 9.4, 4.3 Hz).

ν_{max} (neat) / cm⁻¹: 2921, 1853, 1486, 1439, 1222, 1184, 1116, 866, 800.

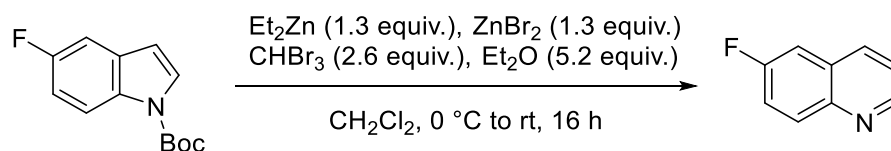
HRMS: calcd. for C₁₅H₁₃FN [M+H]⁺: 226.1027; found (ESI⁺) 226.1025.

m.p. / °C: 63–65 (lit. 61-62).²³²

Characterisation data are consistent with literature values.²³³

5.2.3 Synthesis of 3-*H* quinolines

6-Fluoroquinoline (4)



Under inert atmosphere, Et₂Zn (1.0 M in hexanes, 1.3 mL, 1.3 mmol, 1.3 equiv.) was added dropwise to a rapidly stirring suspension of zinc halide (1.3 mmol, 1.3 equiv.) in dry CH₂Cl₂ (7 mL) at 0 °C. The suspension was warmed to room temperature and stirred until full dissolution of the zinc halide was observed (ca. 2 hours). The solution was cooled back down to 0 °C and bromoform (2.6 mmol, 2.6 equiv.) was added drop-wise and the mixture stirred

for 20 mins. A solution of *N*-*boc*-5-fluoroindole (235 mg, 1.0 mmol) in dry CH₂Cl₂ (3 mL) was then added drop-wise and the reaction mixture warmed to rt, wrapped in foil to exclude light, and stirred overnight. The reaction was quenched by addition of sat. aqueous NaHCO₃ (5 mL) and the CH₂Cl₂ layer separated. The aqueous layer was extracted with CH₂Cl₂ (3 × 10 mL). The combined organics were dried over Na₂SO₄, filtered, and concentrated *in vacuo*. Purification by column chromatography (silica gel; 10-20% EtOAc in CyH) afforded the product as a brown oil (37.0 mg, 0.251 mmol, 25%).

¹H NMR (500 MHz, CDCl₃): δ 8.86 (dd, *J* = 4.3, 1.6 Hz, 1H), 8.13 – 8.03 (m, 2H), 7.47 (td, *J* = 8.8, 2.8 Hz, 1H), 7.43 – 7.35 (m, 2H).

¹³C{¹H} NMR (125 MHz, CDCl₃): δ 160.5 (d, *J* = 248.2 Hz), 149.8 (d, *J* = 2.7 Hz), 145.5, 135.5 (d, *J* = 5.4 Hz), 132.1 (d, *J* = 9.2 Hz), 129.0 (d, *J* = 9.9 Hz), 121.9, 119.8 (d, *J* = 25.8 Hz), 110.8 (d, *J* = 21.5 Hz).

¹⁹F NMR (471 MHz, CDCl₃): δ -113.27 (app td, *J* = 9.2, 5.8 Hz).

ν_{\max} (neat) / cm⁻¹: 1632, 1501, 1466, 1320, 1219, 1137, 1109, 907, 862, 829.

HRMS: calcd. for C₉H₇FN [M+H]⁺: 148.0557; found (ESI⁺): 148.0568

Characterisation data are consistent with literature values.²³⁴

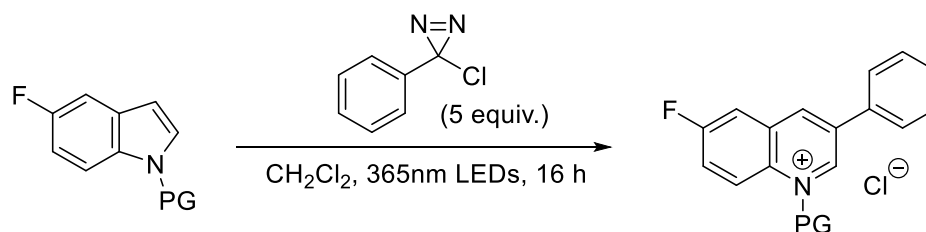
5.3 Experimental details relevant to Chapter 3

5.3.1 Optimisation and General Procedures

General Optimisation:

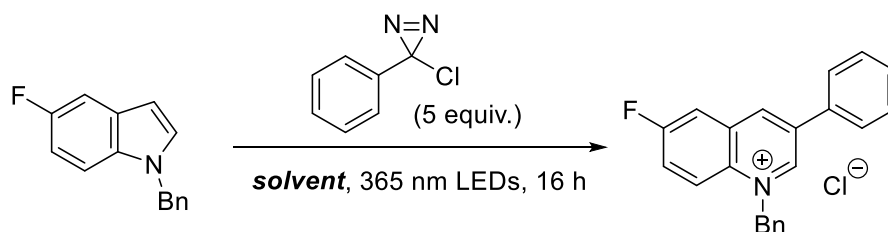
An oven-dried 10 mL microwave tube was charged with *N*-benzyl 5-fluoroindole (45 mg, 0.2 mmol) and 4,4'-bis(trifluoromethyl)-1,1'-biphenyl (internal standard for ¹⁹F NMR spectroscopy) which was then sealed, evacuated and flushed with dinitrogen 3 times. Anhydrous CH₂Cl₂ (2 mL) was then added followed by 3-chloro-3-phenyldiazirine (1.0 mmol). The cap of the reaction flask was then sealed with electrical tape. The reaction mixture was stirred under constant irradiation with UV light (365 nm, 18 W LED, 5 cm from light source) overnight. If any solids precipitated over the course of the reaction, MeOH was added until the mixture was homogenous and an aliquot was taken and analysed by ¹⁹F NMR spectroscopy.

Protecting group optimisation (Table 3.4)



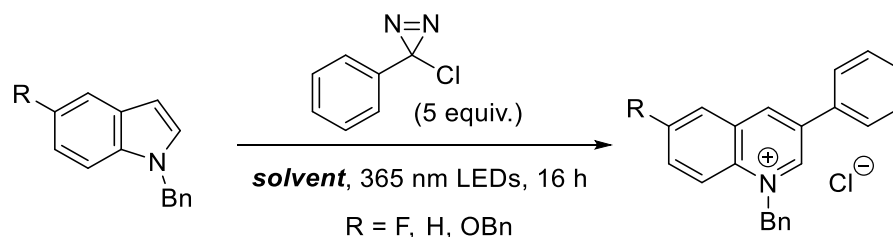
A 10 mL microwave tube was charged with *N*-protected 5-fluoroindole (0.2 mmol) and 4,4'-bis(trifluoromethyl)-1,1'-biphenyl (internal standard for ^{19}F NMR spectroscopy) which was then sealed, evacuated and flushed with dinitrogen 3 times. Anhydrous CH_2Cl_2 (2 mL) was then added followed by 3-chloro-3-phenyldiazirine (1.0 mmol). The cap of the reaction flask was then sealed with electrical tape. The reaction mixture was stirred under constant irradiation with UV light (365 nm, 18 W LED, 5 cm from light source) overnight. If any solids precipitated over the course of the reaction, MeOH was added until the mixture was homogenous and an aliquot was taken and analysed by ^{19}F NMR spectroscopy.

Solvent optimisation (Table 3.5)



A 10 mL microwave tube containing 1-benzyl-5-fluoroindole (45 mg, 0.2 mmol) and 4,4'-bis(trifluoromethyl)-1,1'-biphenyl (internal standard for ^{19}F NMR spectroscopy) was sealed, evacuated, and back-filled with dinitrogen 3 times. Anhydrous solvent (2 mL) was added, followed by 3-chloro-3-phenyldiazirine (153 mg, 1.0 mmol). The cap of the reaction flask was then sealed with electrical tape, and the reaction mixture was stirred under constant irradiation with UV light (365 nm, 18 W LED, 5 cm from light source) overnight. If any solids precipitated over the course of the reaction, MeOH was added until the mixture was homogenous and an aliquot was taken and analysed by ^{19}F NMR spectroscopy.

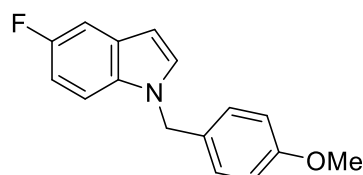
Further solvent screening (Table 3.10)



A 10 mL microwave tube containing *N*-benzylindole (0.2 mmol) which was then sealed, evacuated and flushed with dinitrogen 3 times. The solvent mixture (2 mL) was then added, followed by 3-chloro-3-phenyldiazirine (153 mg, 1.0 mmol). The cap of the reaction flask was then sealed with electrical tape, and the reaction mixture was stirred under constant irradiation with UV light (365 nm, 18 W LED, 5 cm from light source) overnight. The resulting precipitate was isolated by filtration and washed with PhMe (2×5 mL) and dried under a flow of air.

5.3.2 Synthesis of protected azoles

5-Fluoro-1-(4-methoxybenzyl)-1*H*-indole



A flame dried flask under an atmosphere of dinitrogen was charged with 5-fluoroindole (1.35 g, 10.0 mmol) and dry DMF (10 mL). The solution was cooled to 0 °C and NaH (60% in mineral oil, 480 mg, 12.0 mmol) was added portion-wise. The resulting mixture was stirred for 15 mins after which PMBCl (2.0 mL, 15.0 mmol) was added drop-wise. The reaction was stirred at 0 °C for 1 hr and then warmed to rt and stirred overnight. The reaction was quenched with water and the product was extracted with EtOAc (3×15 mL). The combined organics were washed with brine, dried over MgSO₄, filtered, and concentrated *in vacuo*. Purification by column chromatography (silica gel; 10% EtOAc in CyH) afforded the product as a yellow oil. (1.05 g, 3.88 mmol, 39%).

¹H NMR (400 MHz, CDCl₃): δ 7.28 (dd, $J = 9.7, 2.5$ Hz, 1H), 7.18 (dd, $J = 8.9, 4.3$ Hz, 1H), 7.15 (d, $J = 3.1$ Hz, 1H), 7.05 (d, $J = 8.6$ Hz, 2H), 6.91 (app td, $J = 9.1, 2.5$ Hz, 1H), 6.84 (d, $J = 8.6$ Hz, 2H), 6.48 (d, $J = 3.0$ Hz, 1H), 5.24 (s, 2H), 3.78 (s, 3H).

$^{13}\text{C}\{^1\text{H}\}$ NMR (101 MHz, CDCl_3): δ 159.3, 156.8 (d, $J = 234.1$ Hz), 133.0, 129.8, 129.3, 129.1 (d, $J = 10.2$ Hz), 128.3, 114.3, 110.5 (d, $J = 9.8$ Hz), 110.1 (d, $J = 26.4$ Hz), 105.8 (d, $J = 23.3$ Hz), 101.6 (d, $J = 4.7$ Hz), 55.4, 50.1.

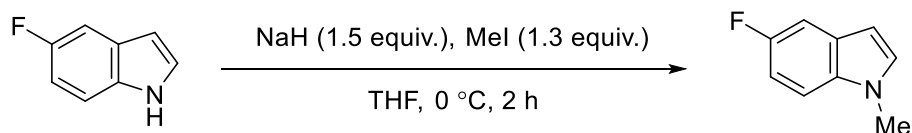
^{19}F NMR (376 MHz, CDCl_3): δ -125.43 (app td, $J = 9.4, 4.3$ Hz).

ν_{max} (neat) / cm^{-1} : 2836, 1612, 1511, 1485, 1463, 1244, 1227, 1175, 1116, 1031, 845, 807.

HRMS: calcd. for $\text{C}_{16}\text{H}_{15}\text{FNO}$ $[\text{M}+\text{H}]^+$: 256.1132; found (ESI $^+$): 256.1136.

Characterisation data are consistent with literature values.²³⁵

5-Fluoro-1-methyl-1*H*-indole



A flame dried flask under an atmosphere of dinitrogen was charged with 5-fluoroindole (676 mg, 5.00 mmol) and dry THF (15 mL). The solution was cooled to 0 °C and NaH (60% dispersion on mineral oil, 300 mg, 7.5 mmol) was added portion-wise. The resulting mixture was stirred for 15 mins and then warmed to rt and stirred for an additional 1 hr. The solution was cooled back to 0 °C and MeI (0.41 mL, 6.5 mmol) added drop-wise. The solution was raised to rt once more and stirred for an additional 1 hr. The reaction was quenched with water (10 mL) and the product extracted with EtOAc (3×15 mL). The combined organics were washed with brine, dried over MgSO_4 , filtered, and concentrated *in vacuo*. Purification by column chromatography (silica gel; 10% EtOAc in CyH) afforded the product as a red solid (637 mg, 4.27 mmol, 85%).

^1H NMR (400 MHz, CDCl_3): δ 7.27 (dd, $J = 9.5, 2.2$ Hz, 1H), 7.23 (dd, $J = 9.0, 4.4$ Hz, 1H), 7.09 (d, $J = 3.1$ Hz, 1H), 6.97 (app td, $J = 9.0, 2.5$ Hz, 1H), 6.44 (d, $J = 3.1$ Hz, 1H), 3.79 (s, 3H).

$^{13}\text{C}\{^1\text{H}\}$ NMR (101 MHz, CDCl_3): δ 158.0 (d, $J = 233.7$ Hz), 133.5, 130.5, 128.8 (d, $J = 10.3$ Hz), 110.0 (d, $J = 19.9$ Hz), 109.9 (d, $J = 3.4$ Hz), 105.7 (d, $J = 23.3$ Hz), 101.0 (d, $J = 4.7$ Hz), 33.2.

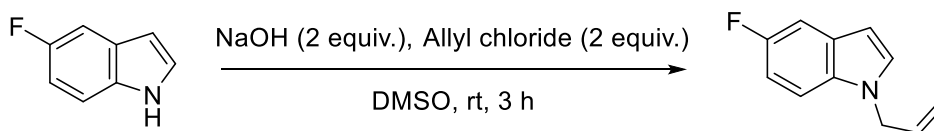
^{19}F NMR (376 MHz, CDCl_3): δ -125.77 (app td, $J = 9.5, 4.4$ Hz).

ν_{max} (neat) / cm^{-1} : 1622, 1574, 1491, 1447, 1424, 1338, 1281, 1237, 1222, 1118, 1078, 947, 857.

m.p. / °C: 54-57 (lit. 55-56).²³⁶

Characterisation data are consistent with literature values.²³⁷

5-Fluoro-*N*-allyl-1*H*-indole



A flame-dried flask under an atmosphere of dinitrogen was charged with 5-fluoroindole (270 mg, 2.0 mmol) and anhydrous DMSO (4 mL). NaOH (160 mg, 4.0 mmol) was then added in one portion and the reaction stirred at rt for 10 mins. Allyl chloride (0.16 mL, 2.0 mmol) was added drop-wise and the reaction stirred for 3 hrs. The reaction was quenched with sat. NH₄Cl (5 mL) and extracted with EtOAc (3 × 10 mL). The combined organics were dried over MgSO₄, filtered, and concentrated *in vacuo*. Purification by column chromatography (silica gel; 5% EtOAc in CyH) afforded the product as a yellow oil. (302 mg, 1.72 mmol, 86%).

¹H-NMR (400 MHz, CDCl₃): δ 7.28 (dd, *J* = 9.5, 2.5 Hz), 7.22 (dd, *J* = 9.0, 4.4 Hz), 7.13 (d, *J* = 3.2 Hz, 1H), 6.95 (app td, *J* = 9.0, 2.5 Hz, 1H), 6.47 (dd, *J* = 3.2, 0.9 Hz), 5.99 (ddt, *J* = 17.2, 10.4, 5.4 Hz, 1H), 5.22 (app dq, *J* = 10.4, 1.7 Hz, 1H), 5.08 (app dq, *J* = 17.2, 1.7 Hz), 4.72 (app dt, *J* = 5.4, 1.7 Hz, 2H).

¹³C{¹H}-NMR (101 MHz, CDCl₃): δ 157.9 (d, *J* = 234.0 Hz), 133.3, 132.8, 129.5, 128.9 (d, *J* = 10.2 Hz), 117.4, 110.2 (d, *J* = 9.8 Hz), 109.9 (d, *J* = 26.3 Hz), 105.6 (d, *J* = 23.2 Hz), 101.4 (d, *J* = 4.7 Hz), 49.1.

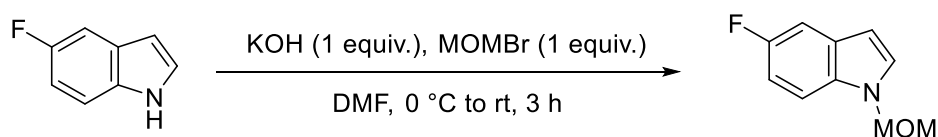
¹⁹F-NMR (376 MHz, CDCl₃): δ -125.54 (app td, *J* = 9.5, 4.4 Hz).

ν_{\max} (neat) / cm⁻¹: 2913, 1484, 1449, 1226, 1115.

HRMS: calcd. for C₁₁H₁₁FN [M+H]⁺: 176.0870; found (ESI⁺): 176.0870.

Characterisation data are consistent with literature values.²³⁸

5-Fluoro-*N*-(methoxymethyl)-1*H*-indole



To a flame-dried flask under an atmosphere of dinitrogen was added anhydrous DMF (4 mL) and pulverised KOH (112 mg, 2.0 mmol) which was then cooled to 0 °C. A solution of 5-fluoroindole (270 mg, 2.0 mmol) in anhydrous DMF (2 mL) was added drop-wise and the reaction stirred for 15 mins. MOMBr (0.16 mL, 2.0 mmol) was added drop-wise to form a white precipitate and the mixture stirred for a further 3 hours. The reaction was quenched with water (10 mL) and diluted with EtOAc (10 mL). The organic layer was separated and the aqueous layer extracted with EtOAc (3 × 10 mL). The combined organics were dried over MgSO₄, filtered, and concentrated *in vacuo*. Purification by column chromatography (silica gel; 5% EtOAc in CyH) to afford the product as a colourless oil (111 mg, 0.619 mmol, 31%).

¹H-NMR (400 MHz, CDCl₃): δ 7.41 (dd, *J* = 9.0, 4.4 Hz, 1H), 7.28 (dd, *J* = 9.3, 2.5 Hz, 1H), 7.21 (d, *J* = 3.2 Hz, 1H), 7.00 (app td, *J* = 9.0, 2.5 Hz, 1H), 6.50 (dd, *J* = 3.2, 0.8 Hz, 1H), 5.43 (s, 2H), 3.24 (s, 3H).

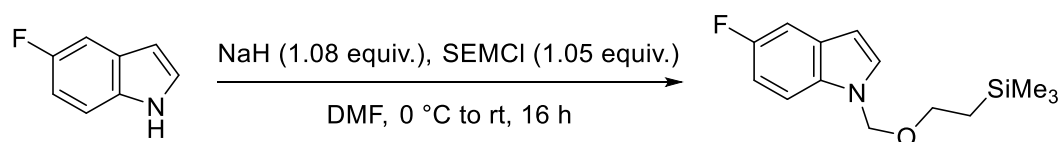
¹³C{¹H}-NMR (101 MHz, CDCl₃): δ 158.4 (d, *J* = 235.0 Hz), 133.0, 129.8, 129.7 (d, *J* = 10.2 Hz), 110.8, 110.6 (d, *J* = 17.2 Hz), 105.9 (d, *J* = 23.5 Hz), 102.6 (d, *J* = 4.6 Hz), 77.9, 56.0.

¹⁹F-NMR (376 MHz, CDCl₃): δ -124.39 (app td, *J* = 9.3, 4.4 Hz).

ν_{max} (neat) / cm⁻¹: 1623, 1580, 1482, 1447, 1398, 1338, 1223, 1096, 1084, 1062, 947, 911, 850.

HRMS: calcd. for C₁₀H₁₀FNO [M+H]⁺: 180.0820; found (ESI⁺):180.0811.

5-Fluoro-*N*-((2-(trimethylsilyl)ethoxy)methyl)-1*H*-indole



A flame dried flask under an atmosphere of dinitrogen was charged with 5-fluoroindole (135 mg, 1.0 mmol) and anhydrous DMF (10 mL). The flask was cooled to 0 °C and NaH (43 mg, 1.08 mmol) was added in one portion and stirred for 20 mins. SEMCl (0.19 mL, 1.05 mmol) was then added drop-wise and the flask was warmed to rt and stirred overnight. The reaction was quenched with water (3 mL) and extracted with Et₂O (3 × 10 mL). The combined

organics were washed with a 10% aqueous solution of LiCl (20 mL) to remove excess DMF and then dried over MgSO₄, filtered, and concentrated *in vacuo*. Purification by column chromatography (silica gel; 5% EtOAc in CyH) afforded the product as a yellow oil (189 mg, 0.71 mmol, 71%).

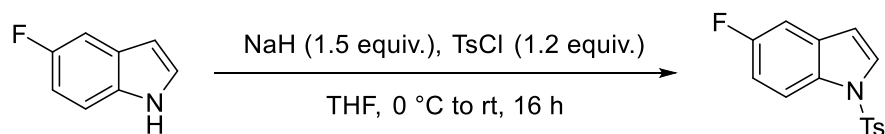
¹H-NMR (400 MHz, CDCl₃): δ 7.40 (dd, *J* = 9.1, 4.4 Hz, 1H), 7.26 (dd, *J* = 9.4, 2.5 Hz, 1H), 7.20 (d, *J* = 3.2 Hz, 1H), 6.98 (app td, *J* = 9.1, 2.5 Hz, 1H), 6.48 (dd, *J* = 3.2, 0.8 Hz, 1H), 5.45 (s, 2H), 2.45 (t, *J* = 8.1 Hz, 2H), 0.88 (t, *J* = 8.1 Hz, 2H), -0.06 (s, 9H).

¹³C{¹H}-NMR (101 MHz, CDCl₃): δ 158.2 (d, *J* = 234.7 Hz), 132.9, 129.6, 129.4 (d, *J* = 10.2 Hz), 110.7 (d, *J* = 26.3 Hz), 110.4 (d, *J* = 9.7 Hz), 105.7 (d, *J* = 23.4 Hz), 102.3 (d, *J* = 4.7 Hz), 75.9, 65.8, 17.7, -1.45.

¹⁹F-NMR (376 MHz, CDCl₃): δ -124.62 (app td, *J* = 9.4, 4.4 Hz).

ν_{max} (neat) / cm⁻¹: 2952, 2893, 1484, 1248, 1226, 1071, 856, 833, 811.

1-Toluenesulfonyl-5-fluoro-1*H*-indole



According to the literature procedure,²³⁹ a flame-dried flask under an atmosphere of dinitrogen was charged with 5-fluoroindole (135 mg, 1.0 mmol) and anhydrous THF (4 mL) and cooled to 0 °C. NaH (60% suspension on mineral oil, 60 mg, 1.5 mmol) was then added in portions and the resulting mixture stirred for 20 mins. TsCl (229 mg, 1.2 mmol) was added in one portion and the reaction mixture warmed to rt and stirred overnight. The reaction was quenched with 2M NaOH solution (5 mL) and the aqueous layer extracted with EtOAc (3 × 10 mL). The combined organics were dried over MgSO₄, filtered, and concentrated *in vacuo*. Recrystallisation from cyclohexane afforded the product as a white solid (201 mg, 0.695 mmol, 69%).

¹H NMR (400 MHz, CDCl₃): δ 7.92 (dd, *J* = 9.1, 4.4 Hz, 1H), 7.75 – 7.72 (m, 2H), 7.59 (d, *J* = 3.6 Hz, 1H), 7.23 (d, *J* = 8.2 Hz, 2H), 7.17 (dd, *J* = 8.8, 2.6 Hz, 1H), 7.03 (app td, *J* = 9.1, 2.6 Hz, 1H), 6.61 (d, *J* = 3.6 Hz, 1H), 2.35 (s, 3H).

$^{13}\text{C}\{^1\text{H}\}$ NMR (101 MHz, CDCl_3): δ 159.6 (d, $J = 240.0$ Hz), 145.1, 135.1, 131.7 (d, $J = 10.2$ Hz), 131.2, 129.9, 128.1, 126.8, 114.6 (d, $J = 9.6$ Hz), 112.6 (d, $J = 25.7$ Hz), 108.9 (d, $J = 4.2$ Hz), 106.8 (d, $J = 24.0$ Hz), 21.6.

^{19}F NMR (376 MHz, CDCl_3): δ -120.01 (app td, $J = 8.8, 4.4$ Hz).

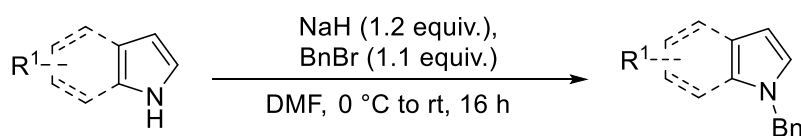
IR (neat) cm^{-1} : 3120, 2924, 1442, 1368, 1215, 1133, 1112, 1088.

HRMS: calcd. for $\text{C}_{15}\text{H}_{12}\text{FNO}_2\text{SNa}$ $[\text{M}+\text{Na}]^+$: 312.0465; found (ESI $^+$): 312.0467.

m.p. / $^\circ\text{C}$: 119-120 (lit. 118-119).²³⁹

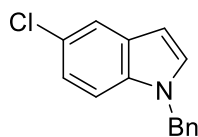
Characterisation data are consistent with literature values.²³⁹

General Procedure 1 (GP-1): *N*-benzylation of azoles



To a flame-dried flask under an atmosphere of dinitrogen was charged the desired azole (2.0 mmol) and anhydrous DMF (2 mL). The solution was added drop-wise to a second flame-dried Schlenk tube containing a suspension of NaH (60% in mineral oil, 2.4 mmol) in anhydrous DMF (2 mL) cooled to 0 °C. The reaction mixture was warmed to rt and stirred for 30 mins. After cooling once more to 0 °C, benzyl bromide (2.2 mmol) was added drop-wise and the reaction mixture warmed to rt and stirred overnight. The reaction was quenched with saturated aqueous NH_4Cl (5 mL) and extracted with EtOAc (3×10 mL). The combined organics were washed with a 10 wt% aqueous solution of LiCl (10 mL) to remove residual DMF and then dried over MgSO_4 , filtered, and concentrated *in vacuo*. Purification by column chromatography using the described eluents or recrystallisation from EtOH afforded the pure product.

1-Benzyl-5-chloroindole



Synthesised according to **GP-1** from 5-chloroindole (303 mg, 2.0 mmol), NaH (60% in mineral oil, 96 mg, 2.4 mmol), and benzyl bromide (0.26 mL, 2.2 mmol). Purification by column chromatography (silica gel; 0-5% EtOAc in CyH) afforded the product as a tan solid (360 mg, 1.49 mmol, 74%).

¹H NMR (400 MHz, CDCl₃): δ 7.63 (d, *J* = 1.4 Hz, 1 H), 7.37–7.26 (m, 4 H), 7.23–7.07 (m, 5 H), 6.52 (d, *J* = 2.9 Hz, 1 H), 5.33 (s, 2 H).

¹³C{¹H} NMR (101 MHz, CDCl₃): δ 137.2, 134.8, 129.8, 129.0, 128.0, 126.8, 125.5, 122.2, 120.5, 110.9, 101.5, 50.5.

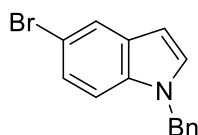
ν_{max} (neat) / cm⁻¹: 1470, 1435, 1330, 1289, 1183, 1062, 1049, 1025, 872.

HRMS: calcd. for C₁₅H₁₃³⁵ClN [M+H]⁺: 242.0731; found (ESI⁺): 242.0718.

m.p. / °C: 62-64 (lit. 63-64).²⁴⁰

Characterisation data are consistent with literature values.²⁴¹

1-Benzyl-5-bromoindole



Synthesised according to **GP-1** from 5-bromoindole (388 mg, 2.0 mmol), NaH (60% in mineral oil, 96 mg, 2.4 mmol), and benzyl bromide (0.26 mL, 2.2 mmol). Purification by column chromatography (silica gel; 0-5% EtOAc in CyH) afforded the product as a colourless solid (423 mg, 1.48 mmol, 74%).

¹H NMR (400 MHz, CDCl₃): δ 7.63 (d, *J* = 1.4 Hz, 1H), 7.37–7.26 (m, 3H), 7.23–7.07 (m, 5H), 6.52 (d, *J* = 2.9 Hz, 1H), 5.33 (s, 2H).

¹³C{¹H} NMR (101 MHz, CDCl₃): δ 137.2, 134.8, 129.9, 129.8, 129.0, 128.0, 126.8, 125.5, 122.2, 120.5, 110.9, 101.5, 50.5.

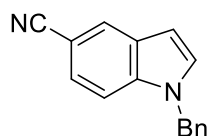
ν_{max} (neat) / cm⁻¹: 1470, 1435, 1330, 1289, 1183, 1062, 1049, 1025, 872.

HRMS: calcd. for $C_{15}H_{13}^{79}BrN$ $[M+H]^+$: 286.0226; found (ESI⁺): 286.0219.

m.p. / °C: 94-96 (lit. 93-95).²⁴²

Characterisation data are consistent with literature values.²⁴¹

1-Benzylindole-5-carbonitrile



Synthesised according to **GP-1** from 5-cyanoindole (284 mg, 2.0 mmol), NaH (60% in mineral oil, 96 mg, 2.4 mmol), and benzyl bromide (0.26 mL, 2.2 mmol). Recrystallisation from EtOH afforded the product as a colourless solid (324 mg, 1.40 mmol, 70%).

¹H NMR (400 MHz, CDCl₃): δ 7.99 (d, $J = 1.5$ Hz, 1H), 7.40 (dd, $J = 8.6, 1.5$ Hz, 1H), 7.39–7.30 (m, 4H), 7.28 (d, $J = 3.5$ Hz, 1H), 7.12 (dd, $J = 7.7, 1.8$ Hz, 2H), 6.66 (dd, $J = 3.3, 0.8$ Hz, 1H), 5.38 (s, 2H).

¹³C{¹H} NMR (101 MHz, CDCl₃): δ 137.9, 136.5, 130.7, 129.1, 128.6, 128.2, 126.9, 126.7, 124.8, 120.9, 110.7, 102.9, 102.8, 50.5.

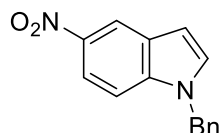
ν_{\max} (neat) / cm^{-1} : 2221, 1604, 1482, 1451, 1436, 1338, 1301, 1183, 884, 805.

HRMS: calcd. for $C_{16}H_{13}N_2$ $[M+H]^+$: 233.1073; found (ESI⁺): 233.1074.

m.p. / °C: 107-109 (lit. 105-106).²⁴³

Characterisation data are consistent with literature values.²⁴⁴

1-Benzyl-5-nitroindole



Synthesised according to **GP-1** from 5-nitroindole (324 mg, 2.0 mmol), NaH (60% on mineral oil, 96 mg, 2.4 mmol), and benzyl bromide (0.26 mL, 2.2 mmol). Purification by column chromatography (silica gel; 10% EtOAc in CyH) afforded the product as a yellow solid (297 mg, 1.18 mmol, 59%).

¹H NMR (400 MHz, CDCl₃): δ 8.62 (d, *J* = 2.2 Hz, 1H), 8.08 (dd, *J* = 9.0, 2.2 Hz, 1H), 7.38–7.26 (m, 5H), 7.16–7.06 (m, 2H), 6.74 (dd, *J* = 3.3, 0.9 Hz, 1H), 5.37 (s, 2H).

¹³C{¹H} NMR (101 MHz, CDCl₃): δ 141.8, 139.1, 136.2, 131.5, 129.1, 128.2, 128.0, 126.8, 118.3, 117.5, 109.6, 104.5, 50.8.

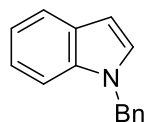
ν_{max} (neat) / cm⁻¹: 3094, 2928, 1606, 1505, 1477, 1440, 1401, 1326, 1311, 1292, 1173, 1069, 906, 808.

HRMS: calcd. for C₁₅H₁₂N₂O₂Na [M+Na]⁺: 275.0796; found (ESI⁺): 275.0801.

m.p. / °C: 106-108 (lit. 96-97).²³²

Characterisation data are consistent with literature values.²⁴⁵

1-Benzylindole (27)



Synthesised according to **GP-1** from indole (234 mg, 2.0 mmol), NaH (60% in mineral oil, 96 mg, 2.4 mmol), and benzyl bromide (0.26 mL, 2.2 mmol). Purification by column chromatography (silica gel; 0-5% EtOAc in CyH) afforded the product as a brown solid (302 mg, 1.46 mmol, 73%).

¹H NMR (400 MHz, CDCl₃): δ 7.66 (app dt, *J* = 7.8, 1.2 Hz, 1H), 7.34–7.26 (m, 4H), 7.18 (app dt, *J* = 7.2, 1.2 Hz, 1H), 7.15–7.09 (m, 4H), 6.57 (dd, *J* = 3.2, 0.9 Hz, 1H), 5.34 (s, 2H).

¹³C{¹H} NMR (101 MHz, CDCl₃): δ 137.7, 136.4, 128.9, 128.8, 128.4, 127.7, 126.9, 121.8, 121.1, 119.7, 109.8, 101.8, 50.2.

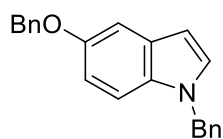
ν_{max} (neat) / cm⁻¹: 1703, 1610, 1509, 1462, 1316, 1158.

HRMS: calcd. for C₁₅H₁₄N [M+H]⁺: 208.1121; found (ESI⁺): 208.1106.

m.p. / °C: 42-44 (lit. 41-42).²³⁷

Characterisation data are consistent with literature values.²⁴¹

1-Benzyl-5-(benzyloxy)indole (28)



Synthesised according to **GP-1** from 5-hydroxyindole (266 mg, 2.0 mmol), NaH (60% on mineral oil, 192 mg, 4.8 mmol), and benzyl bromide (0.53 mL, 4.4 mmol). Purification by recrystallisation from EtOH afforded the product as a colourless solid (344 mg, 1.10 mmol, 55%).

¹H NMR (400 MHz, CDCl₃): δ 7.47 (d, *J* = 7.0 Hz, 2H), 7.38 (app t, *J* = 7.4 Hz, 2H), 7.35 – 7.26 (m, 4H), 7.19 (d, *J* = 2.5 Hz, 1H), 7.16 (d, *J* = 8.9 Hz, 1H), 7.13 – 7.07 (m, 3H), 6.91 (dd, *J* = 8.9, 2.5 Hz, 1H), 6.46 (d, *J* = 3.1 Hz, 1H), 5.29 (s, 2H), 5.10 (s, 2H).

¹³C{¹H} NMR (101 MHz, CDCl₃): δ 153.5, 137.9, 137.7, 132.0, 129.2, 129.0, 128.9, 128.7, 127.9, 127.73, 127.68, 126.9, 112.9, 110.6, 104.3, 101.4, 71.0, 50.4.

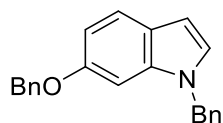
ν_{max} (neat) / cm⁻¹: 1614, 1511, 1486, 1452, 1433, 1363, 1316, 1264, 1219, 1183, 1015, 963, 948.

HRMS: calcd. for C₂₂H₂₀NO [M+H]⁺: 314.1539; found (ESI⁺): 314.1545.

m.p. / °C: 111-113 (lit. 108-109).²⁴⁶

Characterisation data are consistent with literature values.²⁴⁷

1-Benzyl-6-(benzyloxy)indole



Synthesised according to **GP-1** from 6-benzyloxyindole (446 mg, 2.0 mmol), NaH (60% in mineral oil, 96 mg, 2.4 mmol), and benzyl bromide (0.26 mL, 2.2 mmol). Recrystallisation from EtOH afforded the product as a colourless solid (306 mg, 0.98 mmol, 49%).

¹H NMR (400 MHz, CDCl₃): δ 7.52 (d, *J* = 8.5 Hz, 1H), 7.46 – 7.40 (m, 2H), 7.40 – 7.34 (m, 2H), 7.34 – 7.24 (m, 4H), 7.14 – 7.06 (m, 2H), 7.03 (d, *J* = 3.2 Hz, 1H), 6.87 (dd, *J* = 8.6, 2.3 Hz, 1H), 6.82 (d, *J* = 2.3 Hz, 1H), 6.48 (dd, *J* = 3.2, 0.8 Hz, 1H), 5.25 (s, 2H), 5.05 (s, 2H).

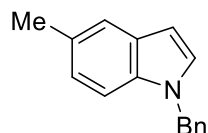
¹³C{¹H} NMR (101 MHz, CDCl₃): δ 155.6, 137.6, 137.6, 137.1, 128.9, 128.7, 128.0, 127.7, 127.5, 126.9, 123.4, 121.6, 110.2, 101.7, 95.1, 70.8, 50.2.

ν_{\max} (neat) / cm^{-1} : 1613, 1511, 1486, 1452, 1433, 1363, 1316, 1263, 1219, 1182, 1014, 962, 948.

HRMS: calcd. for $\text{C}_{22}\text{H}_{20}\text{NO}$ $[\text{M}+\text{H}]^+$: 314.1539; found (ESI⁺): 314.1537.

m.p. / °C: 79-81.

1-Benzyl-5-methylindole



Synthesised according to **GP-1** from 5-methylindole (262 mg, 2.0 mmol), NaH (60% in mineral oil, 96 mg, 2.4 mmol), and benzyl bromide (0.26 mL, 2.2 mmol). Purification by column chromatography (silica gel; CyH) followed by recrystallisation from EtOH afforded the product as a tan solid (176 mg, 0.797 mmol, 40%).

¹H NMR (400 MHz, CDCl₃): δ 7.43 (m, 1H), 7.33 – 7.21 (m, 3H), 7.16 (d, $J = 8.4$ Hz, 1H), 7.13 – 7.05 (m, 3H), 6.99 (dd, $J = 8.4, 1.8$ Hz, 1H), 6.46 (dd, $J = 3.1, 0.9$ Hz, 1H), 5.30 (s, 2H), 2.44 (s, 3H).

¹³C{¹H} NMR (101 MHz, CDCl₃): δ 137.8, 134.9, 129.1, 128.9, 128.5, 127.7, 126.8, 123.4, 120.8, 109.5, 101.2, 50.3, 21.5.

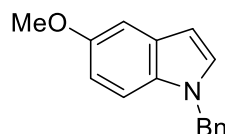
ν_{\max} (neat) / cm^{-1} : 1710, 1486, 1451, 1330, 1234, 1192, 1181.

HRMS: calcd. for $\text{C}_{16}\text{H}_{16}\text{N}$ $[\text{M}+\text{H}]^+$: 222.1277; found (ESI⁺): 222.1290

m.p. / °C: 37-38 (lit. 39-41).²³²

Characterisation data are consistent with literature values.²⁴⁸

1-Benzyl-5-methoxyindole



Synthesised according to **GP-1** from 5-methoxyindole (294 mg, 2.0 mmol), NaH (60% on mineral oil, 96 mg, 2.4 mmol), and benzyl bromide (0.26 mL, 2.2 mmol). Recrystallisation from EtOH afforded the product as an off-white solid (332 mg, 1.40 mmol, 70%).

¹H NMR (400 MHz, CDCl₃): δ 7.33–7.22 (m, 4 H), 7.16 (d, *J* = 8.9, 3.7 Hz, 1 H), 7.14–7.09 (m, 2 H), 6.93 (td, *J* = 9.1, 2.5 Hz, 1 H), 6.53 (dd, *J* = 3.1, 0.9 Hz, 1 H), 5.33 (s, 2 H).

¹³C{¹H} NMR (101 MHz, CDCl₃): δ 154.2, 137.8, 131.8, 129.2, 129.0, 128.9, 127.7, 126.8, 112.2, 110.6, 102.7, 101.3, 56.0, 50.4.

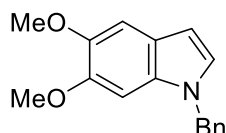
ν_{max} (neat) / cm⁻¹: 1619, 1574, 1486, 1444, 1402, 1344, 1234, 1151, 1132, 1028, 828.

HRMS: calcd. for C₁₆H₁₆NO [M+H]⁺: 238.1225; found (ESI⁺): 238.1226.

m.p. / °C: 77–80 (lit. 69–72).²⁴⁹

Characterisation data are consistent with literature values.²³³

1-Benzyl-5,6-dimethoxyindole



Synthesised according to **GP-1** from 5,6-dimethylindole (354 mg, 2.0 mmol), NaH (60% in mineral oil, 96 mg, 2.4 mmol), and benzyl bromide (0.26 mL, 2.2 mmol). Purification by column chromatography (silica gel; 0–5% EtOAc in CyH) afforded the product as a colourless solid (358 mg, 1.34 mmol, 67%).

¹H NMR (400 MHz, CDCl₃): δ 7.34 – 7.26 (m, 3H), 7.13 – 7.07 (m, 3H), 7.01 (d, *J* = 3.1 Hz, 1H), 6.72 (s, 1H), 6.44 (dd, *J* = 3.1, 0.8 Hz, 1H), 5.28 (s, 2H), 3.92 (s, 3H), 3.84 (s, 3H).

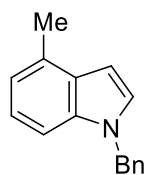
¹³C{¹H} NMR (101 MHz, CDCl₃): δ 147.0, 145.2, 137.7, 130.9, 128.9, 127.7, 126.9, 126.8, 121.5, 102.7, 101.3, 93.4, 56.4, 56.4, 50.4.

ν_{max} (neat) / cm⁻¹: 1487, 1447, 1361, 1257, 1238, 1203, 1144, 1045, 846, 810.

HRMS: calcd. for C₁₇H₁₈NO₂ [M+H]⁺: 268.1332; found (ESI⁺): 268.1318

m.p. / °C: 92–93.

1-Benzyl-4-methylindole



Synthesised according to **GP-1** from 4-methylindole (262 mg, 2.0 mmol), NaH (60% in mineral oil, 96 mg, 2.4 mmol), and benzyl bromide (0.26 mL, 2.2 mmol). Purification by column chromatography (silica gel; CyH) afforded the product as an off-white solid (263 mg, 1.19 mmol, 59%).

¹H NMR (400 MHz, CDCl₃): δ 7.34 – 7.22 (m, 3H), 7.18 – 7.03 (m, 5H), 6.92 (app dt, *J* = 6.9, 1.0 Hz, 1H), 6.57 (dd, *J* = 3.2, 1.0 Hz, 1H), 5.32 (s, 2H), 2.58 (s, 3H).

¹³C{¹H} NMR (101 MHz, CDCl₃): δ 137.8, 136.2, 130.6, 128.9, 128.7, 127.74, 127.69, 126.9, 122.0, 119.9, 107.5, 100.3, 50.3, 18.9.

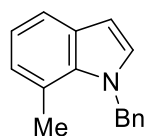
ν_{\max} (neat) / cm⁻¹: 1604, 1583, 1493, 1452, 1423, 1336, 1300, 1212, 1157.

HRMS: calcd. for C₁₆H₁₆N [M+H]⁺: 222.1277; found (ESI⁺): 222.1282

m.p. / °C: 50-53 (lit. 49-50).²³²

Characterisation data are consistent with literature values.²³²

1-Benzyl-7-methylindole



Synthesised according to **GP-1** from 7-methylindole (262 mg, 2.0 mmol), NaH (60% in mineral oil, 96 mg, 2.4 mmol), and benzyl bromide (0.26 mL, 2.2 mmol). Purification by column chromatography (silica gel; CyH) afforded the product as a colourless solid (326 mg, 1.47 mmol, 74%).

¹H NMR (400 MHz, CDCl₃): δ 7.54 (d, *J* = 7.9 Hz, 1H), 7.34 – 7.24 (m, 3H), 7.09 (d, *J* = 3.1 Hz, 1H), 7.03 (app t, *J* = 7.5 Hz, 1H), 6.96 – 6.86 (m, 3H), 6.58 (d, *J* = 3.1 Hz, 1H), 5.62 (s, 2H), 2.56 (s, 3H).

¹³C{¹H} NMR (101 MHz, CDCl₃): δ 139.8, 135.2, 130.3, 129.9, 129.0, 127.4, 125.6, 124.7, 121.2, 120.0, 119.3, 102.2, 52.4, 19.7.

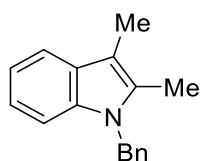
ν_{\max} (neat) / cm^{-1} : 1489, 1445, 1413, 1357, 1312, 1179, 1073, 1031, 961.

HRMS: calcd. for $\text{C}_{16}\text{H}_{16}\text{N}$ $[\text{M}+\text{H}]^+$: 222.1277; found (ESI⁺): 222.1271

m.p. / $^{\circ}\text{C}$: 58-61 (lit. 54-55).²³²

Characterisation data are consistent with literature values.²⁵⁰

1-Benzyl-2,3-dimethylindole



Synthesised according to **GP-1** from 2,3-dimethylindole (266 mg, 2.0 mmol), NaH (60% in mineral oil, 96 mg, 2.4 mmol), and benzyl bromide (0.26 mL, 2.2 mmol). Purification by column chromatography (silica gel; 0-5% EtOAc in CyH) afforded the product as a colourless solid (174 mg, 0.74 mmol, 37%).

¹H NMR (400 MHz, CDCl₃): δ 7.56 – 7.51 (m, 1H), 7.29 – 7.17 (m, 4H), 7.14 – 7.07 (m, 2H), 7.00 – 6.94 (m, 2H), 5.30 (s, 2H), 2.29 (s, 6H).

¹³C{¹H} NMR (101 MHz, CDCl₃): δ 138.3, 136.4, 132.4, 128.72, 128.67, 127.2, 126.0, 120.8, 118.8, 118.0, 108.8, 107.0, 46.5, 10.2, 8.9.

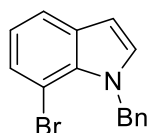
ν_{\max} (neat) / cm^{-1} : 1469, 1450, 1357, 1331, 1196.

HRMS: calcd. for $\text{C}_{17}\text{H}_{18}\text{N}$ $[\text{M}+\text{H}]^+$: 236.1434; found (ESI⁺): 236.1442

m.p. / $^{\circ}\text{C}$: 52-55.

Characterisation data are consistent with literature values.²⁵¹

1-Benzyl-7-bromoindole (40)



Synthesised according to **GP-1** from 7-bromoindole (392 mg, 2.0 mmol), NaH (60% on mineral oil, 96 mg, 2.4 mmol), and benzyl bromide (0.26 mL, 2.2 mmol). Recrystallisation from EtOH afforded the product as a colourless solid. (304 mg, 1.06 mmol, 53%).

¹H NMR (400 MHz, CDCl₃): δ 7.33 – 7.22 (m, 3H), 7.16 – 7.07 (m, 4H), 7.04 (d, *J* = 3.2 Hz, 1H), 6.91 (d, *J* = 8.3 Hz, 1H), 6.66 (d, *J* = 3.1 Hz, 1H), 6.53 (d, *J* = 7.7 Hz, 1H), 5.31 (s, 2H), 3.97 (s, 3H).

¹³C{¹H} NMR (101 MHz, CDCl₃): δ 153.6, 138.0, 137.7, 128.9, 127.7, 126.9, 126.9, 122.7, 119.3, 103.3, 99.6, 99.1, 55.5, 50.4.

ν_{max} (neat) / cm⁻¹: 1554, 1479, 1440, 1416, 1355, 1311, 1176, 1040, 914, 810.

HRMS: calcd. for C₁₅H₁₃N⁷⁹Br [M+H]⁺: 286.0226; found (ESI⁺): 286.0200.

m.p. / °C: 71-74 (lit. 60-62).²⁴¹

Characterisation data are consistent with literature values.²⁴¹

1-Benzyl-7-methoxyindole (41)



Synthesised according to **GP-1** from 7-methoxyindole (294 mg, 2.0 mmol), NaH (60% on mineral oil, 96 mg, 2.4 mmol), and benzyl bromide (0.26 mL, 2.2 mmol). Purification by column chromatography (0-5% EtOAc in CyH) followed by recrystallisation from EtOH afforded the product as a colourless solid. (243 mg, 1.02 mmol, 51%).

¹H NMR (400 MHz, CDCl₃): δ 7.31 – 7.18 (m, 4H), 7.10 (app ddt, *J* = 7.3, 1.3, 0.8 Hz, 2H), 7.04 – 6.97 (m, 2H), 6.62 (dd, *J* = 7.8, 0.8 Hz, 1H), 6.49 (d, *J* = 3.1 Hz, 1H), 5.64 (s, 2H), 3.83 (s, 3H).

¹³C{¹H} NMR (101 MHz, CDCl₃): δ 147.8, 139.9, 131.1, 129.2, 128.6, 127.2, 126.8, 120.1, 113.9, 102.9, 102.2, 55.5, 52.6.

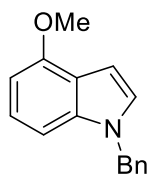
ν_{max} (neat) / cm⁻¹: 2922, 1575, 1488, 1449, 1312, 1260, 1182, 1072, 1031, 971.

HRMS: calcd. for C₁₆H₁₆NO [M+H]⁺: 238.1226; found (ESI⁺): 238.1232.

m.p. / °C: 62-65.

Characterisation data are consistent with literature values.²⁵²

1-Benzyl-4-methoxyindole (42)



Synthesised according to **GP-1** from 4-methoxyindole (294 mg, 2.0 mmol), NaH (60% on mineral oil, 96 mg, 2.4 mmol), and benzyl bromide (0.26 mL, 2.2 mmol). Recrystallisation from EtOH afforded the product as a colourless solid. (413 mg, 1.74 mmol, 87%).

¹H NMR (400 MHz, CDCl₃): δ 7.36 – 7.21 (m, 4H), 7.14 – 7.07 (m, 3H), 7.04 (d, *J* = 3.2 Hz, 1H), 6.91 (d, *J* = 8.2 Hz, 1H), 6.66 (dd, *J* = 3.2, 0.8 Hz, 1H), 6.53 (d, *J* = 7.7 Hz, 1H), 5.31 (s, 2H), 3.97 (s, 3H).

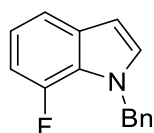
¹³C{¹H} NMR (101 MHz, CDCl₃): δ 153.6, 137.9, 137.7, 128.9, 127.7, 126.93, 126.87, 122.7, 119.3, 103.3, 99.6, 99.1, 55.5, 50.4.

ν_{\max} (neat) / cm⁻¹: 1582, 1494, 1450, 1353, 1253, 1221, 1059.

HRMS: calcd. for C₁₆H₁₆NO [M+H]⁺: 238.1226; found (ESI⁺): 238.1229.

m.p. / °C: 92-93.

1-Benzyl-7-fluoroindole (43)



Synthesised according to **GP-1** from 7-fluoroindole (270 mg, 2.0 mmol), NaH (60% on mineral oil, 96 mg, 2.4 mmol), and benzyl bromide (0.26 mL, 2.2 mmol). Purification by column chromatography (CyH) afforded the product as a colourless solid. (325 mg, 1.44 mmol, 72%).

¹H NMR (400 MHz, CDCl₃): δ 7.38 (d, *J* = 7.9 Hz, 1H), 7.34 – 7.21 (m, 4H), 7.14 (d, *J* = 6.8 Hz, 2H), 7.10 (d, *J* = 3.1 Hz, 1H), 6.98 (app td, *J* = 7.9, 4.6 Hz, 1H), 6.92 – 6.79 (m, 1H), 6.55 (app t, *J* = 2.6 Hz, 1H), 5.49 (s, 2H).

¹³C{¹H} NMR (101 MHz, CDCl₃): δ 150.3 (d, *J* = 243.5 Hz), 138.3, 132.8 (d, *J* = 5.5 Hz), 129.6, 128.7, 127.6, 126.8, 124.2 (d, *J* = 9.6 Hz), 119.8 (d, *J* = 6.5 Hz), 116.8 (d, *J* = 3.5 Hz), 107.4 (d, *J* = 18.1 Hz), 102.7 (d, *J* = 1.8 Hz), 52.3 (d, *J* = 5.6 Hz).

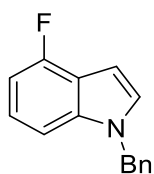
¹⁹F NMR (376 MHz, CDCl₃): δ -135.14 (ddd, *J* = 12.8, 4.6, 2.6 Hz).

ν_{max} (neat) / cm⁻¹: 1630, 1572, 1492, 1431, 1316, 1238, 1194, 1178, 1001.

HRMS: calcd. for C₁₅H₁₃FN [M+H]⁺: 226.1027 ; found (ESI⁺): 226.1035.

m.p. / °C: 41-43.

1-Benzyl-4-fluoroindole (44)



Synthesised according to **GP-1** from 4-fluoroindole (270 mg, 2.0 mmol), NaH (60% on mineral oil, 96 mg, 2.4 mmol), and benzyl bromide (0.26 mL, 2.2 mmol). Purification by column chromatography (CyH) afforded the product as a colourless solid. (226 mg, 1.00 mmol, 50%).

¹H NMR (400 MHz, CDCl₃): δ 7.34 – 7.27 (m, 3H), 7.14 – 7.08 (m, 3H), 7.07 (dd, *J* = 4.0, 2.2 Hz, 2H), 6.78 (ddd, *J* = 10.3, 6.6, 2.0 Hz, 1H), 6.64 (d, *J* = 3.1 Hz, 1H), 5.32 (s, 2H).

¹³C{¹H} NMR (101 MHz, CDCl₃): δ 156.6 (d, *J* = 247.0 Hz), 139.1 (d, *J* = 11.3 Hz), 137.2, 129.0, 128.3, 127.9, 126.9, 122.3 (d, *J* = 7.7 Hz), 117.9 (d, *J* = 22.5 Hz), 106.0 (d, *J* = 3.5 Hz), 104.5 (d, *J* = 19.0 Hz), 98.0, 50.6.

¹⁹F NMR (376 MHz, CDCl₃): δ -122.00 – -122.21 (m).

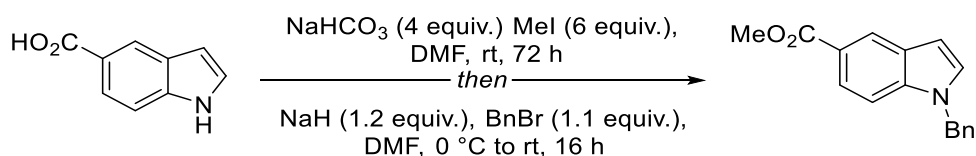
ν_{max} (neat) / cm⁻¹: 1626, 1571, 1493, 1454, 1436, 1370, 1360, 1346, 1292, 1233, 1218, 1195, 977.

HRMS: calcd. for C₁₅H₁₃FN [M+H]⁺: 226.1027 ; found (ESI⁺): 226.1019.

m.p. / °C: 41-43.

Characterisation data are consistent with literature values.²⁵³

Methyl 1-benzyl-1*H*-indole-5-carboxylate (45)



Step 1: To a flame-dried flask under an atmosphere of dinitrogen was added indole 5-carboxylic acid (483 mg, 3.0 mmol), MeI (1.21 mL, 19.5 mmol), and anhydrous DMF (3.5 mL). NaHCO₃ (1.01 g, 12.0 mmol) was added in one portion at rt and the resulting mixture stirred at rt for 72 hrs. The reaction was quenched by addition of water (5 mL) and then extracted with EtOAc (3 × 5 mL). The combined organics were washed with a 10 wt% aqueous LiCl solution (10 mL) and dried over MgSO₄, filtered, and concentrated *in vacuo*. Purification by column chromatography (20% EtOAc in CyH) afforded the product as a colourless solid (375 mg, 2.14 mmol, 71%).

¹H NMR (400 MHz, CDCl₃): δ 8.43 (s, 1H), 8.35 (br s, 1H), 7.91 (dd, *J* = 8.6, 1.6 Hz, 1H), 7.41 (d, *J* = 8.6 Hz, 1H), 7.28 (dd, *J* = 3.3, 2.4 Hz, 1H), 6.69 – 6.61 (m, 1H), 3.94 (s, 3H).

¹³C{¹H} NMR (101 MHz, CDCl₃): δ 168.4, 138.5, 127.6, 125.6, 123.9, 123.6, 122.1, 110.8, 104.2, 52.0.

Step 2: Synthesised according to **GP-1** from methyl 1*H*-indole-5-carboxylate (350 mg, 2.0 mmol), NaH (60% on mineral oil, 96 mg, 2.4 mmol), and benzyl bromide (0.26 mL, 2.2 mmol). Purification by column chromatography (0-10% EtOAc in CyH) afforded the product as a colourless solid. (318 mg, 1.20 mmol, 60%).

¹H NMR (400 MHz, CDCl₃): δ 8.42 (d, *J* = 1.7 Hz, 1H), 7.89 (dd, *J* = 8.7, 1.7 Hz, 1H), 7.35 – 7.27 (m, 4H), 7.18 (d, *J* = 3.3 Hz, 1H), 7.10 (dd, *J* = 7.7, 1.7 Hz, 2H), 6.65 (dd, *J* = 3.3, 0.9 Hz, 1H), 5.34 (s, 2H), 3.93 (s, 3H).

¹³C{¹H} NMR (101 MHz, CDCl₃): δ 168.3, 138.9, 137.0, 129.8, 129.0, 128.4, 128.0, 126.9, 124.2, 123.3, 121.8, 109.5, 103.5, 52.0, 50.4.

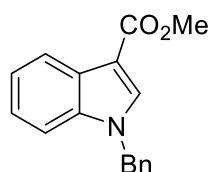
ν_{max} (neat) / cm⁻¹: 1702, 1609, 1453, 1434, 1349, 1296, 1269, 1251, 1196, 1179, 1142, 1080, 905.

HRMS: calcd. for C₁₇H₁₅NO₂ [M+H]⁺: 266.1176; found (ESI⁺): 266.1168.

m.p. / °C: 70-71 (lit. 68-70).²⁵⁴

Characterisation data are consistent with literature values.²⁵⁴

Methyl 1-benzyl-1*H*-indole-3-carboxylate (46)



Synthesised according to **GP-1** from methyl 1*H*-indole-3-carboxylate (350 mg, 2.0 mmol), NaH (60% on mineral oil, 96 mg, 2.4 mmol), and benzyl bromide (0.26 mL, 2.2 mmol). Purification by column chromatography (silica gel; CyH) afforded the product as an off-white solid. (325 mg, 1.44 mmol, 72%).

¹H NMR (400 MHz, CDCl₃): δ 8.22 – 8.18 (m, 1H), 7.85 (s, 1H), 7.35 – 7.27 (m, 5H), 7.26 – 7.22 (m, 1H), 7.19 – 7.12 (m, 2H), 5.34 (s, 2H), 3.91 (s, 3H).

¹³C{¹H} NMR (101 MHz, CDCl₃): δ 165.6, 136.9, 136.0, 134.7, 129.1, 128.3, 127.2, 126.9, 123.1, 122.2, 121.9, 110.4, 107.7, 51.1, 50.8.

ν_{max} (neat) / cm⁻¹: 1688, 1528, 1462, 1433, 1380, 1239, 1176, 1150, 1091, 1074, 1030, 926.

HRMS: calcd. for C₁₇H₁₅NO₂ [M+H]⁺: 266.1176; found (ESI⁺): 266.1167.

m.p. / °C: 95 (decomp.) (lit. 93-95).²⁵⁵

Characterisation data are consistent with literature values.²⁵⁵

1-Benzyl-7-azaindole (48)



Synthesised according to **GP-1** from melatonin (465 mg, 2.0 mmol), NaH (60% on mineral oil, 96 mg, 2.4 mmol), and benzyl bromide (0.26 mL, 2.2 mmol). Purification by column chromatography (silica gel; 10-20% EtOAc in CyH) afforded the product as a colourless solid (294 mg, 1.41 mmol, 70%).

¹H NMR (400 MHz, CDCl₃): δ 8.36 (dd, *J* = 4.7, 1.6 Hz, 1H), 7.93 (dd, *J* = 7.8, 1.6 Hz, 1H), 7.35 – 7.24 (m, 3H), 7.24 – 7.16 (m, 3H), 7.08 (dd, *J* = 7.8, 4.7 Hz, 1H), 6.49 (d, *J* = 3.5 Hz, 1H), 5.52 (s, 2H).

¹³C{¹H} NMR (101 MHz, CDCl₃): δ 147.9, 143.2, 138.0, 128.9, 128.8, 128.0, 127.7, 127.6, 120.6, 116.0, 100.2, 47.9.

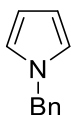
ν_{\max} (neat) / cm^{-1} : 1591, 1566, 1485, 1433, 1420, 1347, 1313, 1297, 1253, 1209, 1183, 889.

HRMS: calcd. for $\text{C}_{14}\text{H}_{13}\text{N}_2$ $[\text{M}+\text{H}]^+$: 209.1073; found (ESI⁺): 209.1078.

m.p. / °C: 77-78.

Characterisation data are consistent with literature values.²⁵⁶

1-Benzylpyrrole (80)



Synthesised according to **GP-1** from pyrrole (2.01 g, 30 mmol), NaH (1.32 g, 33 mmol), and benzyl bromide (3.6 mL, 30 mmol). Purification by column chromatography (silica gel; CyH) afforded the product as a yellow oil (2.64 g, 16.8 mmol, 56%).

¹H NMR (400 MHz, CDCl₃): δ 7.37 – 7.27 (m, 3H), 7.17 – 7.09 (m, 2H), 6.71 (app q, $J = 1.9$ Hz, 2H), 6.21 (app dt, $J = 3.5, 1.9$ Hz, 2H), 5.08 (s, 2H).

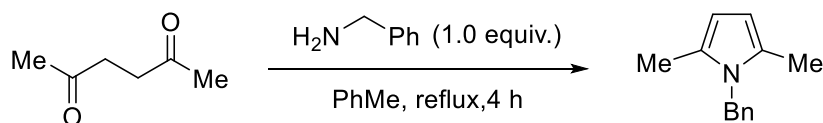
¹³C{¹H} NMR (101 MHz, CDCl₃): δ 138.3, 128.8, 127.7, 127.1, 121.2, 108.6, 53.4.

ν_{\max} (neat) / cm^{-1} : 1496, 1453, 1439, 1355, 1301, 1278, 1087, 1067, 967.

HRMS: calcd. for $\text{C}_{11}\text{H}_{12}\text{N}$ $[\text{M}+\text{H}]^+$: 158.0965; found (ESI⁺): 158.0967.

Characterisation data are consistent with literature values.²⁵⁷

1-Benzyl-2,5-dimethylpyrrole (82)



According to literature procedure,²⁵⁸ 2,5-hexanedione (0.23 mL, 2.0 mmol) and benzylamine (0.22 mL, 2.0 mmol) were dissolved in PhMe (5 mL) and heated to reflux for 4 h. After cooling to rt, the solvent was removed *in vacuo* and the resulting residue purified by column chromatography (silica gel; 2% EtOAc in CyH) to afford the product as a colourless solid (308 mg, 1.42 mmol, 71%).

¹H NMR (400 MHz, CDCl₃): δ 7.35 – 7.19 (m, 3H), 6.89 (d, $J = 7.0$ Hz, 2H), 5.87 (s, 2H), 5.02 (s, 2H), 2.15 (s, 6H).

$^{13}\text{C}\{^1\text{H}\}$ NMR (101 MHz, CDCl_3): δ 138.7, 128.8, 128.2, 127.1, 125.8, 105.5, 46.9, 12.6.

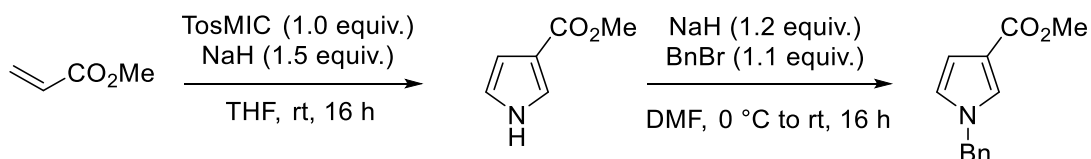
HRMS: calcd. for $\text{C}_{13}\text{H}_{16}\text{N}$ $[\text{M}+\text{H}]^+$: 186.1277; found (ESI $^+$): 186.1267.

ν_{max} (neat) / cm^{-1} : 1658, 1494, 1447, 1406, 1355, 1302.

m.p. / $^{\circ}\text{C}$: 46-47 (lit. 43-45).²⁵⁹

Characterisation data are consistent with literature values.²⁶⁰

1-Benzylpyrrole-3-methyl ester



Step 1: A solution of methyl acrylate (0.45 mL, 5.0 mmol) and TosMIC (976 mg, 5.0 mmol) in anhydrous THF (5 mL) was added drop-wise to a flame-dried flask containing a suspension of *t*BuOK (1.12 g, 10 mmol) in anhydrous THF (5 mL). The resulting suspension was stirred for 1 hr at rt. The reaction was quenched by addition of water (10 mL), then EtOAc (20 mL) was added. The organic phase was separated and the aqueous phase was extracted with EtOAc (3 \times 10 mL). The combined organic portions were washed with brine, dried over MgSO_4 , filtered, and concentrated *in vacuo*. Purification by column chromatography (silica gel; 20% EtOAc in CyH) afforded the product as a yellow oil (130 mg, 1.04 mmol, 21%).

^1H NMR (400 MHz, CDCl_3): δ 8.48 (br s, 1H), 7.44 (app dt, J = 3.3, 1.6 Hz, 1H), 6.76 (app q, J = 2.4 Hz, 1H), 6.66 (app td, J = 2.8, 1.6 Hz, 1H), 3.82 (s, 3H).

Step 2: Synthesised according to **GP-1** from pyrrole-3-methyl ester (188 mg, 1.5 mmol), NaH (72 mg, 1.8 mmol), and benzyl bromide (0.20 mL, 1.65 mmol). Purification by column chromatography (silica gel; 10% EtOAc in CyH) afforded the product as a yellow oil (203 mg, 0.942 mmol, 63%).

^1H NMR (400 MHz, CDCl_3): δ 7.38 – 7.28 (m, 4H), 7.17 – 7.11 (m, 2H), 6.65 – 6.59 (m, 2H), 5.05 (s, 2H), 3.79 (s, 3H).

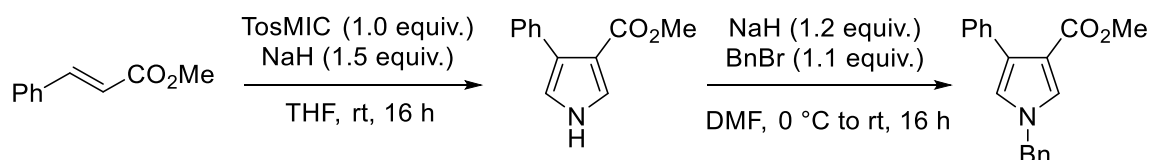
$^{13}\text{C}\{^1\text{H}\}$ NMR (101 MHz, CDCl_3): δ 165.3, 129.0, 128.2, 127.3, 126.4, 122.2, 116.2, 110.5, 53.9, 51.1.

ν_{max} (neat) / cm^{-1} : 2947, 1697, 1539, 1543, 1440, 1362, 1218, 181, 1112, 991, 923.

HRMS: calcd. for C₁₃H₁₄NO₂ [M+H]⁺: 216.1019; found (ESI⁺): 216.1024.

Characterisation data are consistent with literature values.²⁶¹

Methyl 1-benzyl-4-phenyl-1*H*-pyrrole-3-carboxylate



Step 1: A solution of methyl cinnamate (811 mg, 5.0 mmol) and TosMIC (976 mg, 5.0 mmol) in anhydrous THF (10 mL) was added drop-wise to a flame-dried flask containing a suspension of NaH (60% in mineral oil; 300 mg, 7.5 mmol) in anhydrous THF (10 mL). The resulting suspension was stirred overnight at rt. The reaction was quenched by addition of water (20 mL), then EtOAc (20 mL) was added. The organic phase was separated and the aqueous phase was extracted with EtOAc (3 × 20 mL). The combined organic portions were washed with brine, dried over MgSO₄, filtered, and concentrated *in vacuo*. Purification by column chromatography (silica gel; 30% EtOAc in CyH) afforded the product as a yellow oil (621 mg, 2.59 mmol, 52%).

¹H NMR (400 MHz, CDCl₃): δ 8.53 (brs, 1H), 7.56 – 7.42 (m, 3H), 7.39 – 7.33 (m, 2H), 7.31 – 7.27 (m, 1H), 6.78 (app t, *J* = 2.4 Hz, 1H), 3.74 (s, 3H).

¹³C{¹H} NMR (101 MHz, CDCl₃): δ 165.3, 134.8, 129.4, 127.9, 127.0, 126.7, 125.5, 118.4, 113.7, 51.1.

Characterisation data are consistent with literature values.²⁶²

Step 2: Carried out according to **GP-1** employing methyl 4-phenyl-1*H*-pyrrole-3-carboxylate (402 mg, 1.5 mmol), NaH (60% in mineral oil; 72 mg, 1.8 mmol), and BnBr (0.18 mL, 1.65 mmol). Purification by column chromatography (silica gel; 5% EtOAc in CyH) afforded the product as a colourless oil (218 mg, 0.749 mmol, 49%).

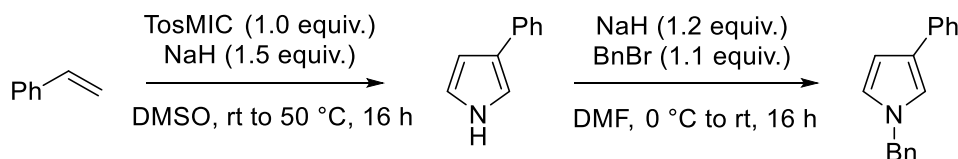
¹H NMR (400 MHz, CDCl₃): δ 7.52 – 7.47 (m, 2H), 7.40 (d, *J* = 2.5 Hz, 1H), 7.39 – 7.30 (m, 5H), 7.29 – 7.24 (m, 1H), 7.24 – 7.19 (m, 2H), 6.68 (d, *J* = 2.5 Hz, 1H), 5.07 (s, 1H), 3.72 (s, 2H).

$^{13}\text{C}\{^1\text{H}\}$ NMR (101 MHz, CDCl_3): δ 165.1, 136.5, 134.7, 129.3, 129.1, 128.4, 128.3, 127.9, 127.6, 127.5, 126.6, 121.7, 113.3, 54.1, 50.9.

ν_{max} (neat) / cm^{-1} : 1707, 1521, 1446, 1386, 1271, 1164, 1101, 994, 941.

HRMS: calcd. for $\text{C}_{19}\text{H}_{18}\text{NO}_2$ $[\text{M}+\text{H}]^+$: 292.1332; found (ESI $^+$): 292.1333.

1-Benzyl-3-phenylpyrrole



Step 1: According to literature procedure,²⁶³ a solution of styrene (0.57 mL, 5.0 mmol) and TosMIC (1.27 g, 6.5 mmol) in anhydrous THF (12 mL) was added drop-wise to a flame-dried flask containing a solution of *t*BuOK (961 mg, 10 mmol) in anhydrous DMSO (12 mL). The resulting solution was heated to 50 °C and stirred overnight. The reaction was quenched by addition of water (20 mL), then EtOAc (20 mL) was added. The organic phase was separated and the aqueous phase was extracted with EtOAc (3 × 20 mL). The combined organic portions were washed with brine, dried over Na_2SO_4 , filtered, and concentrated *in vacuo*. Purification by column chromatography (silica gel; 10% EtOAc in CyH) afforded the product as a colourless solid (214 mg, 1.49 mmol, 30%).

^1H NMR (400 MHz, CDCl_3): δ 8.25 (brs, 1H), 7.60 – 7.52 (m, 2H), 7.40 – 7.31 (m, 2H), 7.22 – 7.15 (m, 1H), 7.10 (app dt, $J = 2.7, 1.9$ Hz, 1H), 6.85 (app td, $J = 2.7, 1.9$ Hz, 1H), 6.56 (app td, $J = 2.7, 1.6$ Hz, 1H).

Characterisation data are consistent with literature values.²⁶³

Step 2: Carried out according to **GP-1** employing methyl 3-phenylpyrrole (143 mg, 1.0 mmol), NaH (60% in mineral oil, 48 mg, 1.2 mmol), and BnBr (0.13 mL, 1.1 mmol). Purification by column chromatography (silica gel; CyH) afforded the product as a white solid (131 mg, 0.561 mmol, 56%).

^1H NMR (400 MHz, CDCl_3): δ 7.55 – 7.47 (m, 2H), 7.38 – 7.27 (m, 5H), 7.22 – 7.11 (m, 3H), 6.99 (app t, $J = 2.0$ Hz, 1H), 6.71 (app t, $J = 2.5$ Hz, 1H), 6.50 (dd, $J = 2.8, 1.8$ Hz, 1H), 5.09 (s, 2H).

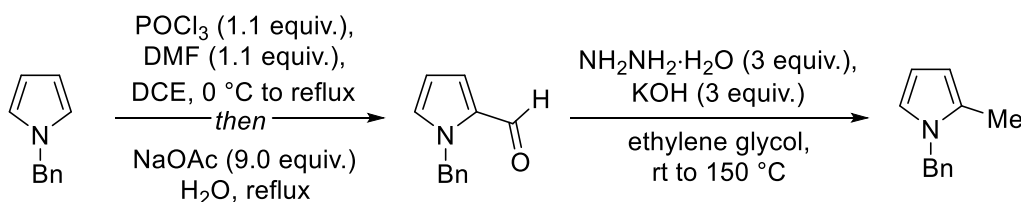
$^{13}\text{C}\{^1\text{H}\}$ NMR (101 MHz, CDCl_3): δ 138.0, 136.0, 128.9, 128.7, 127.9, 127.2, 125.5, 125.4, 125.1, 122.4, 118.1, 106.8, 53.7.

ν_{max} (neat) / cm^{-1} : 1701, 1602, 1494, 1449, 1353, 1265, 1072, 1028.

HRMS: calcd. for $\text{C}_{17}\text{H}_{16}\text{N}$ $[\text{M}+\text{H}]^+$: 234.1278; found (ESI $^+$): 234.1285.

Characterisation data are consistent with literature values.²⁵⁷

1-Benzyl-2-methylpyrrole



Step 1: POCl₃ (206 μL , 2.2 mmol) was added drop-wise to a flask containing DMF (171 μL , 2.2 mmol) cooled to 0 °C to give a white solid. 1,2-DCE (2.5 mL) was then added and the mixture was warmed to rt until full dissolution was observed. A solution of *N*-benzylpyrrole (346 μL , 2.0 mmol) in 1,2-DCE (2.5 mL) was added drop-wise, then heated to reflux and stirred for 15 mins. After cooling to rt, a solution of NaOAc (1.48 g, 18 mmol) in water (9 mL) was added and the mixture was heated to reflux for a further 10 mins. After cooling to rt once more, the reaction mixture was diluted with Et₂O (20 mL) and the aqueous phase was removed. The organic phase was washed with sat. aqueous NaHCO₃ (20 mL), dried over MgSO₄, filtered, and concentrated *in vacuo*. Purification by column chromatography (silica gel; 10% EtOAc in CyH) afforded the product as a yellow liquid (212 mg, 1.14 mmol, 57%).

Step 2: To a mixture of 1-benzyl-2-formylpyrrole (212 mg, 1.14 mmol) in ethylene glycol (4.5 mL) was added KOH (202 mg, 3.6 mmol) and hydrazine hydrate (187 μL , 3.6 mmol) after which the mixture was stirred for 30 mins at rt to give a pale green colour. The reaction mixture was then heated to 150 °C and stirred for 2 h. After cooling to rt, water (10 mL) was added followed by Et₂O (10 mL). The organic phase was separated and the aqueous layer was extracted with Et₂O (3 \times 10 mL). The combined organic portions were washed with brine, dried over Na₂SO₄, filtered, and concentrated *in vacuo* to give a yellow oil that was used without further purification (195 mg, 1.14 mmol, 99%).

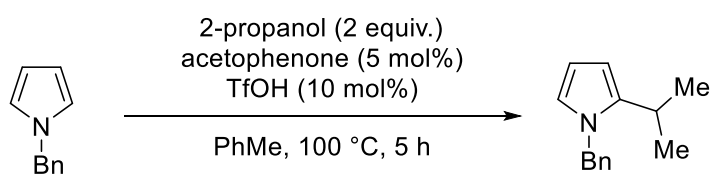
¹H NMR (400 MHz, CDCl₃): δ 7.37 – 7.25 (m, 3H), 7.03 (m, 2H), 6.66 (dd, *J* = 2.8, 1.9 Hz, 1H), 6.14 (app t, *J* = 3.1 Hz, 1H), 5.97 (ddd, *J* = 3.5, 1.9, 1.0 Hz, 1H), 5.06 (s, 2H), 2.17 (s, 3H).

¹³C NMR (101 MHz, CDCl₃): δ 138.6, 128.9, 128.8, 127.4, 126.5, 121.0, 107.2, 77.2, 50.5, 12.1.

***v*_{max} (neat) / cm⁻¹:** 1493, 1452, 1420, 1355, 1299, 1074, 1028.

HRMS: calcd. for C₁₅H₁₈N₃ [M+C₃H₅N₂]⁺: 240.1495; found (ESI⁺): 240.1489.

1-Benzyl-2-isopropylpyrrole



According to literature procedure,²⁶⁴ to a solution of *N*-benzylpyrrole (314 mg, 2.0 mmol), acetophenone (12.0 mg, 5 mol%), and 2-propanol (305 μL, 4.0 mmol) in PhMe (10 mL) was added TfOH (18 μL, 10 mol%) at rt. The resulting red solution was heated to 100 °C and stirred for 5 hrs. After cooling to rt, the reaction was diluted with EtOAc (10 mL) and washed with sat. aqueous NaHCO₃ (20 mL). The aqueous phase was extracted with EtOAc (3 × 10 mL), then the combined organic portions were washed with brine, dried over MgSO₄, filtered, and concentrated *in vacuo*. Purification by column chromatography (silica gel; CyH) afforded the product as a yellow oil (148 mg, 0.741 mmol, 37%).

¹H NMR (400 MHz, CDCl₃): δ 7.40 – 7.29 (m, 3H), 7.19 – 7.11 (m, 2H), 6.63 (app t, *J* = 2.5 Hz, 1H), 6.51 – 6.46 (m, 1H), 6.10 (dd, *J* = 2.5, 1.8 Hz, 1H), 5.03 (s, 2H), 2.85 (hept, *J* = 6.8 Hz, 1H), 1.23 (d, *J* = 6.8 Hz, 6H).

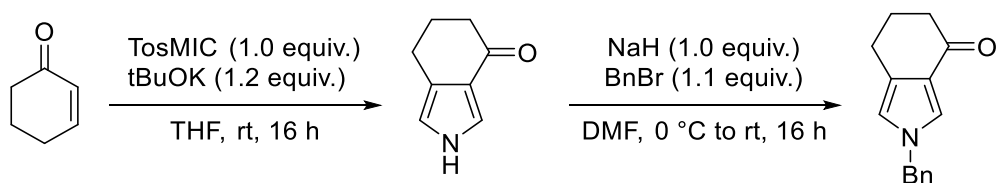
¹³C{¹H} NMR (101 MHz, CDCl₃): δ 138.5, 132.4, 128.8, 127.7, 127.2, 121.0, 117.1, 107.1, 53.5, 26.6, 24.2.

***v*_{max} (neat) / cm⁻¹:** 2956, 1497, 1453, 1358, 1294, 1176, 1076.

HRMS: calcd. for C₁₄H₁₇NNa [M+Na]⁺: 222.1253; found (ESI⁺): 222.1246.

Characterisation data are consistent with literature values.²⁶⁴

2-Benzyl-2,5,6,7-tetrahydro-4*H*-isoindol-4-one



Step 1: According to literature procedure,²⁶⁵ a solution of 2-cyclohexenone (0.48 mL, 5.0 mmol) and TosMIC (976 mg, 5.0 mmol) in anhydrous THF (10 mL) was added drop-wise to a flame-dried flask containing a suspension of *t*BuOK (673 mg, 6.0 mmol) in anhydrous THF (10 mL). The resulting suspension was stirred overnight at rt. The reaction was quenched by addition of water (20 mL), then EtOAc (20 mL) was added. The organic layer was separated and the aqueous layer extracted with EtOAc (3 × 20 mL). The combined organic portions were washed with brine, dried over MgSO₄, filtered, and concentrated *in vacuo*. Purification by column chromatography (silica gel; 50% EtOAc in CyH) afforded the product as a yellow oil (249 mg, 1.84 mmol, 37%).

¹H NMR (400 MHz, CDCl₃): δ 8.83 (br s, 1H), 7.37 (dd, *J* = 3.2, 1.9 Hz, 1H), 6.56 (br s, *J* = 2.1, 1.1 Hz, 1H), 2.72 (td, *J* = 6.2, 1.1 Hz, 2H), 2.49 (dd, *J* = 7.0, 5.6 Hz, 2H), 2.15 – 1.97 (m, 2H).

¹³C{¹H} NMR (101 MHz, CDCl₃): δ 196.4, 126.5, 122.1, 119.6, 113.8, 39.5, 25.2, 21.6.

Step 2: Carried out according to **GP-1** employing 2,5,6,7-tetrahydro-4*H*-isoindol-4-one (135 mg, 1.0 mmol), NaH (40 mg, 1.0 mmol), and BnBr (188 mg, 1.1 mmol). Purification by column chromatography (30% EtOAc in CyH) afforded the product as a colourless solid (109 mg, 0.482 mmol, 48%).

¹H NMR (400 MHz, CDCl₃): δ 7.38 – 7.30 (m, 2H), 7.27 (d, *J* = 2.0 Hz, 1H), 7.20 – 7.13 (m, 2H), 6.41 (d, *J* = 2.0 Hz, 1H), 5.01 (s, 2H), 2.66 (t, *J* = 6.5 Hz, 1H), 2.58 – 2.36 (m, 1H), 2.04 (app p, *J* = 6.2 Hz, 1H).

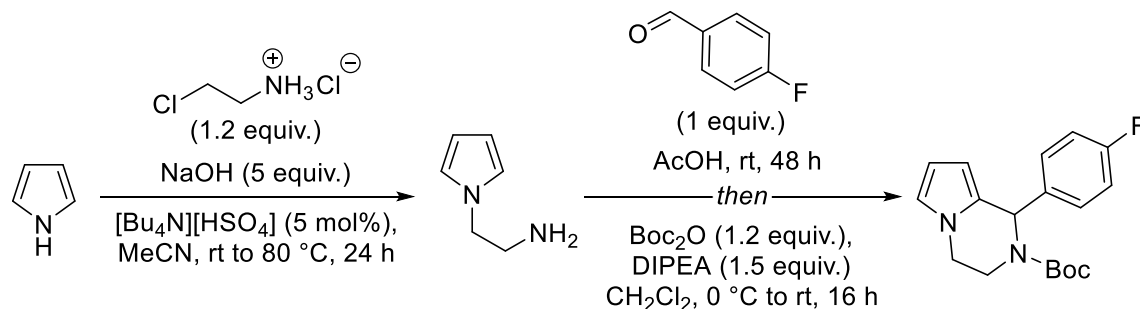
¹³C{¹H} NMR (101 MHz, CDCl₃): δ 195.8, 136.5, 129.1, 128.4, 127.8, 127.7, 122.4, 122.2, 117.2, 54.1, 39.4, 25.3, 21.8.

ν_{max} (neat) / cm⁻¹: 1645, 1518, 1453, 1380, 1250, 1242, 1174, 1135, 1002, 898.

HRMS: calcd. for C₁₅H₁₅NONa [M+Na]⁺: 248.1046; found (ESI⁺): 248.1055.

m.p. / °C: 77-78 (lit. 78-79).²⁶⁶

2-(*tert*-Butoxycarbonyl)-1-(4-Fluorophenyl)-1,2,3,4-tetrahydropyrrolo[1,2-*a*]pyrazine



Step 1: To a solution of pyrrole (335 mg, 5.0 mmol) and tetrabutylammonium hydrogensulfate (TBAS, 85 mg, 5 mol%) in MeCN (15 mL) was added pulverised NaOH (1.00 g, 25 mmol) in one portion. The resulting mixture was stirred at rt for 30 mins, then 2-chloroethylamine hydrochloride (696 mg, 6.0 mmol) was added in one portion. The reaction mixture was heated to reflux and stirred for 24 h. After cooling to rt, the mixture was poured onto water (50 mL) and extracted with Et₂O (3 × 20 mL). The combined organic portions were dried over MgSO₄, filtered, and concentrated *in vacuo* to afford the product as a yellow oil which was used without further purification.

¹H NMR (400 MHz, CDCl₃): δ 6.71 (app t, *J* = 2.1 Hz, 2H), 6.19 (app t, *J* = 2.1 Hz, 2H), 4.04 – 3.89 (m, 2H), 3.14 – 2.99 (m, 2H), 1.03 (brs, 2H).

Step 2: To a solution of 1-(2-aminoethyl)pyrrole (551 mg, 5.0 mmol) in AcOH (12.5 mL) was added 4-fluorobenzaldehyde (621 mg, 5.0 mmol) in one portion. The mixture was stirred at rt for 48 h, then poured onto sat. aqueous Na₂CO₃ (30 mL) and extracted with CH₂Cl₂ (3 × 10 mL). The combined organic portions were washed with brine, dried over Na₂SO₄, filtered, and concentrated *in vacuo*. Purification by recrystallisation from 2-propanol afforded the product as a beige solid (523 mg, 2.42 mmol, 48%).

¹H NMR (400 MHz, CDCl₃): δ 7.50 – 7.34 (m, 2H), 7.18 – 6.97 (m, 2H), 6.63 (app t, *J* = 2.2 Hz, 1H), 6.14 (dd, *J* = 3.5, 2.7 Hz, 1H), 5.55 (app dt, *J* = 3.0, 1.4 Hz, 1H), 5.09 (s, 1H), 4.11 (ddd, *J* = 11.7, 10.1, 4.8 Hz, 1H), 4.01 (ddd, *J* = 11.7, 4.3, 3.1 Hz, 1H), 3.38 (ddd, *J* = 12.6, 4.8, 3.1 Hz, 1H), 3.30 (ddd, *J* = 12.6, 10.1, 4.3 Hz, 1H).

¹³C{¹H} NMR (101 MHz, CDCl₃): δ 162.5 (d, *J* = 245.6 Hz), 138.9 (d, *J* = 3.2 Hz), 130.7, 130.0 (d, *J* = 8.0 Hz), 119.2, 115.3 (d, *J* = 21.3 Hz), 107.8, 105.0, 58.6, 45.6, 43.3.

¹⁹F NMR (376 MHz, CDCl₃): δ -114.93 (tt, *J* = 8.6, 5.4 Hz).

HRMS: calcd. for C₁₃H₁₄FN₂O [M+H]⁺: 217.1136; found (ESI⁺): 217.1135.

Step 3: To a solution of 1-(4-fluorophenyl)-1,2,3,4-tetrahydropyrrolo[1,2-a]pyrazine (198 mg, 1.0 mmol) and DIPEA (0.26 mL, 1.5 mmol) in CH₂Cl₂ (10 mL) cooled to 0 °C was added Boc₂O (0.28 mL, 1.2 mmol) drop-wise. The reaction mixture was warmed to rt and stirred overnight. The volatiles were removed *in vacuo*. Purification by column chromatography (silica gel; 5% EtOAc in pentane) afforded the product as a colourless solid (274 mg, 0.867 mmol, 87%).

¹H NMR (400 MHz, CDCl₃): δ 7.23 (dd, *J* = 8.6, 5.5 Hz, 2H), 6.97 (app t, *J* = 8.7 Hz, 2H), 6.64 (dd, *J* = 2.7, 1.7 Hz, 1H), 6.38 (s, 1H), 6.21 (dd, *J* = 3.5, 2.7 Hz, 1H), 5.91 (s, 1H), 4.22 (brs, 1H), 4.02 (td, *J* = 11.6, 4.3 Hz, 1H), 3.94 (ddd, *J* = 12.1, 4.3, 2.5 Hz, 1H), 3.27 (ddd, *J* = 13.7, 11.1, 4.3 Hz, 1H), 1.49 (s, 9H).

¹³C{¹H} NMR (101 MHz, CDCl₃): δ 162.1 (d, *J* = 245.9 Hz), 154.2, 138.0 (d, *J* = 3.2 Hz), 129.0 (d, *J* = 8.0 Hz), 126.6, 119.2, 115.1 (d, *J* = 21.4 Hz), 108.4, 105.9, 80.8, 53.8, 44.4, 38.3, 28.5.

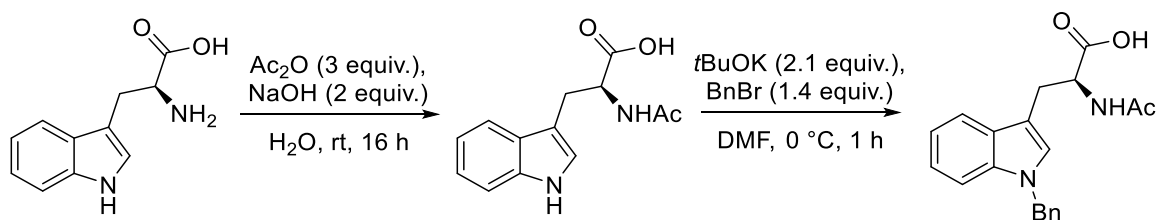
¹⁹F NMR (376 MHz, CDCl₃): δ -115.29 (br s).

ν_{max} (neat) / cm⁻¹: 1682, 1502, 1411, 1287, 1218, 1168, 1149, 1098, 1077, 980, 863.

HRMS: calcd. for C₁₈H₂₁FN₂O₂ [M+H]⁺: 317.1660; found (ESI⁺): 317.1678.

m.p. / °C: 68-70.

N^α-Acetyl-1-benzyltryptophan



Step 1: To a suspension of *L*-tryptophan (2.04 g, 10 mmol) in water (20 mL) was added pulverised NaOH (800 mg, 20 mmol) in one portion. Full dissolution of the suspended solid was observed, and the reaction mixture was stirred at rt for 30 mins. Ac₂O (2.84 mL, 30 mmol) was then added, and a white precipitate formed. The reaction was stirred at rt overnight after which time the precipitate was collected by vacuum filtration, washed with water (10 mL) and dried under reduced pressure to afford the pure product as a colourless solid (1.34 g, 5.44 mmol, 54%).

¹H NMR (400 MHz, DMSO-*d*₆): δ 12.61 (brs, 1H), 10.83 (s, 1H), 8.12 (d, *J* = 7.8 Hz, 1H), 7.53 (d, *J* = 7.8 Hz, 1H), 7.39 – 7.30 (m, 1H), 7.14 (d, *J* = 2.4 Hz, 1H), 7.07 (ddd, *J* = 8.2, 7.0, 1.2 Hz, 1H), 6.98 (ddd, *J* = 8.2, 7.0, 1.2 Hz, 1H), 4.45 (app td, *J* = 8.2, 5.1 Hz, 1H), 3.16 (dd, *J* = 14.7, 5.1 Hz, 1H), 2.98 (dd, *J* = 14.7, 8.7 Hz, 1H), 1.80 (s, 3H).

¹³C{¹H} NMR (101 MHz, DMSO-*d*₆): δ 173.6, 169.2, 136.1, 127.2, 123.5, 120.9, 118.3, 118.1, 111.4, 110.0, 53.0, 27.1, 22.4.

HRMS: calcd. for C₁₃H₁₄N₂O₃Na [M+Na]⁺: 269.0897; found (ESI⁺): 269.0894.

Step 2: According to the literature procedure,²⁶⁷ the *N*-acetyl tryptophan (1.23 g, 5.0 mmol) was transferred to a Schlenk flask under an atmosphere of dinitrogen, and dissolved in anhydrous DMF (25 mL). *t*BuOK (1.18 g, 10.5 mmol) was added in one portion at rt and stirred for 5 mins until all solids fully dissolved. The reaction mixture was cooled to 0 °C and BnBr (0.84 mL, 7.0 mmol) was added drop-wise. The resulting solution was warmed to rt and stirred for 1 hr. The reaction was quenched by addition of 1 M aqueous HCl (10 mL) and then extracted with EtOAc (3 × 20 mL). The combined organics were washed with a 10 wt% aqueous LiCl solution (2 × 30 mL) and dried over Na₂SO₄, filtered, and concentrated *in vacuo*. Purification by recrystallisation from EtOH afforded the product as a colourless solid (1.05 g, 3.12 mmol, 42%).

¹H NMR (400 MHz, DMSO-*d*₆): δ 12.64 (s, 1H), 8.17 (d, *J* = 7.9 Hz, 1H), 7.56 (d, *J* = 7.8 Hz, 1H), 7.38 (d, *J* = 8.1 Hz, 1H), 7.28 (d, *J* = 7.8 Hz, 3H), 7.25 – 7.20 (m, 1H), 7.18 – 7.12 (m, 2H), 7.09 (d, *J* = 7.5 Hz, 1H), 7.02 (d, *J* = 7.5 Hz, 1H), 5.37 (s, 2H), 4.49 (td, *J* = 8.4, 5.2 Hz, 1H), 3.19 (dd, *J* = 14.5, 5.2 Hz, 1H), 3.00 (dd, *J* = 14.6, 8.8 Hz, 1H), 1.80 (s, 3H).

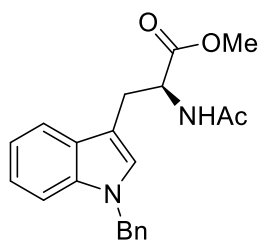
¹³C{¹H} NMR (101 MHz, DMSO-*d*₆): δ 173.5, 169.2, 138.4, 136.0, 128.5, 127.8, 127.5, 127.2, 126.9, 121.2, 118.7, 118.6, 110.1, 110.0, 52.9, 48.9, 27.1, 22.4.

ν_{max} (neat) / cm⁻¹: 3373, 1713, 1582, 1534, 1438, 1327, 1195, 1130.

HRMS: calcd. for C₂₀H₁₉N₂O₃ [M-H]⁻: 335.1401; found (ESI⁻): 335.1386.

m.p. / °C: 157-159.

N α -Acetyl-1-benzyl-*L*-tryptophan methyl ester (95)



To a solution of *N* α -acetyl-1-benzyltryptophan (1.68 g, 5.0 mmol) in MeOH (15 mL) was added SOCl₂ (0.51 mL, 7.0 mmol) drop-wise and the reaction stirred at 0 °C for 30 mins. It was then heated to 50 °C and stirred for 1 hr until consumption of starting material by TLC. The volatiles were then removed *in vacuo* and the residue purified by column chromatography (silica gel; 50% EtOAc in CyH) to afford the product as a colourless solid (918 mg, 2.62 mmol, 48%).

¹H NMR (400 MHz, CDCl₃): δ 7.54 (d, *J* = 7.8 Hz, 1H), 7.33 – 7.23 (m, 4H), 7.18 (app td, *J* = 6.9, 0.9 Hz, 1H), 7.15 – 7.10 (m, 1H), 7.08 (m, 2H), 6.87 (s, 1H), 5.98 (d, *J* = 7.7 Hz, 1H), 5.28 (s, 2H), 4.95 (app dt, *J* = 7.9, 5.2 Hz, 1H), 3.64 (s, 3H), 3.38 – 3.25 (m, 2H), 1.94 (s, 2H).

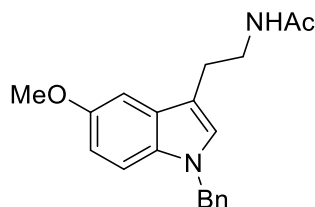
¹³C{¹H} NMR (101 MHz, CDCl₃): δ 172.5, 169.7, 137.5, 136.7, 128.9, 128.6, 127.8, 126.9, 126.8, 122.2, 119.6, 119.0, 109.9, 109.5, 53.3, 52.4, 50.0, 27.8.

ν_{max} (neat) / cm⁻¹: 3309, 1752, 1646, 1543, 1467, 1431, 1372, 1338, 1272, 1210, 1176, 1126.

HRMS: calcd. for C₂₁H₂₃N₂O₃ [M+H]⁺: 351.1703; found (ESI⁺): 351.1693.

m.p. / °C: 152-155.

1-Benzylmelatonin (97)



Synthesised according to **GP-1** from melatonin (465 mg, 2.0 mmol), NaH (60% in mineral oil, 96 mg, 2.4 mmol), and benzyl bromide (0.26 mL, 2.2 mmol). Recrystallisation from EtOAc afforded the product as a colourless solid (379 mg, 1.18 mmol, 59%).

¹H NMR (400 MHz, CDCl₃): δ 7.38 – 7.25 (m, 3H), 7.19 (d, *J* = 8.9 Hz, 1H), 7.15 – 7.09 (m, 2H), 7.07 (d, *J* = 2.4 Hz, 1H), 6.96 (s, 1H), 6.87 (dd, *J* = 8.9, 2.4 Hz, 1H), 5.56 (br s, 1H), 5.27 (s, 2H), 3.88 (s, 3H), δ 3.58 (app q, *J* = 6.6 Hz, 1H), 2.96 (t, *J* = 6.6 Hz, 2H), 1.94 (s, 3H).

¹³C{¹H} NMR (101 MHz, CDCl₃): 170.1, 154.1, 137.7, 132.2, 128.9, 128.5, 127.8, 126.91, 126.85, 112.4, 111.8, 110.8, 100.8, 56.1, 50.3, 39.9, 25.4, 23.5.

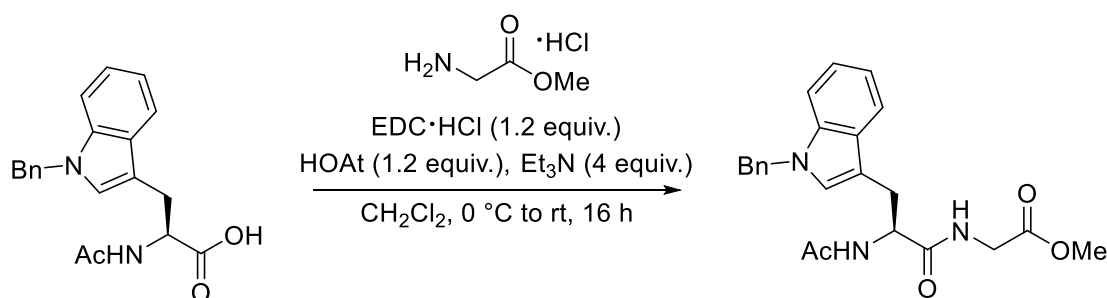
ν_{max} (neat) / cm⁻¹: 3313, 2913, 1637, 1556, 1488, 1434, 1230, 1057, 1042, 857.

HRMS: calcd. for C₂₀H₂₃N₂O₂ [M+H]⁺: 323.1755; found (ESI⁺): 323.1754.

m.p. / °C: 118-120 (lit. 115).²⁶⁸

Characterisation data are consistent with literature values.²⁶⁸

Methyl N^α-acetyl-1-benzyltryptophylglycinate (99)



To a suspension of glycine methyl ester hydrochloride (252 mg, 2.0 mmol) in CH₂Cl₂ (20 mL) at 0 °C was added sequentially Et₃N (1.1 mL, 8.0 mmol), HOAt (327 mg, 2.4 mmol), and N^α-acetyl-1-benzyltryptophan (673 mg, 2.0 mmol) which was stirred until homogenous. EDC·HCl (460 mg, 2.4 mmol) was then added and the reaction mixture warmed to rt and stirred overnight. The reaction was quenched by addition of 1 M HCl (10 mL) and extracted with CH₂Cl₂ (3 × 10 mL). The combined organics were washed with sat. aqueous NaHCO₃ (50 mL) and the new aqueous layer extracted with CH₂Cl₂ (3 × 10 mL). The combined organics were dried over MgSO₄, filtered, and concentrated *in vacuo*. Purification by column chromatography (silica gel; 2-5% MeOH in CH₂Cl₂) afforded the pure product as a colourless solid (481 mg, 1.18 mmol, 59%).

¹H NMR (400 MHz, DMSO-*d*₆): δ 8.46 (app t, *J* = 5.9 Hz, 1H), 8.08 (d, *J* = 8.3 Hz, 1H), 7.70 – 7.54 (m, 1H), 7.37 (d, *J* = 8.3 Hz, 1H), 7.32 – 7.17 (m, 4H), 7.14 (dd, *J* = 6.9, 1.6 Hz, 2H), 7.07 (ddd, *J* = 8.2, 7.0, 1.2 Hz, 1H), 7.00 (ddd, *J* = 7.8, 7.1, 1.1 Hz, 1H), 5.35 (s, 2H), 4.58

(app td, $J = 9.0, 4.8$ Hz, 1H), 3.84 (s, 1H), 3.83 (s, 1H), 3.62 (s, 2H), 3.14 (dd, $J = 14.6, 4.8$ Hz, 1H), 2.88 (dd, $J = 14.6, 9.4$ Hz, 1H), 1.75 (s, 3H).

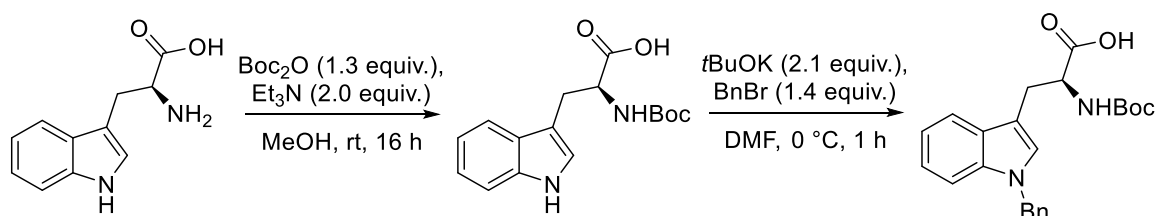
$^{13}\text{C}\{^1\text{H}\}$ NMR (101 MHz, DMSO- d_6): δ 172.7, 170.7, 169.5, 138.9, 136.4, 128.9, 128.4, 127.9, 127.7, 127.4, 121.6, 119.3, 119.0, 110.7, 110.4, 53.5, 52.2, 49.3, 41.1, 31.2, 28.2, 23.0.

ν_{max} (neat) / cm^{-1} : 3300, 1751, 1632, 1545, 1468, 1359, 1199, 1176.

HRMS: calcd. for $\text{C}_{23}\text{H}_{26}\text{N}_3\text{O}_4$ $[\text{M}+\text{H}]^+$: 408.1918; found (ESI $^+$): 408.1924.

m.p. / $^{\circ}\text{C}$: 116-117.

N^{α} -Boc 1-benzyltryptophan



Step 1: To a suspension of *L*-tryptophan (1.02 g, 5.0 mmol) in MeOH (40 mL) was added Et_3N (1.40 mL, 10.0 mmol) followed by Boc_2O (1.50 mL, 6.5 mmol) at rt after which full dissolution was observed. The reaction was stirred at rt overnight. The volatiles were removed *in vacuo* and the resulting solid re-dissolved in CH_2Cl_2 (30 mL). The organics were washed with 1 M HCl (30 mL) and the aqueous layer washed with CH_2Cl_2 (3×20 mL). The combined organics were dried over Na_2SO_4 , filtered, and concentrated *in vacuo* to afford the pure product as a colourless solid (1.42 g, 4.65 mmol, 93%).

^1H NMR (400 MHz, DMSO- d_6): δ 12.53 (s, 1H), 10.82 (s, 1H), 7.52 (d, $J = 7.9$ Hz, 1H), 7.33 (d, $J = 7.9$ Hz, 1H), 7.14 (d, $J = 2.4$ Hz, 1H), 7.10 – 7.02 (m, 1H), 7.02 – 6.91 (m, 2H), 4.15 (td, $J = 8.8, 4.8$ Hz, 1H), 3.13 (dd, $J = 14.6, 4.8$ Hz, 1H), 2.97 (dd, $J = 14.6, 9.3$ Hz, 1H), 1.33 (s, 9H).

$^{13}\text{C}\{^1\text{H}\}$ NMR (101 MHz, DMSO- d_6): δ 174.0, 155.4, 136.1, 127.2, 123.6, 120.9, 118.3, 118.1, 111.4, 110.2, 78.0, 54.5, 28.2, 26.8.

Step 2: According to the literature procedure,²⁶⁷ the *N*-Boc tryptophan (1.22 g, 4.0 mmol) was transferred to a Schlenk flask under an atmosphere of dinitrogen, and dissolved in anhydrous DMF (25 mL). $t\text{BuOK}$ (943 mg, 8.4 mmol) was added in one portion at rt and stirred for

5 mins until all solids fully dissolved. The reaction mixture was cooled to 0 °C and BnCl (0.65 mL, 5.6 mmol) was added drop-wise. The resulting solution was warmed to rt and stirred for 1 hr. The reaction was quenched by addition of 1 M aqueous HCl (10 mL) and then extracted with EtOAc (3 × 20 mL). The combined organics were washed with a 10 wt% aqueous LiCl solution (2 × 30 mL) and dried over Na₂SO₄, filtered, and concentrated *in vacuo*. Purification by column chromatography (silica gel; 0-40% EtOAc in CyH with 1% AcOH) afforded the product as a colourless solid (1.32 g, 3.34 mmol, 83%).

¹H NMR (400 MHz, DMSO-*d*₆): δ 12.57 (s, 1H), 7.56 (d, *J* = 7.7 Hz, 1H), 7.38 (d, *J* = 8.1 Hz, 1H), 7.34 – 7.20 (m, 4H), 7.19 – 7.12 (m, 2H), 7.09 (app t, *J* = 7.7 Hz, 1H), 7.05 – 6.96 (m, 2H), 5.37 (s, 2H), 4.18 (td, *J* = 8.8, 4.8 Hz, 1H), 3.16 (dd, *J* = 14.6, 4.7 Hz, 1H), 3.00 (dd, *J* = 14.6, 9.3 Hz, 1H), 1.33 (s, 9H).

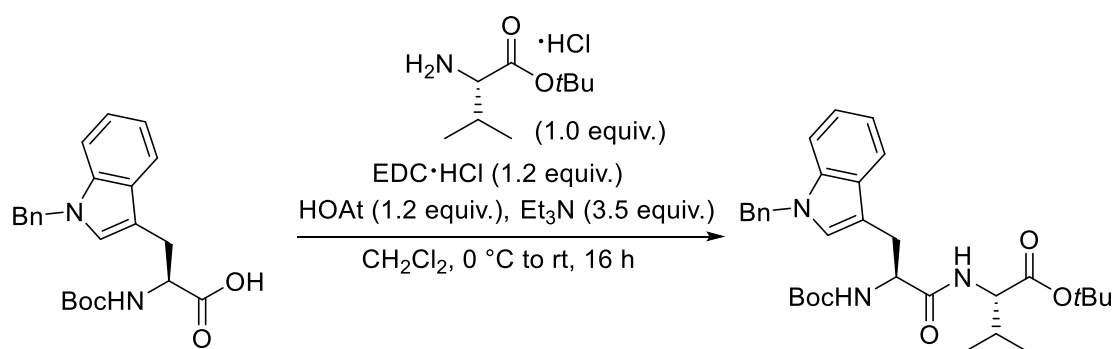
¹³C{¹H} NMR (101 MHz, DMSO-*d*₆): δ 173.8, 155.4, 138.3, 135.9, 128.4, 127.8, 127.4, 127.2, 126.9, 121.2, 118.7, 118.6, 110.3, 110.1, 78.0, 54.5, 48.9, 28.2, 26.7.

ν_{max} (neat) / cm⁻¹: 1711, 1657, 1494, 1467, 1453, 1392, 1366, 1250, 1156, 1054, 1014, 736.

HRMS: calcd. for C₂₃H₂₇N₂O₄ [M+H]⁺: 395.1965; found (ESI⁺): 395.1957.

m.p. / °C: 123-127.

***tert*-Butyl 1-benzyl-N^α-Boc-tryptophylvalinate (101)**



To a suspension of valine *tert*-butyl ester hydrochloride (419 mg, 2.0 mmol) in CH₂Cl₂ (20 mL) at 0 °C was added sequentially Et₃N (0.98 mL, 7.0 mmol), HOAt (327 mg, 2.4 mmol), and N^α-Boc-1-benzyltryptophan (789 mg, 2.0 mmol) which was stirred until homogenous. EDC·HCl (460 mg, 2.4 mmol) was then added and the reaction mixture warmed to rt and stirred overnight. The reaction was quenched by addition of 1 M HCl (10 mL) and extracted with CH₂Cl₂ (3 × 10 mL). The combined organics were washed with sat. aqueous NaHCO₃ (50 mL) and the new aqueous layer extracted with CH₂Cl₂ (3×10 mL). The combined organics

were dried over MgSO₄, filtered, and concentrated *in vacuo*. Purification by column chromatography (silica gel; 0-5% MeOH in CH₂Cl₂) afforded the pure product as a white solid (913 mg, 1.66 mmol, 83%).

¹H NMR (400 MHz, DMSO-d₆): δ 7.93 (d, *J* = 8.4 Hz, 1H), 7.63 (d, *J* = 7.8 Hz, 1H), 7.38 (d, *J* = 8.1 Hz, 1H), 7.32 – 7.21 (m, 4H), 7.19 – 7.13 (m, 2H), 7.12 – 7.05 (m, 1H), 7.02 (app t, *J* = 7.4 Hz, 1H), 6.85 (d, *J* = 8.6 Hz, 1H), 5.36 (s, 2H), 4.34 (td, *J* = 9.0, 4.4 Hz, 1H), 4.14 (dd, *J* = 8.3, 5.7 Hz, 1H), 3.11 (dd, *J* = 14.7, 4.4 Hz, 1H), 2.95 (dd, *J* = 14.7, 9.6 Hz, 1H), 2.07 (sept, *J* = 6.6 Hz, 1H), 1.42 (s, 9H), 1.30 (s, 9H), 0.91 (d, *J* = 6.6 Hz, 5H), 0.89 (d, *J* = 6.6 Hz, 2H).

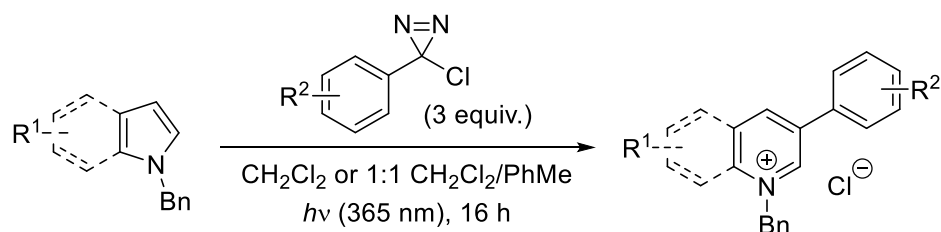
¹³C{¹H} NMR (101 MHz, DMSO-d₆): δ 172.0, 170.5, 155.1, 138.3, 135.9, 128.4, 128.0, 127.4, 127.2, 126.9, 121.1, 118.9, 118.5, 110.4, 109.9, 80.7, 78.0, 57.6, 48.9, 30.3, 28.1, 27.6, 18.8, 17.9.

ν_{max} (neat) / cm⁻¹: 2970, 2930, 1724, 1716, 1654, 1520, 1495, 1467, 1390, 1520, 1219, 1144, 735.

HRMS: calcd. for C₃₂H₄₄N₃O₅ [M+H]⁺: 550.3275; found (ESI⁺): 550.3273.

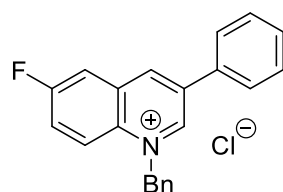
m.p. / °C: 61-63.

5.3.3 General Procedure 2 (GP-2): Ring expansion of *N*-benzylindoles



A 10 mL microwave tube was charged with *N*-benzylindole (0.2 mmol) which was then sealed, evacuated and flushed with dinitrogen 3 times. Anhydrous CH_2Cl_2 or a 1:1 v/v mixture of anhydrous $\text{CH}_2\text{Cl}_2/\text{PhMe}$ (2 mL) was then added followed by 3-chloro-3-aryldiazirine (0.6 mmol unless specified). The cap of the reaction flask was then sealed with electrical tape. The reaction mixture was stirred under constant irradiation with UV light (365 nm, 18 W LED, 5 cm from light source) overnight. Unless specified, the resulting precipitate was isolated by filtration and washed with PhMe (2×5 mL) to afford the pure product.

1-Benzyl-6-fluoro-3-phenylquinolin-1-ium chloride (13)



Synthesised according to **GP-2** from *N*-benzyl-5-fluoroindole (45 mg, 0.2 mmol) and 3-chloro-3-phenyldiazirine (92 mg, 0.6 mmol) in CH_2Cl_2 (2 mL) as an off-white solid (57.3 mg, 0.164 mmol, 82%).

^1H NMR (400 MHz, CD_3OD): δ 10.01 (d, $J = 2.0$ Hz, 1H), 9.53 (d, $J = 2.0$ Hz, 1H), 8.56 (dd, $J = 9.7, 4.3$ Hz, 1H), 8.23 (dd, $J = 8.0, 2.9$ Hz, 1H), 8.04–7.94 (m, 3H), 7.72–7.56 (m, 3H), 7.49–7.33 (m, 5H), 6.46 (s, 2H).

$^{13}\text{C}\{^1\text{H}\}$ NMR (101 MHz, CD_3OD): δ 163.4 (d, $J = 254.8$ Hz), 149.9, 145.2 (d, $J = 5.3$ Hz), 137.6, 135.6, 134.7, 134.5, 133.7 (d, $J = 11.0$ Hz), 131.5, 130.9, 130.6, 130.4, 128.8, 128.3, 126.5 (d, $J = 27.0$ Hz), 123.6 (d, $J = 9.5$ Hz), 115.5 (d, $J = 23.3$ Hz), 62.9.

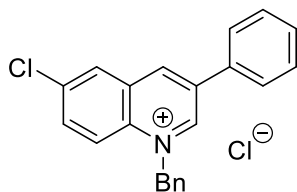
^{19}F NMR (376 MHz, CD_3OD): δ -108.40 (app td, $J = 8.0, 4.3$ Hz).

ν_{max} (neat) / cm^{-1} : 3025, 2941, 1584, 1492, 1454, 1364.

HRMS: calcd. for $\text{C}_{22}\text{H}_{17}\text{FN}$ $[\text{M}-\text{Cl}]^+$: 314.1340; found (ESI $^+$): 314.1351.

m.p. / °C: 256-258.

1-Benzyl-6-chloro-3-phenylquinolin-1-ium chloride (23)



Synthesised according to **GP-2** from *N*-benzyl-5-chloroindole (48 mg, 0.2 mmol) 3-chloro-3-phenyldiazirine (153 mg, 1.0 mmol) in CH₂Cl₂ (2 mL) as an off-white solid (52.1 mg, 0.142 mmol, 71%).

¹H NMR (400 MHz, CD₃OD): δ 10.03 (d, *J* = 2.0 Hz, 1H), 9.52 (d, *J* = 2.0 Hz, 1H), 8.58 (dd, *J* = 2.4 Hz, 1H), 8.49 (dd, *J* = 9.5 Hz, 1H), 8.14 (m, 3H), 8.05–7.97 (m, 2H), 7.73–7.61 (m, 3H), 7.51–7.35 (m, 3H), 6.45 (s, 2H).

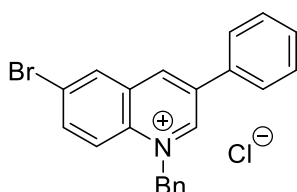
¹³C{¹H} NMR (101 MHz, CD₃OD): δ 150.5, 144.9, 137.8, 137.7, 137.1, 137.0, 134.7, 134.4, 132.9, 131.5, 131.0, 130.7, 130.7, 130.5, 128.8, 128.3, 122.3, 62.8.

ν_{max} (neat) / cm⁻¹: 2925, 1523, 1492, 1376, 1357, 1096, 909, 833.

HRMS: calcd. for C₂₂H₁₇N³⁵Cl [M-Cl]⁺: 330.1044; found (ESI⁺): 330.1048.

m.p. / °C: 247-251.

1-Benzyl-6-bromo-3-phenylquinolin-1-ium chloride (24)



Synthesised according to **GP-2** from *N*-benzyl-5-bromoindole (57 mg, 0.2 mmol) and 3-chloro-3-phenyldiazirine (153 mg, 1.0 mmol) in CH₂Cl₂ (2 mL) as an off-white solid (47.3 mg, 0.115 mmol, 58%).

¹H NMR (400 MHz, CD₃OD): δ 10.03 (d, *J* = 2.0 Hz, 1H), 9.51 (d, *J* = 2.0 Hz, 1H), 8.75 (d, *J* = 2.2 Hz, 1H), 8.40 (d, *J* = 9.5 Hz, 1H), 8.26 (dd, *J* = 9.4, 2.2 Hz, 1H), 8.05 – 7.93 (m, 2H), 7.73 – 7.59 (m, 3H), 7.51 – 7.37 (m, 5H), 6.44 (s, 2H).

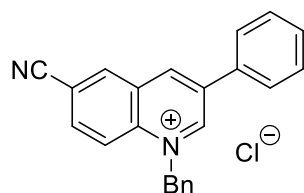
$^{13}\text{C}\{^1\text{H}\}$ NMR (101 MHz, CD_3OD): δ 150.6, 144.8, 139.6, 137.8, 137.3, 134.7, 134.4, 134.1, 133.2, 131.5, 131.0, 130.7, 130.5, 128.8, 128.3, 125.7, 122.1, 62.7.

ν_{max} (neat) / cm^{-1} : 3017, 2922, 1521, 1491, 1452, 1375, 1354, 833.

HRMS: calcd. for $\text{C}_{22}\text{H}_{17}\text{N}^{79}\text{Br}$ $[\text{M}-\text{Cl}]^+$: 374.0539; found (ESI $^+$): 374.0542.

m.p. / $^{\circ}\text{C}$: 236-238.

1-Benzyl-6-cyano-3-phenylquinolin-1-ium chloride (25)



Synthesised according to **GP-2** from *N*-benzylindole-5-carbonitrile (50 mg, 0.2 mmol) and 3-chloro-3-phenyldiazirine (92 mg, 0.6 mmol) in CH_2Cl_2 (2 mL) as an off-white solid (39.8 mg, 0.111 mmol, 56%).

^1H NMR (400 MHz, CD_3OD): δ 10.19 (d, $J = 2.1$ Hz, 1H), 9.68 (d, $J = 2.1$ Hz, 1H), 9.01 (d, $J = 1.9$ Hz, 1H), 8.64 (d, $J = 9.3$ Hz, 1H), 8.35 (dd, $J = 9.3, 1.9$ Hz, 1H), 8.08 – 7.99 (m, 2H), 7.77 – 7.60 (m, 3H), 7.44 (m, 5H), 6.50 (s, 2H).

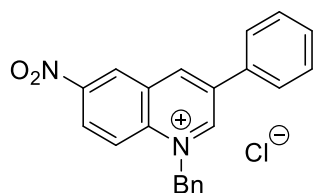
$^{13}\text{C}\{^1\text{H}\}$ NMR (101 MHz, CD_3OD): δ 152.9, 146.3, 139.5, 138.3, 138.1, 136.9, 134.4, 134.2, 131.7, 131.6, 131.0, 130.7, 130.6, 128.8, 128.4, 122.0, 117.6, 115.6, 62.9.

ν_{max} (neat) / cm^{-1} : 2925, 1529, 1492, 1360, 836.

HRMS: calcd. for $\text{C}_{23}\text{H}_{17}\text{N}_2$ $[\text{M}-\text{Cl}]^+$: 341.1285; found (ESI $^+$): 341.1284.

m.p. / $^{\circ}\text{C}$: 234-237.

1-Benzyl-6-nitro-3-phenylquinolin-1-ium chloride (26)



Synthesised according to **GP-2** from *N*-benzyl-5-nitroindole (50 mg, 0.2 mmol) and 3-chloro-3-phenyldiazirine (153 mg, 1.0 mmol) in CH₂Cl₂ (2 mL) as a yellow solid (19.9 mg, 0.54 mmol, 27%).

¹H NMR (400 MHz, CD₃OD): δ 10.23 (d, *J* = 2.0 Hz, 1H), 9.83 (d, *J* = 2.0 Hz, 1H), 9.46 (d, *J* = 2.5 Hz, 1H), 8.85 (dd, *J* = 9.7, 2.5 Hz, 1H), 8.71 (d, *J* = 9.7 Hz, 1H), 8.07–8.01 (m, 2H), 7.77–7.62 (m, 3H), 7.49–7.40 (m, 5H), 6.52 (s, 2H).

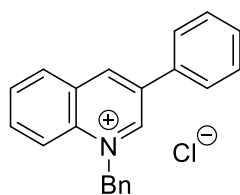
¹³C{¹H} NMR (101 MHz, CD₃OD): δ 153.3, 149.0, 147.5, 140.3, 138.5, 134.3, 134.2, 131.9, 131.8, 131.0, 130.7, 130.6, 129.4, 128.9, 128.4, 128.1, 122.7, 63.2.

ν_{max} (neat) / cm⁻¹: 3002, 2924, 1631, 1609, 1345, 1184, 823.

HRMS: calcd. for C₂₂H₁₇N₂O₂ [M-Cl]⁺: 341.1285; found (ESI⁺): 341.1284.

m.p. / °C: 229-230.

1-Benzyl-3-phenylquinolin-1-ium chloride (29)



Synthesised according to **GP-2** from *N*-benzylindole (41 mg, 0.2 mmol) and 3-chloro-3-phenyldiazirine (92 mg, 0.6 mmol) in 1:1 CH₂Cl₂/PhMe (2 mL) as an off-white solid (46.4 mg, 0.140 mmol, 70%).

¹H NMR (400 MHz, CD₃OD): δ 10.00 (d, *J* = 2.1 Hz, 1H), 9.57 (d, *J* = 1.6 Hz, 1H), 8.48 (dd, *J* = 8.7, 1.2 Hz, 1H), 8.16 (ddd, *J* = 8.7, 7.0, 1.6 Hz, 1H), 8.06–7.95 (m, 3H), 7.71–7.56 (m, 3H), 7.47–7.34 (m, 5H), 6.45 (s, 2H).

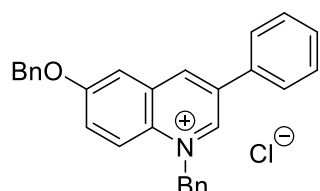
¹³C{¹H} NMR (101 MHz, CD₃OD): δ 150.1, 146.0, 138.5, 136.9, 136.7, 135.0, 134.7, 132.4, 132.1, 131.7, 131.2, 130.9, 130.6, 130.3, 128.8, 128.2, 120.2, 62.5.

ν_{\max} (neat) / cm^{-1} : 2941, 1584, 1528, 1492, 1364.

HRMS: calcd. for $\text{C}_{22}\text{H}_{18}\text{N}$ $[\text{M}-\text{Cl}]^+$: 296.1434; found (ESI⁺): 296.1428.

m.p. / $^{\circ}\text{C}$: 229-231.

1-Benzyl-6-(benzyloxy)-3-phenylquinolin-1-ium chloride (30)



Synthesised according to **GP-2** from *N*-benzyl-5benzyloxyindole (62 mg, 0.2 mmol) and 3-chloro-3-phenyldiazirine (92 mg, 0.6 mmol) in 1:1 $\text{CH}_2\text{Cl}_2/\text{PhMe}$ (2 mL) as a yellow solid (66.2 mg, 0.151 mmol, 76%).

¹H NMR (400 MHz, CD₃OD): δ 9.78 (d, $J = 2.0$ Hz, 1H), 9.38 (d, $J = 2.0$ Hz, 1H), 8.38 (d, $J = 9.7$ Hz, 1H), 8.00-7.94 (m, 2H), 7.92 (d, $J = 2.8$ Hz, 1H), 7.83 (dd, $J = 9.7, 2.8$ Hz, 1H), 7.70–7.57 (m, 2H), 7.54–7.48 (m, 2H), 7.46–7.31 (m, 8H), 6.38 (s, 2H), 5.36 (s, 2H).

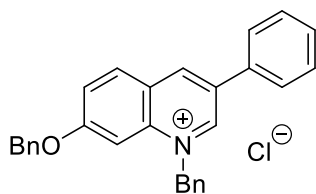
¹³C{¹H} NMR (101 MHz, CD₃OD): δ 160.8, 147.0, 144.1, 137.1, 137.0, 135.2, 134.8, 134.3, 134.2, 131.2, 130.9, 130.6, 130.3, 129.8, 129.5, 129.0, 128.7, 128.1, 121.8, 110.5, 72.1, 62.5.

ν_{\max} (neat) / cm^{-1} : 3030, 2947, 1612, 1531, 1453, 1397, 1272, 1212, 1153.

HRMS: calcd. for $\text{C}_{29}\text{H}_{24}\text{NO}$ $[\text{M}-\text{Cl}]^+$: 402.1853; found (ESI⁺): 402.1868.

m.p. / $^{\circ}\text{C}$: 200-203.

1-Benzyl-7-(benzyloxy)-3-phenylquinolin-1-ium chloride (31)



Synthesised according to **GP-2** from *N*-benzyl-6methoxyindole (62 mg, 0.2 mmol) and 3-chloro-3-phenyldiazirine (92 mg, 0.6 mmol) in 1:1 $\text{CH}_2\text{Cl}_2/\text{PhMe}$ (2 mL) as a yellow solid (62.7 mg, 0.143 mmol, 72%).

¹H NMR (400 MHz, CD₃OD): δ 9.81 (d, *J* = 2.0 Hz, 1H), 9.43 (d, *J* = 2.0 Hz, 1H), 8.49 – 8.29 (m, 1H), 8.00 – 7.87 (m, 2H), 7.74 – 7.62 (m, 4H), 7.61 – 7.55 (m, 1H), 7.47 – 7.31 (m, 10H), 6.35 (s, 2H), 5.32 (s, 2H).

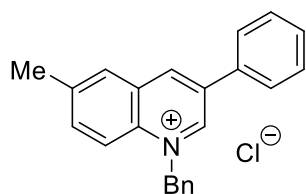
¹³C{¹H} NMR (101 MHz, CD₃OD): δ 166.1, 148.4, 145.2, 141.1, 136.5, 135.2, 134.6, 134.2, 134.0, 130.8, 130.7, 130.3, 129.9, 129.7, 128.9, 128.5, 128.2, 127.8, 124.7, 100.8, 72.5, 62.1, 49.6.

ν_{max} (neat) / cm⁻¹: 2960, 1630, 1607, 1496, 1454, 1383, 1269, 1201, 1020, 837.

HRMS: calcd. for C₂₉H₂₄NO [M-Cl]⁺: 402.1853; found (ESI⁺): 402.1847.

m.p. / °C: 212-214.

1-Benzyl-6-methyl-3-phenylquinolin-1-ium chloride (32)



Synthesised according to **GP-2** from N-benzyl-5-methylindole (44 mg, 0.2 mmol) and 3-chloro-3-phenyldiazirine (92 mg, 1.0 mmol) in 1:1 CH₂Cl₂/PhMe (2 mL) as an off-white solid (50.5 mg, 0.163 mmol, 81%).

¹H NMR (400 MHz, CD₃OD): δ 9.93 (d, *J* = 2.1 Hz, 1H), 9.47 (dd, *J* = 2.1, 0.9 Hz, 1H), 8.37 (d, *J* = 9.1 Hz, 1H), 8.29 (t, *J* = 1.5 Hz, 1H), 8.01 (app td, *J* = 8.6, 8.0, 1.5 Hz, 3H), 7.73 – 7.55 (m, 3H), 7.48 – 7.33 (m, 5H), 6.44 (s, 2H), 2.67 (s, 3H).

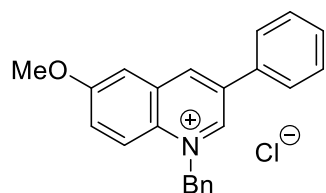
¹³C{¹H} NMR (101 MHz, CD₃OD): δ 148.9, 145.1, 143.0, 139.0, 137.1, 136.61, 135.1, 134.8, 132.3, 131.2, 130.9, 130.8, 130.3, 128.7, 128.2, 119.9, 62.4, 21.3.

ν_{max} (neat) / cm⁻¹: 2935, 1535, 1493, 1384, 1362, 817.

HRMS: calcd. for C₂₃H₂₀N [M-Cl]⁺: 310.1590; found (ESI⁺): 310.1595.

m.p. / °C: 236-238.

1-Benzyl-6-methoxy-3-phenylquinolin-1-ium chloride (33)



Synthesised according to **GP-2** from *N*-benzyl-5-methoxyindole (47 mg, 0.2 mmol) and 3-chloro-3-phenyldiazirine (92 mg, 0.6 mmol) in 1:1 CH₂Cl₂/PhMe (2 mL) as a red solid (42.2 mg, 0.117 mmol, 58%).

¹H NMR (400 MHz, CD₃OD): δ 9.80 (d, *J* = 2.0 Hz, 1H), 9.41 (dd, *J* = 2.0, 0.9 Hz, 1H), 8.38 (dd, *J* = 9.7, 0.9 Hz, 1H), 8.04–7.95 (m, 2H), 7.86 (d, *J* = 2.9 Hz, 1H), 7.77 (dd, *J* = 9.7, 2.9 Hz, 1H), 7.71–7.59 (m, 3H), 7.49–7.33 (m, 5H), 6.40 (s, 2H), 4.07 (s, 3H).

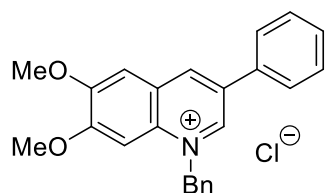
¹³C{¹H} NMR (101 MHz, CD₃OD): δ 161.9, 146.8, 144.0, 137.0, 135.2, 134.8, 134.3, 131.2, 130.9, 130.6, 130.3, 129.5, 129.5, 128.7, 128.1, 121.7, 109.2, 62.5, 57.0.

ν_{max} (neat) / cm⁻¹: 2946, 1621, 1534, 1492, 1464, 1398, 1273, 1215.

HRMS: calcd. for C₂₃H₂₀NO [M-Cl]⁺: 326.1539; found (ESI⁺): 326.1536.

m.p. / °C: 225-228.

1-Benzyl-6,7-dimethoxy-3-phenylquinolin-1-ium chloride (34)



Synthesised according to **GP-2** from *N*-benzyl-5,6-dimethoxyindole (53 mg, 0.2 mmol) and 3-chloro-3-phenyldiazirine (92 mg, 0.6 mmol) in 1:1 CH₂Cl₂/PhMe (2 mL) as a yellow solid (58.5 mg, 0.150 mmol, 75%).

¹H NMR (400 MHz, CD₃OD): δ 9.64 (d, *J* = 1.9 Hz, 1H), 9.29 (d, *J* = 1.9 Hz, 1H), 8.00 – 7.86 (m, 2H), 7.80 (s, 1H), 7.69 – 7.62 (m, 2H), 7.62 – 7.55 (m, 2H), 7.49 – 7.39 (m, 5H), 6.38 (s, 2H), 4.09 (s, 3H), 4.01 (s, 3H).

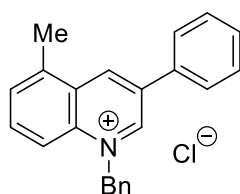
¹³C{¹H} NMR (101 MHz, CD₃OD): δ 159.1, 153.9, 144.8, 142.7, 136.6, 135.5, 134.8, 134.6, 130.8, 130.8, 130.6, 130.3, 129.1, 128.5, 128.4, 108.7, 99.5, 62.3, 57.7, 57.2.

ν_{\max} (neat) / cm^{-1} : 2954, 1626, 1508, 1427, 1281, 1256, 1230, 990.

HRMS: calcd. for $\text{C}_{24}\text{H}_{22}\text{NO}_2$ $[\text{M}-\text{Cl}]^+$: 356.1645; found (ESI⁺): 356.1647.

m.p. / °C: 211-212.

1-Benzyl-5-methyl-3-phenylquinolin-1-ium chloride (35)



Synthesised according to **GP-2** from *N*-benzyl-4-methylindole (44 mg, 0.2 mmol) and 3-chloro-3-phenyldiazirine (92 mg, 0.6 mmol) in 1:1 $\text{CH}_2\text{Cl}_2/\text{PhMe}$ (2 mL) as an amber solid (24.4 mg, 0.071 mmol, 35%).

¹H NMR (400 MHz, CD_3OD): δ 9.99 (d, $J = 1.9$ Hz, 1H), 9.57 (d, $J = 1.9$ Hz, 2H), 8.31 (d, $J = 9.1$ Hz, 8H), 8.07 – 7.97 (m, 3H), 7.87 (d, $J = 7.2$ Hz, 1H), 7.75 – 7.57 (m, 3H), 7.51 – 7.34 (m, 5H), 6.45 (s, 1H), 3.00 (s, 3H).

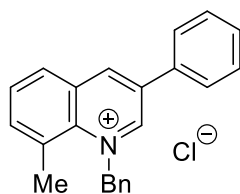
¹³C{¹H} NMR (101 MHz, CD_3OD): δ 152.3, 147.2, 142.0, 139.8, 137.0, 135.9, 134.5, 134.0, 131.9, 131.4, 131.3, 130.9, 130.7, 130.5, 129.9, 128.5, 126.6, 65.3, 24.5.

ν_{\max} (neat) / cm^{-1} : 2946, 1587, 1491, 1434, 1367, 1343.

HRMS: calcd. for $\text{C}_{23}\text{H}_{20}\text{N}$ $[\text{M}-\text{Cl}]^+$: 310.1590; found (ESI⁺): 310.1595.

m.p. / °C: 214-216.

1-Benzyl-8-methyl-3-phenylquinolin-1-ium chloride (36)



Synthesised according to **GP-2** from *N*-benzyl-7-methylindole (44 mg, 0.2 mmol) and 3-chloro-3-phenyldiazirine (92 mg, 0.6 mmol) in 1:1 $\text{CH}_2\text{Cl}_2/\text{PhMe}$ (2 mL) as an amber solid (23.4 mg, 0.068 mmol, 34%).

¹H NMR (400 MHz, CD₃OD): δ 9.99 (d, *J* = 2.0 Hz, 1H), 9.57 (dd, *J* = 2.0, 1.0 Hz, 1H), 8.31 (d, *J* = 9.0 Hz, 1H), 8.08 – 7.97 (m, 3H), 7.88 (dt, *J* = 7.1, 1.0 Hz, 1H), 7.73 – 7.66 (m, 2H), 7.66 – 7.60 (m, 1H), 7.47 – 7.35 (m, 5H), 6.45 (s, 2H), 3.00 (s, 3H).

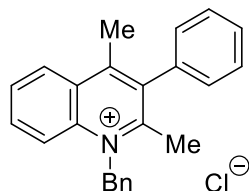
¹³C{¹H} NMR (101 MHz, CD₃OD): δ 149.5, 142.6, 140.9, 139.1, 136.6, 136.2, 135.4, 134.9, 132.1, 131.5, 131.1, 130.9, 130.6, 130.3, 129.0, 128.1, 118.2, 62.8, 19.2.

ν_{max} (neat) / cm⁻¹: 3031, 2957, 1533, 1494, 1451, 1352, 1231, 1170, 1022, 967, 818.

HRMS: calcd. for C₂₃H₂₀N [M-Cl]⁺: 310.1590; found (ESI⁺): 310.1587.

m.p. / °C: 158-161.

1-Benzyl-2,4-dimethyl-3-phenylquinolin-1-ium chloride (37)



Synthesised according to **GP-2** from *N*-benzyl-7methylindole (47 mg, 0.2 mmol) and 3-chloro-3-phenyldiazirine (92 mg, 0.6 mmol) in 1:1 CH₂Cl₂/PhMe (2 mL). The solvent was removed *in vacuo* and the product triturated from PhMe to afford the product as a brown solid (42.3 mg, 0.118 mmol, 59%).

¹H NMR (400 MHz, CD₃OD): δ 8.64 (dd, *J* = 8.5, 1.5 Hz, 1H), 8.37 (d, *J* = 8.9 Hz, 1H), 8.14 (ddd, *J* = 8.9, 7.0, 1.5 Hz, 1H), 8.03 (ddd, *J* = 8.2, 7.0, 1.0 Hz, 1H), 7.73 – 7.55 (m, 3H), 7.48 – 7.33 (m, 6H), 7.23 – 7.12 (m, 2H), 6.38 (s, 2H), 2.77 (s, 3H), 2.75 (s, 3H).

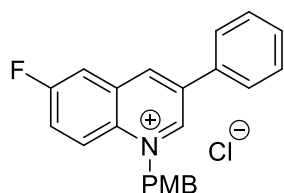
¹³C{¹H} NMR (101 MHz, CD₃OD): δ 160.7, 157.6, 139.0, 137.4, 136.3, 134.2, 130.8, 130.5, 129.7, 128.6, 126.7, 120.7, 56.8, 22.0, 18.9.

ν_{max} (neat) / cm⁻¹: 3032, 1579, 1510, 1494, 1446, 1346, 1163.

HRMS: calcd. for C₂₄H₂₂N [M-Cl]⁺: 324.1747; found (ESI⁺): 324.1751.

m.p. / °C: 94 (decomp.).

1-(4-methoxybenzyl)-6-fluoro-3-phenylquinolin-1-ium chloride (38)



Synthesised according to **GP-2** from *N*-(4-methoxybenzyl)-5-fluoroindole (51 mg, 0.2 mmol) and 3-chloro-3-phenyldiazirine (92 mg, 0.6 mmol) in 1:1 CH₂Cl₂/PhMe (2 mL) as a yellow solid (40.4 mg, 0.106 mmol, 53%).

¹H NMR (400 MHz, CD₃OD): δ 9.92 (d, *J* = 1.8 Hz, 1H), 9.50 (d, *J* = 1.8 Hz, 1H), 8.64 (dd, *J* = 9.7, 4.3 Hz, 1H), 8.22 (dd, *J* = 8.0, 2.8 Hz, 1H), 8.03 (ddd, *J* = 9.7, 8.1, 2.8 Hz, 1H), 7.99 – 7.94 (m, 2H), 7.66 (m, 2H), 7.41 (d, *J* = 8.8 Hz, 2H), 7.00 (d, *J* = 8.8 Hz, 1H), 6.36 (s, 2H), 3.80 (s, 3H).

¹⁹F NMR (376 MHz, CD₃OD): δ -108.48 (td, *J* = 8.0, 4.3 Hz).

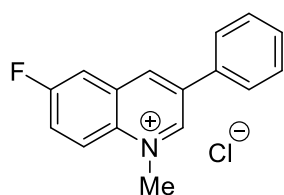
¹³C{¹H} NMR (101 MHz, CD₃OD): δ 164.6 (d, *J* = 254.5 Hz), 162.1, 149.4 (d, *J* = 1.2 Hz), 145.0 (d, *J* = 5.3 Hz), 137.5, 135.6, 134.8, 133.7 (d, *J* = 10.9 Hz), 131.4, 131.0, 130.3, 128.8, 126.4 (d, *J* = 26.9 Hz), 125.9, 123.6 (d, *J* = 9.5 Hz), 116.0, 115.4 (d, *J* = 23.2 Hz), 62.6, 55.9.

ν_{\max} (neat) / cm⁻¹:

HRMS: calcd. for C₂₃H₁₉FNO [M-Cl]⁺: 344.1445; found (ESI⁺): 344.1444.

m.p. / °C: 183-185.

1-Methyl-6-fluoro-3-phenylquinolin-1-ium chloride (39)



Synthesised according to **GP-2** from *N*-methyl-5-fluoroindole (30 mg, 0.2 mmol) and 3-chloro-3-phenyldiazirine (92 mg, 0.6 mmol) in 1:1 CH₂Cl₂/PhMe (2 mL) as a colourless solid (22.3 mg, 0.082 mmol, 41%).

¹H NMR (400 MHz, CD₃OD): δ 9.81 (d, *J* = 2.0 Hz, 1H), 9.45 (d, *J* = 2.0 Hz, 1H), 8.64 (dd, *J* = 9.7, 4.3 Hz, 1H), 8.22 (dd, *J* = 8.0, 2.8 Hz, 1H), 8.13 (ddd, *J* = 9.7, 8.0, 2.9 Hz, 1H), 8.04 – 7.94 (m, 2H), 7.78 – 7.57 (m, 3H), 4.81 (s, 3H).

¹³C{¹H} NMR (101 MHz, CD₃OD): δ 163.5 (d, *J* = 254.2 Hz), 150.2, 144.0 (d, *J* = 5.3 Hz), 137.3, 136.3, 134.8, 132.9 (d, *J* = 10.9 Hz), 131.3, 130.9, 128.7, 126.3 (d, *J* = 26.9 Hz), 123.1 (d, *J* = 9.6 Hz), 115.0 (d, *J* = 23.2 Hz), 46.7.

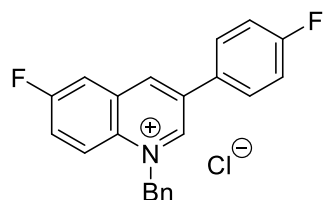
¹⁹F NMR (376 MHz, CD₃OD): δ -108.88 (app td, *J* = 8.0, 4.3 Hz).

***v*_{max} (neat) / cm⁻¹:** 3034, 2961, 1617, 1535, 1389, 1272, 1231, 1173, 967, 814.

HRMS: calcd. for C₁₆H₁₃FN [M-Cl]⁺: 238.1027; found (ESI⁺): 238.1033.

m.p. / °C: 240 (decomp.).

1-Benzyl-6-fluoro-3-(4-fluorophenyl)quinolin-1-ium chloride (71)



Synthesised according to **GP-2** from *N*-benzyl-5-fluoroindole (45 mg, 0.2 mmol) and 3-chloro-3-(4-fluorophenyl)diazirine (102 mg, 0.6 mmol) in 1:1 CH₂Cl₂/PhMe (2 mL) as an offwhite solid (52.9 mg, 0.144 mmol, 72%).

¹H NMR (400 MHz, CD₃OD): δ 10.02 (d, *J* = 2.0 Hz, 1H), 9.52 (d, *J* = 2.0 Hz, 1H), 8.56 (dd, *J* = 9.7, 4.4 Hz, 1H), 8.23 (dd, *J* = 8.2, 2.9 Hz, 1H), 8.12 – 7.90 (m, 4H), 7.43 (m, 10H), 6.46 (s, 2H).

¹³C{¹H} NMR (101 MHz, CD₃OD): δ 165.7 (d, *J* = 250.4 Hz), 163.4 (d, *J* = 254.5 Hz), 149.9, 145.1 (d, *J* = 5.1 Hz), 136.6, 135.5, 134.5, 133.7 (d, *J* = 10.8 Hz), 131.2 (d, *J* = 8.7 Hz), 130.6, 130.5, 128.2, 126.6 (d, *J* = 27.1 Hz), 123.6 (d, *J* = 9.5 Hz), 117.9 (d, *J* = 22.3 Hz), 115.4 (d, *J* = 23.4 Hz), 63.0.

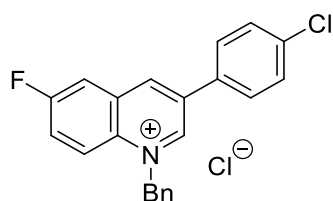
¹⁹F NMR (376 MHz, CD₃OD): -108.26 (app td, *J* = 8.2, 4.5 Hz), -112.71 (app td, *J* = 8.7, 4.4 Hz).

***v*_{max} (neat) / cm⁻¹:** 3004, 2950, 1601, 1513, 1492, 1384, 1245, 1203, 1166, 842.

HRMS: calcd. for C₂₂H₁₆F₂N [M-Cl]⁺: 332.1245; found (ESI⁺): 332.1261.

m.p. / °C: 226-229.

1-Benzyl-6-fluoro-3-(4-bromophenyl)quinolin-1-ium chloride (72)



Synthesised according to **GP-2** from *N*-benzyl-5-fluoroindole (45 mg, 0.2 mmol) and 3-chloro-3-(4-chlorophenyl)diazirine (112 mg, 0.6 mmol) in 1:1 CH₂Cl₂/PhMe (2 mL) as a pale yellow solid (38.9 mg, 0.101 mmol, 51%).

¹H NMR (400 MHz, CD₃OD): δ 10.03 (d, *J* = 2.0 Hz, 1H), 9.55 (d, *J* = 2.0 Hz, 1H), 8.56 (dd, *J* = 9.8, 4.2 Hz, 1H), 8.23 (dd, *J* = 8.1, 2.9 Hz, 1H), 8.05 – 7.98 (m, 3H), 7.73 – 7.67 (m, 2H), 7.42 (m, 5H), 6.46 (s, 2H).

¹³C{¹H} NMR (101 MHz, CD₃OD): δ 163.4 (d, *J* = 255.0 Hz), 149.9, 145.3 (d, *J* = 5.3 Hz), 137.8, 136.4, 135.6, 134.5, 133.7 (d, *J* = 11.1 Hz), 133.4, 131.0, 130.6, 130.4, 128.2, 126.9, 126.6, 123.6 (d, *J* = 9.5 Hz), 115.5 (d, *J* = 23.3 Hz), 63.0.

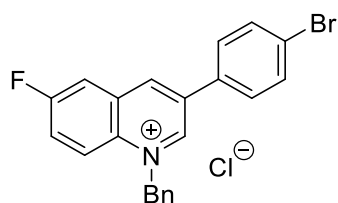
¹⁹F NMR (376 MHz, CD₃OD): δ -108.19 (app td, *J* = 8.1, 4.2 Hz).

ν_{max} (neat) / cm⁻¹: 3027, 2948, 1632, 1536, 1498, 1454, 1384, 1350, 1278, 1213, 1091, 1036, 1010.

HRMS: calcd. for C₂₂H₁₆FN³⁵Cl [M-Cl]⁺: 348.0950; found (ESI⁺): 348.0961.

m.p. / °C: 238-241.

1-Benzyl-6-fluoro-3-(4-bromophenyl)quinolin-1-ium chloride (73)



Synthesised according to **GP-2** from *N*-benzyl-5-fluoroindole (45 mg, 0.2 mmol) and 3-chloro-3-(4-bromophenyl)diazirine (139 mg, 0.6 mmol) in 1:1 CH₂Cl₂/PhMe (2 mL) as a pale yellow solid (76.1 mg, 0.163 mmol, 84%).

¹H NMR (400 MHz, CD₃OD): δ 10.03 (d, *J* = 2.0 Hz, 1H), 9.55 (d, *J* = 2.0 Hz, 1H), 8.56 (dd, *J* = 9.7, 4.4 Hz, 1H), 8.23 (dd, *J* = 8.1, 2.9 Hz, 1H), 8.02 (ddd, *J* = 9.7, 8.1, 2.9 Hz, 1H), 7.97 – 7.90 (m, 2H), 7.90 – 7.81 (m, 2H), 7.51 – 7.36 (m, 5H), 6.45 (s, 2H).

¹³C{¹H} NMR (101 MHz, CD₃OD): δ 163.4 (d, *J* = 255.1 Hz), 149.9, 145.3, 136.4, 135.7, 134.4, 134.1, 133.9, 133.7, 133.6, 130.6 (d, *J* = 5.1 Hz), 130.5, 128.2, 126.8 (d, *J* = 27.0 Hz), 126.0, 123.6 (d, *J* = 9.6 Hz), 115.5 (d, *J* = 23.4 Hz), 63.0.

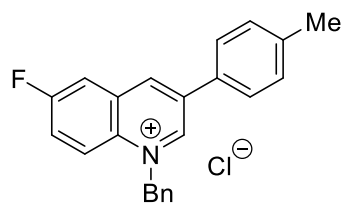
¹⁹F NMR (376 MHz, CD₃OD): δ -108.16 (app td, *J* = 8.1, 4.4 Hz).

ν_{max} (neat) / cm⁻¹: 2947, 1631, 1535, 1491, 1454, 1349, 1278, 1213, 1075, 1004, 827.

HRMS: calcd. for C₂₂H₁₆FN⁷⁹Br [M-Cl]⁺: 392.0445; found (ESI⁺): 392.0439.

m.p. / °C: 239-243.

1-Benzyl-6-fluoro-3-(4-methylphenyl)quinolin-1-ium chloride (74)



Synthesised according to **GP-2** from *N*-benzyl-5-fluoroindole (45 mg, 0.2 mmol) and 3-chloro-3-(4-methylphenyl)diazirine (112 mg, 0.6 mmol) in 1:1 CH₂Cl₂/PhMe (2 mL) as a tan solid (40.0 mg, 0.110 mmol, 55%).

¹H NMR (400 MHz, CD₃OD): δ 9.99 (d, *J* = 2.2 Hz, 1H), 9.50 (d, *J* = 2.2 Hz, 1H), 8.55 (dd, *J* = 9.7, 4.4 Hz, 1H), 8.21 (dd, *J* = 8.2, 3.0 Hz, 1H), 7.99 (ddd, *J* = 10.1, 7.9, 3.0 Hz, 1H), 7.95 – 7.86 (m, 3H), 7.56 – 7.47 (m, 2H), 7.42 (m, 5H), 6.44 (s, 2H), 2.49 (s, 3H).

¹³C{¹H} NMR (101 MHz, CD₃OD): δ 163.4 (d, *J* = 254.8 Hz), 149.8, 144.6 (d, *J* = 5.3 Hz), 142.2, 137.6, 135.4, 134.5, 133.8 (d, *J* = 11.0 Hz), 131.8, 131.6, 130.6, 130.4, 128.6, 128.2, 126.3 (d, *J* = 27.0 Hz), 123.6 (d, *J* = 9.5 Hz), 115.3 (d, *J* = 23.2 Hz), 62.9, 21.3.

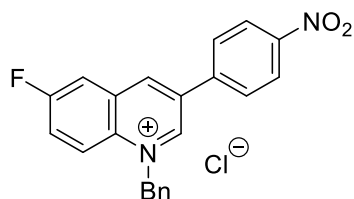
¹⁹F NMR (377 MHz, CD₃OD) δ -108.51 (app td, *J* = 8.2, 4.4 Hz).

ν_{max} (neat) / cm⁻¹: 3030, 2934, 1632, 1535, 1384, 1194, 834, 816.

HRMS: calcd. for C₂₃H₁₉FN [M-Cl]⁺: 328.1496; found (ESI⁺): 328.1506.

m.p. / °C: 231-234.

1-Benzyl-6-fluoro-3-(4-nitrophenyl)quinolin-1-ium chloride (75)



Synthesised according to **GP-2** from *N*-benzyl-5-fluoroindole (45 mg, 0.2 mmol) and 3-chloro-3-(4-nitrophenyl)diazirine (119 mg, 0.6 mmol) in 1:1 CH₂Cl₂/PhMe (2 mL) as a brown solid (35.9 mg, 0.091 mmol, 45%).

¹H NMR (400 MHz, CD₃OD): δ 10.13 (d, *J* = 1.8 Hz, 1H), 9.68 (d, *J* = 1.8 Hz, 1H), 8.60 (dd, *J* = 9.7, 4.2 Hz, 1H), 8.58 – 8.52 (m, 3H), 8.35 – 8.25 (m, 4H), 8.07 (ddd, *J* = 9.7, 7.9, 2.9 Hz, 2H), 7.51 – 7.37 (m, 6H), 6.49 (s, 3H).

¹³C{¹H} NMR (101 MHz, CD₃OD): δ 163.5 (d, *J* = 255.4 Hz), 150.3, 150.2, 146.5 (d, *J* = 5.2 Hz), 140.9, 136.0, 135.3, 134.4, 133.6 (d, *J* = 11.1 Hz), 130.7, 130.5, 130.2, 128.2, 127.4 (d, *J* = 26.9 Hz), 125.7, 123.7 (d, *J* = 9.6 Hz), 115.8 (d, *J* = 23.4 Hz), 63.2.

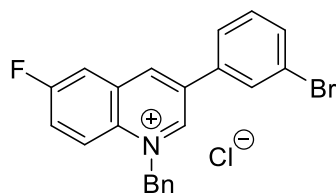
¹⁹F NMR (376 MHz, CD₃OD): δ -107.76 (app td, *J* = 7.9, 4.2 Hz).

ν_{max} (neat) / cm⁻¹: 3084, 2947, 1518, 1345, 830.

HRMS: calcd. for C₂₂H₁₆FN₂O₂ [M-Cl]⁺: 359.1190; found (ESI⁺): 359.1202.

m.p. / °C: 228-231.

1-Benzyl-6-fluoro-3-(3-bromophenyl)quinolin-1-ium chloride (76)



Synthesised according to **GP-2** from *N*-benzyl-5-fluoroindole (45 mg, 0.2 mmol) and 3-chloro-3-(3-bromophenyl)diazirine (139 mg, 0.6 mmol) in 1:1 CH₂Cl₂/PhMe (2 mL) as a brown solid (38.8 mg, 0.090 mmol, 45%).

¹H NMR (400 MHz, CD₃OD): δ 10.06 (d, *J* = 2.0 Hz, 1H), 9.57 (d, *J* = 2.0 Hz, 1H), 8.57 (dd, *J* = 9.7, 4.3 Hz, 1H), 8.26 – 8.22 (m, 2H), 8.04 (dd, *J* = 8.0, 2.9 Hz, 1H), 7.99 (dd, *J* = 8.7,

2.5 Hz, 1H), 7.81 (ddd, $J = 8.0, 2.0, 0.9$ Hz, 1H), 7.61 (app t, $J = 8.0$ Hz, 1H), 7.48 – 7.39 (m, 5H), 6.46 (s, 2H).

$^{13}\text{C}\{^1\text{H}\}$ NMR (101 MHz, CD_3OD): δ 164.7 (d, $J = 255.5$ Hz), 150.1, 145.8, 145.7, 137.0, 136.0, 134.5, 134.4, 133.6 (d, $J = 10.8$ Hz), 132.6, 131.8, 130.6, 130.4, 128.2, 127.7, 126.9 (d, $J = 27.0$ Hz), 124.7, 123.6 (d, $J = 9.6$ Hz), 115.6 (d, $J = 23.2$ Hz), 63.1.

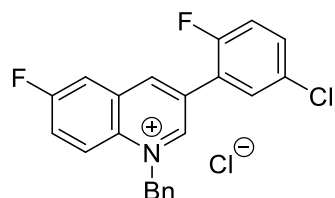
^{19}F NMR (376 MHz, CD_3OD): δ -107.76 (app td, $J = 7.9, 4.3$ Hz).

ν_{max} (neat) / cm^{-1} : 3000, 2933, 1630, 1566, 1535, 1487, 1388, 1275, 1197, 835.

HRMS: calcd. for $\text{C}_{22}\text{H}_{16}\text{FN}^{79}\text{Br}$ $[\text{M}-\text{Cl}]^+$: 392.0445; found (ESI $^+$): 392.0446.

m.p. / $^{\circ}\text{C}$: 196-199.

1-Benzyl-6-fluoro-3-(3-bromophenyl)quinolin-1-ium chloride (77)



Synthesised according to **GP-2** from *N*-benzyl-5-fluoroindole (45 mg, 0.2 mmol) and 3-chloro-3-(5-chloro-2-fluorophenyl)diazirine (123 mg, 0.6 mmol) in 1:1 $\text{CH}_2\text{Cl}_2/\text{PhMe}$ (2 mL) as an orange solid (45.3 mg, 0.113 mmol, 56%).

^1H NMR (400 MHz, CD_3OD): δ 9.93 (s, 1H), 9.53 (s, 1H), 8.63 (dd, $J = 9.8, 4.3$ Hz, 1H), 8.27 (dd, $J = 8.0, 2.9$ Hz, 1H), 8.09 (ddd, $J = 9.8, 8.0, 2.9$ Hz, 1H), 7.98 (dd, $J = 6.7, 2.7$ Hz, 1H), 7.68 (ddd, $J = 8.9, 4.3, 2.7$ Hz, 1H), 7.51 – 7.38 (m, 6H), 6.45 (s, 2H).

$^{13}\text{C}\{^1\text{H}\}$ NMR (101 MHz, CD_3OD): δ 163.5 (d, $J = 255.4$ Hz), 159.8 (d, $J = 249.4$ Hz), 150.8, 148.1, 135.9, 134.2, 133.5 (d, $J = 8.9$ Hz), 133.5 (d, $J = 11.2$ Hz), 131.9, 131.8 (d, $J = 2.4$ Hz), 131.1, 130.7, 130.6, 128.5, 127.4 (d, $J = 27.0$ Hz), 124.5 (d, $J = 14.5$ Hz), 123.7 (d, $J = 9.6$ Hz), 119.4 (d, $J = 24.2$ Hz), 115.8 (d, $J = 23.4$ Hz), 63.0.

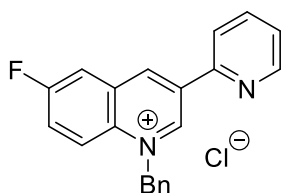
^{19}F NMR (376 MHz, CD_3OD): δ -107.82 (app td, $J = 8.0, 4.3$ Hz), -122.17 (app dt, $J = 10.8, 5.7$ Hz).

ν_{max} (neat) / cm^{-1} : 3047, 3009, 2936, 1633, 1535, 1491, 1387, 1271, 1213, 965, 809.

HRMS: calcd. for $\text{C}_{22}\text{H}_{15}\text{NF}_2^{35}\text{Cl}$ $[\text{M}-\text{Cl}]^+$: 366.0856; found (ESI $^+$): 366.0853.

m.p. / $^{\circ}\text{C}$: 216-219.

1-benzyl-6-fluoro-3-(pyridin-2-yl)quinolin-1-ium chloride (78)



Synthesised according to **GP-2** from *N*-benzyl-5-fluoroindole (45 mg, 0.2 mmol) and 3-chloro-3-(2-pyridyl)diazirine (92 mg, 0.6 mmol) in 1:1 CH₂Cl₂/PhMe (2 mL) as a brown solid (30.7 mg, 0.091 mmol, 45%).

¹H NMR (400 MHz, CD₃OD): δ 10.34 (d, *J* = 1.9 Hz, 1H), 9.86 (d, *J* = 1.9 Hz, 1H), 8.83 (ddd, *J* = 4.9, 1.9, 1.0 Hz, 1H), 8.60 (dd, *J* = 9.7, 4.3 Hz, 1H), 8.34 (dt, *J* = 7.9, 1.0 Hz, 1H), 8.27 (dd, *J* = 8.0, 2.8 Hz, 1H), 8.10 (td, *J* = 7.9, 1.8 Hz, 1H), 8.04 (ddd, *J* = 9.7, 7.9, 2.9 Hz, 1H), 7.59 (ddd, *J* = 7.9, 4.9, 1.0 Hz, 1H), 7.48 – 7.38 (m, 5H), 6.48 (s, 2H).

¹³C{¹H} NMR (101 MHz, CD₃OD): δ 162.0 (d, *J* = 255.2 Hz), 150.2, 150.1, 148.5, 143.5 (d, *J* = 5.1 Hz), 138.1, 134.9, 134.2, 132.9, 132.1 (d, *J* = 11.0 Hz), 129.3, 129.1, 127.2, 125.7, 125.4, 124.9, 122.3 (d, *J* = 9.5 Hz), 121.5, 114.5 (d, *J* = 23.4 Hz), 61.6.

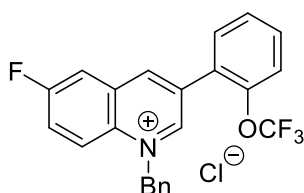
¹⁹F NMR (376 MHz, CD₃OD): δ -108.25 (app td, *J* = 8.0, 4.3 Hz).

ν_{max} (neat) / cm⁻¹: 3002, 2946, 1526, 1384, 1196, 1147.

HRMS: calcd. for C₂₁H₁₆N₂F [M-Cl]⁺: 315.1292; found (ESI⁺) 315.1295.

m.p. / °C: 210 (decomp.).

1-Benzyl-6-fluoro-3-(2-(trifluoromethoxy)phenyl)quinolin-1-ium chloride (79)



Synthesised according to **GP-2** from *N*-benzyl-5-fluoroindole (45 mg, 0.2 mmol) and 3-chloro-3-(2-trifluoromethoxy)diazirine (142 mg, 0.6 mmol) in 1:1 CH₂Cl₂/PhMe (2 mL) as an orange solid (30.0 mg, 0.072 mmol, 36%).

¹H NMR (400 MHz, CD₃OD): δ 9.86 (d, *J* = 1.9 Hz, 1H), 9.45 (d, *J* = 1.9 Hz, 1H), 8.69 (dd, *J* = 9.7, 4.3 Hz, 1H), 8.28 (dd, *J* = 8.0, 2.9 Hz, 1H), 8.11 (ddd, *J* = 9.7, 8.0, 2.9 Hz, 1H), 7.88

(dd, $J = 7.6, 1.8$ Hz, 1H), 7.77 (td, $J = 7.8, 1.8$ Hz, 1H), 7.72 – 7.60 (m, 2H), 7.51 – 7.38 (m, 5H), 6.45 (s, 2H).

$^{13}\text{C}\{^1\text{H}\}$ NMR (101 MHz, CD_3OD): δ 162.1 (d, $J = 255.6$ Hz), 149.6, 146.9, 146.1, 134.4, 132.7, 132.1, 132.1, 132.0 (d, $J = 5.1$ Hz), 131.9, 129.3, 129.3, 128.2, 127.3, 127.1, 126.0 (d, $J = 26.9$ Hz), 122.2 (d, $J = 9.7$ Hz), 121.6, 121.3, 119.1, 114.2 (d, $J = 23.4$ Hz), 61.3.

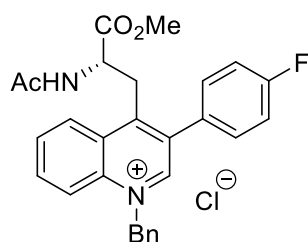
^{19}F NMR (376 MHz, CD_3OD): δ -58.80 (d, $J = 1.6$ Hz), -107.67 (td, $J = 7.9, 4.3$ Hz).

ν_{max} (neat) / cm^{-1} : 2949, 1531, 1252, 1220, 1202, 1160, 1035.

HRMS: calcd. for $\text{C}_{23}\text{H}_{16}\text{F}_4\text{NO}$ $[\text{M}-\text{Cl}]^+$ 398.1163; found (ESI $^+$): 1398.1158.

m.p. / $^{\circ}\text{C}$: 162-164.

Methyl (S)-4-(2-acetamido-3-(4-fluorophenyl)-1-benzyl-3-(4-fluorophenyl)quinolin-1-ium chloride (96)



Synthesised according to **GP-2** from *N*^α-Ac-1-benzyltryptophan methyl ester (70 mg, 0.2 mmol) and 3-chloro-3-(4-fluorophenyl)diazirine (102 mg, 0.6 mmol) in 1:1 $\text{CH}_2\text{Cl}_2/\text{PhMe}$ (2 mL) as an orange solid (69.2 mg, 0.144 mmol, 72%).

^1H NMR (400 MHz, CD_3OD): δ 9.55 (s, 1H), 8.75 (dd, $J = 8.8, 1.4$ Hz, 1H), 8.47 (d, $J = 8.8$ Hz, 1H), 8.18 (ddd, $J = 8.8, 7.0, 1.4$ Hz, 1H), 8.13 – 8.04 (m, 1H), 7.76 – 7.65 (m, 2H), 7.48 – 7.37 (m, 5H), 7.37 – 7.28 (m, 2H), 6.36 (d, $J = 3.4$ Hz, 2H), 4.77 (dd, $J = 9.7, 5.3$ Hz, 1H), 4.01 (dd, $J = 13.7, 5.3$ Hz, 1H), 3.89 (dd, $J = 13.7, 9.7$ Hz, 1H), 3.64 (s, 3H), 1.60 (s, 3H).

$^{13}\text{C}\{^1\text{H}\}$ NMR (101 MHz, CD_3OD): δ 172.7, 171.2, 164.9 (d, $J = 248.7$ Hz), 157.7, 150.6, 138.5, 137.6, 136.4, 134.8, 133.4 (d, $J = 8.6$ Hz), 131.8 (d, $J = 3.4$ Hz), 131.5, 131.4, 130.6, 130.2, 128.8, 127.9, 121.0, 117.4 (d, $J = 22.2$ Hz), 62.1, 53.7, 53.3, 33.4, 28.0, 22.1.

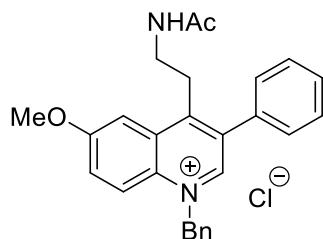
^{19}F NMR (376 MHz, CD_3OD): δ -113.40 (tt, $J = 9.1, 5.3$ Hz).

ν_{max} (neat) / cm^{-1} : 2948, 1727, 1653, 1509, 1371, 1219, 1162, 846.

HRMS: calcd. for $\text{C}_{28}\text{H}_{26}\text{FN}_2\text{O}_3$ $[\text{M}-\text{Cl}]^+$: 457.1922; found (ESI $^+$): 457.1955.

m.p. / °C: 195 (decomp.).

4-(2-Acetamidoethyl)-1-benzyl-6-methoxy-3-phenylquinolin-1-ium chloride (98)



Synthesised according to **GP-2** from *N*-benzylmelatonin (64 mg, 0.2 mmol) and 3-chloro-3-phenyldiazirine (92 mg, 0.6 mmol) in 1:1 CH₂Cl₂/PhMe (2 mL) as a yellow solid (25.7 mg, 0.056 mmol, 29%).

¹H NMR (400 MHz, CD₃OD): δ 8.96 (s, 1H), 8.23 (app t, *J* = 6.2 Hz, 1H), 8.14 (d, *J* = 9.7 Hz, 1H), 7.94 (d, *J* = 2.7 Hz, 1H), 7.69 – 7.63 (m, 2H), 7.60 (dd, *J* = 9.7, 2.7 Hz, 1H), 7.54 – 7.44 (m, 3H), 7.40 – 7.32 (m, 3H), 7.29 (dd, *J* = 7.5, 2.0 Hz, 2H), 6.30 (s, 2H), 4.10 (s, 3H), 3.54 (t, *J* = 6.6 Hz, 2H), 3.38 (app q, *J* = 6.6 Hz, 2H), 1.70 (s, 3H).

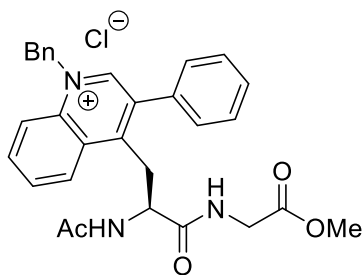
¹³C{¹H} NMR (101 MHz, CD₃OD): δ 173.8, 162.1, 155.9, 147.1, 138.3, 136.1, 134.9, 134.1, 133.4, 130.8, 130.6, 130.6, 130.4, 130.3, 128.9, 128.1, 122.4, 106.5, 62.0, 57.4, 40.5, 31.7, 22.4.

ν_{max} (neat) / cm⁻¹: 2931, 1616, 1532, 1368, 1242, 1027.

HRMS: calcd. for C₂₇H₂₇N₂O₂ [M-Cl]⁺: 411.2067; found (ESI⁺): 411.2076.

m.p. / °C: 115 (decomp.).

(S)-4-(2-Acetamido-3-((2-methoxy-2-oxoethyl)amino)-3-oxopropyl)-1-benzyl-3-phenylquinolin-1-ium chloride (100)



Synthesised according to modified **GP-2** from methyl *N*α-acetyl-1-benzyl-*L*-tryptophylglycinate (82 mg, 0.2 mmol) and 3-chloro-3-phenyldiazirine (92 mg, 0.6 mmol) in

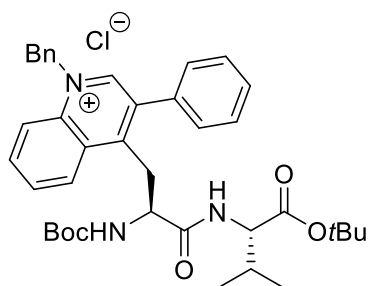
CH₂Cl₂ (2 mL). The solvent was removed *in vacuo* and the crude material purified by column chromatography (C₁₈; MeCN) to afford the product as an orange solid (22.5 mg, 0.041 mmol, 21%).

¹H NMR (400 MHz, CD₃OD): δ 9.51 (s, 1H), 8.83 (dd, *J* = 8.6, 1.3 Hz, 1H), 8.48 (d, *J* = 8.8 Hz, 1H), 8.18 (ddd, *J* = 8.8, 6.9, 1.3 Hz, 1H), 8.13 – 8.03 (m, 1H), 7.64 (m, 5H), 7.50 – 7.32 (m, 5H), 6.38 (s, 2H), 4.80 (dd, *J* = 8.5, 6.0 Hz, 1H), 4.08 (dd, *J* = 13.6, 6.1 Hz, 1H), 3.93 – 3.75 (m, 3H), 3.71 (s, 3H), 1.69 (s, 3H).

¹³C{¹H} NMR (101 MHz, CD₃OD): δ 172.9, 171.6, 171.6, 157.6, 150.6, 138.6, 138.4, 136.2, 135.8, 134.8, 131.5, 131.4, 131.2, 130.6, 130.5, 130.4, 130.2, 129.0, 128.1, 120.9, 62.0, 54.8, 52.7, 41.8, 33.5, 22.4.

HRMS: calcd. for C₃₀H₃₀N₃O₄ [M-Cl]⁺: 496.2231; found (ESI⁺): 496.2241.

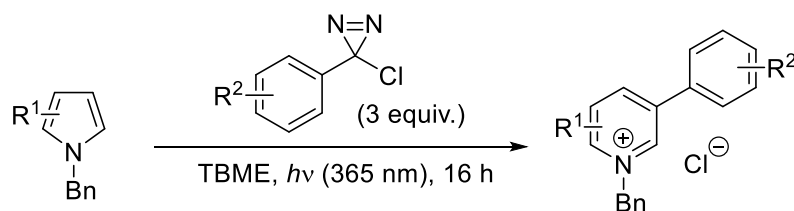
1-Benzyl-4-((*S*)-3-(((*S*)-1-(*tert*-butoxy)-3-methyl-1-oxobutan-2-yl)amino)-2-((*tert*-butoxycarbonyl)amino)-3-oxopropyl)-3-phenylquinolin-1-ium chloride (102)



Synthesised according to modified **GP-2** from methyl *N*α-Boc-1-benzyl-*L*-tryptophylvalinate *tert*-butyl ester (110 mg, 0.2 mmol) and 3-chloro-3-phenyldiazirine (92 mg, 0.6 mmol) in 1:1 CH₂Cl₂/PhMe (2 mL). The solvent was removed *in vacuo* and the crude material purified by column chromatography (C₁₈, MeCN) to afford the impure product as an orange solid (18.7 mg, 0.028 mmol, 14%).

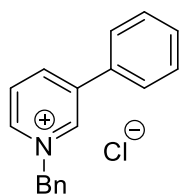
¹H NMR (400 MHz, CD₃OD): δ 9.57 (s, 1H), 8.86 (d, *J* = 8.6 Hz, 1H), 8.50 (d, *J* = 8.9 Hz, 1H), 8.20 (t, *J* = 8.0 Hz, 1H), 8.13 – 8.05 (m, 1H), 7.74 – 7.56 (m, 5H), 7.49 – 7.34 (m, 5H), 6.38 (d, *J* = 4.4 Hz, 2H), 4.48 (dd, *J* = 8.6, 5.7 Hz, 1H), 4.11 (d, *J* = 5.4 Hz, 1H), 3.95 (dd, *J* = 13.5, 5.7 Hz, 1H), 3.80 (dd, *J* = 13.5, 8.7 Hz, 1H), 2.08 (sept, *J* = 6.9 Hz, 1H), 1.45 (s, 9H), 1.17 (s, 9H), 0.90 (dd, *J* = 6.9, 6H).

5.3.4 General Procedure 3 (GP-3): Ring expansion of *N*-benzylpyrroles



A 10 mL microwave tube was charged with *N*-benzylpyrrole (0.2 mmol) which was then sealed, evacuated and flushed with dinitrogen 3 times. Anhydrous TBME (2 mL) was then added followed by 3-chloro-3-aryldiazirine (0.6 mmol). The cap of the reaction flask was then sealed with electrical tape. The reaction mixture was stirred under constant irradiation with UV light (365 nm, 18 W LED, 5 cm from light source) overnight. The resulting precipitate was isolated by filtration and washed with TBME (2 × 5 mL) to afford the pure product.

1-Benzyl-3-phenylpyridinium chloride (81)



Synthesised according to **GP-3** from *N*-benzylpyrrole (31 mg, 0.2 mmol) and 3-chloro-3-phenyldiazirine (92 mg, 0.6 mmol) in TBME (2 mL) as a viscous gum (36.5 mg, 0.130 mmol, 65%).

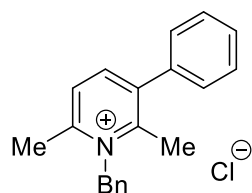
¹H NMR (400 MHz, CD₃OD): δ 9.51 (app t, *J* = 1.7 Hz, 1H), 9.02 (app dt, *J* = 6.0, 1.4 Hz, 1H), 8.88 (app dt, *J* = 8.3, 1.4 Hz, 1H), 8.18 (dd, *J* = 8.2, 6.1 Hz, 1H), 7.90 – 7.79 (m, 2H), 7.68 – 7.53 (m, 5H), 7.53 – 7.41 (m, 3H), 5.97 (s, 2H).

¹³C{¹H} NMR (101 MHz, CD₃OD): δ 143.4, 142.6, 142.4, 141.8, 133.3, 133.2, 130.3, 129.7, 129.5, 129.4, 128.7, 128.3, 127.2, 64.5.

ν_{\max} (neat) / cm⁻¹: 3025, 2984, 1678, 1488, 1433, 1153.

HRMS: calcd. for C₁₈H₁₆N [M-Cl]⁺: 246.1277; found (ESI⁺): 246.1273.

1-Benzyl-2,6-dimethyl-3-phenylpyridin-1-ium chloride (83)



Synthesised according to **GP-3** from *N*-benzyl-2,5-dimethylpyrrole (38 mg, 0.2 mmol) and 3-chloro-3-phenyldiazirine (92 mg, 0.6 mmol) in TBME (2 mL) as a viscous gum (55.0 mg, 0.189 mmol, 88%).

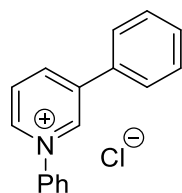
¹H NMR (400 MHz, CD₃OD): δ 8.47 (d, *J* = 8.2 Hz, 1H), 8.09 (d, *J* = 8.2 Hz, 1H), 7.62 – 7.53 (m, 3H), 7.52 – 7.48 (m, 2H), 7.48 – 7.36 (m, 3H), 7.17 – 7.07 (m, 2H), 6.00 (s, 2H), 2.80 (s, 3H), 2.62 (s, 3H).

¹³C{¹H} NMR (101 MHz, CD₃OD): δ 155.9, 154.8, 146.2, 140.5, 136.7, 132.7, 129.8, 129.6, 129.4, 128.7, 127.9, 126.0, 56.8, 21.6, 19.7.

ν_{\max} (neat) / cm⁻¹: 2971, 2818, 1615, 1481, 1447, 1029.

HRMS: calcd. for C₂₀H₂₀N [M-Cl]⁺: 274.1590; found (ESI⁺): 274.1597.

1,3-Diphenylpyridin-1-ium chloride (84)



Synthesised according to **GP-3** from 1-phenylpyrrole (29 mg, 0.2 mmol) and 3-chloro-3-phenyldiazirine (92 mg, 0.6 mmol) in TBME (2 mL) as a yellow solid (50.2 mg, 0.196 mmol, 98%).

¹H NMR (400 MHz, CD₃OD): δ 9.51 (app t, *J* = 1.7 Hz, 1H), 9.18 (app dt, *J* = 6.2, 1.4 Hz, 1H), 9.04 (app dt, *J* = 8.3, 1.4 Hz, 1H), 8.32 (dd, *J* = 8.3, 6.1 Hz, 1H), 7.91 (ddd, *J* = 7.7, 4.4, 2.3 Hz, 4H), 7.81 – 7.75 (m, 3H), 7.66 – 7.57 (m, 3H).

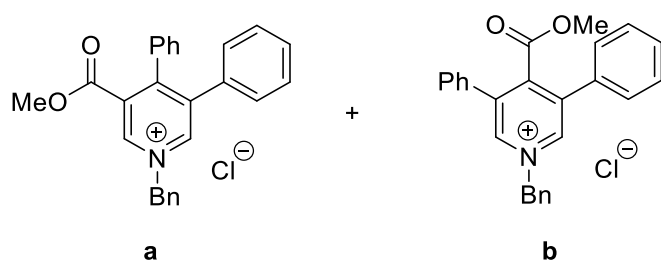
¹³C{¹H} NMR (101 MHz, CD₃OD): δ 145.4, 144.2, 144.1, 143.2, 134.6, 132.8, 131.7, 131.7, 130.9, 129.4, 128.9, 125.8.

ν_{\max} (neat) / cm⁻¹: 3025, 1573, 1482, 1413, 1309, 1229, 1024.

HRMS: calcd. for C₁₇H₁₄N [M-Cl]⁺: 232.1121; found (ESI⁺): 232.1125.

m.p. / °C: 100-103.

1-benzyl-3-(methoxycarbonyl)-4,5-diphenylpyridin-1-ium chloride^a (86a) and 1-benzyl-4-(methoxycarbonyl)-3,5-diphenylpyridin-1-ium chloride^b (86b)



Synthesised according to **GP-3** from *N*-benzyl-3-phenyl-4-(carboxymethyl)pyrrole (58 mg, 0.2 mmol) and 3-chloro-3-phenyldiazirine (92 mg, 0.6 mmol) in TBME (2 mL) as a tan solid (58.5 mg, 0.141 mmol, 70%, 3.3:1 mixture of isomers).

¹H NMR (400 MHz, DMSO-*d*₆): δ 9.70^a (d, *J* = 2.1 Hz, 1H), 9.65^b (d, *J* = 2.0 Hz, 0.6H), 9.63^a (d, *J* = 1.7 Hz, 1H), 7.75 – 7.71^a (m, 3H), 7.62 (dd, *J* = 7.3, 3.3 Hz, 2H), 7.54 – 7.45^a (m, 6H), 7.40 – 7.28 (m, 8H), 7.23 – 7.19 (m, 2H), 7.17 – 7.12 (m, 2H), 7.08 (d, *J* = 2.5 Hz, 0.3H), 6.00^a (s, 2H), 3.65^a (s, 3H), 3.53^b (s, 0.9H).

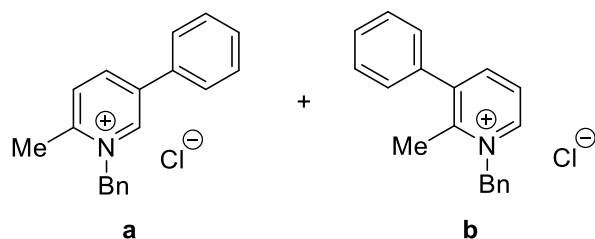
¹³C{¹H} NMR (101 MHz, DMSO-*d*₆): δ 164.8^b, 164.1, 163.4^a, 155.1, 146.5^a, 144.8^b, 144.4, 143.2^a, 141.5, 138.4, 137.7, 134.5, 133.9, 133.7, 133.2, 132.5, 132.1, 130.1, 129.9, 129.5, 129.4, 129.4, 129.3, 129.2, 129.2, 129.2, 129.0, 128.8, 128.7, 128.58, 128.57, 128.4, 128.2, 127.8, 127.7, 127.6, 126.0, 125.8, 122.1, 111.6, 63.7^b, 63.2^a, 53.3^a, 52.6, 50.5.

ν_{max} (neat) / cm⁻¹: 2947, 1737, 1627, 1432, 1330, 1275, 1219, 1167, 1100.

HRMS: calcd. for C₂₆H₂₂NO₂ [M-Cl]⁺: 380.1645; found (ESI⁺): 380.1640.

Peak assignment for regioisomers determined by relative integrations and 2D multinuclear correlation spectroscopy. Ambiguous peaks have been left unassigned.

1-benzyl-2-methyl-5-phenylpyridin-1-ium chloride (88a) and 1-benzyl-2-methyl-3-phenylpyridin-1-ium chloride (88b)



Synthesised according to **GP-3** from *N*-benzyl-2-methylpyrrole (34 mg, 0.2 mmol) and 3-chloro-3-phenyldiazirine (92 mg, 0.6 mmol) in TBME (2 mL) as a tan solid (26.7 mg, 0.090 mmol, 45%, 3.7:1 mixture of isomers).

^1H NMR (400 MHz, CD_3OD): δ 9.65^a (d, J = 2.1 Hz, 1H), 9.14^b (d, J = 7.2 Hz, 0.25H), 8.94^a (dd, J = 8.3, 2.1 Hz, 1H), 8.54^b (d, J = 6.8 Hz, 0.25H), 8.18^a (d, J = 8.4 Hz, 1H), 8.13^b (d, J = 7.7 Hz, 0.25H), 7.97 – 7.91 (m, 2H), 7.68 – 7.55 (m, 3H), 7.52 – 7.40 (m, 3H), 7.37 – 7.30 (m, 3H), 6.00^b (s, 0.5H), 5.98^a (s, 2H), 2.74 (s, 3H), 2.62 (s, 0.75H).

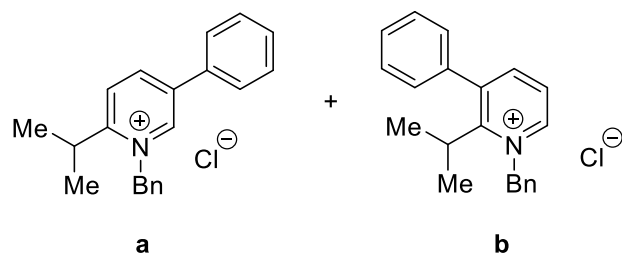
$^{13}\text{C}\{^1\text{H}\}$ NMR (101 MHz, CD_3OD): δ 153.9^a, 153.8^b, 146.1^b, 145.5^b, 144.1^a, 143.7, 143.1^a, 142.3, 141.7, 137.6^a, 133.2, 132.9, 132.6, 130.5, 130.0, 129.5, 129.3, 129.3, 129.2, 128.9, 128.8, 128.7, 127.6, 127.4, 127.33, 125.3^b, 61.1^b, 60.7^a, 19.5^a, 18.3^b.

ν_{max} (neat) / cm^{-1} : 3064, 2964, 2820, 1628, 1538, 1493, 1476, 1454, 1028.

HRMS: calcd. for $\text{C}_{26}\text{H}_{22}\text{NO}_2$ $[\text{M}-\text{Cl}]^+$: 380.1645; found (ESI⁺): 380.1640.

Peak assignment for regioisomers determined by relative integrations and 2D multinuclear correlation spectroscopy. Ambiguous peaks have been left unassigned.

1-benzyl-2-isopropyl-5-phenylpyridin-1-ium chloride (89a) and 1-benzyl-2-isopropyl-3-phenylpyridin-1-ium chloride (89b)



Synthesised according to **GP-3** from *N*-benzyl-2-isopropylpyrrole (40 mg, 0.2 mmol) and 3-chloro-3-phenyldiazirine (92 mg, 0.6 mmol) in TBME (2 mL) as a tan solid (47.9 mg, 0.148 mmol, 74%, 1.2:1 mixture of isomers).

^1H NMR (400 MHz, CD_3OD): δ 9.28^a (app t, $J = 1.6$ Hz, 1H), 9.00^a (d, $J = 1.6$ Hz, 1H), 8.98 – 8.92^{a,b} (m, 1.8H), 8.81 – 8.76^a (m, 1H), 8.18^b (d, $J = 6.4$ Hz, 0.8H), 7.87 – 7.81^a (m, 2H), 7.67 – 7.54 (m, 9H), 7.54 – 7.43 (m, 8H), 5.93^a (s, 2H), 5.83^b (s, 1.6H), 3.31^{a,b} (sept, $J = 6.8$ Hz, 1.8H), 1.44^a (d, $J = 7.0$ Hz, 6H), 1.28^b (d, $J = 6.8$ Hz, 5H).

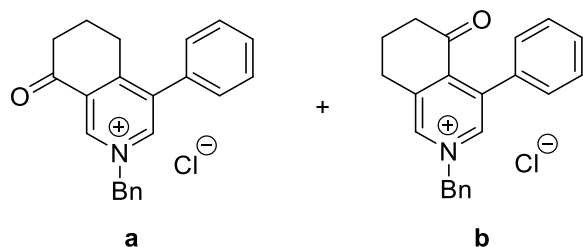
$^{13}\text{C}\{^1\text{H}\}$ NMR (101 MHz, CD_3OD): δ 168.6^a, 151.7^a, 145.2^b, 144.0^b, 143.1^a, 143.0, 142.9, 142.3^a, 141.7^a, 135.0, 134.9, 134.82, 134.79, 131.5, 131.0, 130.96, 130.8, 130.7, 130.4, 130.2, 130.1, 129.8, 128.7^a, 127.0^b, 65.8^a, 64.9^b, 33.5^a, 31.9^b, 23.3^a, 22.8^b.

ν_{max} (neat) / cm^{-1} : 2964, 2931, 2819, 1632, 1489, 1454, 1032.

HRMS: calcd. for $\text{C}_{21}\text{H}_{22}\text{N}$ $[\text{M}-\text{Cl}]^+$: 288.1747; found (ESI⁺): 288.1752.

Peak assignment for regioisomers determined by relative integrations and 2D multinuclear correlation spectroscopy. Ambiguous peaks have been left unassigned.

2-Benzyl-8-oxo-4-phenyl-5,6,7,8-tetrahydroisoquinolin-2-ium chloride (90a) and 2-Benzyl-5-oxo-4-phenyl-5,6,7,8-tetrahydroisoquinolin-2-ium chloride (90b)



Synthesised according to **GP-3** from *N*-benzyl-2,5-dimethylpyrrole (38 mg, 0.2 mmol) and 3-chloro-3-phenyldiazirine (92 mg, 0.6 mmol) in TBME (2 mL) as a viscous gum (55.0 mg, 0.189 mmol, 88%, 10:1 mixture of isomers).

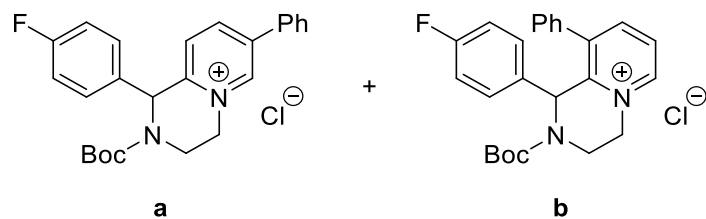
¹H NMR (400 MHz, DMSO-*d*₆): δ 9.56^a (d, *J* = 1.5 Hz, 1H), 9.46^b (d, *J* = 1.4 Hz, 0.1H), 9.40^a (d, *J* = 1.5 Hz, 1H), 9.26^b (d, *J* = 1.4 Hz, 0.1H), 7.68 – 7.59^a (m, 5H), 7.57 – 7.53 (m, 2H), 7.50 – 7.41^a (m, 4H), 7.39 – 7.33^b (m, 0.4H), 7.33 – 7.25^b (m, 0.5H), 6.68^b (d, *J* = 2.1 Hz, 0.1H), 5.95^a (s, 2H), 5.87^b (s, 0.2H), 3.08^a (t, *J* = 6.0 Hz, 2H), 2.79^a (dd, *J* = 7.3, 5.7 Hz, 2H), 2.58^b (t, *J* = 6.1 Hz, 0.2H), 2.29^b (dd, *J* = 7.1, 5.6 Hz, 0.2H), 2.13 – 2.03^a (m, 2H), 1.91^b (app p, *J* = 6.3 Hz, 0.2H).

¹³C{¹H} NMR (101 MHz, DMSO-*d*₆): δ 194.3^a, 193.6^b, 160.8^a, 145.2^a, 141.9^a, 141.1, 134.3, 132.6, 131.5, 129.8^a, 129.5^a, 129.4^a, 129.2^a, 129.2, 129.0^a, 128.9^a, 128.6^b, 128.3^b, 127.8^b, 127.7^b, 126.4, 122.0, 117.3^b, 63.5^b, 63.0^a, 52.6, 37.3^a, 27.9^a, 26.6, 24.8, 21.1, 20.8^a.

ν_{max} (neat) / cm⁻¹: 2932, 1702, 1627, 1160, 1029, 905.

HRMS: calcd. for C₂₂H₂₀NO [M-Cl]⁺: 314.1539; found (ESI⁺): 314.1546.

2-Boc-1-(4-fluorophenyl)-7-phenyl-1,2,3,4-tetrahydropyrido[1,2-a]pyrazin-5-ium chloride (91a) and 2-Boc-1-(4-fluorophenyl)-9-phenyl-1,2,3,4-tetrahydropyrido[1,2-a]pyrazin-5-ium chloride (91b)



Synthesised according to **GP-3** from 1-phenylpyrrole (65 mg, 0.2 mmol) and 3-chloro-3-phenyldiazirine (92 mg, 0.6 mmol) in TBME (2 mL) as a tan solid (76.4 mg, 0.173 mmol, 87%, 4.0:1 mixture of isomers).

¹H NMR (400 MHz, CD₃OD): δ 9.48^a (d, J = 2.1 Hz, 1H), 9.16^b (d, J = 6.1 Hz, 0.25H), 8.92^a (d, J = 8.5 Hz, 1H), 8.58^b (d, J = 7.9 Hz, 0.25H), 8.26^b (dd, J = 8.1, 6.1 Hz, 0.25H), 7.95 – 7.86^a (m, 2H), 7.69 – 7.55^a (m, 3H), 7.49^a (s, 2H), 7.28 (t, J = 8.8 Hz, 2H), 7.12^b (app t, J = 8.7 Hz, 0.5H), 7.03 – 6.90^b (m, 0.5H), 4.88 (dt, J = 11.4, 5.5 Hz, 1H), 4.74^a (s, 1H), 4.51^b (s, 0.25H), 4.11 (s, 1H), 4.01^b (m, 1H), 3.99 – 3.88^a (m, 1H), 1.43 (s, 12H)^{a,b}.

¹³C{¹H} NMR (101 MHz, CD₃OD): δ 163.2, 163.0, 160.7, 160.6, 153.1, 150.1^a, 149.8^b, 146.8, 146.0^b, 143.9, 142.5^a, 140.1, 137.5^a, 134.2, 132.9^a, 130.2^a, 129.8, 129.5, 129.4, 128.7, 128.2, 127.3^a, 126.5, 116.0, 115.9, 115.6, 81.0, 80.9, 55.7, 54.1^a, 53.6, 27.9^{a,b}.

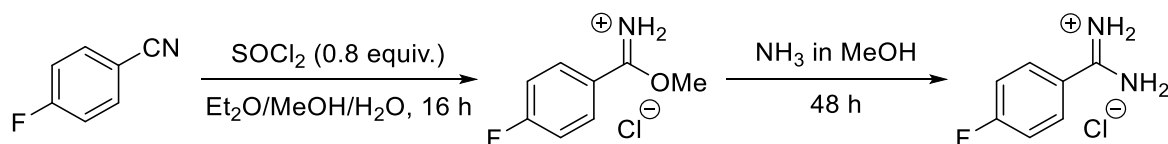
ν_{max} (neat) / cm⁻¹: 2975, 1690, 1507, 1391, 1365, 1224, 1160, 1138, 959, 842.

HRMS: calcd. for C₂₅H₂₆FN₂O₂ [M-Cl]⁺: 405.1973; found (ESI⁺): 405.1986.

Peak assignment for regioisomers determined by relative integrations and 2D multinuclear correlation spectroscopy. Ambiguous peaks have been left unassigned.

5.3.5 Synthesis of Amidine Hydrochlorides

4-Fluorobenzamidine hydrochloride (49)



4-Fluorobenzonitrile (3.03 g, 25 mmol) was dissolved in a 6:2:1 mixture of $\text{Et}_2\text{O}/\text{MeOH}/\text{water}$ (4 mL) and the solution cooled to 0 °C by use of an ice-water bath. SOCl_2 (1.46 mL, 20 mmol) was then added drop-wise and the reaction stirred at 0 °C for 1 h. The reaction was then warmed to rt and stirred overnight. The resulting precipitate was isolated by filtration and transferred to a second flask and suspended in MeOH (5 mL). NH_3 (2 M in MeOH , 18.8 mL, 37.5 mmol) was then added. The suspension fully dissolved within 2 hrs and the resulting solution was stirred at rt for 48 h. The volatiles were removed *in vacuo* and the resulting solid was washed with Et_2O (3×20 mL) to afford the pure product as an off-white solid (3.68 g, 21.1 mmol, 84%).

$^1\text{H NMR}$ (400 MHz, CDCl_3): δ 9.23 (br s, 4H), 8.01 – 7.81 (m, 2H), 7.53 – 7.46 (m, 2H).

$^{13}\text{C NMR}$ (101 MHz, CDCl_3): δ 166.4 (d, $J = 252.7$ Hz), 164.72, 131.2 (d, $J = 9.7$ Hz), 124.5 (d, $J = 3.2$ Hz), 116.1 (d, $J = 22.3$ Hz).

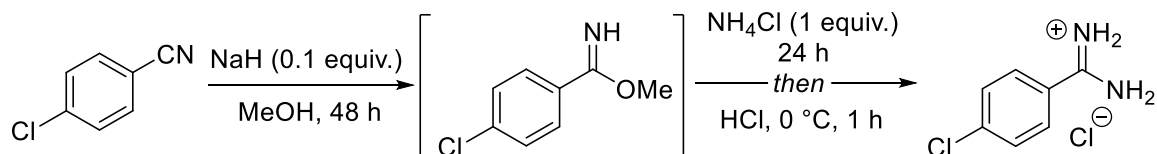
$^{19}\text{F NMR}$ (376 MHz, CDCl_3): δ -105.13 (tt, $J = 8.5, 5.5$ Hz).

ν_{max} (neat) / cm^{-1} : 3251, 3052, 1656, 1609, 1491, 1245, 1088, 848.

HRMS: calcd. for $\text{C}_7\text{H}_8\text{FN}_2$ $[\text{M}-\text{Cl}]^+$: 139.0667; found (ESI $^+$): 139.0663.

m.p. / °C: 210-211.

4-Chlorobenzamidine hydrochloride (50)



A flame-dried flask under an atmosphere of dinitrogen was charged 4-chlorobenzonitrile (4.13 g, 30.0 mmol) and MeOH (90 mL). NaH (60% on mineral oil, 120 mg, 3.0 mmol) was then added in one portion and the reaction stirred at rt for 48 hrs. Anhydrous NH_4Cl (1.61 g,

30.0 mmol) was added in one portion and the reaction stirred for a further 24 hrs. Any unreacted NH_4Cl was removed by filtration and the reaction mixture concentrated *in vacuo*. The resulting solid was suspended in Et_2O (20 mL) and basified by addition of 2 M NaOH (20 mL). The organic layer was separated and dried over Na_2SO_4 , filtered, and the volatiles were removed *in vacuo*. The residue was re-dissolved in Et_2O (10 mL) and HCl (4 M in dioxane, 8 mL, 32 mmol) was added at 0 °C and the suspension stirred at rt for 1 hr. The resulting solid isolated by filtration and washed with Et_2O (2×10 mL) to afford the pure product as a colourless solid (3.38 g, 17.8 mmol, 59%).

^1H NMR (400 MHz, CDCl_3): δ 8.77 (br s, 4H), 7.84 (d, $J = 8.4$ Hz, 2H), 7.67 (d, $J = 8.4$ Hz, 2H).

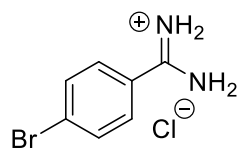
$^{13}\text{C}\{^1\text{H}\}$ NMR (101 MHz, CDCl_3): δ 164.0, 137.7, 129.7, 128.8, 128.8.

ν_{max} (neat) / cm^{-1} : 3239, 3123, 1672, 1595, 1482, 1089, 1013, 845.

HRMS: calcd. for $\text{C}_7\text{H}_8\text{N}_2^{35}\text{Cl}$ $[\text{M}-\text{Cl}]^+$: 155.0371; found (ESI⁺): 155.0374.

m.p. / °C: 247-250 (lit. 239-241).²⁶⁹

4-Bromobenzamidine hydrochloride (51)



Synthesised according to the above procedure from 4-bromobenzonitrile (1.82 g, 10.0 mmol) to afford the pure product as a colourless solid (1.43 g, 6.09 mmol, 61%).

^1H NMR (400 MHz, CDCl_3): δ 8.92 (br s, 4H), 7.82 (d, $J = 8.6$ Hz, 2H), 7.75 (d, $J = 8.6$ Hz, 2H).

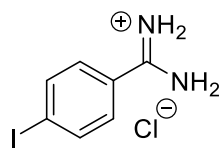
$^{13}\text{C}\{^1\text{H}\}$ NMR (101 MHz, CDCl_3): δ 162.9, 131.9, 131.4, 129.4, 125.1.

ν_{max} (neat) / cm^{-1} : 3070, 1673, 1594, 1479, 1072, 1012, 842.

HRMS: calcd. for $\text{C}_7\text{H}_8\text{N}_2^{79}\text{Br}$ $[\text{M}-\text{Cl}]^+$: 198.9865; found (ESI⁺): 198.9874.

m.p. / °C: 258 (decomp.) (lit. 259-260, decomp.).²⁷⁰

4-Iodobenzamidinium hydrochloride (52)



Synthesised according to the above procedure from 4-iodobenzonitrile (2.23 g, 10.0 mmol) to afford the pure product as a colourless solid (2.03 g, 7.19 mmol, 72%).

^1H NMR (400 MHz, CDCl_3): δ 9.25 (br s, 4H) 8.11 – 7.86 (m, 2H), 7.79 – 7.61 (m, 2H).

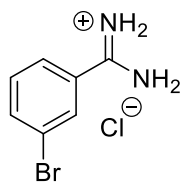
$^{13}\text{C}\{^1\text{H}\}$ NMR (101 MHz, CDCl_3): δ 165.3, 137.8, 129.8, 127.3, 102.3.

ν_{max} (neat) / cm^{-1} : 3251, 3052, 1668, 1589, 1470, 1394, 1308, 1284, 1012, 845.

HRMS: calcd. for $\text{C}_7\text{H}_8\text{N}_2\text{I}$ $[\text{M}-\text{Cl}]^+$: 246.9727; found (ESI⁺): 246.9723.

m.p. / $^{\circ}\text{C}$: 288-290.

3-Bromobenzamidinium hydrochloride (53)



Synthesised according to the above procedure from 3-bromobenzonitrile (1.82 g, 10 mmol) to afford the pure product as a colourless solid (1.41 g, 6.00 mmol, 60%).

^1H NMR (400 MHz, CDCl_3): δ 9.34 (br s, 4H), 8.05 (app t, $J = 2.1$ Hz, 1H), 7.92 (ddd, $J = 8.0, 2.0, 1.0$ Hz, 1H), 7.84 (ddt, $J = 8.0, 2.0, 1.0$ Hz, 1H), 7.56 (app t, $J = 8.0$ Hz, 1H).

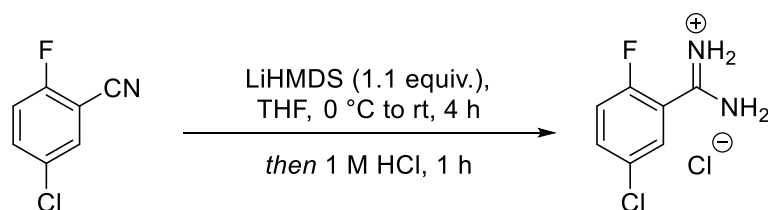
$^{13}\text{C}\{^1\text{H}\}$ NMR (101 MHz, CDCl_3): δ 164.6, 136.4, 131.0, 130.8, 130.2, 127.3, 122.0.

ν_{max} (neat) / cm^{-1} : 3035, 1579, 1516, 1463, 1411, 1078.

HRMS: calcd. for $\text{C}_7\text{H}_8\text{N}_2^{79}\text{Br}$ $[\text{M}-\text{Cl}]^+$: 198.9865; found (ESI⁺): 198.9884.

m.p. / $^{\circ}\text{C}$: 121-124 (lit. 129-131).²⁷⁰

5-Chloro-2-fluorobenzamidine hydrochloride (54)



To a flame-dried flask under an atmosphere of dinitrogen was added a solution of LiHMDS (1 M in THF, 22 mL, 22 mmol). The flask was cooled to 0 °C and 5-chloro-2-fluorobenzonitrile (3.11 g, 20 mmol) was added portion-wise over 5 mins. The reaction mixture was warmed to rt and stirred for 4 hrs. The mixture was cooled to 0 °C and aqueous HCl (2 M, 25 mL, 25 mmol) was added and the reaction stirred for a further 1 hr. EtOAc (20 mL) was then added and the organic layer separated. The aqueous layer was washed with EtOAc (3 × 20 mL) after which it was basified with 2M NaOH until pH > 10 and the aqueous solution extracted with CH₂Cl₂ (3 × 30 mL). The combined CH₂Cl₂ extracts were dried over Na₂SO₄, filtered, and concentrated *in vacuo* to give an orange oil which solidified over time. The crude material was dissolved in Et₂O (30 mL) and cooled to 0 °C. HCl (4 M in dioxane, 6 mL, 24 mmol) was then added drop-wise to produce a yellow precipitate. The reaction mixture was stirred at rt for 1 hr and the solid isolated by filtration and washed with Et₂O (2 × 20 mL) to afford the pure product as a yellow solid (3.15 g, 15.1 mmol, 75%).

¹H NMR (400 MHz, DMSO-*d*₆): δ 9.66 (br s, 2H), 9.65 (br s, 2H), 7.87 (dd, *J* = 5.9, 2.7 Hz, 1H), 7.81 (ddd, *J* = 9.0, 4.5, 2.7 Hz, 1H), 7.55 (t, *J* = 9.3 Hz, 1H).

¹³C NMR (101 MHz, DMSO-*d*₆): δ 160.9, 158.7 (d, *J* = 252.4 Hz), 134.3 (d, *J* = 8.9 Hz), 129.9 (d, *J* = 2.0 Hz), 128.6 (d, *J* = 3.3 Hz), 119.3 (d, *J* = 14.9 Hz), 118.5 (d, *J* = 22.9 Hz).

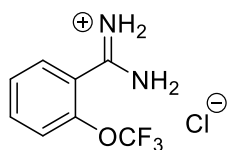
¹⁹F NMR (376 MHz, DMSO-*d*₆): δ -115.70 (app td, *J* = 9.7, 9.0, 4.5 Hz).

ν_{\max} (neat) / cm⁻¹: 3034, 2917, 2849, 1674, 1617, 1540, 1476, 1236, 1105.

HRMS: calcd. for C₇H₇N₂FCl [M-Cl]⁺: 173.0276; found (ESI⁺): 173.0287.

m.p. / °C: 219-221.

2-(Trifluoromethoxy)benzamidinium hydrochloride (55)



Synthesised as described above from 2-(trifluoromethoxy)benzonitrile (3.74 g, 20 mmol) as a colourless solid (715 mg, 2.97 mmol, 15%).

¹H NMR (400 MHz, DMSO-*d*₆): δ 9.58 (br s, 4H), 7.81 (app td, *J* = 7.8, 1.7 Hz, 1H), 7.77 (dd, *J* = 7.7, 1.7 Hz, 1H), 7.63 (app t, *J* = 7.7 Hz, 2H).

¹³C NMR (101 MHz, DMSO-*d*₆): δ 163.0 (q, *J* = 6.0 Hz), 144.8 (q, 1.6 Hz), 134.1, 130.6, 127.9, 123.7 (q, *J* = 2.9 Hz), 121.7, 119.9 (q, 258.6 Hz).

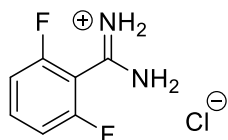
¹⁹F NMR (376 MHz, DMSO-*d*₆): δ -56.79

ν_{\max} (neat) / cm⁻¹: 3049, 1674, 1477, 1259, 1217, 1158.

HRMS: calcd. for C₈H₇N₂OF₃ [M-Cl]⁺: 205.0583; found (ESI⁺): 205.0597.

m.p. / °C: 276-278.

2,6-difluorobenzamidinium hydrochloride (56)



Synthesised as described above from 2,6-difluorobenzonitrile (3.74 g, 10 mmol) as a colourless solid (728 mg, 3.78 mmol, 38%).

¹H NMR (400 MHz, DMSO-*d*₆): δ 9.91 (s, 2H), 9.84 (s, 2H), 7.75 (tt, *J* = 8.6, 6.6 Hz, 1H), 7.36 (t, *J* = 8.6 Hz, 2H).

¹³C NMR (101 MHz, DMSO-*d*₆): δ 158.7 (dd, *J* = 252.4, 5.8 Hz), 157.7, 134.8 (t, *J* = 10.3 Hz), 112.38 (d, *J* = 23.8 Hz), 112.37 (dd, *J* = 17.0, 1.8 Hz), 108.1 (t, *J* = 19.7 Hz).

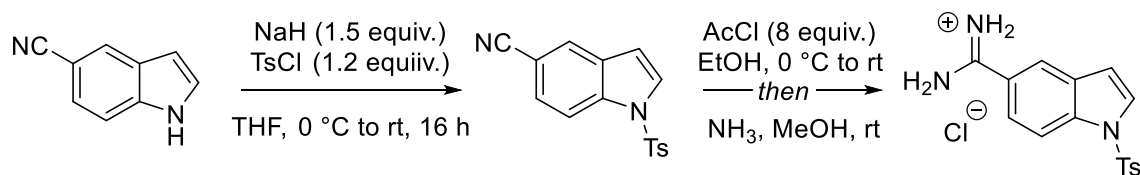
¹⁹F NMR (376 MHz, DMSO-*d*₆): δ -112.62 (dd, *J* = 8.2, 6.5 Hz).

ν_{\max} (neat) / cm⁻¹: 3210, 2999, 1672, 1637, 1470, 1282, 1238, 1014.

HRMS: calcd. for C₇H₇F₂N₂ [M-Cl]⁺: 157.0572; found (ESI⁺): 157.0578.

m.p. / °C: 235 (decomp.).

5-(1-Tosyl-indolyl)amidinium hydrochloride (57)



Step 1: To a flame-dried flask under an atmosphere of dinitrogen was added 5-cyanoinidole (1.42 g, 10 mmol) and anhydrous THF (30 mL). The solution was cooled to 0 °C and NaH (60% on mineral oil, 600 mg, 15 mmol) was added in portions. After stirring for 30 mins, TsCl (2.29 g, 12.0 mmol) was added in one portion and the reaction mixture warmed to rt and stirred overnight. The reaction was quenched by addition of 2 M NaOH until the resulting white precipitate dissolved and extracted with Et₂O (3 × 30 mL). The combined organics were washed with brine, dried over MgSO₄, filtered, and concentrated *in vacuo*. Purification by recrystallisation from EtOH afforded the product as a colourless solid (2.54 g, 8.59 mmol, 86%).

¹H NMR (400 MHz, DMSO-d₆): δ 8.07 (d, *J* = 8.6 Hz, 1H), 7.87 (d, *J* = 1.6 Hz, 1H), 7.81 – 7.75 (m, 2H), 7.69 (d, *J* = 3.7 Hz, 1H), 7.55 (dd, *J* = 8.6, 1.6 Hz, 1H), 7.26 (d, *J* = 8.1 Hz, 2H), 6.71 (dd, *J* = 3.8, 0.8 Hz, 1H), 2.36 (s, 3H).

¹³C NMR (101 MHz, DMSO-d₆): δ 145.9, 136.6, 134.9, 130.8, 130.3, 128.6, 127.7, 127.0, 126.5, 119.4, 114.4, 108.6, 107.0, 21.8.

Step 2: To a suspension of 1-tosyl-5-cyanoinidole (2.22 g, 7.5 mmol) in EtOH (7 mL) cooled to 0 °C was added AcCl (4.3 mL, 6.0 mmol) drop-wise. After complete addition, the resulting mixture was warmed to rt and stirred overnight to afford a white precipitate. The volatiles were removed *in vacuo* and MeOH (5 mL) was added. NH₃ (2 M in MeOH, 5.7 mL, 11.25 mmol) was added in one portion and the reaction stirred for 48 hrs. The volatiles were removed *in vacuo* to afford the product as a tan solid (2.47 g, 7.08 mmol, 94%).

¹H NMR (400 MHz, DMSO-d₆): δ 9.51 (s, 4H), 8.33 (d, *J* = 1.8 Hz, 1H), 8.29 (d, *J* = 8.7 Hz, 1H), 8.19 (d, *J* = 3.7 Hz, 1H), 8.14 – 8.09 (m, 2H), 7.95 (dd, *J* = 8.8, 1.9 Hz, 1H), 7.58 (d, *J* = 8.2 Hz, 2H), 7.19 (d, *J* = 3.7 Hz, 1H), 2.50 (s, 3H).

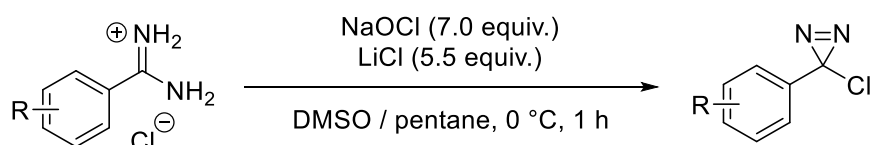
¹³C NMR (101 MHz, DMSO-d₆): δ 166.0, 146.1, 136.5, 130.4, 130.2, 129.1, 126.9, 124.2, 123.3, 122.5, 113.3, 109.4, 21.0.

ν_{max} (neat) / cm⁻¹: 3030, 1666, 1541, 1446, 1369, 1169, 1129, 1089, 991.

HRMS: calcd. for C₁₆H₁₆N₃O₂S [M-Cl]⁺: 314.0958; found (ESI⁺): 314.0961.

m.p. / °C: 152-155.

5.3.6 Synthesis of 3-chloro-3-aryl-3*H*-diazirines (GP-4)



CAUTION! As indicated by the DSC data, arylchlorodiazirines are thermally and photolytically unstable and are potentially explosive at temperatures at and above ambient. Any operations involving the use or isolation of these diazirines should be performed behind a blast shield and shielded from light.

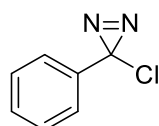
According to a modified literature procedure,²⁷¹ a two-necked round-bottom flask fitted with a thermometer and a pressure-equalising dropping funnel was charged with DMSO (18 mL) followed by LiCl (1.17 g, 27.5 mmol) and amidine hydrochloride (5.0 mmol). The solution was cooled to 0 °C by use of an external ice-water bath, then pentane (10 mL) was added. A solution of aqueous sodium hypochlorite (0.48 M, 73 mL, 35 mmol) saturated with NaCl was added drop-wise from the addition funnel at a rate that maintained the temperature below 30 °C. After complete addition, the resulting mixture was stirred at 0 °C for a further 1 hr and then poured onto ice-cold water (50 mL). The pentane layer was separated, and the aqueous layer was extracted with Et₂O (3 × 20 mL). The combined organic portions were washed with water (2 × 20 mL) and dried over MgSO₄, filtered and concentrated *in vacuo* by rotary evaporation (bath temperature 25 °C and the flask shielded from light with aluminium foil behind a blast shield; see below). Purification by column chromatography (silica gel) eluting with solvents listed afforded the pure product after additional careful rotary evaporation. The diazirines were typically isolated >95% pure with the remaining mass balance being residual solvent, and were stored in a freezer (-20 °C).

Arylchlorodiazirines are known to be energetic materials. Therefore, we recommend the following safety precautions when isolating the pure diazidine *via* rotary evaporation.

- Set cooling bath to 25 °C

- Avoid pressures below 100 mbar
- Cover RBF in elastic mesh to contain fragments in case of explosion
- Shield flask from light with aluminium foil
- Employ a blast shield at all times, and work with the fume-hood sash lowered

3-Chloro-3-phenyl-3*H*-diazirine (11)



Synthesised according to **GP-4** from benzamidine hydrochloride hydrate (3.13 g, 20.0 mmol), LiCl (4.66 g, 110 mmol), and NaOCl (292 mL, 140 mmol). Purification by column chromatography (silica gel; pentane) afforded a yellow liquid (1.81 g, 11.9 mmol, 59%).

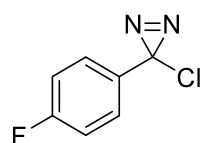
¹H NMR (400 MHz, CDCl₃): δ 7.48-7.34 (m, 3 H), 7.21-7.05 (m, 2 H).

¹³C{¹H} NMR (101 MHz, CDCl₃): δ 135.7, 129.3, 128.5, 126.0, 47.1.

HRMS: calcd. for C₇H₆³⁵Cl [M-N₂+H]⁺: 125.0153; found (ESI⁺): 125.0157.

Characterisation data are consistent with literature values.¹⁸⁷

3-Chloro-3-(4-fluorophenyl)-3*H*-diazirine (58)



Synthesised according to **GP-4** from 4-fluorobenzamidine hydrochloride (1.75 g, 10 mmol), LiCl (2.33 g, 55 mmol), and NaOCl (146 mL, 70 mmol). Purification by column chromatography (silica gel; pentane) afforded a yellow liquid (1.14 g, 6.65 mmol, 67%).

¹H NMR (400 MHz, CDCl₃): δ 7.15-7.05 (m, 4H).

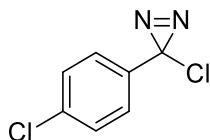
¹³C{¹H} NMR (101 MHz, CDCl₃): δ 163.3 (d, *J* = 250.2 Hz), 131.6 (d, *J* = 3.2 Hz), 128.0 (d, *J* = 8.9 Hz), 115.7 (d, *J* = 22.3 Hz), 46.6.

¹⁹F NMR (376 MHz, CDCl₃): δ -111.14 (tt, *J* = 8.9, 5.1 Hz).

HRMS: calcd. for C₇H₅F³⁵Cl [M-N₂+H]⁺: 143.0059; found (ESI⁺): 143.0049.

Characterisation data are consistent with literature values.¹⁸⁷

3-Chloro-3-(4-chlorophenyl)-3*H*-diazirine (59)



Synthesised according to **GP-4** from 4-chlorobenzamidine hydrochloride (955 mg, 5.0 mmol) LiCl (1.16 g, 27.5 mmol), and NaOCl (73 mL, 35 mmol). Purification by column chromatography (silica gel; pentane) afforded a colourless liquid (320 mg, 1.71 mmol 34%).

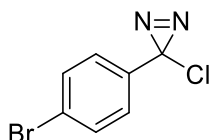
¹H NMR (400 MHz, CDCl₃): δ 7.43 – 7.34 (m, 2H), 7.11 – 6.97 (m, 2H).

¹³C{¹H} NMR (101 MHz, CDCl₃): δ 135.8, 134.4, 128.9, 127.5, 46.6.

HRMS: calcd. for C₇H₅³⁵Cl₂ [M-N₂+H]⁺: 160.9734; found (ESI⁺): 160.9747.

Characterisation data are consistent with literature values.¹⁸⁷

3-Chloro-3-(4-bromophenyl)-3*H*-diazirine (60)



Synthesised according to **GP-4** from 4-bromobenzamidine hydrochloride (1.18 g, 5.0 mmol), LiCl (1.16 g, 27.5 mmol), and NaOCl (73 mL, 35 mmol). Purification by column chromatography (silica gel; pentane) afforded a colourless liquid (246 mg, 1.06 mmol, 21%).

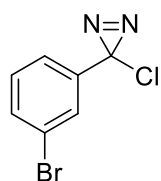
¹H NMR (400 MHz, CDCl₃): δ 7.60 – 7.51 (m, 2H), 7.05 – 6.95 (m, 2H).

¹³C{¹H} NMR (101 MHz, CDCl₃): δ 134.9, 131.9, 127.7, 124.0, 46.7.

HRMS: calcd. for C₇H₅⁷⁹Br³⁵Cl [M-N₂+H]⁺: 202.9258; found (ESI⁺): 202.9253.

Characterisation data are consistent with literature values.¹⁸⁷

3-Chloro-3-(3-bromophenyl)-3*H*-diazirine (62)



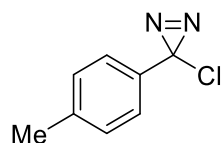
Synthesised according to **GP-4** from 3-bromobenzamidine hydrochloride (1.18 g, 5.0 mmol), LiCl (1.16 g, 27.5 mmol), and NaOCl (73 mL, 35 mmol). Purification by column chromatography (silica gel; pentane) afforded a colourless liquid (446 mg, 1.93 mmol, 39%).

¹H NMR (400 MHz, CDCl₃): δ 7.53 (ddd, *J* = 7.9, 1.9, 1.0 Hz, 1H), 7.31 (app t, *J* = 1.9 Hz, 1H), 7.26 (app t, *J* = 7.9 Hz, 1H), 7.00 (ddd, *J* = 7.9, 1.9, 1.0 Hz, 1H).

¹³C{¹H} NMR (101 MHz, CDCl₃): δ 137.9, 132.6, 130.1, 129.4, 124.7, 123.0, 46.2.

Characterisation data are consistent with literature values.¹⁸⁷

3-Chloro-3-(4-methylphenyl)-3*H*-diazirine (63)



Synthesised according to **GP-4** from 4-methylbenzamidine hydrochloride (853 mg, 5.0 mmol), LiCl (1.16 g, 27.5 mmol), and NaOCl (73 mL, 35 mmol). Purification by column chromatography (silica gel; pentane) afforded a yellow liquid (464 mg, 2.79 mmol, 56%).

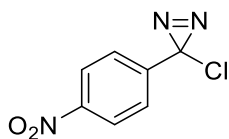
¹H NMR (400 MHz, CDCl₃): δ 7.24 – 7.20 (m, 2H), 7.08 – 6.96 (m, 2H), 2.40 (s, 3H).

¹³C{¹H} NMR (101 MHz, CDCl₃): 139.6, 133.0, 129.3, 126.0, 47.3, 21.3.

HRMS: calcd. for C₈H₈³⁵Cl [M-N₂+H]⁺: 139.0309; found (ESI⁺): 139.0308.

Characterisation data are consistent with literature values.¹⁸⁷

3-Chloro-3-(4-nitrophenyl)-3*H*-diazirine (64)



Synthesised according to **GP-4** from 4-nitrobenzamidinium hydrochloride (1.01 g, 5.0 mmol), LiCl (1.16 g, 27.5 mmol), and NaOCl (73 mL, 35 mmol). Purification by column chromatography (silica gel; 5% Et₂O in pentane) afforded the product as a yellow solid (227 mg, 1.15 mmol, 23%).

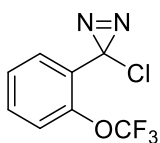
¹H NMR (400 MHz, CDCl₃): δ 8.26 (d, *J* = 8.9 Hz, 1H), 7.30 (d, *J* = 8.9 Hz, 1H).

¹³C{¹H} NMR (101 MHz, CDCl₃): δ 148.3, 142.2, 127.1, 123.7, 45.8.

m.p. / °C: 58-63 (DSC).

Characterisation data are consistent with literature values.¹⁸⁷

3-Chloro-3-(2-trifluoromethoxy)-3*H*-diazirine (65)



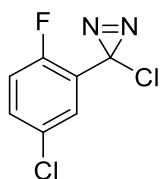
Synthesised according to **GP-4** from 2-(trifluoromethoxy)benzamidinium hydrochloride (1.20 g, 10.0 mmol), LiCl (1.16 g, 27.5 mmol), and NaOCl (73 mL, 35 mmol). Purification by column chromatography (silica gel; pentane) afforded a colourless liquid (219 mg, 0.926 mmol, 19%).

¹H NMR (400 MHz, CDCl₃): δ 7.62 (dd, *J* = 7.7, 0.4 Hz, 1H), 7.46 (ddd, *J* = 8.3, 7.5, 1.7 Hz, 1H), 7.34 (td, *J* = 7.6, 1.2 Hz, 1H), 7.32 – 7.29 (m, 1H).

¹³C NMR (101 MHz, CDCl₃): δ 147.5 (q, *J* = 1.8 Hz), 131.9, 129.4, 128.0, 127.3, 121.4 (q, *J* = 1.6 Hz), 120.5 (q, *J* = 258.9 Hz), 43.1.

¹⁹F NMR (376 MHz, CDCl₃): δ -57.12 (s).

3-Chloro-3-(2-fluoro-5-chlorophenyl)-3*H*-diazirine (66)



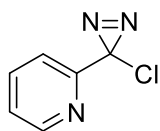
Synthesised according to **GP-4** from 2-fluoro-5-chlorobenzamidine hydrochloride (2.09 g, 10.0 mmol), LiCl (2.33 g, 55 mmol), and NaOCl (146 mL, 70 mmol). Purification by column chromatography (silica gel; pentane) afforded a colourless liquid (1.47 g, 7.18 mmol, 72%).

¹H NMR (400 MHz, CDCl₃): δ 7.50 (dd, *J* = 6.3, 2.6 Hz, 1H), 7.35 (ddd, *J* = 8.8, 4.2, 2.6 Hz, 1H), 7.04 (dd, *J* = 10.1, 8.8 Hz, 1H).

¹³C{¹H} NMR (101 MHz, CDCl₃): δ 159.0 (d, *J* = 254.3 Hz), 132.0 (d, *J* = 8.4 Hz), 129.9 (d, *J* = 3.6 Hz), 129.2 (d, *J* = 2.2 Hz), 124.2 (d, *J* = 12.9 Hz), 118.2 (d, *J* = 22.5 Hz), 42.4.

¹⁹F NMR (376 MHz, CDCl₃): δ -115.89 (ddd, *J* = 10.1, 6.3, 4.2 Hz).

2-(3-chloro-3*H*-diazirin-3-yl)pyridine (68)



Synthesised according to **GP-4** from 2-pyridine carboximidamide hydrochloride (788 mg, 5.0 mmol), LiCl (1.16 g, 27.5 mmol), and NaOCl (73 mL, 35 mmol). Purification by column chromatography (silica gel; 10% Et₂O in pentane) afforded a yellow liquid (309 mg, 2.01 mmol, 40%).

¹H NMR (400 MHz, CDCl₃): δ 8.55 (app dt, *J* = 4.8, 1.3 Hz, 1H), 7.82 (td, *J* = 7.9, 1.8 Hz, 1H), 7.72 (app dt, *J* = 7.9, 1.3 Hz, 1H), 7.32 (ddd, *J* = 7.6, 4.8, 1.1 Hz, 1H).

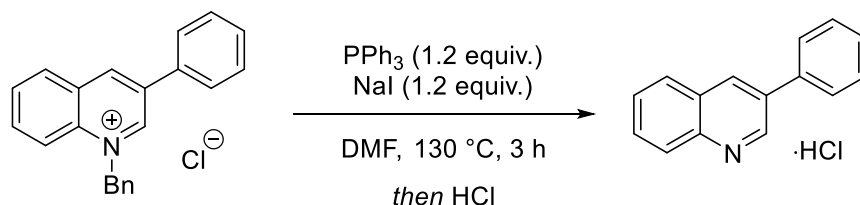
¹³C{¹H} NMR (101 MHz, CDCl₃): δ 153.7, 149.2, 137.1, 123.6, 122.8, 47.4.

HRMS: calcd. for C₆H₅N³⁵Cl [M-N₂+H]⁺: 126.0106; found (ESI⁺): 126.0113.

Characterisation data are consistent with literature values.¹⁸⁷

5.3.7 Functionalisation of Azinium Salts

6-Fluoro-3-phenylquinolinium hydrochloride



A round bottom flask was charged with 1-benzyl-3-phenylquinolin-1-ium chloride (66 mg, 0.2 mmol), PPh₃ (63 mg, 0.24 mmol), NaI (36 mg, 0.24 mmol) and DMF (2 mL). The solution was heated to 130 °C and stirred for 3 h. After cooling to rt, water (2 mL) and the mixture was poured onto Et₂O (5 mL). The ether layer was separated and the aqueous layer was washed with Et₂O (3 × 5 mL). The combined organic portions were dried over Na₂SO₄, filtered, and concentrated *in vacuo*. Et₂O (5 mL) was then added followed by HCl (4 M in dioxane, 0.1 mL). The resulting precipitate was isolated by filtration to afford the product as a colourless powder (38.1 mg, 0.158 mmol, 79%).

¹H-NMR (400 MHz, DMSO-*d*₆): δ 9.51 (d, *J* = 2.3 Hz, 1H), 9.13 (d, *J* = 1.1 Hz, 1H), 8.29 – 8.21 (m, 2H), 8.02 – 7.94 (m, 3H), 7.84 (ddd, *J* = 8.0, 6.9, 1.1 Hz, 1H), 7.65 – 7.58 (m, 2H), 7.56 – 7.49 (m, 1H).

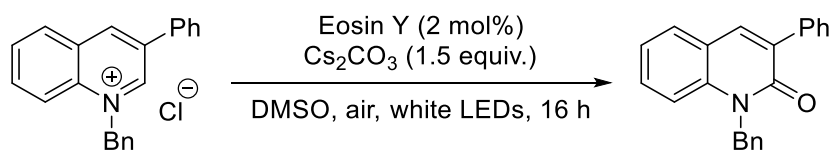
¹³C{¹H} NMR (101 MHz, DMSO-*d*₆): δ 145.6, 139.7, 134.9, 133.5, 132.9, 129.4, 129.2, 129.1, 128.3, 127.5, 123.0.

ν_{max} (neat) / cm⁻¹: 2536, 2030, 1571, 1501, 1360, 1328, 1301, 1150, 1030, 900.

HRMS: calcd. for C₁₅H₁₂N [M-Cl]⁺: 206.0964; found (ESI⁺): 206.0967.

m.p. / °C: 160 (decomp.)

1-Benzyl-3-phenylquinolin-2(1H)-one



According to literature procedure,²¹⁰ a microwave tube was charged with the quinolinium salt (66 mg, 0.2 mmol), Eosin Y (2.8 mg, 0.004 mmol, 2.0 mol%), Cs₂CO₃ (98 mg, 0.3 mmol) and DMSO (2 mL). The reaction mixture was stirred under constant irradiation (white LEDs, 6200K) overnight. The reaction mixture was poured onto EtOAc (10 mL), filtered through a silica plug and washed through with EtOAc. The filtrate was washed with water (10 mL) and the aqueous layer was extracted with EtOAc (3 × 10 mL). The combined organic portions were washed with brine, dried over MgSO₄, filtered, and concentrated *in vacuo*. Purification by column chromatography (silica gel; 20% EtOAc in CyH) afforded the product as a colourless solid (37.5 mg, 0.120 mmol, 60%).

¹H NMR (400 MHz, CDCl₃): δ 7.88 (s, 1H), 7.79 (dd, *J* = 7.2, 1.8 Hz, 2H), 7.63 (dd, *J* = 7.8, 1.5 Hz, 1H), 7.50 – 7.36 (m, 4H), 7.34 – 7.28 (m, 5H), 7.26 – 7.18 (m, 2H), 5.64 (s, 2H).

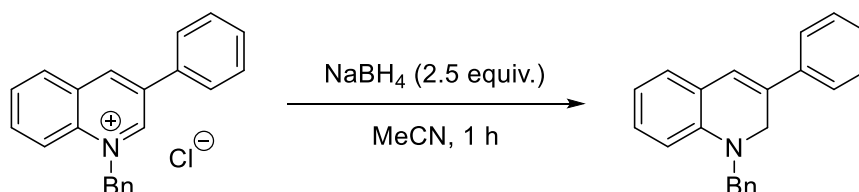
¹³C{¹H} NMR (101 MHz, CDCl₃): δ 161.8, 139.3, 137.5, 136.8, 136.7, 132.5, 130.4, 129.2, 129.1, 128.9, 128.3, 128.3, 127.4, 127.0, 122.4, 121.2, 115.0, 46.7.

ν_{max} (neat) / cm⁻¹: 1633, 1576, 1493, 1448, 1238, 1216, 1183.

HRMS: calcd. for C₂₂H₁₇NO [M+H]⁺: 312.1383; found (ESI⁺): 312.1385.

m.p. / °C: 102-104.

1-Benzyl-3-phenyl-1,2-dihydroquinoline



To a suspension of quinolinium salt (66 mg, 0.2 mmol) in MeCN (1 mL) cooled to 0 °C was added NaBH₄ (19 mg, 0.5 mmol) in one portion. Dissolution of the solids was accompanied by formation of a fluorescent yellow colour. The reaction was stirred for 1 h, then quenched with sat. aqueous NH₄Cl (5 mL) and diluted with CH₂Cl₂ (5 mL). The CH₂Cl₂ layer was separated and the aqueous layer extracted with CH₂Cl₂ (3 × 10 mL). The combined organic

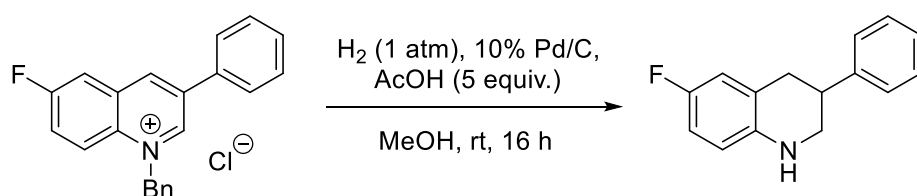
portions were dried over Na_2SO_4 , filtered and concentrated *in vacuo* to afford the crude product as a fluorescent yellow oil (51.1 mg, 0.172 mmol, 86%).

^1H NMR (400 MHz, CDCl_3): δ 7.47 – 7.40 (m, 2H), 7.36 (dt, $J = 8.2, 5.5$ Hz, 6H), 7.32 – 7.24 (m, 2H), 7.03 (app t, $J = 7.5$ Hz, 2H), 6.85 (s, 1H), 6.65 (app t, $J = 7.5$ Hz, 1H), 6.56 (d, $J = 8.1$ Hz, 1H), 4.55 (d, $J = 1.4$ Hz, 2H), 4.54 (s, 2H).

$^{13}\text{C}\{^1\text{H}\}$ NMR (101 MHz, CDCl_3): δ 144.5, 138.0, 137.3, 130.5, 129.3, 128.8, 128.6, 127.9, 127.7, 127.3, 127.2, 124.3, 122.7, 122.4, 117.2, 110.1, 54.0, 52.2.

HRMS: calcd. for $\text{C}_{22}\text{H}_{20}\text{N}$ $[\text{M}+\text{H}]^+$: 298.1590; found (ESI⁺): 298.1591.

3-Phenyl-6-fluoro-1,2,3,4-tetrahydroquinoline



Prior to reaction, MeOH was degassed by sparging with dinitrogen for 30 minutes. An oven-dried round-bottom flask was charged with 1-benzyl-3-phenyl-6-fluoroquinolinium chloride (70 mg, 0.2 mmol) and Pd/C (30 mg), then sealed with a rubber septum. The flask was evacuated and back-filled with dinitrogen three times, then degassed MeOH (2 mL) was added slowly followed by AcOH (57 μL , 1.0 mmol). The flask was then evacuated by use of a water aspirator until boiling of the solvent was observed and then filled with H_2 *via* balloon; this process was repeated five times. The reaction was stirred for 16 h at rt under balloon pressure of hydrogen. The reaction mixture was filtered through Celite and washed with MeOH (10 mL). The solvent was removed *in vacuo*, then water (10 mL) and Et_2O (10 mL) were added. The biphasic mixture was separated, and the organic phase was washed with sat. aqueous NaHCO_3 (20 mL). The combined aqueous portions were extracted with Et_2O (3×5 mL) and the combined organic portions were dried over Na_2SO_4 , filtered, and concentrated *in vacuo*. Purification by column chromatography (silica gel; 10% EtOAc in CyH) afforded the product as a colourless powder (41.8 mg, 0.184 mmol, 92%).

^1H NMR (400 MHz, CDCl_3): δ 7.44 – 7.33 (m, 2H), 7.32 – 7.24 (m, 3H), 6.76 (m, 2H), 6.51 (dd, $J = 9.5, 4.8$ Hz, 1H), 3.94 (s, 1H), 3.48 (ddd, $J = 11.2, 3.6, 1.9$ Hz, 1H), 3.34 (app t, $J = 10.7$ Hz, 1H), 3.16 (tdd, $J = 10.0, 5.7, 3.6$ Hz, 1H), 3.09 – 2.93 (m, 2H).

$^{13}\text{C}\{^1\text{H}\}$ NMR (101 MHz, CDCl_3): δ 155.7 (d, $J = 235.1$ Hz), 143.6, 140.4 (d, $J = 1.8$ Hz), 128.8, 127.3, 126.9, 122.8 (d, $J = 6.7$ Hz), 115.7 (d, $J = 21.7$ Hz), 115.0 (d, $J = 7.7$ Hz), 113.7 (d, $J = 22.5$ Hz), 48.6, 38.7, 34.7.

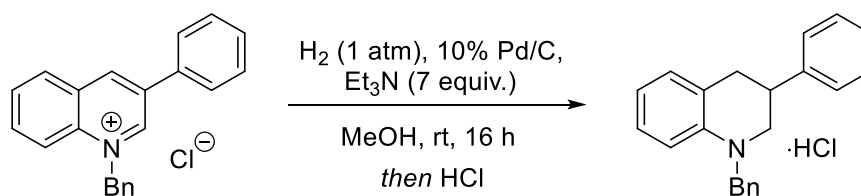
^{19}F NMR (376 MHz, CDCl_3): δ -128.11 (app td, $J = 8.8, 4.8$ Hz).

ν_{max} (neat) / cm^{-1} : 3390, 1503, 1490, 1236, 1214, 1140, 1098, 1078, 952, 869.

HRMS: calcd. for $\text{C}_{15}\text{H}_{15}\text{FN}$ $[\text{M}+\text{H}]^+$: 228.1183; found (ESI $^+$): 228.1192.

m.p. / $^{\circ}\text{C}$: 112-113.

3-Phenyl-1,2,3,4-tetrahydroquinoline



Prior to reaction, MeOH was degassed by sparging with dinitrogen for 30 minutes. An oven-dried round-bottom flask was charged with 1-benzyl-3-phenylquinolinium chloride (66 mg, 0.2 mmol) and Pd/C (30 mg), then sealed with a rubber septum. The flask was evacuated and back-filled with dinitrogen three times, then degassed MeOH (2 mL) was added slowly followed by Et $_3$ N (0.20 mL, 1.4 mmol). The flask was then evacuated by use of a water aspirator until boiling of the solvent was observed and then filled with H $_2$ *via* balloon; this process was repeated five times. The reaction was then stirred for 16 h under balloon pressure of hydrogen. The reaction mixture was filtered through Celite and eluted with MeOH (10 mL). The solvent was removed *in vacuo* and the resulting residue was taken up in Et $_2$ O. The solids were removed by filtration, then HCl (4 M in dioxane, 0.1 mL) was added to the filtrate. After standing in a fridge (4 $^{\circ}\text{C}$) overnight, the resulting solid was isolated by filtration to afford the product as a yellow solid (41.6 mg, 0.124 mmol, 62%).

^1H NMR (400 MHz, CDCl_3): δ 7.36 – 7.18 (m, 10H), 6.98 (dd, $J = 7.4, 1.6$ Hz, 1H), 6.96 – 6.89 (m, 1H), 6.56 – 6.48 (m, 2H), 4.59 (d, $J = 16.9$ Hz, 1H), 4.49 (d, $J = 16.9$ Hz, 1H), 3.51 (app q, $J = 11.3$ Hz, 1H), 3.44 (ddd, $J = 11.3, 4.4, 2.0$ Hz, 1H), 3.26 – 3.12 (m, 2H), 3.05 (dd, $J = 15.5, 11.3$ Hz, 1H), 2.92 (ddd, $J = 15.5, 4.4, 2.0$ Hz, 1H).

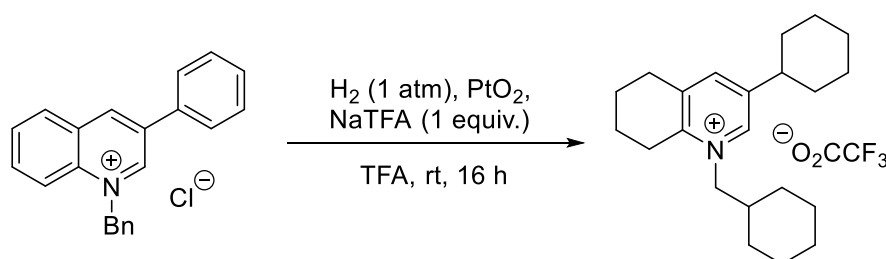
$^{13}\text{C}\{^1\text{H}\}$ NMR (101 MHz, CDCl_3): δ 144.4, 143.4, 138.9, 128.9, 128.4, 128.4, 127.2, 127.0, 126.7, 126.6, 126.5, 121.8, 115.5, 110.8, 55.7, 54.2, 37.7, 34.8.

ν_{\max} (neat) / cm^{-1} : 1601, 1495, 1449, 1354, 1336, 1276, 1241, 1112, 1076, 1058, 1022, 962.

HRMS: calcd. for $\text{C}_{22}\text{H}_{22}\text{N}$ $[\text{M}+\text{H}]^+$: 300.1747; found (ESI⁺): 300.1747.

m.p. / °C: 145 (decomp.)

3-Cyclohexyl-1-(cyclohexylmethyl)-5,6,7,8-tetrahydroquinolin-1-ium trifluoroacetate



Prior to reaction, trifluoroacetic acid (TFA) was degassed by sparging with dinitrogen for 30 minutes. According to the literature procedure,²¹⁷ an oven-dried round-bottom flask was charged with 1-benzyl-3-phenylquinolinium chloride (66 mg, 0.2 mmol), PtO₂ hydrate (10 mg), and sodium trifluoroacetate (27 mg, 0.2 mmol), then sealed with a rubber septum. The flask was evacuated and back-filled with dinitrogen three times, then degassed TFA (1 mL) was added slowly. The flask was evacuated by use of a water aspirator until boiling of the solvent was observed and then filled with H₂ *via* balloon; this process was repeated five times. The reaction was then stirred for 16 hrs at rt under balloon pressure. The reaction mixture was diluted with EtOAc (5 mL) and filtered through Celite. The organics were washed with H₂O (10 mL) and the aqueous layer extracted with EtOAc (3 × 10 mL). The combined organics were dried over Na₂SO₄, filtered, and concentrated *in vacuo* to afford the product as a viscous yellow oil (55.6 mg, 0.131 mmol, 65%).

¹H NMR (400 MHz, DMSO-*d*₆): δ 8.21 (s, 1H), 7.87 (s, 1H), 4.33 (d, *J* = 7.2 Hz, 2H), 3.21 – 2.84 (m, 4H), 2.64 (d, *J* = 10.6 Hz, 1H), 2.15 – 0.98 (m, 25H).

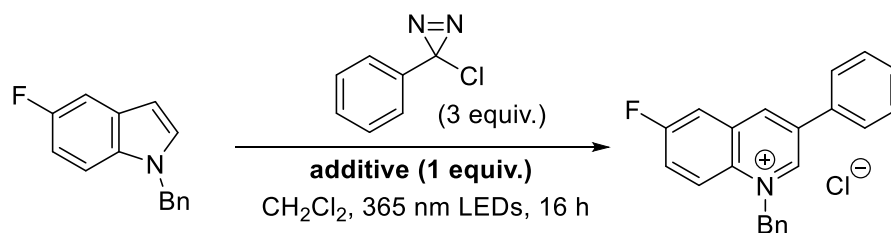
¹³C{¹H} NMR (101 MHz, DMSO-*d*₆): δ 158.2 (q, *J* = 34.7 Hz), 151.4, 143.7, 143.1, 142.5, 138.6, 116.2 (q, *J* = 294.8 Hz), 61.9, 36.8, 32.8, 32.7, 29.3, 28.2, 26.0, 25.8, 25.6, 25.1, 25.0, 21.2, 20.2.

¹⁹F NMR (376 MHz, DMSO-*d*₆): δ -74.32 (s).

ν_{\max} (neat) / cm^{-1} : 2928, 2856, 1736, 1450, 1180, 1132, 932.

HRMS: calcd. for $\text{C}_{22}\text{H}_{34}\text{N}$ $[\text{M}-\text{O}_2\text{CCF}_3]^+$: 312.2686; found (ESI⁺): 312.2702.

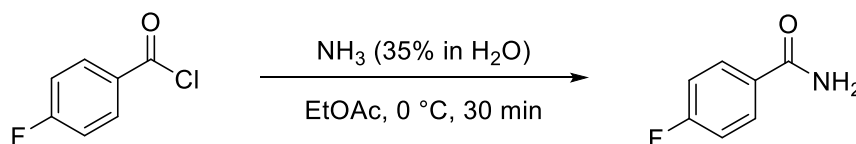
5.3.8 Robustness Screen



General Procedure: A 10 mL microwave tube was charged with 5-fluoroindole (46 mg, 0.2 mmol), the additive (0.2 mmol, if solid, liquid additives were added prior to addition of diazirine) and 4,4'-bis(trifluoromethyl)-1,1'-biphenyl (internal standard for ^{19}F NMR spectroscopy) which was then sealed, evacuated and flushed with dinitrogen 3 times. Anhydrous CH_2Cl_2 (2 mL) was then added followed by 3-chloro-3-phenyldiazirine (92 mg, 0.6 mmol) and an aliquot taken for initial ^{19}F NMR analysis. The cap of the reaction flask was then sealed with electrical tape. The reaction mixture was stirred under constant irradiation with UV light (365 nm, 18 W LED, 5 cm from light source) overnight. If solids precipitated, the reaction was diluted with MeOH until homogenous and an aliquot was taken and analysed by ^{19}F NMR spectroscopy.

Synthesis of additives for robustness screen

4-Fluorobenzamide



NH_3 (35% in H_2O , 6.4 mL) was added to a flask containing EtOAc (30 mL) and cooled to $0\text{ }^\circ\text{C}$. 4-Fluorobenzoyl chloride (0.47 mmol, 4.0 mmol) was then added drop-wise. The resulting mixture was stirred at $0\text{ }^\circ\text{C}$ for 30 mins. The layers were separated and the organic layer washed with water (20 mL) and brine (20 mL). The organics were dried over MgSO_4 , filtered, and concentrated *in vacuo* to afford the pure product as a colourless solid (539 mg, 3.87 mmol, 97%).

^1H NMR (400 MHz, $\text{DMSO}-d_6$): δ 7.89 – 7.78 (m, 2H), 7.18 – 7.07 (m, 2H), 5.93 (br s, 2H).

$^{13}\text{C}\{^1\text{H}\}$ NMR (101 MHz, $\text{DMSO}-d_6$): δ 166.8, 163.9 (d, $J = 248.3$ Hz), 130.8 (d, $J = 2.9$ Hz), 130.1 (d, $J = 9.0$ Hz), 115.1 (d, $J = 21.6$ Hz).

¹⁹F NMR (376 MHz, DMSO-d₆): δ -109.60 (tt, *J* = 8.9, 5.5 Hz).

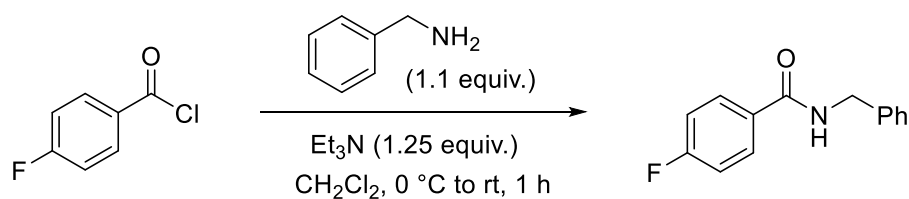
ν_{max} (neat) / cm⁻¹: 3307, 3140, 1669, 1621, 1598, 1586, 1413, 1396, 1224, 1156, 843, 825.

HRMS: calcd. for C₇H₇FNO [M+H]⁺: 140.0506; found (ESI⁺): 140.0514.

m.p. / °C: 156-159 (lit. 155-157).²⁷²

Characterisation data are consistent with literature values.²⁷³

***N*-Benzyl-4-fluorobenzamide**



According to the literature procedure,²⁷⁴ to a solution of benzylamine (0.12 mL, 1.10 mmol) in CH₂Cl₂ (2 mL) was added Et₃N (0.18 mL, 1.25 mmol) which was then cooled to 0 °C by use of an ice-water bath. 4-Fluorobenzoyl chloride (0.12 mL, 1.1 mmol) was then added drop-wise after which the mixture was warmed to rt and stirred for 1 hr. The solvent was removed *in vacuo* and residue filtered through a silica plug eluting with 1:1 EtOAc/CyH to afford the pure product as a colourless solid (205 mg, 89%).

¹H NMR (400 MHz, CDCl₃): δ 7.85 – 7.74 (m, 2H), 7.39 – 7.23 (m, 5H), 7.07 (app t, *J* = 8.6 Hz, 2H), 6.62 (s, 1H), 4.60 (d, *J* = 5.7 Hz, 2H).

¹³C{¹H} NMR (101 MHz, CDCl₃): δ 166.5, 164.8 (d, *J* = 251.9 Hz), 138.2, 130.6 (d, *J* = 3.2 Hz), 129.5 (d, *J* = 8.9 Hz), 128.9, 128.0, 127.8, 115.7 (d, *J* = 21.9 Hz), 44.3.

¹⁹F NMR (376 MHz, CDCl₃): δ -108.10 (tt, *J* = 13.7, 5.2 Hz).

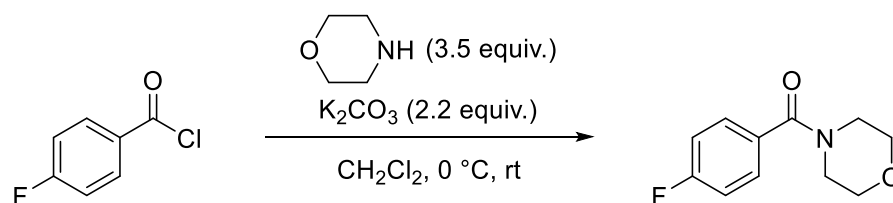
ν_{max} (neat) / cm⁻¹: 3319, 1639, 1592, 1547, 1495, 1450, 1420, 1318, 1289, 1225, 1158, 987, 853.

HRMS: calcd. for C₁₄H₁₃FNO [M+H]⁺: 230.0976; found (ESI⁺): 230.0975.

m.p. / °C: 142-145 (lit. 140-141).²⁷⁵

Characterisation data are consistent with literature values.²⁷⁶

(4-Fluorophenyl)(morpholino)methanone



According to the literature procedure,²⁷⁷ to a solution of morpholine (1.23 mL, 14.0 mmol) in CH_2Cl_2 (8 mL) was added K_2CO_3 (1.22 g, 14 mmol) and the suspension cooled to $0\text{ }^\circ\text{C}$ by use of an ice-water bath. 4-Fluorobenzoyl chloride (0.47 mL, 4.0 mmol) was then added drop-wise after which the reaction was warmed to rt and stirred for 24 hrs. The resulting suspension was filtered to remove any solids and washed with 1 M HCl (10 mL) and saturated aq. $NaHCO_3$ (10 mL). The organic layer was removed and the aqueous layer extracted with CH_2Cl_2 (3×10 mL). The combined organics were washed with brine, dried over $MgSO_4$, filtered, and concentrated *in vacuo* to afford the pure product as a colourless solid (593 mg, 71%).

1H NMR (400 MHz, $CDCl_3$): δ 7.54 – 7.34 (m, 2H), 7.24 – 7.01 (m, 2H), 4.06 – 3.27 (m, 8H).

$^{13}C\{^1H\}$ NMR (101 MHz, $CDCl_3$): δ 169.5, 163.5 (d, $J = 250.3$ Hz), 131.3 (d, $J = 3.5$ Hz), 129.5 (d, $J = 8.6$ Hz), 115.7 (d, $J = 21.8$ Hz), 66.9, 48.3, 42.8.

^{19}F NMR (376 MHz, $CDCl_3$): δ -109.88 (dd, $J = 8.5, 5.2$ Hz).

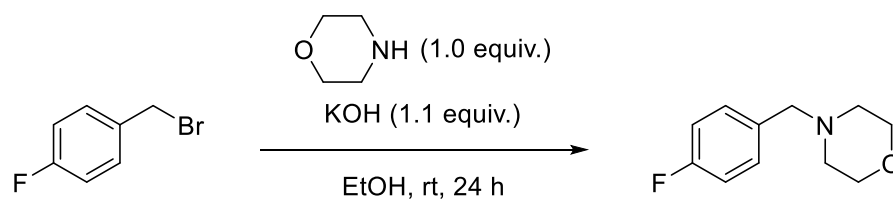
ν_{max} (neat) / cm^{-1} : 2857, 1627, 1602, 1509, 1428, 1276, 1256, 1218, 1112, 1021, 1010, 843.

HRMS: calcd. for $C_{11}H_{13}FNO_2$ $[M+H]^+$: 210.0925; found (ESI⁺): 210.0925.

m.p. / $^\circ\text{C}$: 39-42.

Characterisation data are consistent with literature values.²⁷⁸

4-(4-Fluorobenzyl)morpholine



According to a modified literature procedure,²⁷⁹ To a solution of morpholine (0.35 mL, 2.0 mmol) in EtOH (8 mL) was added 4-fluorobenzyl bromide (0.50 mL, 4.0 mmol) and KOH

(247 mg, 4.4 mmol) at rt and the resulting solution was stirred for 24 hrs. Water (5 mL) was then added followed by EtOAc (10 mL). The organic layer was separated and the aqueous layer extracted with EtOAc (3 × 10 mL). The combined organics were washed with brine, dried over MgSO₄, filtered, and concentrated *in vacuo*. Purification by column chromatography (silica gel; 20% EtOAc in CyH with 1% Et₃N) afforded the product as a colourless oil (331 mg, 1.69 mmol, 42%).

¹H NMR (400 MHz, CDCl₃): δ 7.28 (dd, *J* = 8.3, 5.5 Hz, 2H), 6.99 (app t, *J* = 8.5 Hz, 2H), 3.73 – 3.66 (m, 4H), 3.45 (s, 2H), 2.42 (m, 4H).

¹³C{¹H} NMR (101 MHz, CDCl₃): δ 162.2 (d, *J* = 245.1 Hz), 133.5 (d, *J* = 3.1 Hz), 130.7 (d, *J* = 7.8 Hz), 115.2 (d, *J* = 21.2 Hz), 67.1, 62.7, 53.6.

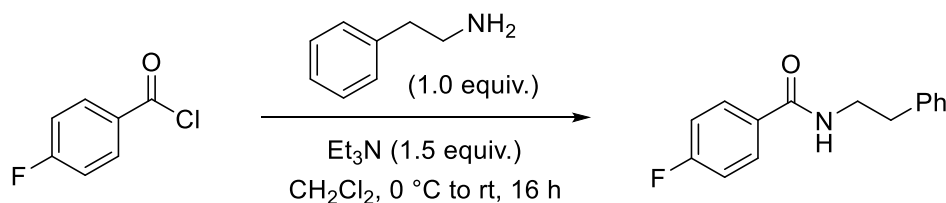
¹⁹F NMR (376 MHz, CDCl₃): δ -115.76 (tt, *J* = 8.8, 5.5 Hz).

ν_{max} (neat) / cm⁻¹: 2804, 1602, 1509, 1454, 1367, 1349, 1263, 1219, 1114, 1006, 865, 827.

HRMS: calcd. for C₁₄H₁₃FNO [M+H]⁺: 196.1132; found (ESI⁺): 196.1140.

Characterisation data are consistent with literature values.²⁸⁰

***N*-Phenethyl-4-fluorobenzamide**



To a solution of phenethylamine (0.63 mL, 5.0 mmol) and Et₃N (1.05 mL, 7.5 mmol) in CH₂Cl₂ (10 mL) was added 4-fluorobenzoyl chloride (0.65 mL, 5.5 mmol) drop-wise at 0 °C. After stirring at 0 °C for 30 mins, the reaction was warmed to rt and stirred overnight. The reaction mixture was then poured onto water (20 mL) and the organic layer separated. The aqueous layer was then extracted with EtOAc (3 × 10 mL). The combined organics were washed with 1 M HCl (10 mL) followed by sat. aqueous NaHCO₃ (10 mL). The organics were then dried over MgSO₄, filtered, and concentrated *in vacuo*. Recrystallisation from EtOH afforded the product as a colourless solid (1.11 g, 4.57 mmol, 91%)

¹H NMR (400 MHz, CDCl₃): δ 7.75 – 7.64 (m, 1H), 7.39 – 7.30 (m, 1H), 7.29 – 7.18 (m, 2H), 7.14 – 7.02 (m, 1H), 6.07 (s, 1H), 3.72 (dd, *J* = 6.9, 6.1 Hz, 1H), 2.94 (t, *J* = 6.9 Hz, 1H).

$^{13}\text{C}\{^1\text{H}\}$ NMR (101 MHz, CDCl_3): δ 166.6, 164.8 (d, $J = 251.8$ Hz), 138.9, 130.9 (d, $J = 3.2$ Hz), 129.2 (d, $J = 8.9$ Hz), 128.9, 128.8, 126.8, 115.7 (d, $J = 21.9$ Hz), 41.3, 35.8.

^{19}F NMR (376 MHz, CDCl_3): δ -108.34 (tt, $J = 8.4, 5.2$ Hz).

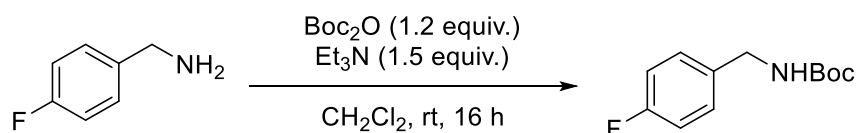
ν_{max} (neat) / cm^{-1} : 3346, 1639, 1601, 1543, 1501, 1314, 1291, 1231, 1156, 1095, 1007, 845.

HRMS: calcd. for $\text{C}_{15}\text{H}_{15}\text{FNO}$ $[\text{M}+\text{H}]^+$: 244.1132; found 244.1137.

m.p. / $^{\circ}\text{C}$: 123-126.²⁸¹

Characterisation data are consistent with literature values.²⁸²

***N*-Boc-4-fluorobenzylamine**



To a solution of 4-fluorobenzylamine (0.46 mL, 4.0 mmol) and Et_3N (0.84 mL, 6.0 mmol) in CH_2Cl_2 (20 mL) was added Boc_2O (1.10 mL, 4.8 mmol) drop-wise at rt. The mixture was stirred overnight after which the reaction was quenched with 1 M HCl (10 mL) and the organic layer separated. The aqueous layer was then extracted with Et_2O (3×10 mL). The combined organics were washed with brine (20 mL) and then dried over MgSO_4 , filtered, and concentrated *in vacuo* to afford the product as a colourless solid (868 mg, 3.85 mmol, 96%)

^1H NMR (400 MHz, CDCl_3): δ 7.30 – 7.17 (m, 2H), 7.07 – 6.95 (m, 2H), 4.88 (br s, 1H), 4.28 (s, 1H), 4.26 (s, 1H), 1.45 (s, 9H).

$^{13}\text{C}\{^1\text{H}\}$ NMR (101 MHz, CDCl_3): δ 162.2 (d, $J = 245.2$ Hz), 156.0, 134.9, 129.2 (d, $J = 8.0$ Hz), 115.5 (d, $J = 21.4$ Hz), 79.7, 44.1, 28.5.

^{19}F NMR (376 MHz, CDCl_3): δ -115.47 (tt, $J = 9.1, 5.3$ Hz).

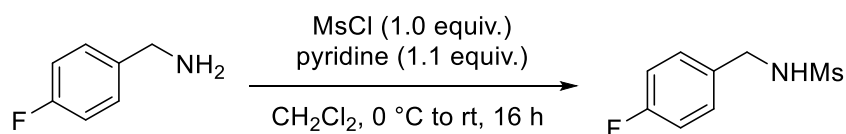
ν_{max} (neat) / cm^{-1} : 3362, 1676, 1501, 1491, 1464, 1365, 1242, 1218, 1151, 1121, 1097, 1046, 834.

HRMS: calcd. for $\text{C}_{12}\text{H}_{17}\text{FNO}_2$ $[\text{M}+\text{H}]^+$: 226.1238; found (ESI⁺): 226.1249.

m.p. / $^{\circ}\text{C}$: 68-71 (lit. 64-66).²⁸³

Characterisation data are consistent with literature values.²⁸⁴

N-methanesulfonyl-4-fluorobenzylamine



To a flame-dried flask under an atmosphere of dinitrogen was added 4-fluorobenzylamine (0.46 mL, 4.0 mmol), pyridine (0.36 mL, 4.4 mmol) and anhydrous CH₂Cl₂ (12 mL). After cooling to 0 °C, MsCl (1.10 mL, 4.8 mmol) was added drop-wise to afford a yellow solution. The reaction mixture was warmed to rt and stirred overnight. The reaction was quenched with 1 M HCl (10 mL) and the organic layer separated. The aqueous layer was then extracted with CH₂Cl₂ (3 × 10 mL). The combined organics were washed with brine (20 mL) and then dried over MgSO₄, filtered, and concentrated *in vacuo* to afford the product as a yellow solid (298 mg, 1.46 mmol, 37%)

¹H NMR (400 MHz, CDCl₃): δ 7.35 – 7.27 (m, 2H), 7.07 – 6.99 (m, 2H), 5.15 (t, *J* = 6.1 Hz, 1H), 4.25 (d, *J* = 6.1 Hz, 2H), 2.82 (s, 3H).

¹³C{¹H} NMR (101 MHz, CDCl₃): δ 162.2 (d, *J* = 245.2 Hz), 156.0, 134.9, 129.2 (d, *J* = 8.0 Hz), 115.5 (d, *J* = 21.4 Hz), 79.7, 44.1, 28.5.

¹⁹F NMR (376 MHz, CDCl₃): -114.01 (tt, *J* = 8.8, 5.3 Hz).

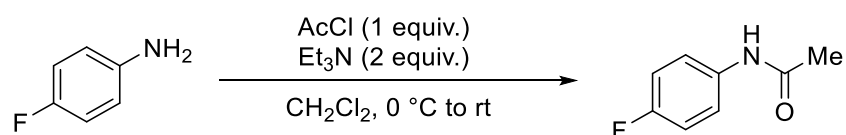
ν_{max} (neat) / cm⁻¹: 3235, 1607, 1507, 1434, 1406, 1297, 1229, 1153, 1133, 1061, 1008, 964, 849.

HRMS: calcd. for C₈H₁₀FNO₂SNa [M+Na]⁺: 226.0308; found 226.0310.

m.p. / °C: 57-60 (lit. 52-53).²⁸⁵

Characterisation data are consistent with literature values.²⁸⁵

N-(4-Fluorophenyl)acetamide



According to the literature procedure,²⁸⁶ to a solution of 4-fluoroaniline (0.19 mL, 2.0 mmol) in CH₂Cl₂ (10 mL) at 0 °C was added Et₃N (0.56 mL, 4.0 mmol). Acetyl chloride (0.16 mL, 2.2 mmol) was then added drop-wise after which the solution was warmed to rt and stirred for 90 mins. The reaction was quenched with sat. aqueous NH₄Cl (10 mL) and the CH₂Cl₂ layer

separated. The organic layer was washed with sat. aqueous NaHCO₃ (10 mL), dried over Na₂SO₄, filtered, and concentrated *in vacuo* to afford the pure product as a colourless solid (291 mg, 1.90 mmol, 95%).

¹H NMR (400 MHz, CDCl₃): δ 7.49 – 7.41 (m, 2H), 7.32 (br s, 1H), 7.04 – 6.96 (m, 2H), 2.16 (s, 3H).

¹³C{¹H} NMR (101 MHz, CDCl₃): δ 168.6, 159.5 (d, *J* = 243.5 Hz), 134.0 (d, *J* = 2.8 Hz), 122.0 (d, *J* = 7.8 Hz), 115.7 (d, *J* = 22.5 Hz), 24.5.

¹⁹F NMR (376 MHz, CDCl₃): δ -118.00 (tt, *J* = 8.5, 4.7 Hz).

ν_{max} (neat) / cm⁻¹: 3270, 1662, 1617, 1503, 1401, 1366, 1320, 1221, 1157, 1013, 831.

HRMS: calcd. for C₈H₉FNO [M+H]⁺: 154.0663; found (ESI⁺): 154.0664.

m.p. / °C: 153-156 (lit. 154-156).²⁸⁷

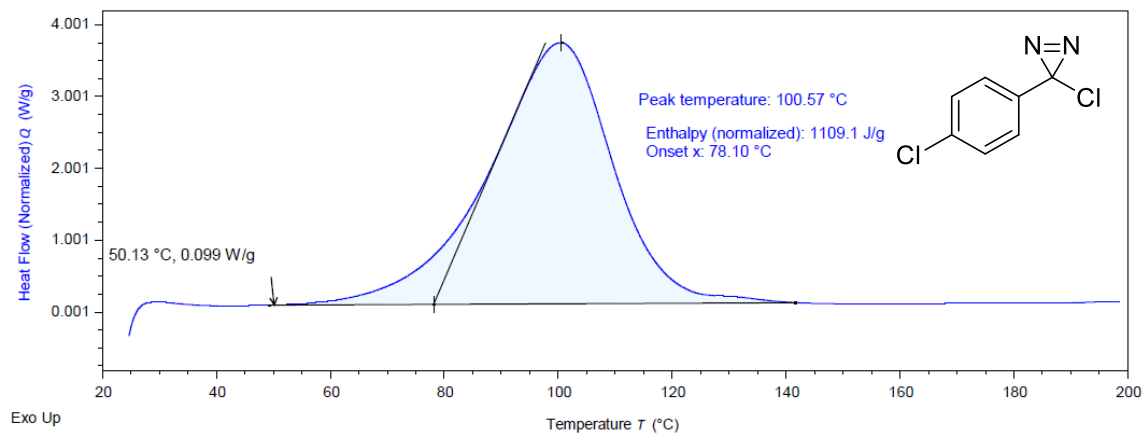
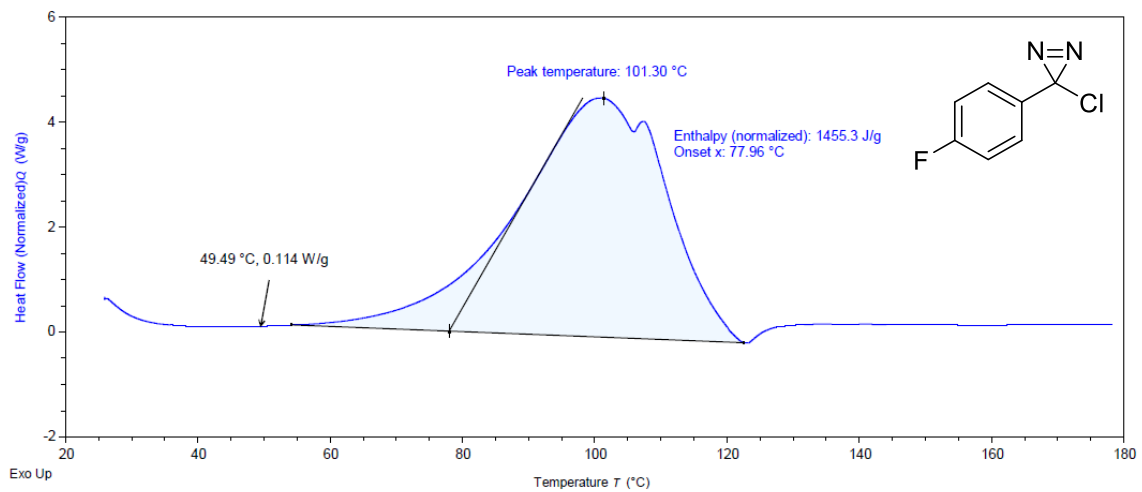
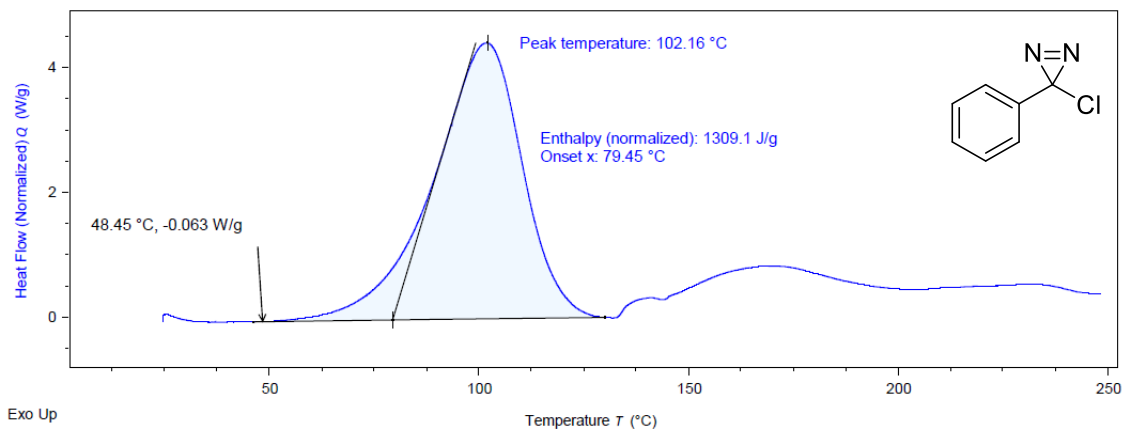
Characterisation data are consistent with literature values.²⁸⁸

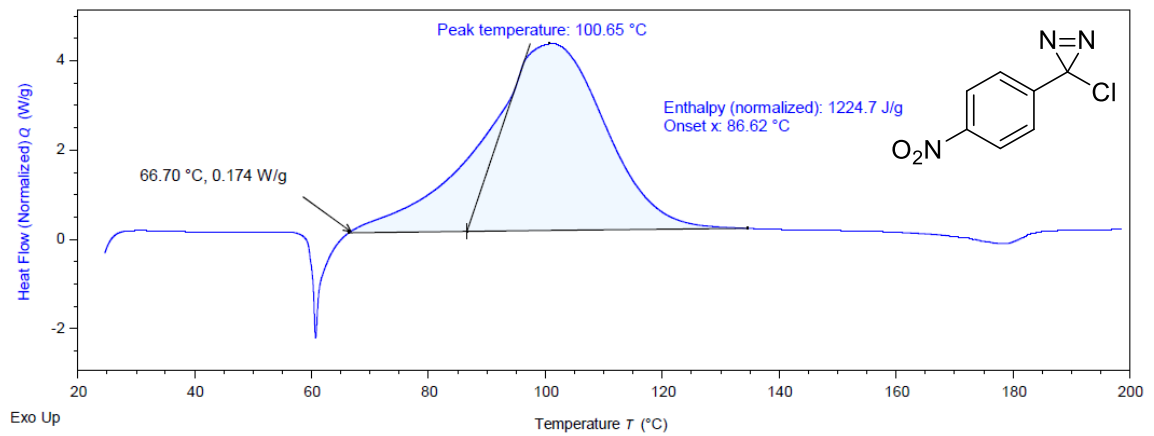
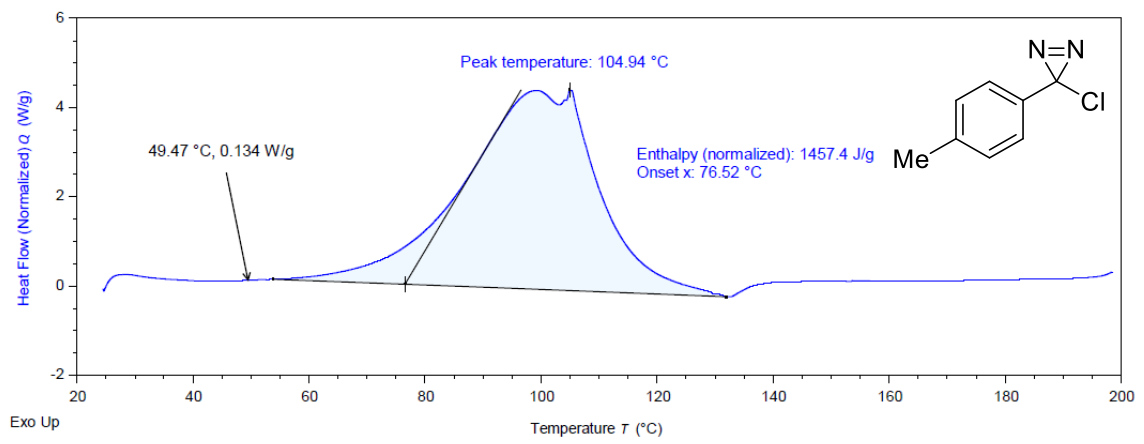
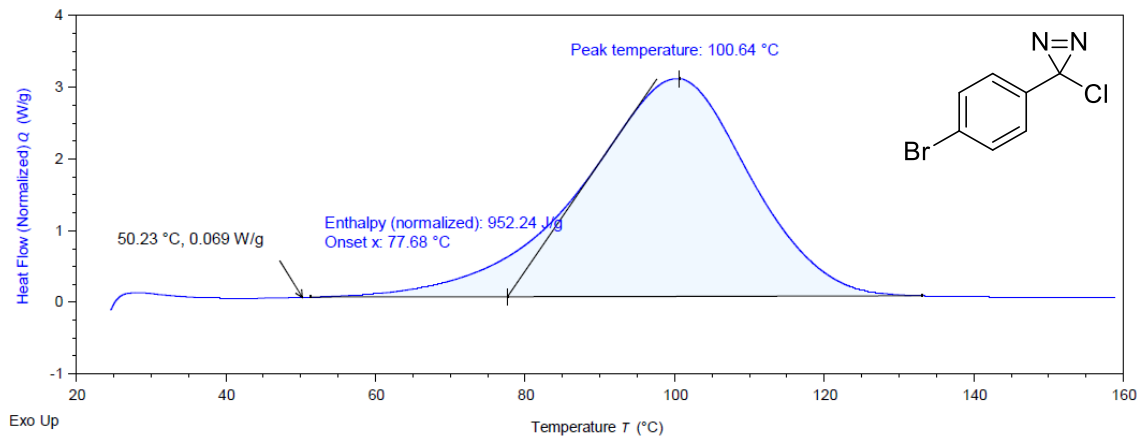
5.4 DSC Analysis

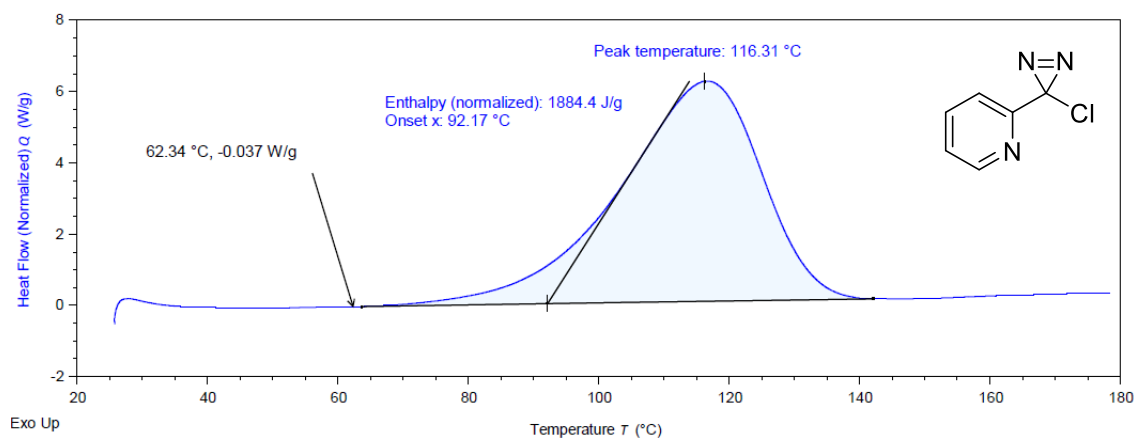
DSC Method:

Approximately 5 mg of material was weighed into a high pressure stainless-steel crucible (TA Instruments; #900808.901) using a 7-place balance. The crucible was fitted with a disposable gold-coated copper seal (TA Instruments; 900814.901), then sealed under air. After equilibrating the sample at 25 °C, the sample was heated at 5 °C/min. Initial measurements were made to 250 °C; repeat measurements were made to 200 °C or 180 °C once it was clear that the exotherms concluded <160 °C.

Temperatures denoted by the arrow are *T*_{init} and correspond to temperatures 0.01 W g⁻¹ above the baseline value (not necessarily 0 W g⁻¹). Exothermic events are positive in the *y*-axis.







6

References

- [1] M. E. Vitaku, D. T. Smith and J. T. Njardarson, *J Med Chem*, 2014, **57**, 16–16.
- [2] J. A. Joule, in *Advances in Heterocyclic Chemistry*, eds. E. F. V. Scriven and C. A. Ramsden, Academic Press, 2016, vol. 119, pp. 81–106.
- [3] M. Solà, *Nat. Chem.*, 2022, **14**, 585–590.
- [4] Joule, J. A. and Mills, K., *Heterocyclic Chemistry*, Wiley, 5th edn., 2010.
- [5] S. C. A. H. Pierrefixe and F. M. Bickelhaupt, *Chem. Eur. J.*, 2007, **13**, 6321–6328.
- [6] N. Martín and L. T. Scott, *Chem. Soc. Rev.*, 2015, **44**, 6397–6400.
- [7] A. R. Katritzky, C. A. Ramsden, J. A. Joule and V. Zhandkin, *Handbook of Heterocyclic Chemistry*, Elsevier, 3rd edn., 2010.
- [8] L. Nyulászi, *Chem. Rev.*, 2001, **101**, 1229–1246.
- [9] J. Clayden, N. Greaves and S. Warren, *Organic Chemistry*, Oxford University Press, 2nd edn., 2012.
- [10] F. F. Runge, *Ann. Phys.*, 1834, **107**, 65–78.
- [11] A. L. Harreus, in *Ullmann's Encyclopedia of Industrial Chemistry*, Wiley-VCH Verlag GmbH & Co. KGaA, 2000, pp. 615–617.
- [12] G. Collin and H. Höke, in *Ullmann's Encyclopedia of Industrial Chemistry*, John Wiley & Sons, Ltd, 2000.
- [13] R. L. Hinman and J. Lang, *J. Am. Chem. Soc.*, 1964, **86**, 3796–3806.
- [14] H. Walba and R. W. Isensee, *J. Org. Chem.*, 1961, **26**, 2789–2791.
- [15] G. P. Bean, *J. Chem. Soc., Chem. Commun.*, 1971, 421.
- [16] A. Cipiciani, S. Clementi, P. Linda, G. Marino and G. Savelli, *J. Chem. Soc. Perkin Trans. 2*, 1977, 1284–1287.
- [17] T. V. Sravanthi and S. L. Manju, *Eur. J. Pharm. Sci.*, 2016, **91**, 1–10.
- [18] V. Bhardwaj, D. Gumber, V. Abbot, S. Dhiman and P. Sharma, *RSC Adv.*, 2015, 15233–15266.
- [19] T. Zarganes-Tzitzikas, C. G. Neochoritis and A. Dömling, *ACS Med. Chem. Lett.*, 2019, **10**, 389–392.
- [20] C. Walsh, S. Garneau-Tsodikova and A. Howard-Jones, *Nat. Prod. Rep.*, 2006, **23**, 517–31.
- [21] M. Inman and C. J. Moody, *Chem Sci*, 2013, **4**, 29–41.
- [22] E. R. Radwanski and R. L. Last, *Plant Cell*, 1995, **7**, 921–934.
- [23] B. Robinson, *Chem. Rev.*, 1963, **63**, 373–401.

- [24] M. Małkosza and K. Wojciechowski, *Chem. Heterocycl. Compd.*, 2015, **51**, 210–222.
- [25] A. Batcho and W. Leimgruber, *Org. Synth.*, 1985, **63**, 214.
- [26] A. Reissert, *Berichte Dtsch. Chem. Ges.*, 1897, **30**, 1030–1053.
- [27] R. C. Larock and E. K. Yum, *J. Am. Chem. Soc.*, 1991, **113**, 6689–6690.
- [28] R. C. Larock, E. K. Yum and M. D. Refvik, *J. Org. Chem.*, 1998, **63**, 7652–7662.
- [29] E. K. Jaffe, *Acc. Chem. Res.*, 2016, **49**, 2509–2517.
- [30] O. H. Oldenziel, D. Van Leusen and A. M. Van Leusen, *J. Org. Chem.*, 1977, **42**, 3114–3118.
- [31] C. Paal, *Berichte Dtsch. Chem. Ges.*, 1884, **17**, 2756–2767.
- [32] L. Knorr, *Berichte Dtsch. Chem. Ges.*, 1884, **17**, 2863–2870.
- [33] T. Anderson, *Trans. R. Soc. Edin.*, 1851, **20**, 247–260.
- [34] W. Koerner, *G. Sci. Nat. Ed Econ.*, 1869, **5**, 111–114.
- [35] J. Dewar, *Chem. News*, 1871, **23**, 38–41.
- [36] W. Ramsay, *Lond. Edinb. Dublin Philos. Mag. J. Sci.*, 1876, **2**, 269–281.
- [37] C. Gerhardt, *Ann. Chem. Pharm.*, 1842, **42**, 310–313.
- [38] M. Lökov, S. Tshepelevitsh, A. Heering, P. G. Plieger, R. Vianello and I. Leito, *Eur. J. Org. Chem.*, 2017, **2017**, 4475–4489.
- [39] P. Gros and Y. Fort, *Eur. J. Org. Chem.*, 2002, 3375–3383.
- [40] M. W. Austin and J. H. Ridd, *J. Chem. Soc.*, 1963, 4204–4210.
- [41] J. Miller and P. G. Lutz, *J. Chem. Soc.*, 1954, 1265–1266.
- [42] G. Bartoli and P. E. Todesco, *Acc. Chem. Res.*, 1977, **10**, 125–132.
- [43] E. E. Kwan, Y. Zeng, H. A. Besser and E. N. Jacobsen, *Nat. Chem.*, 2018, **10**, 917–923.
- [44] A. A. Aly, M. Ramadan, G. E.-D. A. Abu-Rahma, Y. A. M. M. Elshaier, M. A. I. Elbastawesy, A. B. Brown and S. Bräse, in *Advances in Heterocyclic Chemistry*, Elsevier, 2021, vol. 135, pp. 147–196.
- [45] P. J. Boratyński, M. Zielińska-Blajet and J. Skarżewski, in *The Alkaloids: Chemistry and Biology*, Academic Press, 2019, vol. 82, pp. 29–145.
- [46] T. Marcelli and H. Hiemstra, *Synthesis*, 2010, 1229–1279.
- [47] J. W. Foster and A. G. Moat, *Microbiol. Rev.*, 1980, **44**, 83–105.
- [48] J. B. Tarr and J. Arditti, *Plant Physiol.*, 1982, **69**, 553–556.
- [49] A. Hantzsch, *Berichte Dtsch. Chem. Ges.*, 1881, **14**, 1637–1638.
- [50] P. Z. Wang, J.-R. Chen and W. J. Xiao, *Org. Biomol. Chem.*, 2019, **17**, 6936–6951.
- [51] C. Zheng and S. L. You, *Chem. Soc. Rev.*, 2012, **41**, 2498–2518.
- [52] M. C. Bagley, C. Glover and E. A. Merritt, *Synlett*, 2007, **2007**, 2459–2482.
- [53] M. C. Bagley, J. W. Dale and J. Bower, *Synlett*, 2001, **2001**, 1149–1151.
- [54] X. Xiong, M. C. Bagley and K. Chapaneri, *Tetrahedron Lett.*, 2004, **45**, 6121–6124.

- [55] M. C. Bagley, V. Fusillo, R. L. Jenkins, M. C. Lubinu and C. Mason, *Beilstein J. Org. Chem.*, 2013, **9**, 1957–1968.
- [56] J. Dohe and T. J. J. Müller, *Z. Für Naturforschung B*, 2016, **71**, 705–718.
- [57] W. Zecher and F. Kröhnke, *Chem. Ber.*, 1961, **94**, 690–697.
- [58] F. Kröhnke, W. Zecher, J. Curtze, D. Drechsler, K. Pflegar, K. E. Schnalke and W. Weis, *Angew. Chem. Int. Ed.*, 1962, **1**, 626–632.
- [59] T. R. Kelly and H. Liu, *J. Am. Chem. Soc.*, 1985, **107**, 4998–4999.
- [60] J. J. Li, Ed., in *Name Reactions: A Collection of Detailed Reaction Mechanisms*, Springer, Berlin, Heidelberg, 2006, pp. 144–146.
- [61] Z. H. Skraup, *Berichte*, 1880, **13**, 2086.
- [62] R. H. Manske, *Chem. Rev.*, 1942, **30**, 113–144.
- [63] H. T. Clarke and A. W. Davis, *Org. Synth.*, 1922, **2**, 79.
- [64] O. Doebner and W. v. Miller, *Berichte Dtsch. Chem. Ges.*, 1881, **14**, 2812–2817.
- [65] S. E. Denmark and S. Venkatraman, *J. Org. Chem.*, 2006, **71**, 1668–1676.
- [66] P. Friedländer and C. F. Gohring, *Berichte Dtsch. Chem. Ges.*, 1883, **16**, 1833–1839.
- [67] J. Marco-Contelles, E. Pérez-Mayoral, A. Samadi, M. do C. Carreiras and E. Soriano, *Chem. Rev.*, 2009, **109**, 2652–2671.
- [68] Y. Kwon, *Handbook of Essential Pharmacokinetics, Pharmacodynamics and Drug Metabolism for Industrial Scientists*, Springer Science & Business Media, 2007.
- [69] J. Sangster, *Octanol–Water Partition Coefficients: Fundamentals and Physical Chemistry*, John Wiley & Sons, Ltd, 1997, vol. 2.
- [70] H. Pajouhesh and G. R. Lenz, *NeuroRX*, 2005, **2**, 541–553.
- [71] D. C. Blakemore, L. Castro, I. Churcher, D. C. Rees, A. W. Thomas, D. M. Wilson and A. Wood, *Nat Chem*, 2018, **10**, 383–394.
- [72] H. C. van der Plas, in *Advances in Heterocyclic Chemistry*, A. R. Katritzky, Academic Press, 2003, vol. 84, pp. 31–70.
- [73] D. Moderhack, *J. Für Prakt. Chemie Chemiker-Ztg.*, 1998, **340**, 687–709.
- [74] J. Jurczyk, J. Woo, S. F. Kim, B. D. Dherange, R. Sarpong and M. D. Levin, *Nat. Synth.*, 2022, **1**, 352–364.
- [75] G. R. Krow, in *Organic Reactions*, John Wiley & Sons, Ltd, 2004, pp. 251–798.
- [76] L. Guy Donaruma and W. Z. Heldt, in *Organic Reactions*, John Wiley & Sons, Ltd, 2011, pp. 1–156.
- [77] E. Buchner and T. Curtius, *Berichte Dtsch. Chem. Ges.*, 1885, **18**, 2377–2379.
- [78] B. J. Andre Anciaux, A. Demonceau, A. J. Hubert, N. Petiniot and P. Teyssie, *J. Chem., Soc. Chem. Commun.*, 1980, 765–766.
- [79] A. J. Anciaux, A. Demonceau, A. F. Noels, A. J. Hubert, R. Warin and P. Teyssié, *J. Org. Chem.*, 1981, **46**, 873–876.
- [80] A. R. Maguire, P. O’leary, F. Harrington, S. E. Lawrence and A. J. Blake, *J. Org. Chem.*, 2001, **66**, 7166–7177.

- [81] A. R. Maguire, N. R. Buckley, P. O’leary and G. Ferguson, *J. Chem. Soc. Perkin. Trans. 1*, 1998, 4077–4091.
- [82] S. E. Reisman, R. R. Nani and S. Levin, *Synlett*, 2011, 2437–2442.
- [83] G. S. Fleming and A. B. Beeler, *Org. Lett.*, 2017, **19**, 5268–5271.
- [84] P. Piacentini, T. W. Bingham and D. Sarlah, *Angew. Chem. Int. Ed.*, 2022, **61**, e202208014.
- [85] Z. Siddiqi, W. Wertjes and D. Sarlah, *J. Am. Chem. Soc.*, 2020, **142**, 10125–10131.
- [86] G. L. Ciamician and M. Dennstedt, *Ber. Dtsch. Chem. Ges.*, 1881, **14**, 1153–1163.
- [87] Z. Wang, in *Comprehensive Organic Name Reactions and Reagents*, John Wiley & Sons, Inc., 2010, pp. 646–648.
- [88] D. Ma, B. S. Martin, K. S. Gallagher, T. Saito and M. Dai, *J. Am. Chem. Soc.*, 2021, **143**, 16383–16387.
- [89] M. Mortén, M. Hennem and T. Bonge-Hansen, *Beilstein J. Org. Chem.*, 2015, **11**, 1944–1949.
- [90] S. Peeters, L. Neerbye Berntsen, P. Rongved and T. Bonge-Hansen, *Beilstein J. Org. Chem.*, 2019, **15**, 2156–2160.
- [91] E. E. Hyland, P. Q. Kelly, A. M. Mckillop, B. D. Dherange and M. D. Levin, *J. Am. Chem. Soc.*, 2022, **144**, 19258–19264.
- [92] Kumar P R, *Heterocycles*, 1987, **26**, 1257–1262.
- [93] S. Atkinson and B. J. Kelly, *J. Chem. Soc., Chem. Commun.*, 1987, 1362–1363.
- [94] J. C. Reisenbauer, O. Green, A. Franchino, P. Finkelstein and B. Morandi, *Science*, 2022, **377**, 1104–1109.
- [95] K. Maeda and T. Hayashi, *Bull. Chem. Soc. Jpn.*, 1971, **44**, 533–536.
- [96] K. Maeda, T. Mishima and T. Hayashi, *Bull. Chem. Soc. Jpn.*, 1974, **47**, 334–338.
- [97] C. Kaneko, H. Fujii, S. Kawai, A. Yamamoto, K. Hashiba, T. Kimata, R. Hayashi and M. Somei, *Chem. Pharm. Bull. (Tokyo)*, 1980, **28**, 1157–1171.
- [98] C. Kaneko, H. Fujii, S. Kawai, K. Hashiba, Y. Karasawa, M. Wakai, R. Hayashi and M. Somei, *Chem. Pharm. Bull. (Tokyo)*, 1982, **30**, 74–85.
- [99] J. Woo, A. H. Christian, S. A. Burgess, Y. Jiang, U. F. Mansoor and M. D. Levin, *Science*, 2022, **376**, 527–532.
- [100] B. Takashi Tsuchiya, S. Okajima, M. Enkaku and J. Kurita, *J. Chem. Soc., Chem. Commun.*, 1981, 211–213.
- [101] T. Tsuchiya, S. Okajima, Enkakum Michiko and J. Kurita, *Chem. Pharm. Bull. (Tokyo)*, 1982, **30**, 3757–3763.
- [102] K. Lempert, J. Fetter, J. Nyitrai, F. Bertha and J. Möller, *J. Chem. Soc. Perkin Trans.*, 1986, **1**, 269–275.
- [103] G. L. Bartholomew, F. Carpaneto and R. Sarpong, *J. Am. Chem. Soc.*, 2022, **144**, 22309–22315.
- [104] A. R. Katritzky and C. M. Marson, *Angew. Chem. Int. Ed.*, 1984, **23**, 420–429.
- [105] J. T. M. Correia, V. A. Fernandes, B. T. Matsuo, J. A. C. Delgado, W. C. de Souza and M. W. Paixão, *Chem. Commun.*, 2020, **56**, 503–514.

- [106] C. Ghiazza, T. Faber, A. Gómez-Palomino and J. Cornella, *Nat. Chem.*, 2022, **14**, 78–84.
- [107] D. Moser, Y. Duan, F. Wang, Y. Ma, M. J. O'Neill and J. Cornella, *Angew. Chem. Int. Ed.*, 2018, **57**, 11035–11039.
- [108] S. C. Patel and N. Z. Burns, *J. Am. Chem. Soc.*, 2022, **144**, 17797–17802.
- [109] P. de Frémont, N. Marion and S. P. Nolan, *Coord. Chem. Rev.*, 2009, **253**, 862–892.
- [110] P. Zuev and R. S. Sheridan, *J. Am. Chem. Soc.*, 1994, **116**, 4123–4124.
- [111] D. Bourissou, O. Guerret, F. P. Gabbaï and G. Bertrand, *Chem. Rev.*, 2000, **100**, 39–92.
- [112] S. Henkel, P. Costa, L. Klute, P. Sokkar, M. Fernandez-Oliva, W. Thiel, E. Sanchez-Garcia and W. Sander, *J. Am. Chem. Soc.*, 2016, **138**, 1689–1697.
- [113] K. Hirai, T. Itoh and H. Tomioka, *Chem. Rev.*, 2009, **109**, 3275–3332.
- [114] M. P. Doyle, R. Duffy, M. Ratnikov and L. Zhou, *Chem. Rev.*, 2010, **110**, 704–724.
- [115] I. D. Jurberg and H. M. L. Davies, *Chem. Sci.*, 2018, **9**, 5112–5118.
- [116] R. A. Moss, *Acc. Chem. Res.*, 1980, **13**, 58–64.
- [117] J. L. Miesusset and U. H. Brinker, *J. Org. Chem.*, 2008, **73**, 1553–1558.
- [118] A. Geuther, *Ann.*, 1862, **123**, 121.
- [119] C. Aouf and M. Santelli, *Tetrahedron Lett.*, 2011, **52**, 688–691.
- [120] J. P. Oliver and U. V. Rao, *J. Org. Chem.*, 1966, **31**, 2696–2697.
- [121] W. E. Parham and E. E. Schweizer, *J. Org. Chem.*, 1959, **24**, 1733–1735.
- [122] W. R. Dolbier, F. Tian, J. X. Duan, A. R. Li, S. Ait-Mohand, O. Bautista, S. Buathong, J. Marshall Baker, J. Crawford, P. Anselme, X. H. Cai, A. Modzelewska, H. Koroniak, M. A. Battiste and Q.-Y. Chen, *J. Fluor. Chem.*, 2004, **125**, 459–469.
- [123] F. Wang, T. Luo, J. Hu, Y. Wang, H. S. Krishnan, P. V. Jog, S. K. Ganesh, G. K. S. Prakash and G. A. Olah, *Angew. Chem. Int. Ed.*, 2011, **50**, 7153–7157.
- [124] Ł. W. Ciszewski, K. Rybicka-Jasińska and D. Gryko, *Org. Biomol. Chem.*, 2019, **17**, 432–448.
- [125] V. H. Gessner, *Chem. Commun.*, 2016, **52**, 12011–12023.
- [126] G. Maas, in *Organic Synthesis, Reactions and Mechanisms*, Springer, Berlin, Heidelberg, 1987, pp. 75–253.
- [127] R. H. Crabtree, *The Organometallic Chemistry of the Transition Metals*, Wiley, 6th edn., 2014.
- [128] T. E. Taylor and M. B. Hall, *J. Am. Chem. Soc.*, 1984, **106**, 1576–1584.
- [129] K. H. Dötz and J. Jr. Stendel, *Chem. Rev.*, 2009, **109**, 3227–3274.
- [130] J. Santamaría and E. Aguilar, *Org. Chem. Front.*, 2016, **3**, 1561–1588.
- [131] D. Gillingham and N. Fei, *Chem. Soc. Rev.*, 2013, **42**, 4918.
- [132] S. P. Green, K. M. Wheelhouse, A. D. Payne, J. P. Hallett, P. W. Miller and J. A. Bull, *Org. Process Res. Dev.*, 2020, **24**, 67–84.
- [133] M. Mortén, M. Hennem and T. Bonge-Hansen, *Beilstein J. Org. Chem.*, 2016, **12**, 1590–1597.

- [134] H. Wang, D. M. Guptill, A. Varela-Alvarez, D. G. Musaev and H. M. L. Davies, *Chem. Sci.*, 2013, **4**, 2844.
- [135] H. Lebel, J. F. Marcoux, C. Molinaro and A. B. Charette, *Chem. Rev.*, 2003, **103**, 977–1050.
- [136] G. Wittig and F. Wingler, *Chem. Ber.*, 1964, **97**, 2146–2164.
- [137] J. Furukawa, N. Kawabata and J. Nishimura, *Tetrahedron Lett.*, 1966, **7**, 3353–3354.
- [138] A. B. Charette and A. Beauchemin, in *Organic Reactions*, John Wiley & Sons, Ltd, 2004, pp. 1–415.
- [139] M. Nakamura, A. Hirai and E. Nakamura, *J. Am. Chem. Soc.*, 2003, **125**, 2341–2350.
- [140] C. Ebner and E. M. Carreira, *Chem. Rev.*, 2017, **117**, 11651–11679.
- [141] A. B. Charette and J. Lemay, *Angew. Chem. Int. Ed.*, 1997, **36**, 1090–1092.
- [142] Z. Yang, J. C. Lorenz and Y. Shi, *Tetrahedron Lett.*, 1998, **39**, 8621–8624.
- [143] A. B. Charette, S. Francoeur, J. Martel and N. Wilb, *Angew. Chem. Int. Ed.*, 2000, **39**, 4539–4542.
- [144] A. Voituriez, L. E. Zimmer and A. B. Charette, *J. Org. Chem.*, 2010, **75**, 1244–1250.
- [145] H. Takahashi, M. Yoshioka, M. Ohno and S. Kobayashi, *Tetrahedron Lett.*, 1992, **33**, 2575–2578.
- [146] A. B. Charette, B. Cote and J. F. Marcoux, *J. Am. Chem. Soc.*, 1991, **113**, 8166–8167.
- [147] A. B. Charette, H. Juteau, H. Lebel and C. Molinaro, *J. Am. Chem. Soc.*, 1998, **120**, 11943–11952.
- [148] E. Schmitz, D. Habisch and A. Stark, *Angew. Chem. Int. Ed.*, 1963, **2**, 548–548.
- [149] M. T. H. Liu, *Chem Soc Rev*, 1982, **11**, 127–140.
- [150] R. A. G. Smith and J. R. Knowles, *J. Chem. Soc. Perkin Trans. 2*, 1975, 686–694.
- [151] J. B. Geri, J. V. Oakley, T. Reyes-Robles, T. Wang, S. J. McCarver, C. H. White, F. P. Rodriguez-Rivera, D. L. Parker, E. C. Hett, O. O. Fadeyi, R. C. Oslund and D. W. C. MacMillan, *Science*, 2020, **367**, 1091–1097.
- [152] H. Zhang, Y. Song, Y. Zou, Y. Ge, Y. An, Y. Ma, Z. Zhu and C. J. Yang, *Chem. Commun.*, 2014, **50**, 4891–4894.
- [153] Y. Kornii, O. Shablykin, T. Tarasiuk, O. Stepaniuk, V. Matvienko, D. Aloslyn, N. Zahorodniuk, I. V. Sadkova and P. K. Mykhailiuk, *J. Org. Chem.*, 2023, **88**, 1–17.
- [154] Y. Chang, D. Zhu, H. Guo, X. Yin, K. Ding and Z. Li, *ChemBioChem*, 2019, **20**, 1783–1788.
- [155] S. S. Husain, S. Nirthanan, D. Ruesch, K. Solt, Q. Cheng, G.-D. Li, E. Arevalo, R. W. Olsen, D. E. Raines, S. A. Forman, J. B. Cohen and K. W. Miller, *J. Med. Chem.*, 2006, **49**, 4818–4825.
- [156] S. S. Husain, M. R. Ziebell, D. Ruesch, F. Hong, E. Arevalo, J. A. Kosterlitz, R. W. Olsen, S. A. Forman, J. B. Cohen and K. W. Miller, *J. Med. Chem.*, 2003, **46**, 1257–1265.
- [157] W. H. Graham, *J. Am. Chem. Soc.*, 1965, **87**, 4396–4397.
- [158] R. A. Moss, *Acc. Chem. Res.*, 1989, **22**, 15–21.
- [159] R. A. Moss, *Acc. Chem. Res.*, 2006, **39**, 267–272.

- [160] W. P. Dailey, *Tetrahedron Lett.*, 1987, **28**, 5801–5804.
- [161] K. Krogh-Jespersen, C. M. Young, R. A. Moss and M. Wloostowski, *Tetrahedron Lett.*, 1982, **23**, 2339–2342.
- [162] R. A. Moss, M. Wloostowski, J. Terpinski, G. Kmicik-Lawrynowicz and K. Krogh-Jespersen, *J. Am. Chem. Soc.*, 1987, **109**, 3811–3812.
- [163] R. A. Moss, M. Fedorynski, G. Kmicik-Lawrynowicz and J. Terpinski, *Tetrahedron Lett.*, 1986, **27**, 2707–2710.
- [164] R. A. Moss, G. Chu and R. R. Sauers, *J. Am. Chem. Soc.*, 2005, **127**, 2408–2409.
- [165] J. Nishimura and J. Furukawa, *J. Chem. Soc. Chem. Commun.*, 1971, 1375.
- [166] S. Miyano and H. Hashimoto, *Bull. Chem. Soc. Jpn.*, 1974, **47**, 1500–1503.
- [167] H. Y. Kim, A. E. Lurain, P. García-García, P. J. Carroll and P. J. Walsh, *J. Am. Chem. Soc.*, 2005, **127**, 13138–13139.
- [168] H. Y. Kim, L. Salvi, P. J. Carroll and P. J. Walsh, *J. Am. Chem. Soc.*, 2009, **131**, 954–962.
- [169] L. P. B. Beaulieu, L. E. Zimmer and A. B. Charette, *Chem. Eur. J.*, 2009, **15**, 11829–11832.
- [170] E. M. D. Allouche, S. Taillemaud and A. B. Charette, *Chem. Commun.*, 2017, **53**, 9606–9609.
- [171] C. Navuluri and A. B. Charette, *Org. Lett.*, 2015, **17**, 4288–4291.
- [172] S. Taillemaud, N. Diercxsens, A. Gagnon and A. B. Charette, *Angew. Chem. Int. Ed.*, 2015, **54**, 14108–14112.
- [173] L. P. B. Beaulieu, L. E. Zimmer, A. Gagnon and A. B. Charette, *Chem. Eur. J.*, 2012, **18**, 14784–14791.
- [174] G. Benoit and A. B. Charette, *J. Am. Chem. Soc.*, 2017, **139**, 1364–1367.
- [175] W. A. Ma and Z.-X. Wang, *Organometallics*, 2011, **30**, 4364–4373.
- [176] C. J. Fahrni and T. V. O'Halloran, *J. Am. Chem. Soc.*, 1999, **121**, 11448–11458.
- [177] X. Zhang, C. Du, H. Zhang, X.-C. Li, Y.-L. Wang, J.-L. Niu and M.-P. Song, *Synthesis*, 2019, **51**, 889–898.
- [178] H. Xu, Y. P. Li, Y. Cai, G. P. Wang, S. F. Zhu and Q. L. Zhou, *J. Am. Chem. Soc.*, 2017, **139**, 7697–7700.
- [179] C. M. Sonleitner, S. Park, R. Eckl, T. Ertl and O. Reiser, *Angew. Chem. Int. Ed.*, 2020, **59**, 18110–18115.
- [180] J. C. Lorenz, J. Long, Z. Yang, S. Xue, Y. Xie and Y. Shi, *J. Org. Chem.*, 2004, **69**, 327–334.
- [181] S. F. Musolino, Z. Pei, L. Bi, G. A. Dilabio and J. E. Wulff, *Chem. Sci.*, 2021, **12**, 12138–12148.
- [182] A. Padwa, M. J. Pulwer and T. J. Blacklock, *Org. Synth.*, 1990, **7**, 203.
- [183] Y. N. Romashin, M. T. H. Liu and R. Bonneau, *Chem. Commun.*, 1999, 447–448.
- [184] J. E. Jackson, N. Soundararajan, M. S. Platz and M. T. H. Liu, *J. Am. Chem. Soc.*, 1988, **110**, 5595–5596.

- [185] A. Padwa, T. J. Blacklock, D. M. Cordova and R. Loza, *J. Am. Chem. Soc.*, 1980, **102**, 5648–5656.
- [186] Y. N. Romashin, M. T. H. Liu, S. S. Nijjar and O. A. Attanasi, *Chem. Commun.*, 2000, 1147–1148.
- [187] B. D. Dherange, P. Q. Kelly, J. P. Liles, M. S. Sigman and M. D. Levin, *J. Am. Chem. Soc.*, 2021, **143**, 11337–11344.
- [188] A. Ruffoni, C. Hampton, M. Simonetti and D. Leonori, *Nature*, 2022, **610**, 81–86.
- [189] D. E. Wise, E. S. Gogarnoiu, A. D. Duke, J. M. Paolillo, T. L. Vacala, W. A. Hussain and M. Parasram, *J. Am. Chem. Soc.*, 2022, **144**, 15437–15442.
- [190] M. Kischkewitz, B. Marinic, N. Kratena, Y. Lai, H. B. Hepburn, M. Dow, K. E. Christensen and T. J. Donohoe, *Angew. Chem. Int. Ed.*, 2022, **61**, e202204682.
- [191] Z. Bao, M. Huang, Y. Xu, X. Zhang, Y.-D. Wu and J. Wang, *Angew. Chem. Int. Ed.*, 2023, **62**, e202216356.
- [192] Q.-Y. Zhang, Y. Wang, S.-J. Li, Y. Wang and D. Wei, *Catal. Sci. Technol.*, 2022, **12**, 947–953.
- [193] P. A. Cox, M. Reid, A. G. Leach, A. D. Campbell, E. J. King and G. C. Lloyd-Jones, *J. Am. Chem. Soc.*, 2017, **139**, 13156–13165.
- [194] X. A. F. Cook, A. de Gombert, J. McKnight, L. R. E. Pantaine and M. C. Willis, *Angew. Chem. Int. Ed.*, 2021, **60**, 11068–11091.
- [195] P. A. Cox, A. G. Leach, A. D. Campbell and G. C. Lloyd-Jones, *J. Am. Chem. Soc.*, 2016, **138**, 9145–9157.
- [196] T. Martinu and W. P. Dailey, *J. Org. Chem.*, 2006, **71**, 5012–5015.
- [197] K. D. Collins and F. Glorius, *Nat. Chem.*, 2013, **5**, 597–601.
- [198] P. Ertl, E. Altmann and J. M. McKenna, *J. Med. Chem.*, 2020, **63**, 8408–8418.
- [199] L.-B. Yu, D. Chen, J. Li, J. Ramirez, P. G. Wang and S. G. Bott, *J. Org. Chem.*, 1997, **62**, 208–211.
- [200] S. Peixoto, T. M. Nguyen, D. Crich, B. Delpech and C. Marazano, *Org. Lett.*, 2010, **12**, 4760–4763.
- [201] S. Kulchat and J. M. Lehn, *Chem. Asian. J.*, 2015, **10**, 2484–2496.
- [202] L. W. Deady and W. L. Finlayson, *Synth. Commun.*, 1980, **10**, 947–950.
- [203] L. W. Deady and O. L. Korytsky, *Tetrahedron Lett.*, 1979, **20**, 451–452.
- [204] U. Berg, R. Gallo and J. Metzger, *J. Org. Chem.*, 1976, **41**, 2621–2624.
- [205] E. M. Arnett and R. Reich, *J. Am. Chem. Soc.*, 1980, **102**, 5892–5902.
- [206] D. C. Batesky, M. J. Goldfogel and D. J. Weix, *J. Org. Chem.*, 2017, **82**, 9931–9936.
- [207] D. Gnecco, C. Marazano, R. G. Enríquez, J. L. Terán, M. del R. Sánchez S and A. Galindo, *Tetrahedron Asymmetry*, 1998, **9**, 2027–2029.
- [208] S. Banu, K. Singh, S. Tyagi, A. Yadav and P. P. Yadav, *Org. Biomol. Chem.*, 2021, **19**, 9433–9438.
- [209] M. Zhou, K. Yu, J. Liu, W. Shi, Y. Pan, H. Tang, X. Peng, Q. Liu and H. Wang, *RSC Adv.*, 2021, **11**, 16246–16251.

- [210] Y. Jin, L. Ou, H. Yang and H. Fu, *J. Am. Chem. Soc.*, 2017, **139**, 14237–14243.
- [211] F. Lovering, J. Bikker and C. Humblet, *J. Med. Chem.*, 2009, **52**, 6752–6756.
- [212] H. C. Kolb, M. S. Van Nieuwenhze and K. B. Sharpless, *Chem. Rev.*, 1994, **94**, 2483–2547.
- [213] Q. F. Xu-Xu, X. Zhang and S.-L. You, *Org. Lett.*, 2019, **21**, 5357–5362.
- [214] S. Stockerl, T. Danelzik, D. G. Piekarski and O. García Mancheño, *Org. Lett.*, 2019, **21**, 4535–4539.
- [215] V. H. Rawal, R. J. Jones and M. P. Cava, *J. Org. Chem.*, 1987, **52**, 19–28.
- [216] K. Yamada, T. Kurokawa, H. Tokuyama and T. Fukuyama, *J. Am. Chem. Soc.*, 2003, **125**, 6630–6631.
- [217] M. Hönel and F. W. Vierhapper, *J. Chem. Soc. Perkin 1*, 1982, 2607–2610.
- [218] J. B. Sperry, C. J. Minter, J. Tao, R. Johnson, R. Duzguner, M. Hawksworth, S. Oke, P. F. Richardson, R. Barnhart, D. R. Bill, R. A. Giusto and J. D. Weaver, *Org. Process Res. Dev.*, 2018, **22**, 1262–1275.
- [219] S. Bräse, C. Gil, K. Knepper and V. Zimmermann, *Angew. Chem. Int. Ed.*, 2005, **44**, 5188–5240.
- [220] G. L. Closs and R. A. Moss, *J. Am. Chem. Soc.*, 1964, **86**, 4042–4053.
- [221] Yoshida, Tadao, Yoshizawa, Fujiroku, Ito, Mamoru, Matsunaga, Takehiro, Watanabe, Masatoshi, and Tamura, Masamitsu. *Kogyo Kagaku*, 1987, **48**, 311–316.
- [222] D. J. Frurip, D. G. Gorman, J. Klosin and G. R. Buske, *Chem. Eng. News*, **12**, 1287–1292.
- [223] H. Nefati, B. Diawara and J. J. Legendre, *SAR QSAR Environ. Res.*, 1993, **1**, 131–136.
- [224] F. Stoessel, *Thermal Safety of Chemical Processes*, Wiley-VCH Verlag GmbH, Weinheim, Germany, 2008.
- [225] M. B. Plutschack, B. Pieber, K. Gilmore and P. H. Seeberger, *Chem. Rev.*, 2017, **117**, 11796–11893.
- [226] T. Morofuji, K. Inagawa and N. Kano, *Org. Lett.*, 2021, **23**, 6126–6130.
- [227] H. Sonnenschein, E. Schmitz and W. Pritzkow, *Liebigs Ann. Chem.*, 1990, **1990**, 277–279.
- [228] Y. Y. Zhang, J. D. Lin, X. L. Xu and J. H. Li, *Synth. Comm.*, 2010, **40**, 2556–2563.
- [229] H. Lee, J. Börgel and T. Ritter, *Angew. Chem. Int. Ed.*, 2017, **56**, 6966–6969.
- [230] Y. Yu, Y. Wang, B. Li, Y. Tan, H. Zhao, Z. Li, C. Zhang and W. Ma, *Adv. Synth. Catal.*, 2022, **364**, 838–844.
- [231] M. Schlosser, A. Ginanneschi and F. Leroux, *Eur. J. Org. Chem.*, 2006, **2006**, 2956–2969.
- [232] N. Sun, L. Hong, F. Huang, H. Ren, W. Mo, B. Hu, Z. Shen and X. Hu, *Tetrahedron*, 2013, **69**, 3927–3933.
- [233] J. C. Borghs, V. Zubar, L. M. Azofra, J. Sklyaruk and M. Rueping, *Org. Lett.*, 2020, **22**, 4222–4227.
- [234] K. Y. Kim and J. H. Lee, *Org. Lett.*, 2018, **20**, 7712–7716.
- [235] S. H. Son, J.-W. Shin, H.-J. Won, H.-S. Yoo, Y. Y. Cho, S. L. Kim, Y. H. Jang, B. Y. Park and N.-J. Kim, *Org. Lett.*, 2021, **23**, 7467–7471.

- [236] A. Carbone, M. Pennati, B. Parrino, A. Lopergolo, P. Barraja, A. Montalbano, V. Spanò, S. Sbarra, V. Doldi, M. De Cesare, G. Cirrincione, P. Diana and N. Zaffaroni, *J. Med. Chem.*, 2013, **56**, 7060–7072.
- [237] W. Zhuang, J. Zhang, C. Ma, J. S. Wright, X. Zhang, S.-F. Ni and Q. Huang, *Org. Lett.*, 2022, **24**, 4229–4233.
- [238] H. Wu, W. Chen, W. Deng, L. Yang, X. Li, Y. Hu, Y. Li, L. Chen and Y. Huang, *Org. Lett.*, 2022, **24**, 1412–1417.
- [239] A. J. Cresswell and G. C. Lloyd-Jones, *Chem. Eur. J.*, 2016, **22**, 12641–12645.
- [240] D. Lubriks, I. Sokolovs and E. Suna, *Org. Lett.*, 2011, **13**, 4324–4327.
- [241] S. Islam and I. Larrosa, *Chem. Eur. J.*, 2013, **19**, 15093–15096.
- [242] H. Elokdah, M. Abou-Gharbia, J. K. Hennan, G. McFarlane, C. P. Mugford, G. Krishnamurthy and D. L. Crandall, *J. Med. Chem.*, 2004, **47**, 3491–3494.
- [243] J. Gao, X. Liu, B. Zhang, Q. Mao, Z. Zhang, Q. Zou, X. Dai and S. Wang, *Eur. J. Med. Chem.*, 2020, **190**, 112077.
- [244] M. Shee, S. S. Shah and N. D. P. Singh, *Chem. Commun.*, 2020, **56**, 4240–4243.
- [245] H. Chen, H. Yang, N. Li, X. Xue, Z. He and Q. Zeng, *Org. Process Res. Dev.*, 2019, **23**, 1679–1685.
- [246] G. Ehrhart and I. Hennig, *Arch. Pharm. (Weinheim)*, 1961, **294**, 550–555.
- [247] M. J. Aalam, Deepa and S. Singh, *Eur. J. Org. Chem.*, 2022, **2022**, e202200978.
- [248] V. Yadav, S. G. Jagtap, E. Balaraman and S. B. Mhaske, *Org. Lett.*, 2022, **24**, 9054–9059.
- [249] G. L. Tolnai, S. Ganss, J. P. Brand and J. Waser, *Org. Lett.*, 2013, **15**, 112–115.
- [250] R. Lang, L. Shi, D. Li, C. Xia and F. Li, *Org. Lett.*, 2012, **14**, 4130–4133.
- [251] A. F. G. Maier, S. Tussing, T. Schneider, U. Flörke, Z.-W. Qu, S. Grimme and J. Paradies, *Angew. Chem. Int. Ed.*, 2016, **55**, 12219–12223.
- [252] P. Y. Choy, C. P. Lau and F. Y. Kwong, *J. Org. Chem.*, 2011, **76**, 80–84.
- [253] P. Tang, W. Wang and T. Ritter, *J. Am. Chem. Soc.*, 2011, **133**, 11482–11484.
- [254] D. A. Evans, K. A. Scheidt, K. R. Fandrick, H. W. Lam and J. Wu, *J. Am. Chem. Soc.*, 2003, **125**, 10780–10781.
- [255] D. I. Bugaenko, A. A. Dubrovina, M. A. Yurovskaya and A. V. Karchava, *Org. Lett.*, 2018, **20**, 7358–7362.
- [256] P. Kannaboina, K. A. Kumar and P. Das, *Org. Lett.*, 2016, **18**, 900–903.
- [257] B. Emayavaramban, M. Sen and B. Sundararaju, *Org. Lett.*, 2017, **19**, 6–9.
- [258] R. Honeker, J. B. Ernst and F. Glorius, *Chem. Eur. J.*, 2015, **21**, 8047–8051.
- [259] A. Walia, S. Kang and R. B. Silverman, *J. Org. Chem.*, 2013, **78**, 10931–10937.
- [260] W. Fu, L. Zhu, S. Tan, Z. Zhao, X. Yu and L. Wang, *J. Org. Chem.*, 2022, **87**, 13389–13395.
- [261] S. Liu and C. C. Tzschucke, *Eur. J. Org. Chem.*, 2016, **2016**, 3509–3513.
- [262] S. Sengmany, S. Vasseur, A. Lajnef, E. Le Gall and E. Léonel, *Eur. J. Org. Chem.*, 2016, **2016**, 4865–4871.

- [263] N. D. Smith, D. Huang and N. D. P. Cosford, *Org. Lett.*, 2002, **4**, 3537–3539.
- [264] X. Han and J. Wu, *Angew Chem Int Ed*, 2013, **52**, 4637–4640.
- [265] Y. Li, J. Han, H. Luo, Q. An, X.-P. Cao and B. Li, *Org. Lett.*, 2019, **21**, 6050–6053.
- [266] P. Barraja, V. Spanò, D. Patrizia, A. Carbone, G. Cirrincione, D. Vedaldi, A. Salvador, G. Viola and F. Dall'Acqua, *Bioorg. Med. Chem. Lett.*, 2009, **19**, 1711–1714.
- [267] L. Junk, E. Papadopoulos and U. Kazmaier, *Synthesis*, 2021, **53**, 2503–2511.
- [268] M. Righi, F. Topi, S. Bartolucci, A. Bedini, G. Piersanti and G. Spadoni, *J. Org. Chem.*, 2012, **77**, 6351–6357.
- [269] P. R. Golubev, A. S. Pankova and M. A. Kuznetsov, *Eur. J. Org. Chem.*, 2014, **2014**, 3614–3621.
- [270] O. Dann, H. Fick, B. Pietzner, E. Walkenhorst, R. Fernbach and D. Zeh, *Justus Liebigs Ann. Chem.*, 1975, **1975**, 160–194.
- [271] M. G. Rosenberg and U. H. Brinker, *J. Org. Chem.*, 2003, **68**, 4819–4832.
- [272] F. M. Kalimani and A. Khorshidi, *RSC Adv.*, 2023, **13**, 6909–6918.
- [273] A. R. Mazzotti, M. G. Campbell, P. Tang, J. M. Murphy and T. Ritter, *J. Am. Chem. Soc.*, 2013, **135**, 14012–14015.
- [274] S. Das, B. Join, K. Junge and M. Beller, *Chem. Commun.*, 2012, **48**, 2683–2685.
- [275] T. K. Achar and P. Mal, *J. Org. Chem.*, 2015, **80**, 666–672.
- [276] M. Boyle, K. Livingstone, M. C. Henry, J. M. L. Elwood, J. D. Lopez-Fernandez and C. Jamieson, *Org. Lett.*, 2022, **24**, 334–338.
- [277] A. Cederbalk, M. Lysén, J. Kehler and J. L. Kristensen, *Tetrahedron*, 2017, **73**, 1576–1582.
- [278] Md. M. Rahman, G. Li and M. Szostak, *J. Org. Chem.*, 2019, **84**, 12091–12100.
- [279] N. J. Taylor, E. Emer, S. Preshlock, M. Schedler, M. Tredwell, S. Verhoog, J. Mercier, C. Genicot and V. Gouverneur, *J. Am. Chem. Soc.*, 2017, **139**, 8267–8276.
- [280] A. Steiner, J. D. Williams, O. de Frutos, J. A. Rincón, C. Mateos and C. O. Kappe, *Green Chem.*, 2020, **22**, 448–454.
- [281] K. Singha, S. C. Ghosh and A. B. Panda, *Eur. J. Org. Chem.*, 2021, **2021**, 657–662.
- [282] A. O. Gálvez, C. P. Schaack, H. Noda and J. W. Bode, *J. Am. Chem. Soc.*, 2017, **139**, 1826–1829.
- [283] G. A. Molander and I. Shin, *Org. Lett.*, 2013, **15**, 2534–2537.
- [284] R. S. Mega, V. K. Duong, A. Noble and V. K. Aggarwal, *Angew. Chem. Int. Ed.*, 2020, **59**, 4375–4379.
- [285] Z. Lin, L. Huang and G. Yuan, *Chem. Commun.*, 2021, **57**, 3579–3582.
- [286] J. A. R. Tilden, A. T. Lubben, S. B. Reeksting, G. Kociok-Köhn and C. G. Frost, *Chem. Eur. J.*, 2022, **28**, e202104385.
- [287] P. S. Mahajan, V. T. Humne, S. D. Tanpure and S. B. Mhaske, *Org. Lett.*, 2016, **18**, 3450–3453.
- [288] C. Qin, P. Feng, Y. Ou, T. Shen, T. Wang and N. Jiao, *Angew. Chem. Int. Ed.*, 2013, **52**, 7850–7854.